



UNIVERSITY OF BURGOS

HIGHER POLYTECHNIC SCHOOL

PhD THESIS

PERFORMANCE OF SELF-COMPACTING CONCRETE
MANUFACTURED WITH COARSE AND FINE RECYCLED
CONCRETE AGGREGATE AND SLAG-BASED BINDER

VÍCTOR REVILLA CUESTA

Supervisors:

Dr. Mr. Juan Manuel Manso Villalaín

Dr. Mrs. Vanesa Ortega López



Burgos, September 2021

PhD THESIS

PERFORMANCE OF SELF-COMPACTING CONCRETE
MANUFACTURED WITH COARSE AND FINE RECYCLED
CONCRETE AGGREGATE AND SLAG-BASED BINDER

VÍCTOR REVILLA CUESTA

Supervisors:

Dr. Mr. Juan Manuel Manso Villalaín

Dr. Mrs. Vanesa Ortega López

Burgos, September 2021

*To you, dear reader.
That my PhD thesis is worthy of your perusal is an honor and,
at the same time, an enormous responsibility*

*A ti, estimado lector.
Que mi tesis doctoral sea digna de tu lectura es un honor y,
al mismo tiempo, una enorme responsabilidad*

*Existentialism and raciovitalism, contemporary ways of thinking,
opposed in many aspects, but both true in their own way*

*"In the end, I am the architect of my own being, my own character and destiny.
It is no use pretending what I could have been,
because I am what I have made, and nothing more"*

Jean-Paul Sartre

"What is most valuable in human is their capacity for dissatisfaction"

José Ortega y Gasset

*Existencialismo y raciovitalismo, formas de pensar contemporáneas,
en muchos aspectos opuestas, pero ambas ciertas a su manera*

*"Al final, yo soy el arquitecto de mi propio ser, mi propio carácter y destino.
No sirve de nada aparentar lo que podría haber sido,
porque yo soy lo que he hecho, y nada más"*

Jean-Paul Sartre

"Lo que más vale en el hombre es su capacidad de insatisfacción"

José Ortega y Gasset

Agradecimientos/Acknowledgements

Agradecimientos breves y ordenados. Quien me conoce sabe que el orden no es un problema, pero creo que la brevedad nunca será uno de mis puntos fuertes. Además, sois muchos...

En primer lugar, a mi director de tesis, Dr. D. Juan Manuel Manso. Gracias por haber apostado y confiado en mí, incluso cuando era un simple número en una lista hecha en secretaría. Sin embargo, en particular quiero agradecerle una llamada de teléfono que hiciste a un estudiante de segundo curso del Máster de Ingeniería de Caminos, Canales y Puertos en diciembre de 2017, cuatro días antes del comienzo de las vacaciones de Navidad. No se puede entender quién soy ahora sin la decisión que tomé aquel día.

En segundo lugar, es obvio que esta Tesis Doctoral tampoco habría sido posible sin mi codirectora, Dra. Dña. Vanesa Ortega. Gracias por tu apoyo constante, tu preocupación, tu orientación y, especialmente, por haber tenido la paciencia, que te ha hecho mucha falta, para haber soportado durante tres largos años a un hombre tremendamente insatisfecho con un grave problema de impaciencia.

Mención especial merece también la Dra. Dña. Marta Skaf. Pobres directores si no hubieses estado ahí tú también... Todo lo que he dicho por Vanesa también puede aplicarse a ti. Mi insatisfacción y necesidad de hacer las cosas deprisa te ha llevado a tener una carga de trabajo para nada despreciable, de la cual en ningún momento te has desentendido. Gracias por tu continua ayuda a lo largo de todo este tiempo.

Vanesa y Marta, pasada la lógica fase de cautela que existe cuando alguien nuevo empieza, este periodo de tiempo me ha permitido conoceros. Cada una con su particular forma de ser, una más seria, otra más espontánea, pero ambas con una fortaleza envidiable. Gracias por este tiempo, el cual ha sido un regalo, por no haberos hundido bajo mi peso y por haber tenido incluso la capacidad de erguirnos soportándolo. A vosotras, y a Manolo incluido, gracias por haberme tratado siempre como un igual y no haber hecho jamás caso a mi posición, la de un simple becario. Al resto de miembros del grupo de investigación SUCONS, incluido José Antonio aunque ya esté jubilado, por el apoyo que me habéis brindado cuando lo he necesitado.

A mi amigo por correspondencia durante estos dos últimos años, Dr. D. Javier Jesús González. Gracias por la infinidad de correos electrónicos durante el confinamiento, mientras estuve en Portugal y tras volver de allí. Con cada uno de ellos he aprendido un poco más de esta complicada labor del investigador. Solo tuvimos la oportunidad de debatir en persona durante mi etapa de mayor carga de trabajo en el laboratorio, tenemos pendientes muchos debates de mi fase redactora.

A todo el grupo de investigación de la Universidad del País Vasco que D. Javier lleva detrás y que se encuentra comandado por el Dr. D. *JTSJL*, pues todos vosotros habéis jugado un pequeño papel durante este tiempo. La pandemia ha fastidiado muchísimas cosas, y una de ellas es no haber tenido la oportunidad de haberos conocido mejor durante estos años. Eso es algo que tenemos pendiente y que no se me va a olvidar.

Despite the uncertainty caused by the pandemic, I went to Lisbon, to the Instituto Superior Técnico (IST), from September to December 2020, where I could meet one of the best researchers in my field, Prof. Dr. Jorge de Brito. To you, Professor, and to Dr. D. Luís Evangelista, thank you for welcoming me, for the clear idea of what I was going to do there, and for teaching me that quality work begins by being rigorous in its approach and execution. Thanks to all the colleagues who helped me while I was there, being alone in a new place is never easy.

Dejamos las plantas altas del edificio y nos movemos a la planta baja, a los talleres de la Universidad de Burgos. Vamos por parejas. Al Dr. Pablo Luís Campos y a D. José Luís Díez, por haberme ayudado en todos los ensayos sobre los que os he preguntado, y por haber soportado el desorden y el trasiego de probetas que en algún momento había en vuestro laboratorio por mi culpa. A D. Jorge Javier Hernández y a D. José Miguel Solaguren-Beascoa, por haberme ayudado a hacer las infinitas amasadas de hormigón y haberme enseñado tanto inglés, sobre todo tú, Josemi. A D. Roberto Lorenzo y D. Antonio Fernández, por haberme ayudado siempre que lo he necesitado cuando pasaba del otro laboratorio. Afortunadamente para vosotros fue un número de veces razonable. A D. Pablo Ausín, por su ayuda durante estos dos últimos años, y por haberme hecho recordar toda la resistencia de materiales que se estudia en la carrera. Y ya sin formalismos, Pablo, José Luís, Jorge, Josemi, Roberto y Antonio, gracias por el buen humor y ambiente que siempre hay en los laboratorios y con el que da gusto trabajar.

Dejo a las personas más cercanas para el final. A mis padres, Candi y Begoña, a mi hermana Andrea, y a mis amigos. Soy perfectamente consciente de que a lo largo de estos tres años ha habido épocas en las que no fue nada fácil convivir conmigo por mi mal humor, mis quejas y lamentos o ambas cosas a la vez. Muchas veces a los que están siempre contigo y no esperan nada a cambio por ello no les damos la importancia que se merecen. No quiero cometer ese error. Gracias simplemente por estar ahí, sin ello podéis estar seguros que me habría derrumbado. En estos momentos no puedo ni quiero imaginar una vida sin vosotros.

Y para acabar, no puedo olvidarme tampoco de agradecer esta tesis al hormigón. Querido compañero, se puede afirmar sin ningún riesgo de equivocarme que mi Tesis Doctoral no sería posible sin ti.

A todos vosotros, muchísimas gracias y espero poder seguir agradeciándoos cosas en el futuro.

Víctor

Financiación: Agradezco al Ministerio de Ciencia e Innovación (MICINN), a la Agencia Estatal de Investigación (AEI) y a los Fondos Europeos de Desarrollo Regional (FEDER) la financiación de la presente Tesis Doctoral a través de la convocatoria de 2017 de las Ayudas para la Formación de Profesorado Universitario, FPU17/03374. Sin esta beca, mi Tesis Doctoral jamás habría existido. A estas mismas instituciones les agradezco también la financiación a través de la convocatoria de 2020 de las Ayudas a la movilidad para estancias breves y traslados temporales para beneficiarios del programa de Formación del Profesorado Universitario, EST19/00263, gracias a la cual pude realizar la estancia en el Instituto Superior Técnico (IST) de la Universidad de Lisboa.

Resumen

El desarrollo sostenible es el gran reto de la sociedad actual. El cambio climático y la sobreexplotación de los recursos naturales lleva a que sea necesario buscar formas de producción alternativas a las tradicionales en todos los sectores productivos. Una mayor sostenibilidad medioambiental, no dañando los recursos existentes y consumiéndolos de forma responsable, junto con una sostenibilidad social y económica, permite alcanzar este objetivo.

El sector de la construcción ha avanzado en los últimos años en el desarrollo sostenible mediante el empleo de subproductos industriales en sustitución a los materiales de construcción tradicionales, en aplicaciones como el hormigón. El empleo de estos materiales alternativos permite aumentar la sostenibilidad medioambiental al reducirse el consumo de recursos naturales y la huella de carbono. Además, el reducido coste de dichos materiales promueve la sostenibilidad económica y, si adicionalmente el diseño del material de construcción es adecuado, contribuye también a la sostenibilidad social. La presente Tesis Doctoral, elaborada por compendio de siete artículos, constituye un avance en el conocimiento sobre el desarrollo sostenible y la economía circular en el sector de la construcción.

En el primer artículo se abordaron las deficiencias bibliográficas existentes en relación con el hormigón autocompactante con árido reciclado de hormigón. Para ello, se realizó un análisis bibliográfico de 108 referencias que abordaban la elaboración de hormigón autocompactante con el citado residuo. Se observó la escasez de los estudios que evaluaban el empleo de árido fino de hormigón reciclado en este tipo de hormigón, así como el estudio prácticamente inexistente de su interacción con el árido grueso de hormigón reciclado y conglomerantes alternativos. Estos aspectos detectados sirvieron de base para el posterior desarrollo del trabajo experimental de la Tesis Doctoral.

El segundo artículo, que conforma la primera fase de trabajo experimental de la Tesis Doctoral junto con el tercer artículo, pretendía arrojar luz sobre la influencia del empleo simultáneo de árido grueso y fino de hormigón reciclado en el comportamiento del hormigón autocompactante. Para ello, se elaboraron cinco hormigones autocompactantes con un 100% de árido grueso de hormigón reciclado y un 0%, 25%, 50%, 75% y 100% de árido fino de hormigón reciclado. Las diferentes propiedades mecánicas de estas mezclas se analizaron a las edades de 7, 28 y 90 días. Con este análisis se pretendió establecer de forma clara el efecto de cada uno de los contenidos de árido fino de hormigón reciclado y que se utilizaron de base para el desarrollo de las mezclas estudiadas en la segunda fase de esta Tesis Doctoral.

En línea con el segundo artículo, el tercer artículo estudió también el comportamiento mecánico de unos hormigones autocompactantes con una composición prácticamente idéntica. Sin embargo, este tercer artículo presentó un enfoque estadístico. Así, en vez de analizarse diferentes propiedades mecánicas, se analizó una única propiedad, la resistencia a compresión. La realización de un elevado número de réplicas, es decir, la rotura de un elevado número de probetas de cada hormigón a cada edad permitió efectuar un análisis estadístico detallado sobre el efecto del árido fino de hormigón reciclado, la predicción de la resistencia a compresión, y el concepto de resistencia característica.

La segunda fase de desarrollo de la Tesis Doctoral se inicia en el cuarto artículo. En él se evaluó la evolución a lo largo del tiempo de la autocompactabilidad de unas mezclas elaboradas no solo con un 100% de árido grueso de hormigón reciclado y un contenido variable (0%, 50%, and 100%) de árido fino de hormigón reciclado, sino también escoria siderúrgica granulada molida (45% del total de conglomerante añadido a la mezcla). La evaluación de la capacidad de llenado, la viscosidad y la

habilidad de paso por lugares angostos de estas mezclas a lo largo del tiempo permitió establecer una visión clara de la viabilidad del transporte de estas mezclas a grandes distancias desde su lugar de producción, una vez completado su proceso de fabricación.

El quinto artículo abordó, en las mismas mezclas que las diseñadas en el cuarto artículo, un aspecto también relevante para una posible generalización del uso de este tipo de hormigón: la estimación indirecta de su resistencia a compresión. Las peculiaridades del diseño de este tipo de hormigones afectan a su dureza superficial, es decir, al valor del índice de rebote que se obtiene en ellos. Por otra parte, su composición más uniforme debido al bajo contenido de árido grueso del hormigón autocompactante también afecta a la velocidad de propagación del impulso ultrasónico. Si además se emplean grandes cantidades de materiales alternativos, la alteración de estas propiedades puede ser incluso mayor. Por ello, en este artículo se recoge un amplio programa experimental que permite analizar estadísticamente la validez de estas medidas indirectas para estimar la resistencia a compresión y, así, poder realizar un control de la calidad del hormigón *in situ* en la propia obra.

Para complementar esta segunda fase de la Tesis Doctoral, en el sexto artículo se analizó de forma detallada el comportamiento plástico en la dirección longitudinal y transversal de las mezclas autocompactantes desarrolladas. En primer lugar, se estudiaron hormigones autocompactantes elaborados con árido natural en su totalidad. Este aspecto fue estudiado debido a su carácter novedoso en la literatura científica y a la casi nula existencia de publicaciones científicas en este aspecto, fundamentalmente en lo referente al comportamiento plástico transversal. Posteriormente, se evaluó en detalle el efecto del empleo de árido grueso y fino de hormigón reciclado, así como de escoria siderúrgica granulada molida. El objetivo era caracterizar de forma detallada este comportamiento en este tipo de hormigones para analizar su uso potencial en aplicaciones reales ante cargas de compresión elevadas.

La presente Tesis Doctoral finaliza con un artículo corto en el cual se recogen los resultados preliminares obtenidos en relación con el comportamiento térmico del hormigón autocompactante y el efecto del empleo de árido reciclado de hormigón. Con este estudio se pretendía caracterizar también los hormigones elaborados en relación con los esfuerzos térmicos que experimentarán en servicio, cuando formen parte de elementos estructurales. Con todo ello, se proporcionó una visión completa del comportamiento deformacional de estos hormigones y de su viabilidad en todo tipo de aplicaciones.

Del análisis conjunto de los resultados expuestos en los siete artículos que se recogen en esta Tesis Doctoral, se pueden señalar o destacar diferentes aspectos relevantes que deben ser tenidos en cuenta a la hora de emplear árido grueso y fino de hormigón reciclado y escoria siderúrgica granulada molida en el hormigón autocompactante:

- Si se emplea árido grueso de hormigón reciclado en hormigón autocompactante, un contenido igual al 100% es lo más recomendable. No se observó una diferencia estadísticamente significativa entre las propiedades mecánicas del hormigón autocompactante elaborado con un 50% o un 100% de árido grueso de hormigón reciclado.
- El empleo de un 25% de árido fino de hormigón reciclado no tuvo un efecto significativo en el comportamiento mecánico del hormigón. El empleo de un 50% de árido reciclado fino proporcionó un hormigón autocompactante con unas propiedades mecánicas intermedias. Tampoco se observó una diferencia significativa entre el empleo de un 75% o de un 100% de árido fino de hormigón reciclado en el descenso general de resistencia y rigidez causado por el empleo de contenidos tan altos de la fracción fina de este árido.
- La adición de árido reciclado de hormigón causó que la resistencia característica del hormigón autocompactante fuese subestimada por la formulación existente. Al mantener la relación agua/cemento efectiva constante se obtuvo una distribución de probabilidad para la resistencia a compresión con una menor dispersión que la del hormigón elaborado exclusivamente con árido natural.

- Ambas fracciones de tamaño (gruesa y fina) de árido reciclado de hormigón aumentaron la deformabilidad térmica del hormigón autocompactante. Esto se tradujo en la necesidad de considerar un coeficiente de dilatación térmica lineal de $1.2 \cdot 10^{-5} \text{ }^\circ\text{C}^{-1}$ para estimar de forma segura la deformabilidad ante cambios de temperatura del hormigón autocompactante elaborado con árido reciclado de hormigón.
- Atendiendo a la interacción del árido reciclado de hormigón con la escoria siderúrgica granulada molida, la adición simultánea de ambos materiales exigió una reducción del contenido de árido grueso, así como un aumento del contenido de conglomerante del hormigón, para conseguir una alta autocompactabilidad sin segregaciones, además de una adecuada resistencia. De ese modo, fue posible mantener la autocompactabilidad de estos hormigones en términos de escurrimiento hasta 60 minutos después de la finalización del proceso de amasado, aunque para ello fue necesario desarrollar un proceso de mezclado por etapas que garantizase una adecuada absorción de agua por parte del árido reciclado de hormigón.
- La menor dureza superficial del hormigón autocompactante y la mayor flexibilidad de los materiales alternativos empleados, en comparación con los materiales convencionales, provocó que tanto el índice de rebote como la velocidad del impulso ultrasónico no permitiesen estimar correctamente la resistencia a compresión de las mezclas elaboradas utilizando las formulaciones clásicas. Sin embargo, un ajuste estadístico basado en un elevado número de determinaciones experimentales permitió desarrollar nuevos modelos para estimar esta resistencia de forma precisa y segura. Con esta nueva formulación propuesta, los métodos de estimación indirecta de la resistencia del hormigón pueden ser también empleados en hormigón autocompactante fabricado con árido reciclado de hormigón y escoria siderúrgica granulada molida.
- El contenido tanto de árido reciclado de hormigón como de escoria siderúrgica granulada molida debe ser estudiado en detalle para evitar daños por fenómenos plásticos transversales bajo cargas cíclicas de compresión de magnitud creciente. Estos daños plásticos transversales se debieron fundamentalmente a una fisuración por hendimiento vertical, así como por la aparición de un abarillamiento (bulging) en la probeta.

Globalmente se demuestra que el empleo de grandes cantidades de árido reciclado de hormigón y de escoria siderúrgica granulada molida permite obtener un hormigón autocompactante con una adecuada conservación temporal de la autocompactabilidad y una correcta resistencia que puede ser evaluada exitosamente de forma indirecta siempre que se realice un diseño adecuado.

PALABRAS CLAVE

Árido reciclado de hormigón; hormigón autocompactante; escoria siderúrgica granulada molida; evolución temporal de la trabajabilidad; resistencia característica; comportamiento plástico; deformabilidad térmica; ensayos no destructivos.

Abstract

Sustainable development is the great challenge of today's society. Both the climate change and the overexploitation of natural resources demand alternative forms of production to the traditional ones in all productive sectors. A greater environmental sustainability, without damaging existing resources and with their responsible consumption, along with a social and economic sustainability, allows achieving this objective.

In recent years, the construction sector has advanced in sustainable development through the use of industrial by-products to replace traditional raw materials in applications such as concrete. The use of these alternative materials increases environmental sustainability by reducing the consumption of natural resources and the carbon footprint. Moreover, the reduced cost of these materials promotes economic sustainability and, if additionally the design of the construction material is adequate, it also contributes to social sustainability. This PhD Thesis, a compendium of seven scientific articles, constitutes an advance in the knowledge of sustainable development and circular economy in the construction sector.

The first article addresses the existing bibliographic shortcomings regarding self-compacting concrete with recycled concrete aggregate. For this purpose, a bibliographic review of 108 references dealing with the development of self-compacting concrete with the aforementioned waste was carried out. A scarcity of studies that evaluated the use of fine recycled concrete aggregate in this type of concrete was observed, as well as the almost non-existent studies concerning its interaction with coarse recycled concrete aggregate and alternative binders. These aspects identified served as the basis for the subsequent experimental work of the PhD Thesis.

The second article, which constitutes the first stage of experimental work of the PhD Thesis together with the third article, aimed to clarify the influence of the simultaneous use of coarse and fine recycled concrete aggregate on the behavior of self-compacting concrete. For this purpose, five self-compacting concretes were produced with 100% coarse recycled concrete aggregate and 0%, 25%, 50%, 75%, and 100% fine recycled concrete aggregate. The different mechanical properties of these mixtures were analyzed at 7, 28 and 90 days. The purpose of this analysis was to clearly establish the effect of each content of fine recycled concrete aggregate. The conclusions established were the basis for the design of the mixes studied in the second phase of this PhD Thesis.

In line with the second article, the third article also studied the mechanical behavior of self-compacting concrete with an almost identical composition. However, this third article presented a statistical approach. Thus, instead of analyzing different mechanical properties, a single property, compressive strength, was evaluated. The compressive-strength testing of a large number of specimens of each concrete mix at each age, allowed a detailed statistical analysis of the effect of the fine recycled concrete aggregate, the prediction of the compressive strength, and the study of the concept of characteristic strength.

The second stage of the PhD Thesis starts in the fourth article. It evaluated the temporal evolution of the self-compactability of concrete mixes made not only with 100% coarse recycled concrete aggregate and a variable content (0%, 50%, and 100%) of fine recycled concrete aggregate, but also ground granulated blast furnace slag (45% of the total amount of binder of the mix). The evaluation over time of the filling capacity, viscosity and passing ability through narrow spaces of these mixes allowed establishing a clear understanding of the feasibility of transporting these mixes over long distances from their production site, once their manufacturing process was completed.

The fifth article addressed, in the same mixes as those designed in the fourth article, an aspect also relevant for a possible generalization of the use of this type of concrete: the indirect estimation of its compressive strength. The peculiarities of the design of this type of concrete affect its surface hardness, *i.e.*, the value of the hammer rebound index obtained. On the other hand, their more uniform composition due to the low coarse aggregate content of self-compacting concrete also affects the ultrasonic pulse velocity. If large quantities of alternative materials are also used, the alteration of these properties can be even greater. Therefore, this paper includes a comprehensive experimental program to statistically analyze the suitability of these indirect measurements for estimating the compressive strength and, therefore, for on-site quality control of the designed concrete mixes.

To complement this second stage of the PhD Thesis, the sixth article analyzed in detail the plastic behavior in the longitudinal and transversal directions of the self-compacting mixes developed. First, self-compacting concretes manufactured with 100% natural aggregate were studied. This aspect was analyzed due to its novelty in the scientific literature and to the almost null existence of scientific publications regarding this issue, mainly in relation to the transversal plastic behavior. Subsequently, the effect of the use of coarse and fine recycled concrete aggregate, as well as ground granulated blast furnace slag, was carefully evaluated. The goal was to characterize in detail the behavior of this type of concrete in order to examine its potential use in real applications under high compressive loads.

This PhD Thesis ends with a letter in which the preliminary results obtained regarding the thermal behavior of self-compacting concrete and the effect of the use of recycled concrete aggregate are collected. With this study, it is also intended to characterize the concrete mixes produced in relation to the thermal stresses that they will experience in service, when structural elements are manufactured with them. In this way, a detailed view of the deformational behavior of these self-compacting concretes and their viability in all types of applications was provided.

From the joint analysis of the results presented in the seven articles included in this PhD Thesis, it is possible to highlight different relevant aspects that should be considered when using coarse and fine recycled concrete aggregate and ground granulated blast furnace slag in self-compacting concrete:

- If coarse recycled concrete aggregate is used in self-compacting concrete, a content equal to 100% is recommended. No statistically significant difference was observed between the mechanical properties of self-compacting concrete produced with 50% or 100% coarse recycled concrete aggregate.
- The use of 25% fine recycled concrete aggregate had no significant effect on the mechanical behavior of self-compacting concrete. The use of 50% fine recycled aggregate allowed obtaining a self-compacting concrete with intermediate mechanical properties. There was also no significant difference between the use of 75% or 100% fine recycled concrete aggregate in the overall decrease of strength and stiffness caused by the use of such high contents of the fine fraction of this aggregate.
- The addition of recycled concrete aggregate caused the characteristic strength of self-compacting concrete to be underestimated by the existing formulation. Maintaining the effective water/cement ratio constant resulted in a probability distribution for the compressive strength of a lower dispersion than that of concrete made exclusively with natural aggregate.
- Both size fractions (coarse and fine) of recycled concrete aggregate increased the thermal deformability of self-compacting concrete. This resulted in the need to consider a linear thermal expansion coefficient of $1.2 \cdot 10^{-5} \text{ } ^\circ\text{C}^{-1}$ to reliably estimate the deformability under temperature variations of self-compacting concrete with recycled concrete aggregate.

- Due to the interaction of recycled concrete aggregate with ground granulated blast furnace slag, the simultaneous addition of both materials required a reduction in the coarse aggregate content as well as an increase in the binder content of concrete in order to achieve high self-compactability without segregation, as well as adequate strength. Thus, it was possible to maintain the self-compactability of these concretes in terms of slump flow up to 60 minutes after the end of the mixing process, although this required the development of a staged mixing process that ensured adequate water absorption by the recycled concrete aggregate.
- The lower surface hardness of self-compacting concrete, and the higher flexibility of the alternative materials compared to conventional ones, provoked that both the hammer rebound index and the ultrasonic pulse velocity did not allow correct estimation of the compressive strength of the mixtures produced through the use of the classical formulation. However, a statistical adjustment based on a large number of experimental determinations enabled the development of new models to accurately and reliably estimate this strength. With this new proposed formulation, the methods for indirect estimation of concrete strength can also be used for self-compacting concrete produced with recycled concrete aggregate and ground granulated blast furnace slag.
- The content of both recycled concrete aggregate and ground granulated blast furnace slag should be studied in detail to avoid damage due to transversal plastic phenomena under cyclic compressive loads of increasing magnitude. This transversal plastic damage was mainly due to vertical-splitting cracking as well as bulging of the specimen.

Overall, it is proved that the use of large quantities of recycled concrete aggregate and ground granulated blast furnace slag allows obtaining a self-compacting concrete with an adequate temporal preservation of its self-compactability and a correct strength that can be successfully evaluated indirectly, as long as an adequate design is performed.

KEYWORDS

Recycled concrete aggregate; self-compacting concrete; ground granulated blast furnace slag; temporal evolution of workability; characteristic strength; plastic behavior; thermal deformability; non-destructive testing.

Table of contents

AGRADECIMIENTOS/ACKNOWLEDGEMENTS

RESUMEN

ABSTRACT

TABLE OF CONTENTS

INTRODUCCIÓN	1
1. Contexto general	1
2. Marco de estudio de la Tesis Doctoral	3
3. Objetivos	4
4. Esquema organizativo y conceptual de la Tesis Doctoral	5
Referencias	9
INTRODUCTION	13
1. General context	13
2. Framework of the Doctoral Thesis Framework of the PhD Thesis	15
3. Objectives	16
4. Organizational and conceptual scheme of the PhD Thesis	17
References	21
ARTICLE 1: <i>Self-compacting concrete manufactured with recycled concrete aggregate: an overview</i>	25
Abstract	25
1. Introduction	25
2. Characterization of Recycled Concrete Aggregate (RCA)	27
3. Self-Compacting Concrete (SCC) reference dosage	27
4. Fresh state performance	28
4.1. Fresh state of SCC with RCA	28
4.2. Fresh state of SCC with RCA and other wastes (fly ash, silica fume, recycled asphalt pavement aggregates, rubber granules, slags)	33
4.3. Fresh state of SCC with RCA and fibers	36
5. Hardened state: mechanical properties	36
5.1. Compressive strength	36

5.1.1. SCC with RCA	36
5.1.2. SCC with RCA and other wastes (fly ash, silica fume, recycled asphalt pavement aggregates, rubber granules, slags)	40
5.1.3. SCC with RCA and fibers	41
5.1.4. Compressive strength conclusions.....	41
5.2. Splitting tensile strength and flexural strength.....	42
5.2.1. SCC with RCA	42
5.2.2. SCC with RCA and other wastes (fly ash, silica fume, recycled asphalt pavement aggregates, rubber granules, slags)	42
5.2.3. SCC with RCA and fibers	43
5.2.4. General conclusions	44
5.3. Modulus of elasticity	44
5.3.1. SCC with RCA	44
5.3.2. SCC with RCA and other wastes (fly ash, silica fume, recycled asphalt pavement aggregates, rubber granules, slags)	44
5.3.3. SCC with RCA and fibers	45
5.4. Volumetric properties and others.....	45
6. Durability	46
6.1. SCC with RCA	47
6.2. SCC with RCA and other wastes (fly ash, silica fume, recycled asphalt pavement aggregates, rubber granules, slags)	47
6.3. SCC with RCA and fibers	48
7. Long-term properties: shrinkage and creep.....	48
7.1. Shrinkage	48
7.2. Creep	49
8. Structural elements. Beams and columns.....	49
9. Other relevant aspects	50
10. Conclusions.....	50
References.....	51
ARTICLE 2: Effect of fine recycled concrete aggregate on the mechanical behavior of self-compacting concrete	57
Abstract	57
1. Introduction.....	57
2. Materials.....	59

2.1. Cement, water, filler and admixtures	59
2.2. Aggregates (RCA, siliceous gravel and siliceous sand)	59
3. Methodology	60
3.1. Experiment design	60
3.2. Mix design	61
3.2.1. Preliminary analysis	61
3.2.2. Mixes with fine RCA	61
3.3. Experimental procedure	62
3.4. Theoretical calculations	63
4. Results and discussion	65
4.1. Fresh properties	65
4.2. Hardened state behavior	67
4.2.1. Density	67
4.2.2. Compressive strength, UPV and hammer rebound index	67
4.2.3. Splitting tensile strength and flexural strength	70
4.2.4. Static modulus of elasticity and Poisson coefficient	72
4.2.5. Stress-strain curves	74
4.2.6. Dynamic modulus of elasticity through the UPV	75
4.2.7. Abrasion resistance	76
4.2.8. Statistical analysis of mechanical properties	77
4.2.9. SEM analysis	78
5. Conclusions	79
References	80
ARTICLE 3: Statistical approach for the design of structural self-compacting concrete with fine recycled concrete aggregate	83
Abstract	83
1. Introduction	84
2. Materials	85
3. Experimental procedure	87
4. In-fresh behavior	88
5. Compressive strength: statistical analysis and strength prediction	90
5.1. Stages of the statistical analysis	90
5.2. Robustness	91

5.3. Normality.....	92
5.4. Confidence intervals.....	93
5.5. Pearson correlations	94
5.6. Effect of age and percentage of fine RCA on compressive strength.....	95
5.7. Compressive strength regression.....	96
5.8. Probability distribution fitting: characteristic strength.....	100
6. Conclusions.....	102
References.....	103
ARTICLE 4: Temporal flowability evolution of slag-based self-compacting concrete with recycled concrete aggregate	107
Abstract	107
1. Introduction.....	107
2. Materials and methods	109
2.1. Materials	109
2.1.1. Binders and admixtures	109
2.1.2. Aggregates.....	110
2.2. Mix design	112
2.3. Experimental plan	114
3. Results and discussion: fresh behavior	114
3.1. Filling ability and viscosity: slump-flow test over time	115
3.1.1. Slump-flow, spreading	115
3.1.2. Viscosity (t_{500})	116
3.1.3. Statistical analysis.....	119
3.1.4. Adjustment model.....	119
3.2. Viscosity: V-funnel test.....	122
3.3. Passing ability: 2-bar L-box test.....	123
3.4. Sieve segregation	124
3.5. Air content.....	125
3.6. Fresh density	126
4. Results and discussion: hardened behavior	127
4.1. Hardened density	127
4.2. Compressive strength.....	128
5. Results and discussion: carbon footprint	129

6. Global overview.....	130
7. Conclusions	130
References.....	131
ARTICLE 5: Models for compressive strength estimation through non-destructive testing of highly self-compacting concrete containing recycled concrete aggregate and slag-based binder	135
Abstract	135
1. Introduction	135
1.1. Novelty of the study.....	138
2. Materials and methods	138
2.1. Materials	138
2.1.1. Cement, water and admixtures	138
2.1.2. Natural and recycled aggregates	139
2.2. Mix design	140
2.3. Experimental procedure	141
2.4. Relationship between indirect measurements and compressive strength in conventional concretes	142
3. Results ad discussion.....	143
3.1. In-fresh performance: slump-flow test.....	143
3.2. Hardened density.....	145
3.3. Compressive strength	146
3.4. Hammer rebound index.....	147
3.4.1. Model of the relationship between the hammer rebound index and compressive strength in conventional concretes	148
3.4.2. Development of a new model for the relationship between the hammer rebound index and compressive strength	149
3.5. UPV	152
3.5.1. Relationship between UPV and density.....	154
3.5.2. Relationship between UPV and compressive strength.....	155
3.6. Joint use of the hammer rebound index and the UPV.....	157
3.7. Validation of the models developed	160
3.8. Use of the models	161
4. Conclusions	161
References.....	162

ARTICLE 6: Assessment of longitudinal and transversal plastic behavior of recycled aggregate self-compacting concrete: a two-way study	167
Abstract	167
1. Introduction.....	167
2. Materials and methods	169
2.1. Materials	169
2.2. Mixes design.....	170
2.3. Mixing and testing.....	172
3. Results and discussion.....	173
3.1. Fresh behavior: slump-flow test.....	173
3.2. Compressive strength and elastic properties.....	174
3.3. Monotonic-load test.....	176
3.3.1. Longitudinal direction	176
3.3.2. Transversal direction.....	179
3.3.3. Relationship between transversal and longitudinal strain levels.....	182
3.3.4. Volumetric variation.....	182
3.4. Loading/unloading test	186
3.4.1. Longitudinal direction	189
3.4.2. Transversal direction.....	193
3.4.3. Relationship between transversal and longitudinal strain	197
4. Conclusions and recommendations	197
References.....	198
ARTICLE 7: Thermal deformability of recycled self-compacting concrete under cyclical temperature variations	203
Abstract	203
1. Introduction.....	203
2. Materials and methods	204
3. Results and discussion.....	204
4. Conclusions.....	206
References.....	206
CONCLUSIONES Y FUTURAS LÍNEAS DE INVESTIGACIÓN	209
1. Conclusiones.....	209
2. Futuras líneas de investigación	211

CONCLUSIONS AND FUTURE RESEARCH LINES	213
1. Conclusions	213
2. Future research lines.....	215
SCIENTIFIC PRODUCTIVITY DURING THE PhD THESIS.....	217
1. Scientific research articles.....	217
2. Book chapters.....	219
3. Teaching innovation articles	220
4. Scientific presentations at national and international congresses and conferences ...	220
5. Teaching innovation presentations at international congresses.....	221
6. Patents	222
7. Stays	223
8. Contracts, knowledge transfer.....	223
8. PhD Thesis funding.....	223

Introducción

La presente Tesis Doctoral se desarrolla por compendio de siete artículos científicos, de modo que, cada uno de ellos es un documento independiente, que puede ser leído y comprendido sin necesidad de los demás. Todos los artículos incluidos responden a la misma necesidad social y se engloban en un mismo campo de investigación, la ciencia de los materiales de construcción. De este modo, cada artículo aborda un aspecto diferente del comportamiento del hormigón autocompactante elaborado con árido reciclado de hormigón y, en algunos casos, escoria siderúrgica granulada molida y materiales de diferente naturaleza para las fracciones finas de árido 0/1 mm o 0/0.5 mm. Por tanto, aunque los artículos pueden tratarse como elementos independientes, todos ellos forman un conjunto cuya lectura permite obtener una visión amplia y completa de la investigación realizada y de los aspectos estudiados.

En esta introducción se incluye la justificación de la investigación llevada a cabo, así como la definición de sus objetivos, novedades e innovación. Además, se muestra el proceso de concepción y desarrollo de los diferentes artículos de la Tesis Doctoral, de modo que se perciba el carácter progresivo de su redacción. Este carácter progresivo hace que cada artículo se base en aspectos recogidos en artículos previos, pudiéndose observar también el propio proceso de aprendizaje del autor a lo largo del periodo de tiempo dedicado a la elaboración de la Tesis Doctoral.

1. CONTEXTO GENERAL

Términos como “cambio climático”, “economía circular” o “sostenibilidad” son cada vez más habituales en cualquier ámbito de nuestra sociedad debido a la necesidad de alcanzar lo que el *Informe Brundtland*, documento más comúnmente conocido como *Nuestro Futuro Común*, denominó en 1987 como desarrollo sostenible [1]. Este concepto hace referencia a la necesidad de que la sociedad sea capaz de satisfacer sus necesidades actuales sin comprometer que las generaciones futuras puedan satisfacer las suyas [2]. Esta frase es breve en su escritura, pero muy amplia en su aplicación, pues abarca los tres ámbitos de la sociedad: el medioambiental, el social y el económico.

- En primer lugar, es necesario alcanzar una sostenibilidad medioambiental, donde los recursos naturales medioambientales no se consideren ilimitados, sino que en su consumo se tenga en cuenta su reposición. Dicho en palabras más sencillas, consumir los recursos al mismo ritmo que se generan y no dañar los ya existentes.
- En segundo lugar, debe conseguirse una sostenibilidad social. Esto implica que todos los miembros de la sociedad vean satisfechas sus necesidades (alimento, vivienda, trabajo, sanidad...) sin perjuicio de los demás.
- Finalmente, la sostenibilidad económica se refiere a que todas las personas deben contar con los recursos económicos necesarios para poder realizar su vida en plenitud.

Estas tres dimensiones están íntimamente ligadas entre sí, y derivan en la idea de una sociedad equitativa, viable y vivible, cuyo esquema conceptual se muestra en la Figura Int.1.

- Una sociedad equitativa es aquella en la que todos sus miembros disponen de los recursos económicos para satisfacer sus necesidades sociales.
- Una sociedad viable es aquella en la que se consigue que todos sus miembros tengan los recursos económicos necesarios consumiendo los recursos naturales a un ritmo adecuado.
- Una sociedad vivible alcanza simultáneamente la sostenibilidad medioambiental y social, de modo que se consigue satisfacer las necesidades sociales de todos los miembros de la sociedad sin sobreexplotar los recursos naturales.

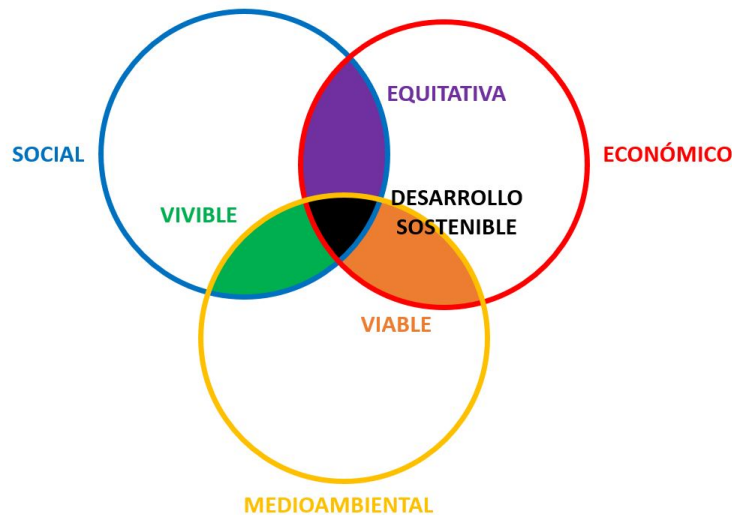


Figura Int.1. Concepto de desarrollo sostenible (Fuente: elaboración propia)

La sociedad que alcance las tres sostenibilidades citadas simultáneamente presentará las sinergias dos a dos y, como consecuencia, conseguirá el desarrollo sostenible. Este concepto, que se ha explicado de forma general en unas pocas líneas, es extremadamente ambicioso, e imposible de alcanzar en su forma ideal. Por este motivo han surgido iniciativas como los 17 Objetivos de Desarrollo Sostenible de la Organización de Naciones Unidas (Figura Int.2), que tratan de simplificar y establecer un camino claro por el que alcanzar una situación lo más próxima posible al desarrollo sostenible [3].



Figura Int.2. Concepto de desarrollo sostenible [3]

La complejidad del propio concepto de desarrollo sostenible, su difícil comprensión, y su laboriosa aplicación hace que el ser humano busque abordarlo aplicando una estrategia de compartimentación. Es habitual que cuando se necesita resolver un problema complejo, su resolución se realice por partes. En el caso que nos ocupa, cada compartimento será un sector productivo de la sociedad en el cual deberán buscarse estrategias para alcanzar la sostenibilidad medioambiental, económica y social, las respectivas sinergias y, finalmente, el desarrollo sostenible. Es aquí donde se puede comenzar a hablar del sector de la construcción.

2. MARCO DE ESTUDIO DE LA TESIS DOCTORAL

El sector de la construcción es uno de los sectores productivos cuyo impacto medioambiental es más elevado. Esta situación se puede observar en la obligatoriedad por ley de realizar un Estudio de Impacto Ambiental en numerosas obras civiles [4], en la elevada huella de carbono que se produce en todas sus actividades [5], o en los grandes impactos medioambientales que se originan durante la fabricación de las materias primas utilizadas para producir los materiales tradicionalmente utilizados en este sector, como el hormigón [6]. Este es un aspecto abordado de forma repetida en la introducción de los diferentes artículos que componen esta Tesis Doctoral, pero hay dos aspectos muy notables en relación con el hormigón, material obtenido al mezclar básicamente cemento, agua y áridos, que conviene destacar:

- Por una parte, durante la fabricación de cada tonelada de cemento Portland ordinario se emite aproximadamente una tonelada de CO₂ a la atmósfera [7]. Si se considera un hormigón con un contenido habitual de 300 kg/m³ de cemento, durante la fabricación de un metro cúbico de hormigón se emiten 300 kg de CO₂ a la atmósfera. Estas emisiones son las mismas que las que emite un coche de gama media que recorre una distancia de aproximadamente 2100 km. Solo en España se producen en torno a 23 millones de metros cúbicos de hormigón al año [8], cuyas emisiones son equivalentes a 23 millones de vehículos que todos los años realizan el trayecto de ida y vuelta desde La Coruña a Málaga pasando por Madrid.
- Por otra parte, entre el 60% y el 70% del volumen del hormigón son áridos [9], los cuales se extraen de canteras y graveras. Los daños medioambientales de este tipo de explotaciones son ampliamente conocidos, como la deforestación, la erosión, la lixiviación y la contaminación de los flujos subterráneos de agua [6]. Teniendo en cuenta las cifras de producción de hormigón anteriores y una densidad del árido de 2.6 Mg/m³, solo en España se consumen para la elaboración de hormigón entre 36 y 42 millones de toneladas de árido al año. Casi una tonelada por habitante y año solo para fabricar hormigón.

Para tratar de aumentar la sostenibilidad medioambiental del sector de la construcción y minimizar estos impactos, a lo largo de este siglo han surgido numerosas líneas de investigación que estudian el efecto de la incorporación de diferentes subproductos industriales o residuos en el hormigón [10, 11]. El objetivo es conocer de forma detallada cómo se comporta el hormigón cuando estos materiales alternativos reemplazan a los materiales tradicionales, es decir, al árido natural y al cemento Portland ordinario. Sin embargo, conseguir una mayor sostenibilidad medioambiental no es suficiente, sino que sería necesario, tal y como se ha dicho anteriormente, alcanzar también tanto una sostenibilidad social como una sostenibilidad económica. Desde el punto de vista social, el material alternativo que se incorpore debe proporcionar al hormigón unas propiedades adecuadas para garantizar su uso en las aplicaciones habituales del sector de la construcción. De este modo, las necesidades sociales cuya resolución corresponde al sector constructivo podrán ser satisfechas, aunque se emplee el material alternativo en cuestión; es decir, se podrá construir la infraestructura o edificio que se necesite. En relación con la sostenibilidad económica, el material alternativo empleado debe, al menos, no encarecer el precio final del hormigón, manteniendo de este modo el equilibrio económico existente en el sector. La incorporación de materiales alternativos en el hormigón, cuando se cumplen estos tres requisitos, promueve el desarrollo sostenible en el sector de la construcción.

Relevantes estudios con el claro objetivo de promover el desarrollo sostenible en el sector de la construcción fueron realizados conjuntamente por investigadores de la Universidad de Burgos y la Universidad del País Vasco hace dos décadas, abordando la incorporación de escoria de horno de arco eléctrico en hormigones como reemplazo del árido natural. Comenzaron su estudio por un hormigón vibrado convencional [12, 13], para posteriormente abordar el desarrollo de hormigones para pavimentos [14, 15] y de hormigones autocompactantes para edificación [16-18].

Recientemente, incluso se han desarrollado hormigones autocompactantes reforzados con fibras [19] y se ha testado su viabilidad en vigas de edificación [20]. Además, en estos estudios se contó con la colaboración de prestigiosos investigadores de la Universidad de Padua [21, 22].

En la década reciente, el grupo de investigación SUCONS de la Universidad de Burgos, junto con investigadores de la Universidad de Cantabria, se inició en la línea de investigación de la reutilización de árido reciclado de hormigón en la fracción gruesa de hormigones autocompactantes, quedando recogidos los primeros resultados en la Tesis Doctoral del Dr. Francisco Fiol [23-25]. La presente Tesis Doctoral avanza en el conocimiento de esta línea de investigación, abordando, en una primera fase, el desarrollo de hormigones autocompactantes fabricados con árido reciclado de hormigón tanto grueso como fino. En una segunda fase, se estudia el comportamiento de estos hormigones cuando este árido se combina con escoria siderúrgica granulada molida, es decir, cuando se utiliza CEM III/A (EN 197-1), y fracciones finas de árido 0/1 mm o 0/0.5 mm de materiales más sostenibles que el filler calizo tradicional. En definitiva, el empleo estos materiales alternativos, de menor coste que los materiales tradicionales, permiten potenciar la sostenibilidad medioambiental y económica. Si además el diseño del hormigón es adecuado y las cantidades empleadas son correctamente ajustadas, su empleo garantizará también la sostenibilidad social del sector de la construcción.

Finalmente, debe destacarse que parte del trabajo llevado a cabo durante el periodo de realización de esta Tesis Doctoral se realizó en el Instituto Superior Técnico (IST) de la Universidad de Lisboa en colaboración con el Prof. Jorge de Brito y el Prof. Luís Evangelista. Su experiencia y reconocido prestigio en el campo del empleo de materiales alternativos en la elaboración del hormigón [26-29] enseñaron al autor de esta Tesis Doctoral que un trabajo de calidad implica necesariamente una alta rigurosidad. El autor espera haber reflejado dichos aspectos en este documento.

3. OBJETIVOS

Se establece como objetivo principal de la presente Tesis Doctoral la caracterización precisa del comportamiento en estado fresco y endurecido del hormigón autocompactante elaborado con árido grueso y fino de hormigón reciclado, el estudio de la interacción de este árido con la escoria siderúrgica granulada molida y con áridos de diferente naturaleza para las fracciones finas 0/1 mm o 0/0.5 mm añadidas para alcanzar la autocompactabilidad y, finalmente, sus consecuencias en el comportamiento del hormigón autocompactante. Sin embargo, esta Tesis Doctoral recoge otros aspectos que permiten identificar una serie de objetivos específicos (OE):

- OE1. Definir las carencias en la bibliografía existente en relación con el estudio del hormigón autocompactante con árido reciclado de hormigón.
- OE2. Establecer pautas del efecto del árido reciclado de hormigón en el hormigón autocompactante a partir de los datos proporcionados por estudios de la bibliografía.
- OE3. Determinar el contenido más adecuado de árido grueso y fino de hormigón reciclado y fino en un hormigón autocompactante.
- OE4. Analizar el concepto de resistencia característica en el hormigón autocompactante elaborado con árido reciclado de hormigón.
- OE5. Definir un proceso de mezcla que permita maximizar la fluidez del hormigón autocompactante con árido reciclado de hormigón a la vez que conservar de forma eficiente su resistencia.
- OE6. Definir una dosificación de hormigón autocompactante de alta fluidez y resistencia con grandes cantidades de árido reciclado grueso y fino, escoria siderúrgica granulada molida y fracciones finas de árido 0/1 mm y 0/0.5 mm de diferentes materiales.
- OE7. Evaluar la viabilidad del transporte a grandes distancias del hormigón autocompactante elaborado con árido reciclado de hormigón, escoria siderúrgica granulada molida y fracciones finas de árido alternativo 0/1 mm o 0/0.5 mm.

- OE8. Mostrar la aplicabilidad de los métodos de ensayo *in situ*, i.e. métodos de ensayo indirecto del hormigón, a las mezclas de alta autocompactabilidad elaboradas con árido reciclado de hormigón y escoria siderúrgica granulada molida.
- OE9. Caracterizar de forma precisa el comportamiento plástico longitudinal y transversal de un hormigón autocompactante elaborado con árido natural, así como el efecto del empleo de árido reciclado de hormigón y de escoria siderúrgica granulada molida.
- OE10. Efectuar una primera aproximación al efecto del árido reciclado de hormigón en la deformabilidad térmica del hormigón autocompactante.

Cada uno de estos objetivos específicos son abordados en uno o varios artículos recogidos en esta Tesis Doctoral. El esquema de desarrollo estos artículos, así como la vinculación entre los artículos y los objetivos establecidos se muestra en el siguiente apartado. Adicionalmente, se proporciona el resumen gráfico (graphical abstract) de cada uno de ellos, el cual sirve como resumen de la temática de cada artículo.

4. ESQUEMA CONCEPTUAL Y ORGANIZATIVO DE LA TESIS DOCTORAL

La presente Tesis Doctoral comienza con una revisión bibliográfica (Figura Int.3) titulada “*Self-compacting concrete manufactured with recycled concrete aggregate: An overview*” (primer artículo) y publicada en *Journal of Cleaner Production* [30]. En este artículo se aborda el estado del arte y las investigaciones realizadas, hasta la fecha de su publicación (marzo de 2020), en hormigón autocompactante elaborado con árido reciclado de hormigón. Su realización permitió detectar la escasa literatura existente en relación con el comportamiento del hormigón autocompactante cuando se incorpora árido reciclado de hormigón en su fracción fina. Esta escasez de estudios era aún mayor cuando el hormigón elaborado era de alta autocompactabilidad (clase de escurrimiento SF3, escurrimiento entre 750 mm y 850 mm) [31] y cuando el árido fino de hormigón reciclado se combinaba con conglomerantes alternativos al cemento Portland ordinario como la escoria siderúrgica granulada molida. Además, esta revisión bibliográfica permitió detectar la ausencia de una tendencia clara del efecto del árido reciclado de hormigón en la resistencia a compresión del hormigón autocompactante. El equilibrio que se necesita entre todos sus componentes para alcanzar la autocompactabilidad justifica estos resultados.

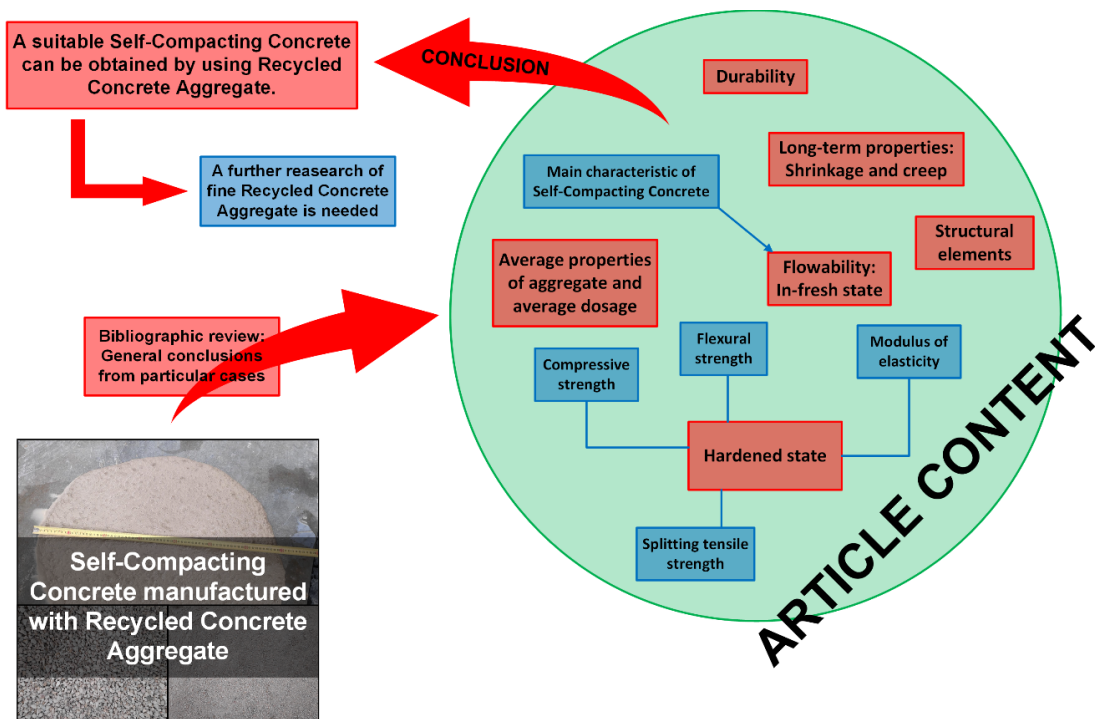


Figura Int.3. Resumen gráfico del primer artículo

“Effect of fine recycled concrete aggregate on the mechanical behavior of self-compacting concrete” es el segundo artículo de esta Tesis Doctoral (Figura Int.4), publicado en *Construction and Building Materials* [32]. Esta publicación pretende arrojar luz sobre el comportamiento del hormigón autocompactante fabricado con árido reciclado fino en hormigones autocompactantes de clase de escurrimiento SF2 (escurrimiento entre 650 mm y 750 mm) [31]. Para ello, en primer lugar, se definió la dosificación base del hormigón autocompactante utilizado en el proceso experimental de esta Tesis Doctoral y se determinó, en base al comportamiento mecánico del hormigón, que el contenido de árido grueso de hormigón reciclado más adecuado para el estudio era un 100%. Posteriormente, se estudió el comportamiento mecánico del hormigón autocompactante a tres edades de curado diferentes (7, 28 y 90 días) añadiéndose un 100% de árido reciclado de hormigón en la fracción gruesa y un 0%, 25%, 50%, 75% o 100% en la fracción fina. Se encontró que los hormigones elaborados se podían clasificar en tres grupos de acuerdo con su comportamiento mecánico en función de su contenido de árido fino de hormigón reciclado: 0-25%, 50%, y 75-100%.

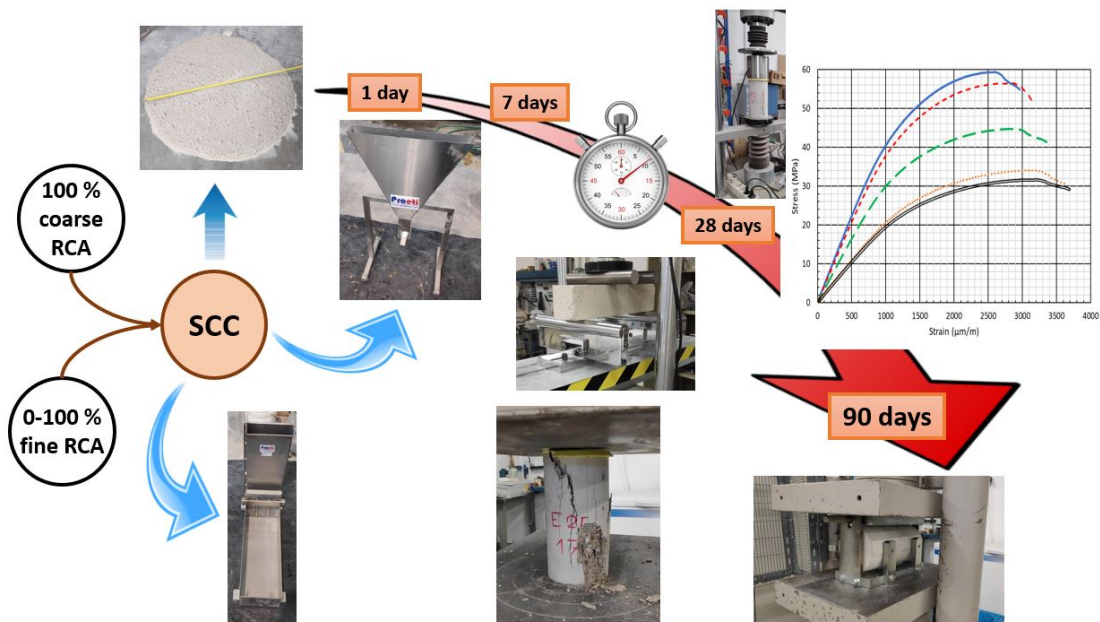


Figura Int.4. Resumen gráfico del segundo artículo

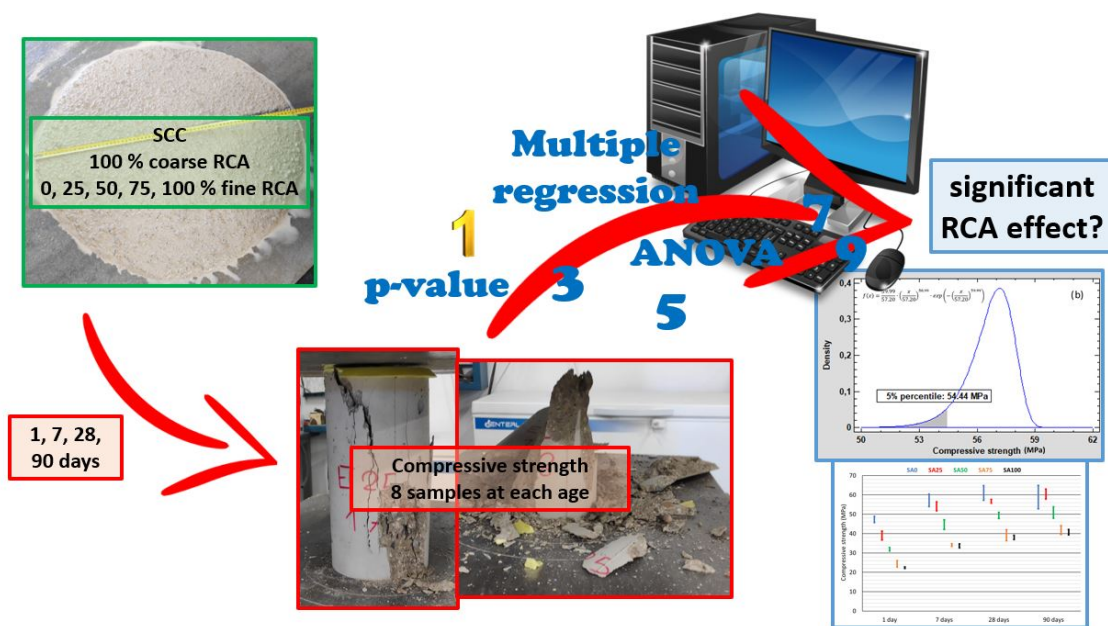


Figura Int.5. Resumen gráfico del tercer artículo

“Statistical approach for the design of structural self-compacting concrete with fine recycled concrete aggregate” (tercer artículo, Figura Int.5), publicado en *Mathematics*, mantiene la misma línea de investigación del segundo artículo [33]. En este documento se describió la elaboración de unos hormigones con una composición similar a los del segundo artículo, pero con una modificación en su proceso de elaboración para tratar de mejorar la autocompactabilidad. Además, se propuso un análisis estadístico de la resistencia a compresión de dichos hormigones, el cual permitió determinar que esta resistencia se encontraba más condicionada por el contenido de árido fino de hormigón reciclado que por la edad. Además, se observó la necesidad de readaptar la forma de calcular la resistencia característica al incorporar este material al hormigón autocompactante.

“Temporal flowability evolution of slag-based self-compacting concrete with recycled concrete aggregate” (cuarto artículo, Figura Int.6) [34] y “Models for compressive strength estimation through non-destructive testing of highly self-compacting concrete containing recycled concrete aggregate and slag-based binder” (quinto artículo, Figura Int.7) [35], publicados en *Journal of Cleaner Production* y *Construction and Building Materials*, respectivamente, forman parte de la segunda etapa de investigación de la presente Tesis Doctoral. En ambos se detalló la composición y el proceso de mezcla necesarios para la obtención de un hormigón autocompactante de clase de escurrimiento SF3 [31] elaborado con un 100% de árido grueso de hormigón reciclado, árido fino de hormigón reciclado, conglomerante a base de escoria siderúrgica granulada molida, y varias fracciones finas de árido 0/1 mm o 0/0.5 mm de naturaleza o características diferentes al filler calizo tradicional. Puede observarse que se abordan simultáneamente las tres carencias en la literatura existente detectadas en el primer artículo. Además, de acuerdo con los resultados del segundo artículo, el contenido de árido fino de hormigón reciclado se definió en un 0%, un 50% o un 100%. A través del cuarto artículo se validó la posibilidad de transportar el hormigón autocompactante elaborado a un punto situado a 60 minutos de la planta de fabricación. En el quinto artículo se reflejó la posibilidad de estimar de forma indirecta la resistencia a compresión de este tipo de hormigón si los modelos existentes se adaptan a él, ya que su comportamiento se encuentra condicionado por el bajo contenido de árido grueso y la mayor flexibilidad del árido reciclado de hormigón en comparación con el árido calizo o silíceo tradicional. La validez de las medidas indirectas muestra la posibilidad de efectuar un eficiente control *in situ* de este tipo de mezclas, al igual que se realiza con el hormigón vibrado convencional en una obra real.

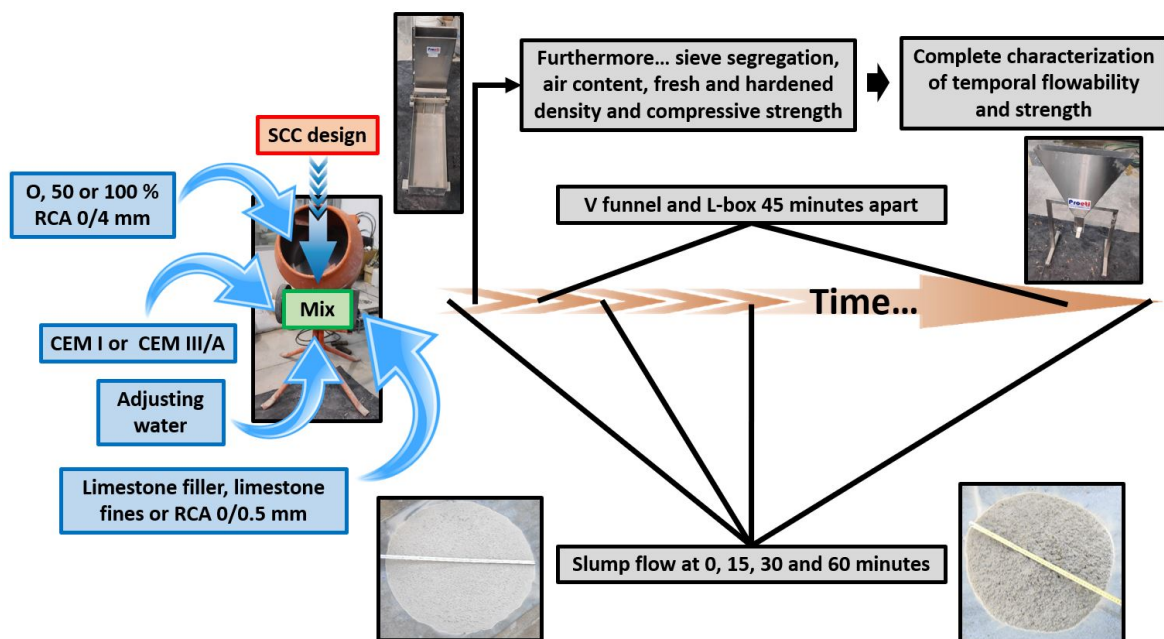


Figura Int.6. Resumen gráfico del cuarto artículo

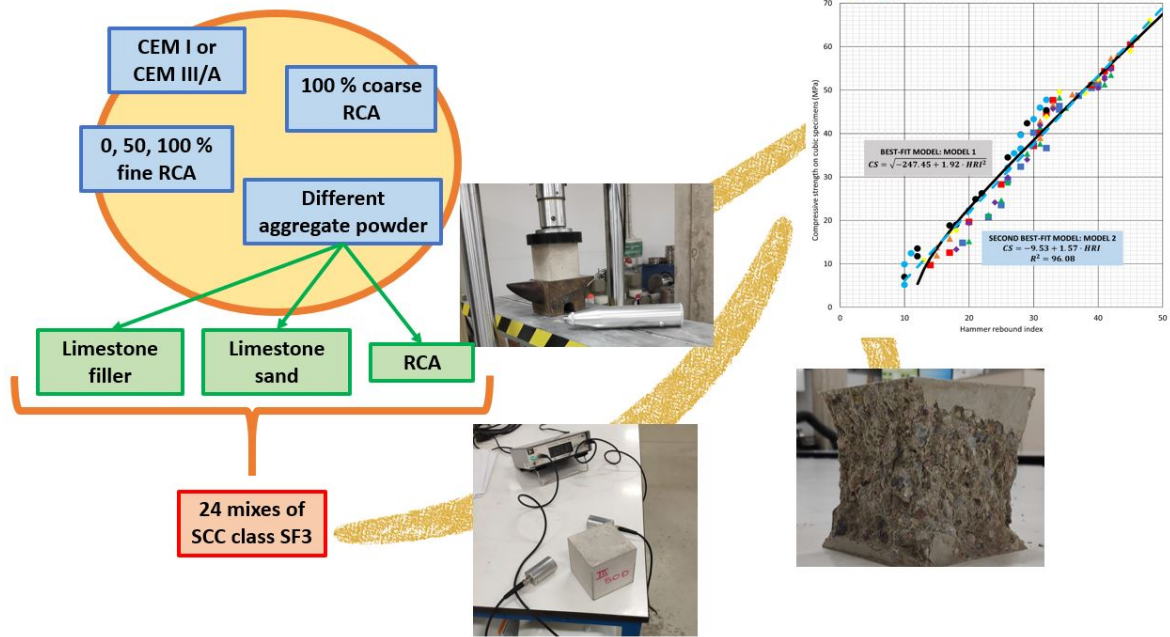


Figura Int.7. Resumen gráfico del quinto artículo

El sexto artículo (Figura Int.8), titulado “*Assessment of longitudinal and transversal plastic behavior of recycled aggregate self-compacting concrete: A two-way study*” y publicado en *Construction and Building Materials* [36], es, desde el punto de vista del autor, el más novedoso de todos ellos. Su objetivo no se limitó a aspectos concretos del árido reciclado de hormigón, sino que tiene un objetivo mucho más amplio, como fue describir el comportamiento plástico transversal de un hormigón autocompactante sin ningún tipo de confinamiento. La influencia de la adición de un 100% de árido grueso de hormigón reciclado y de un 0%, 50% o 100% de árido fino de hormigón reciclado también fue estudiada en detalle.

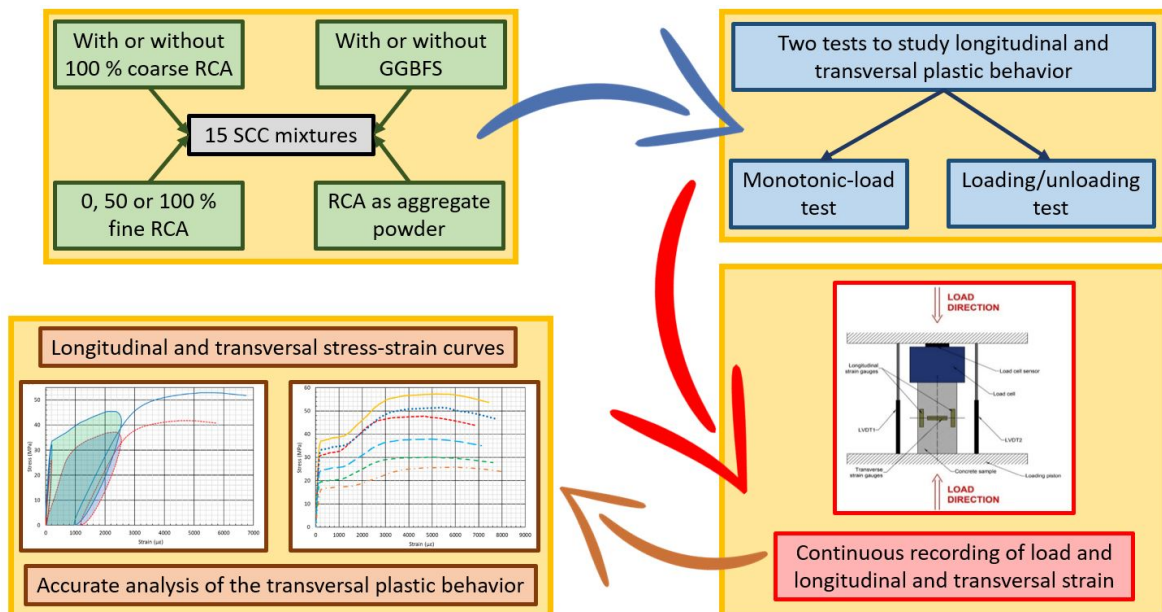


Figura Int.8. Resumen gráfico del sexto artículo

La Tesis Doctoral finaliza con un artículo corto titulado “*Thermal deformability of recycled self-compacting concrete under cyclical temperature variations*” (séptimo artículo, Figura Int.9), publicado en *Materials Letters* [37]. En él se proporcionan unos breves apuntes de la influencia del

empleo de ambas fracciones, gruesa y fina, de árido reciclado de hormigón en la deformabilidad térmica del hormigón autocompactante, mostrando la necesidad, en principio, de adoptar un valor de $1.2 \cdot 10^{-5} \text{ } ^\circ\text{C}^{-1}$ como coeficiente de dilatación térmica en este tipo de hormigones.

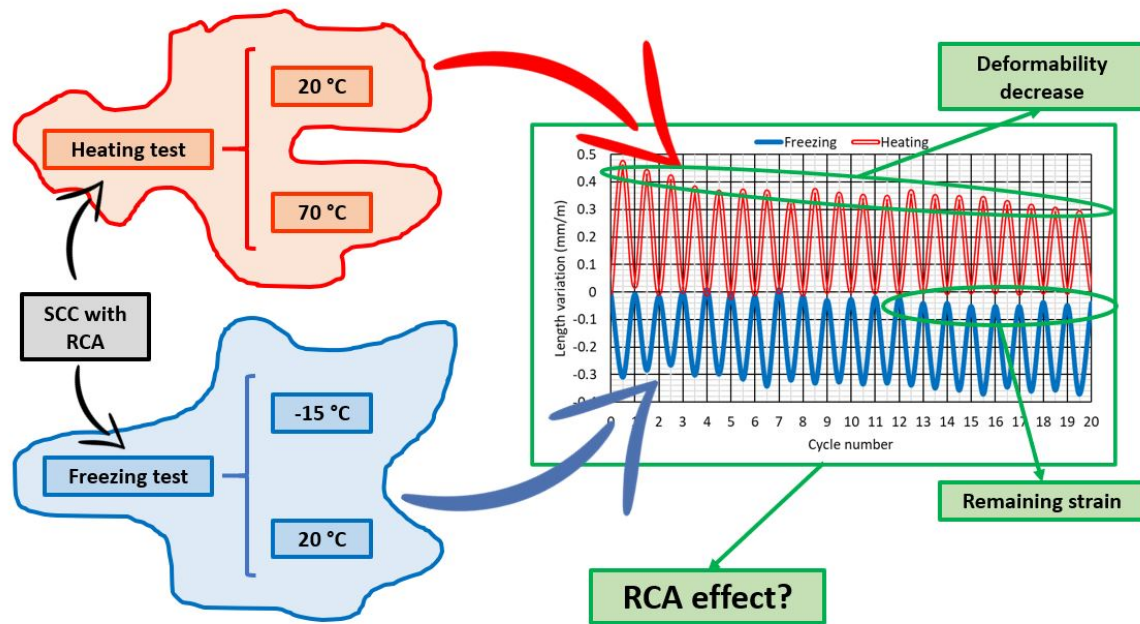


Figura Int.9. Resumen gráfico del séptimo artículo

La Figura Int.10 muestra un esquema conceptual en el que se detalla el desarrollo de los artículos y los objetivos específicos abordados en cada uno de ellos.

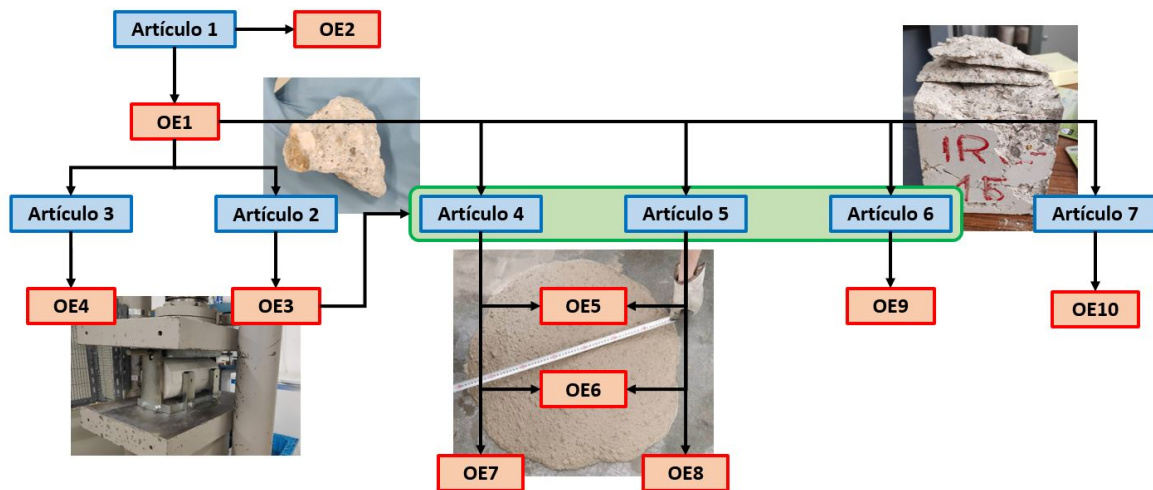


Figura Int.10. Esquema conceptual y organizativo de la Tesis Doctoral

REFERENCIAS

- [1] T. Hák, S. Janoušková, B. Moldan, A.L. Dahl, Closing the sustainability gap: 30 years after “Our Common Future” society lacks meaningful stories and relevant indicators to make the right decisions and build public support, *Ecol. Indic.* 87 (2018) 193-195.
- [2] J. Mistry, C. Tschirhart, C. Verwer, R. Glastra, O. Davis, D. Jafferally, L. Haynes, R. Benjamin, G. Albert, R. Xavier, I. Bovolo, A. Berardi, Our common future? Cross-scalar scenario analysis for social-ecological sustainability of the Guiana Shield, South America, *Environ. Sci. Policy* 44 (2014) 126-148.
- [3] United Nations (UN), Sustainable development goals (<https://sdgs.un.org/es/goals>) (2015).
- [4] Government of Spain, Law 21/2013, of December 9, on environmental assessment (2013).

- [5] F. Pomponi, A. Stephan, Water, energy, and carbon dioxide footprints of the construction sector: A case study on developed and developing economies, *Water Res.* 194 (2021) 116935.
- [6] M.U. Hossain, C.S. Poon, I.M.C. Lo, J.C.P. Cheng, Comparative environmental evaluation of aggregate production from recycled waste materials and virgin sources by LCA, *Resour. Conserv. Recycl.* 109 (2016) 67-77.
- [7] R. Maddalena, J.J. Roberts, A. Hamilton, Can Portland cement be replaced by low-carbon alternative materials? A study on the thermal properties and carbon emissions of innovative cements, *J. Clean Prod.* 186 (2018) 933-942.
- [8] ERMCO, Ready-mixed concrete industry statistics, European Ready-Mixed Concrete Organization (2019).
- [9] ANEFA, Sectorial economic progress reports (2019).
- [10] M. Behera, S.K. Bhattacharyya, A.K. Minocha, R. Deoliya, S. Maiti, Recycled aggregate from C&D waste & its use in concrete - A breakthrough towards sustainability in construction sector: A review, *Constr. Build. Mater.* 68 (2014) 501-516.
- [11] M. Sandanayake, G. Zhang, S. Setunge, Estimation of environmental emissions and impacts of building construction - A decision making tool for contractors, *J. Build. Eng.* 21 (2019) 173-185.
- [12] J.M. Manso, D. Hernández, M.M. Losáñez, J.J. González, Design and elaboration of concrete mixtures using steelmaking slags, *ACI Mater. J.* 108 (6) (2011) 673-681.
- [13] J.M. Manso, J.J. Gonzalez, J.A. Polanco, Electric arc furnace slag in concrete, *J. Mater. Civ. Eng.* 16 (6) (2004) 639-645.
- [14] J.A. Fuente-Alonso, V. Ortega-López, M. Skaf, Á. Aragón, J.T. San-José, Performance of fiber-reinforced EAF slag concrete for use in pavements, *Constr. Build. Mater.* 149 (2017) 629-638.
- [15] V. Ortega-López, J.A. Fuente-Alonso, A. Santamaría, J.T. San-José, Á. Aragón, Durability studies on fiber-reinforced EAF slag concrete for pavements, *Constr. Build. Mater.* 163 (2018) 471-481.
- [16] A. Santamaría, A. Orbe, M.M. Losañez, M. Skaf, V. Ortega-Lopez, J.J. González, Self-compacting concrete incorporating electric arc-furnace steelmaking slag as aggregate, *Mater. Des.* 115 (2017) 179-193.
- [17] A. Santamaría, A. Orbe, J.T. San José, J.J. González, A study on the durability of structural concrete incorporating electric steelmaking slags, *Constr. Build. Mater.* 161 (2018) 94-111.
- [18] A. Santamaría, V. Ortega-López, M. Skaf, J.A. Chica, J.M. Manso, The study of properties and behavior of self compacting concrete containing Electric Arc Furnace Slag (EAFS) as aggregate, *Ain Shams Eng. J.* 11 (1) (2020) 231-243.
- [19] V. Ortega-López, A. García-Llona, V. Revilla-Cuesta, A. Santamaría, J.T. San-José, Fiber-reinforcement and its effects on the mechanical properties of high-workability concretes manufactured with slag as aggregate and binder, *J. Build. Eng.* 43 (2021) 102548.
- [20] A. Santamaría, A. García-Llona, V. Revilla-Cuesta, I. Piñero, V. Ortega-López, Bending tests on building beams containing electric arc furnace slag and alternative binders and manufactured with energy-saving placement techniques, *Structures* 32 (2021) 1921-1933.
- [21] A. Santamaria, F. Faleschini, G. Giacomello, K. Brunelli, J.T. San José, C. Pellegrino, M. Pasetto, Dimensional stability of electric arc furnace slag in civil engineering applications, *J. Clean. Prod.* 205 (2018) 599-609.
- [22] F. Faleschini, A. Santamaria, M.A. Zanini, J.T. San José, C. Pellegrino, Bond between steel reinforcement bars and electric arc furnace slag concrete, *Mater. Struct.* 50 (3) (2017) 170.
- [23] F. Fiol, C. Thomas, C. Muñoz, V. Ortega-López, J.M. Manso, The influence of recycled aggregates from precast elements on the mechanical properties of structural self-compacting concrete, *Constr. Build. Mater.* 182 (2018) 309-323.
- [24] F. Fiol, C. Thomas, J.M. Manso, I. López, Influence of recycled precast concrete aggregate on durability of concrete's physical processes, *Appl. Sci.* 10 (20) (2020) 7348.
- [25] F. Fiol, C. Thomas, J.M. Manso, I. López, Transport mechanisms as indicators of the durability of precast recycled concrete, *Constr. Build. Mater.* 269 (2021) 121263.

- [26] L. Evangelista, M. Guedes, J. De Brito, A.C. Ferro, M.F. Pereira, Physical, chemical and mineralogical properties of fine recycled aggregates made from concrete waste, *Constr. Build. Mater.* 86 (2015) 178-188.
- [27] L. Evangelista, J. De Brito, Concrete with fine recycled aggregates: A review, *Eur. J. Environ. Civ. Eng.* 18 (2) (2014) 129-172.
- [28] L. Evangelista, J. de Brito, Durability performance of concrete made with fine recycled concrete aggregates, *Cem. Concr. Compos.* 32 (1) (2010) 9-14.
- [29] L. Evangelista, J. de Brito, Mechanical behaviour of concrete made with fine recycled concrete aggregates, *Cem. Concr. Compos.* 29 (5) (2007) 397-401.
- [30] V. Revilla-Cuesta, M. Skaf, F. Faleschini, J.M. Manso, V. Ortega-López, Self-compacting concrete manufactured with recycled concrete aggregate: An overview, *J. Clean. Prod.* 262 (2020) 121362.
- [31] EFNARC, Specification Guidelines for Self-compacting Concrete, European Federation of National Associations Representing producers and applicators of specialist building products for Concrete (2002).
- [32] V. Revilla-Cuesta, V. Ortega-López, M. Skaf, J.M. Manso, Effect of fine recycled concrete aggregate on the mechanical behavior of self-compacting concrete, *Constr. Build. Mater.* 263 (2020) 120671.
- [33] V. Revilla-Cuesta, M. Skaf, A.B. Espinosa, A. Santamaría, V. Ortega-López, Statistical approach for the design of structural self-compacting concrete with fine recycled concrete aggregate, *Mathematics* 8 (12) (2020) 2190.
- [34] V. Revilla-Cuesta, M. Skaf, A. Santamaría, J.J. Hernández-Bagaces, V. Ortega-López, Temporal flowability evolution of slag-based self-compacting concrete with recycled concrete aggregate, *J. Clean. Prod.* 299 (2021) 126890.
- [35] V. Revilla-Cuesta, M. Skaf, R. Serrano-López, V. Ortega-López, Models for compressive strength estimation through non-destructive testing of highly self-compacting concrete containing recycled concrete aggregate and slag-based binder, *Constr. Build. Mater.* 280 (2021) 122454.
- [36] V. Revilla-Cuesta, M. Skaf, A. Santamaría, V. Ortega-López, J.M. Manso, Assessment of longitudinal and transversal plastic behavior of recycled aggregate self-compacting concrete: A two-way study *Constr. Build. Mater.* 292 (2021) 123426.
- [37] V. Revilla-Cuesta, M. Skaf, J.A. Chica, J.A. Fuente-Alonso, V. Ortega-López, Thermal deformability of recycled self-compacting concrete under cyclical temperature variations, *Mater. Lett.* 278 (2020) 128417.

Introduction

This PhD Thesis is a compendium of seven scientific articles, so that each one is an independent document that can be read and understood without the others. All these articles address the same social need and are included in the same field of research, the science of construction materials. Thus, each article deals with a different aspect of the behavior of self-compacting concrete manufactured with recycled concrete aggregate and, in some cases, ground granulated blast furnace slag, and aggregate fines 0/1 mm or 0/0.5 mm of different nature. Therefore, although the articles can be considered independent elements, all of them constitute a set whose reading allows obtaining a wide and complete overview of the research carried out and of the aspects studied.

This introduction includes the justification of the research conducted, as well as the definition of its objectives, novelties and innovation. In addition, the process of conception and development of the different articles of the PhD Thesis is shown, so that the progressive character during its writing can be perceived. This progressive nature leads each article to be based on aspects collected in previous articles. Furthermore, the author's own learning process throughout the time spent on the preparation of his PhD Thesis can also be observed.

1. GENERAL CONTEXT

Terms such as "*climate change*", "*circular economy*" or "*sustainability*" are becoming more and more common in any area of our society due to the need to achieve what the *Brundtland Report*, a document more commonly known as *Our Common Future*, referred to in 1987 as sustainable development [1]. This concept refers to the need for society to be able to meet its present needs without compromising the ability of future generations to meet theirs [2]. This sentence is brief in its wording, but very broad in its application, since it covers the three spheres of society: environmental, social and economic.

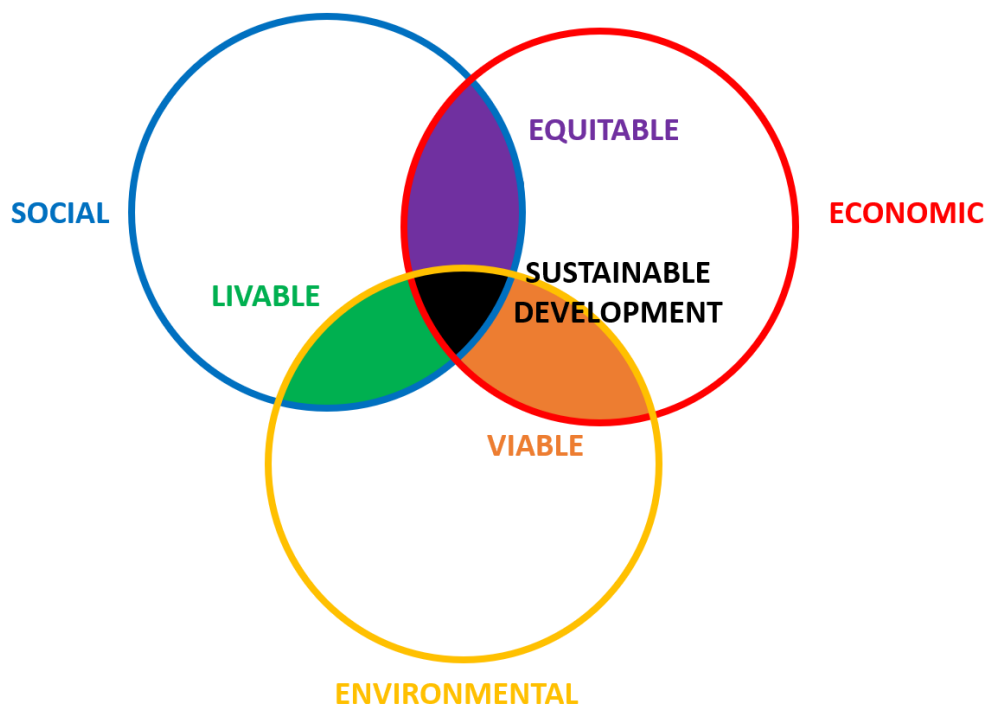


Figure Int.1. Concept of sustainable development (Source: prepared by the author)

- Firstly, it is necessary to achieve environmental sustainability, in which natural resources are not considered unlimited, but in which their consumption considers their replenishment. Put more simply, consuming resources at the same rate at which they are generated and not damaging the existing ones.
- Secondly, social sustainability has to be reached. This implies that all members of society have their needs met (food, housing, work, health...) without detriment to others.
- Finally, economic sustainability refers to the fact that all people must have the necessary economic resources to be able to live their lives to the fullest.

These three dimensions are closely linked to each other, and derive in the idea of an equitable, viable and livable society, whose conceptual scheme is shown in Figure Int.1.

- An equitable society is that society in which all its members have the economic resources to satisfy their social needs.
- A viable society is one in which all its members have the necessary economic resources while consuming natural resources at an adequate rate.
- A livable society simultaneously achieves environmental and social sustainability, so that the social needs of all members are met without overexploiting natural resources.

The society that achieves the three aforementioned sustainability issues simultaneously will have the synergies two by two and, as a consequence, will achieve sustainable development. This concept, which has been explained in general terms in a few lines, is extremely ambitious and impossible to achieve in its ideal form. For this reason, initiatives such as the 17 Sustainable Development Goals of the United Nations have emerged (Figure Int.2), which seek to simplify and establish a clear path to achieve a situation as close as possible to sustainable development [3].



Figure Int.2. Concept of sustainable development [3]

The complexity of the concept of sustainable development itself, its difficult understanding, and its laborious implementation, has led human beings to seek to approach it by applying a compartmentalization strategy. It is usual that when a complex problem needs to be solved, it is resolved by parts. In this case, each compartment will be a productive sector of society in which strategies must be sought to achieve environmental, economic and social sustainability, the

respective synergies and, finally, sustainable development. This is the point at which we can begin to talk about the construction sector.

2. FRAMEWORK OF THE PhD THESIS

The construction sector is one of the productive sectors with the highest environmental impact. This situation can be observed in the obligation by law to carry out an Environmental Impact Study in many civil works [4], in the high carbon footprint that is produced in all its activities [5], or in the major environmental impacts that arise during the production of raw materials used to produce the materials traditionally used in this sector, such as concrete [6]. This is an aspect repeatedly addressed in the introduction of the different articles that compose this PhD Thesis, but there are two very notable aspects regarding concrete, a material obtained by mixing cement, water and aggregates, that should be emphasized:

- On the one hand, approximately one ton of CO₂ is emitted into the atmosphere during the manufacture of each ton of ordinary Portland cement [7]. Considering a concrete with a typical cement content of 300 kg/m³, 300 kg of CO₂ are emitted into the atmosphere during the production of one cubic meter of concrete. These emissions are the same as those emitted by a mid-range car traveling a distance of approximately 2,100 km. In Spain alone, around 23 million cubic meters of concrete are produced every year [8], whose emissions are equivalent to 23 million vehicles that every year make the round trip from La Coruña to Malaga via Madrid.
- On the other hand, between 60% and 70% of the volume of concrete is aggregate [9], which are extracted from quarries and gravel pits. The environmental damages caused by this type of mining are well known, such as deforestation, erosion, leaching, and contamination of groundwater flows [6]. Considering the above concrete production figures and an aggregate density of 2.6 Mg/m³, Spain alone consumes between 36 and 42 million tons of aggregate per year for the production of concrete. Almost one ton per inhabitant per year just to manufacture concrete.

To try to increase the environmental sustainability of the construction sector and minimize these impacts, throughout this century numerous research lines have emerged, which have studied the effect of incorporating different industrial by-products or wastes in concrete [10, 11]. The objective is to know in detail how concrete performs when these alternative materials replace traditional ones, *i.e.*, natural aggregate and ordinary Portland cement. However, achieving greater environmental sustainability is not enough; it would be necessary, as mentioned above, to also achieve both social and economic sustainability. From the social point of view, the alternative material should provide concrete with adequate mechanical and durability properties to ensure its use in the common applications of the construction sector. In this way, the social needs whose resolution corresponds to the construction sector can be satisfied even if the alternative material is used; *i.e.*, it will be possible to build any necessary infrastructure or building. Regarding economic sustainability, the alternative material used should, at least, not increase the final price of concrete, thus maintaining the existing economic balance in the sector. The incorporation of alternative materials in concrete, when these three requirements are met, promotes sustainable development in the construction sector.

Relevant studies with the clear goal of promoting sustainable development in the construction sector were carried out jointly by researchers from the University of Burgos and the University of the Basque Country two decades ago, which addressed the incorporation of electric arc furnace slag in concrete as replacement for natural aggregate. They began their study with conventional vibrated concrete [12, 13], to subsequently address the development of concretes for pavements [14, 15] and building self-compacting concretes [16-18]. Recently, even fiber-reinforced self-compacting concretes have been developed [19] and the feasibility of these concretes in building

beams has been tested [20]. In addition, prestigious researchers from the University of Padua have collaborated on these projects [21, 22].

In the recent decade, the SUCONS research group from the University of Burgos, in collaboration with researchers from the University of Cantabria, started a line of research on the reuse of recycled concrete aggregate in the coarse fraction of self-compacting concretes, whose first results were presented in the PhD Thesis of Dr. Francisco Fiol [23-25]. This PhD Thesis advances in the knowledge of this research line, addressing, in a first stage, the development of self-compacting concretes manufactured with both coarse and fine recycled concrete aggregate. In a second stage, the behavior of these concretes is studied when this aggregate is combined with ground granulated blast furnace slag, that is, when using CEM III/A (EN 197-1), and aggregate fines 0/1 mm or 0/0.5 mm more sustainable than conventional limestone filler. In short, the use of these alternative materials, with lower cost than traditional materials, can enhance environmental and economic sustainability. If the design of concrete is also adequate and the used quantities of these alternative materials are correctly adjusted, their use will also guarantee the social sustainability of the construction sector.

Finally, it should be noted that part of the work performed during this PhD Thesis was carried out at the Instituto Superior Técnico (IST) of the University of Lisbon in collaboration with Prof. Jorge de Brito and Prof. Luís Evangelista. Their experience and recognized prestige in the field of using alternative materials in the production of concrete [26-29] taught the author of this PhD Thesis that quality work necessarily implies a high level of rigor. The author hopes to have reflected these aspects in his PhD Thesis document.

3. OBJECTIVES

The main objective of this PhD Thesis is the accurate characterization of the fresh and hardened behavior of self-compacting concrete prepared with coarse and fine recycled concrete aggregate, the study of the interaction of this aggregate with ground granulated blast furnace slag and with aggregate fines 0/1 mm and 0/0.5 mm of different nature, whose addition allow reaching self-compactability. However, this PhD Thesis collects other aspects that allow identifying a series of specific objectives (SO):

- SO1. Defining the gaps in the existing literature related to the study of self-compacting concrete with recycled concrete aggregate.
- SO2. Establishing guidelines for the effect of recycled concrete aggregate on the performance of self-compacting concrete based on data from the literature.
- SO3. Determining the most appropriate content of coarse and fine recycled concrete aggregate in a self-compacting concrete.
- SO4. Analyzing the concept of characteristic strength in self-compacting concrete produced with recycled concrete aggregate.
- SO5. Defining a mixing process that maximizes the flowability of self-compacting concrete with recycled concrete aggregate while efficiently preserving its strength.
- SO6. Defining a dosage of concrete of high flowability and strength with large quantities of coarse and fine recycled aggregate, ground granulated blast furnace slag and aggregate fines 0/1 mm and 0/0.5 mm of different nature.
- SO7. Evaluating the feasibility of long-distance transport of self-compacting concrete made with recycled concrete aggregate, ground granulated blast furnace slag and aggregate fines 0/1 mm or 0/0.5 mm of different nature.
- SO8. Demonstrating the applicability of *in situ* testing methods, *i.e.*, indirect concrete testing, in concrete mixtures with high self-compactability produced with recycled concrete aggregate and ground granulated blast furnace slag.

- SO9. Accurately characterizing the longitudinal and transversal plastic behavior of self-compacting concrete produced with natural aggregate, as well as defining the effect of using recycled concrete aggregate and ground granulated blast furnace slag.
- SO10. Performing a first approximation of the effect of recycled concrete aggregate on the thermal deformability of self-compacting concrete.

Each specific objective is addressed in one or more of the articles included in this PhD Thesis. The outline of the development process of these articles, as well as the link between the articles and the established objectives is shown in the following section. Additionally, the graphical abstract of each article is provided, which serves as summary of the subject matter of each of them.

4. ORGANIZATIONAL AND CONCEPTUAL SCHEME OF THE PhD THESIS

This PhD Thesis starts with a literature review (Figure Int.3) entitled "*Self-compacting concrete manufactured with recycled concrete aggregate: An overview*" (first article) and published in *Journal of Cleaner Production* [30]. This article addresses the state of the art and research, carried out up to the date of publication (March 2020), on self-compacting concrete manufactured with recycled concrete aggregate. Its preparation allowed detecting the scarce existing literature about the behavior of self-compacting concrete when fine recycled concrete aggregate is added. This scarcity of studies was even greater when the concrete produced was of high self-compactability (slump-flow class SF3, slump flow between 750 mm and 850 mm) [31] and when the fine recycled concrete aggregate was combined with binders alternative to ordinary Portland cement such as ground granulated blast furnace slag. In addition, this literature review detected the absence of a clear trend of the effect of recycled concrete aggregate on the compressive strength of self-compacting concrete. The careful balance required between all its components to achieve self-compactability explains these results.

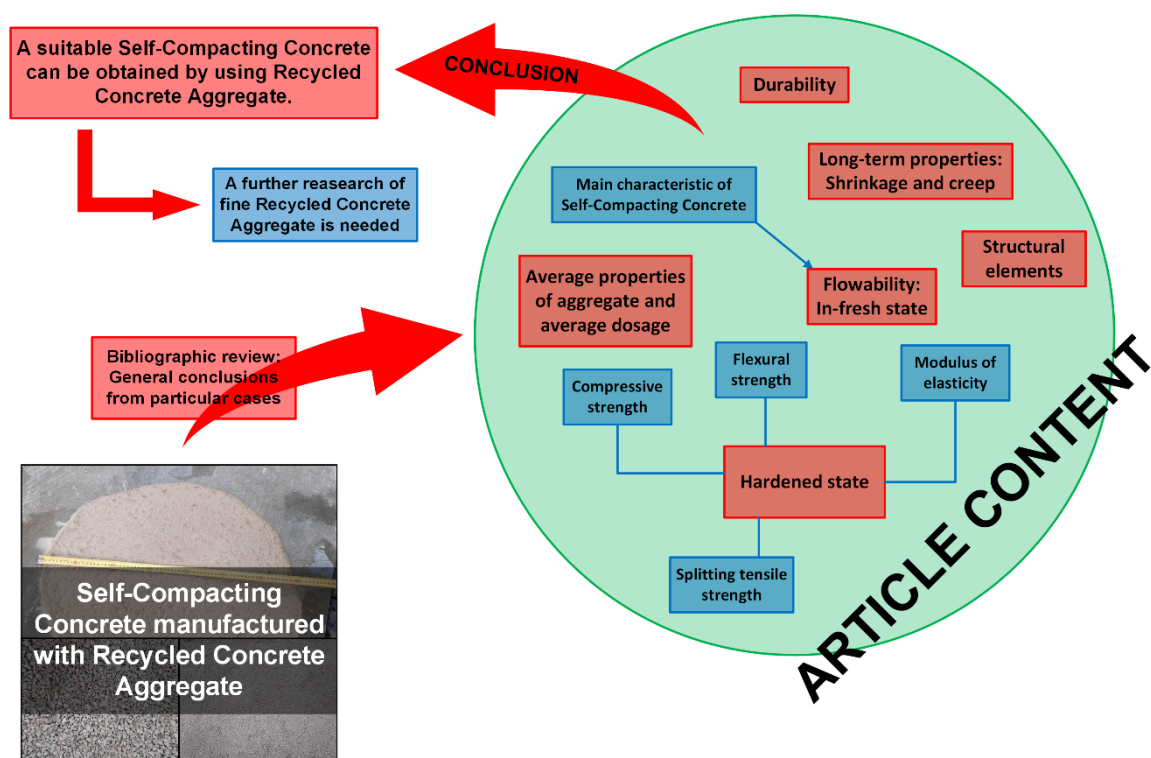


Figure Int.3. Graphical abstract, first article

"*Effect of fine recycled concrete aggregate on the mechanical behavior of self-compacting concrete*" is the second article of this PhD Thesis (Figure Int.4), published in *Construction and Building Materials* [32]. This publication aims to clarify the behavior of self-compacting concrete made with

fine recycled concrete aggregate in self-compacting concrete mixtures of slump-flow class SF2 (slump flow between 650 mm and 750 mm) [31]. For this purpose, first, the basic dosage for self-compacting concrete used in the experimental work of this PhD Thesis was defined and it was determined, based on the mechanical behavior of concrete, that the most suitable content of coarse recycled concrete aggregate for the study was 100%. Subsequently, the mechanical behavior of self-compacting concrete was studied at three different curing ages (7, 28, and 90 days) by adding 100% recycled concrete aggregate in the coarse fraction and 0%, 25%, 50%, 75% or 100% in the fine fraction. It was found that the concretes produced could be classified into three groups according to their mechanical behavior based on their content of fine recycled concrete aggregate: 0-25%, 50%, and 75-100%.

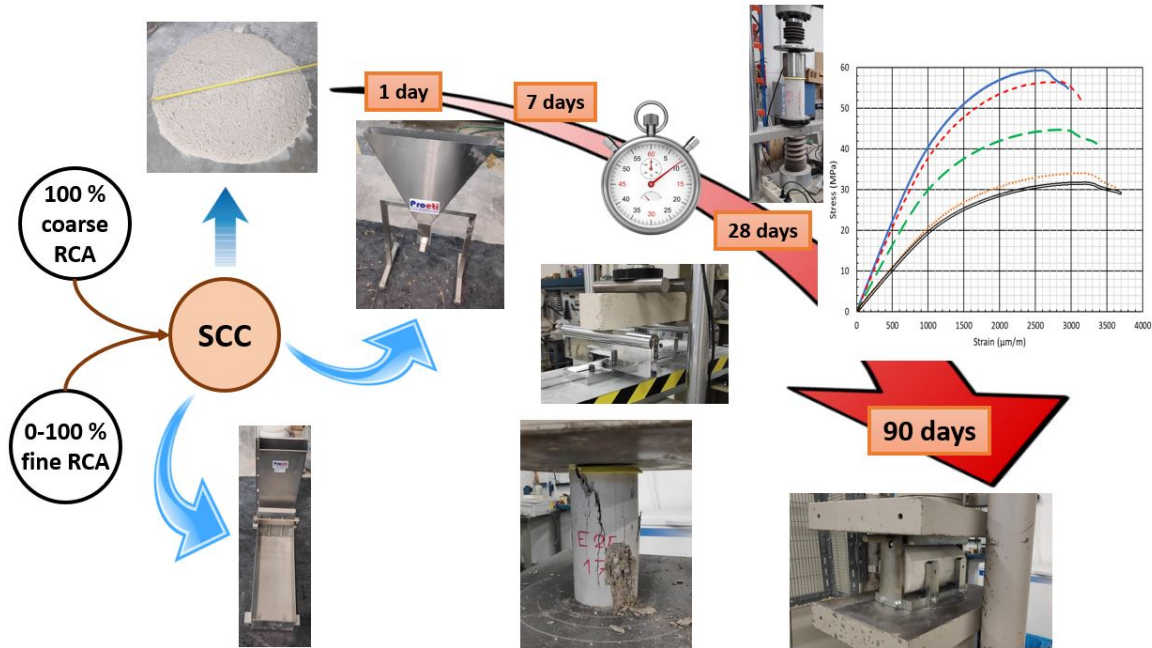


Figure Int.4. Graphical abstract, second article

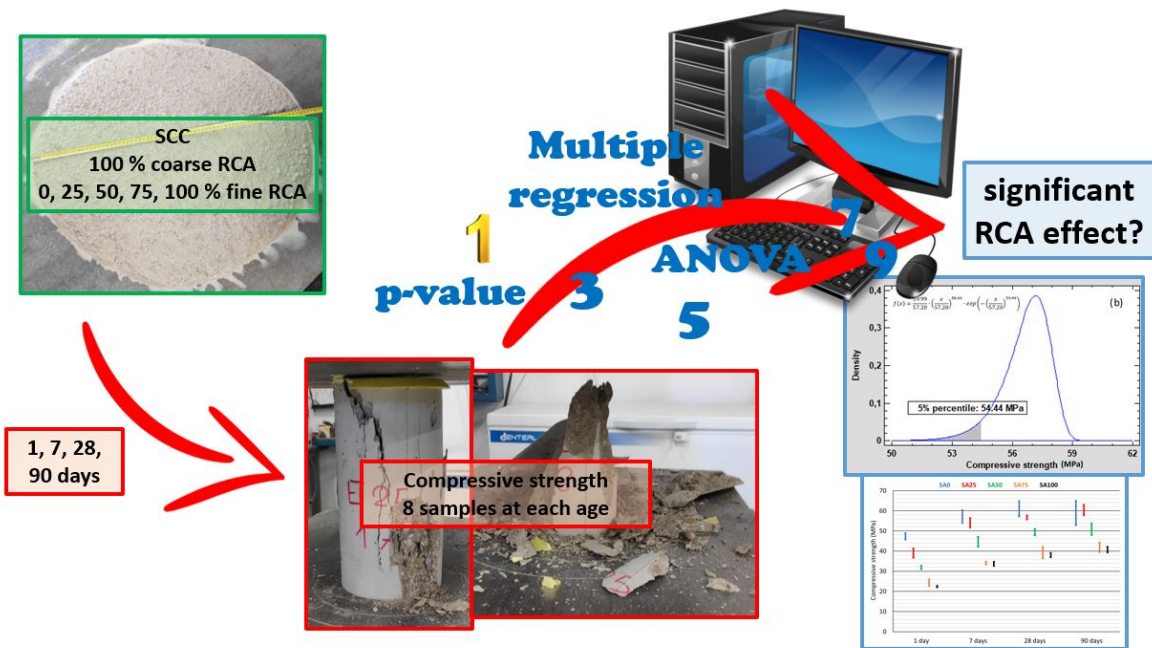


Figure Int.5. Graphical abstract, third article

"Statistical approach for the design of structural self-compacting concrete with fine recycled concrete aggregate" (third article, Figure Int.5), published in *Mathematics*, maintains the same line of research of the second paper [33]. This paper described the design of concretes with a composition similar to that of the concretes included in the second article, but with a modification in its production process to try to improve the self-compactability. In addition, a statistical analysis of the compressive strength of these concretes was proposed, which allowed determining that this strength was more conditioned by the content of fine recycled concrete aggregate than by age. In addition, the need to readapt the way of calculating the characteristic strength when incorporating this type of aggregate to self-compacting concrete was observed.

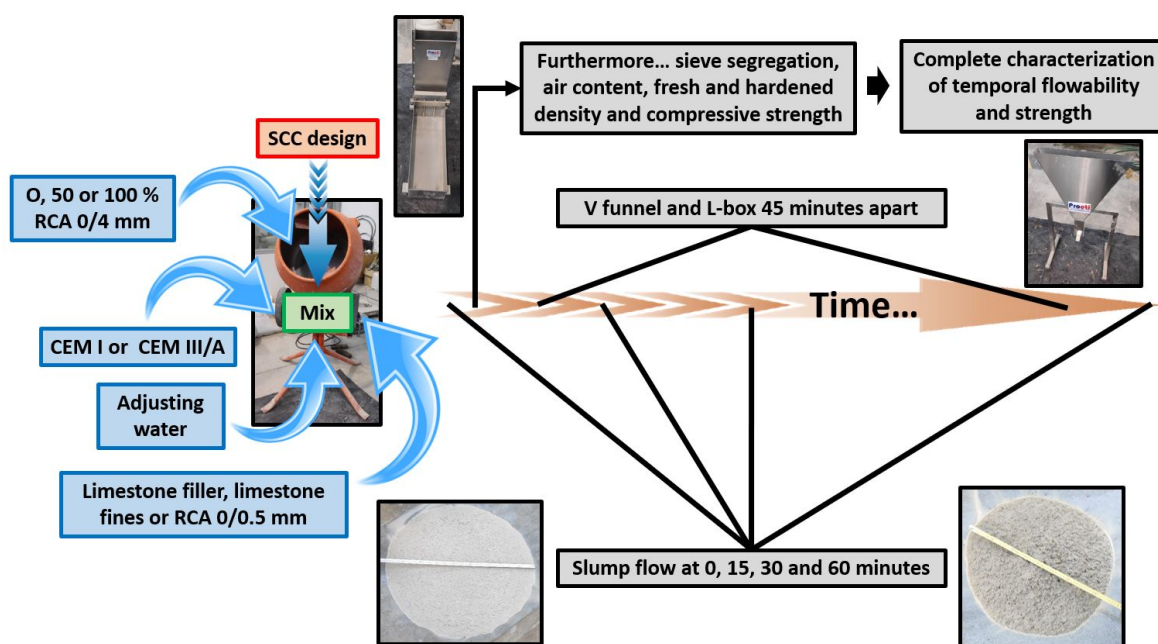


Figure Int.6. Graphical abstract, fourth article

"Temporal flowability evolution of slag-based self-compacting concrete with recycled concrete aggregate" (fourth article, Figure Int.6) [34] and "Models for compressive strength estimation through non-destructive testing of highly self-compacting concrete containing recycled concrete aggregate and slag-based binder" (fifth article, Figure Int.7) [35], published in *Journal of Cleaner Production* and *Construction and Building Materials*, respectively, are part of the second stage of research of this PhD Thesis. In both, the composition and mixing process necessary to get a self-compacting concrete of slump-flow class SF3 [31] made with 100% coarse recycled concrete aggregate, fine recycled concrete aggregate, slag-based binder, and aggregate fines 0/1 mm or 0/0.5 mm more sustainable than traditional limestone filler were detailed. It can be noted that the three gaps in the existing literature identified in the first article were addressed simultaneously. Furthermore, according to the results of the second article, the content of fine recycled concrete aggregate in these two articles was defined as 0%, 50% or 100%. Through the fourth article, the possibility of transportation of these self-compacting concretes to a point located 60 minutes away from the manufacturing plant was validated. The fifth article reflected the possibility of indirectly estimating the compressive strength if the existing models are adapted to it, as its behavior is conditioned by the low coarse aggregate content and the greater flexibility of recycled concrete aggregate compared to ordinary limestone or siliceous aggregate. The suitability of indirect measurements shows the possibility of performing an efficient *in situ* control of this type of mixes, as it is done in conventional vibrated concrete in real civil works.

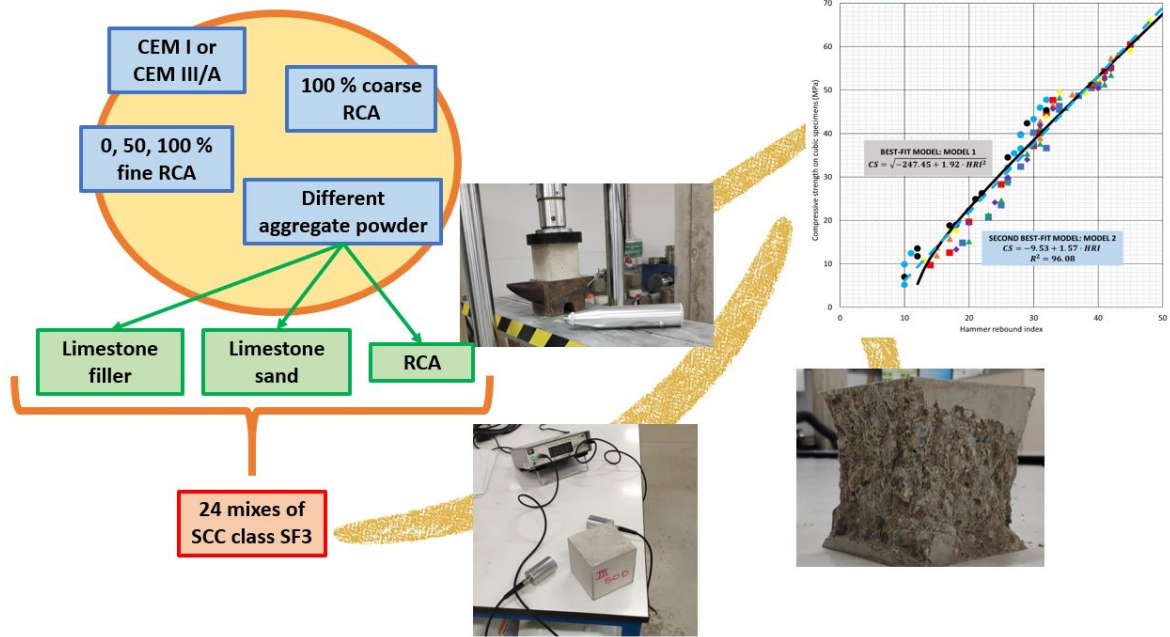


Figure Int.7. Graphical abstract, fifth article

The sixth article (Figure Int.8), entitled "Assessment of longitudinal and transversal plastic behavior of recycled aggregate self-compacting concrete: A two-way study" and published in *Construction and Building Materials* [36], is, from the author's point of view, the most novel of them all. Its goal was not limited to specific aspects of recycled concrete aggregate, but has a much broader objective, as it intended to describe the transverse plastic behavior of a self-compacting concrete without any confinement. The influence of the addition of 100% coarse recycled concrete aggregate and 0%, 50% or 100% fine recycled concrete aggregate was also studied in detail.

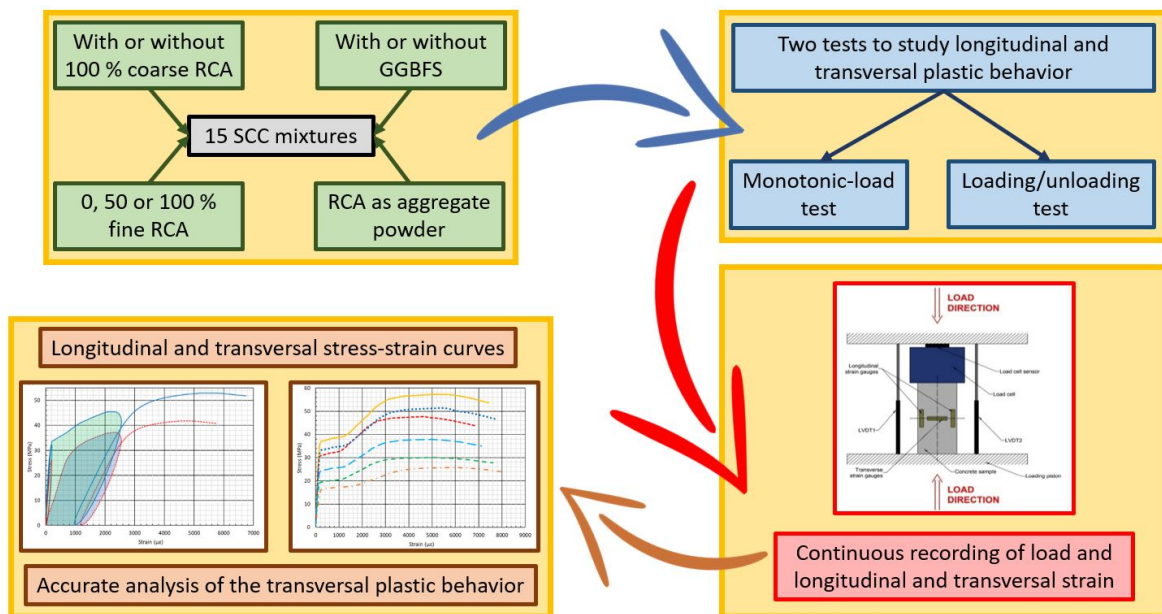


Figure Int.8. Graphical abstract, sixth article

The PhD Thesis ends with a short paper entitled "Thermal deformability of recycled self-compacting concrete under cyclical temperature variations" (seventh paper, Figure Int.9), published in *Materials Letters* [37]. It provides some brief notes on the influence of the use of both coarse and fine fractions of recycled concrete aggregate on the thermal deformability of self-compacting concrete,

showing the need, in principle, to adopt a linear thermal expansion coefficient of $1.2 \cdot 10^{-5} \text{ } ^\circ\text{C}^{-1}$ in this type of concrete.

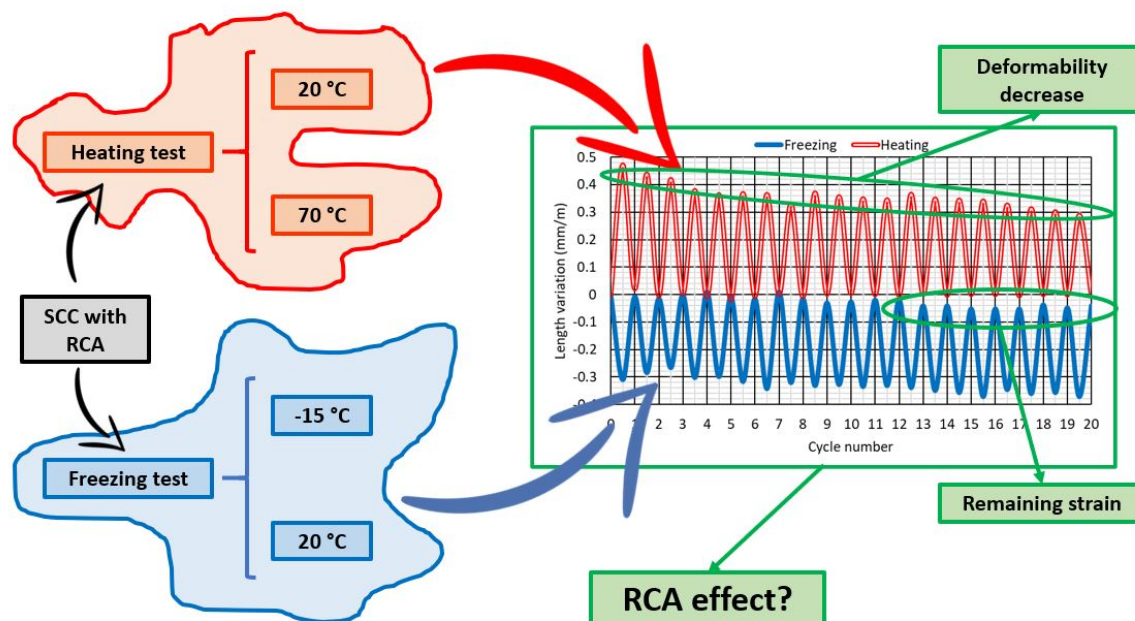


Figure Int.9. Graphical abstract, seventh article

Figure Int.10 shows a conceptual scheme detailing the development of the articles and the specific objectives addressed in each of them.

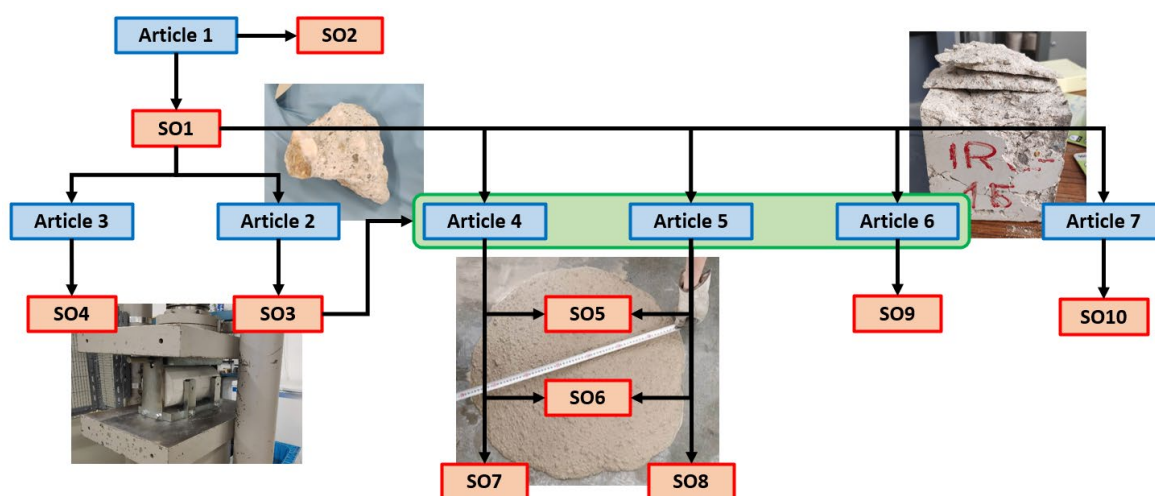


Figure Int.10. Conceptual and organizational outline of the PhD Thesis

REFERENCES

- [1] T. Hák, S. Janoušková, B. Moldan, A.L. Dahl, Closing the sustainability gap: 30 years after “Our Common Future” society lacks meaningful stories and relevant indicators to make the right decisions and build public support, *Ecol. Indic.* 87 (2018) 193-195.
- [2] J. Mistry, C. Tschirhart, C. Verwer, R. Glastra, O. Davis, D. Jafferally, L. Haynes, R. Benjamin, G. Albert, R. Xavier, I. Bovolo, A. Berardi, Our common future? Cross-scalar scenario analysis for social-ecological sustainability of the Guiana Shield, South America, *Environ. Sci. Policy* 44 (2014) 126-148.
- [3] United Nations (UN), Sustainable development goals (<https://sdgs.un.org/es/goals>) (2015).
- [4] Government of Spain, Law 21/2013, of December 9, on environmental assessment (2013).

- [5] F. Pomponi, A. Stephan, Water, energy, and carbon dioxide footprints of the construction sector: A case study on developed and developing economies, *Water Res.* 194 (2021) 116935.
- [6] M.U. Hossain, C.S. Poon, I.M.C. Lo, J.C.P. Cheng, Comparative environmental evaluation of aggregate production from recycled waste materials and virgin sources by LCA, *Resour. Conserv. Recycl.* 109 (2016) 67-77.
- [7] R. Maddalena, J.J. Roberts, A. Hamilton, Can Portland cement be replaced by low-carbon alternative materials? A study on the thermal properties and carbon emissions of innovative cements, *J. Clean Prod.* 186 (2018) 933-942.
- [8] ERMCO, Ready-mixed concrete industry statistics, European Ready-Mixed Concrete Organization (2019).
- [9] ANEFA, Sectorial economic progress reports (2019).
- [10] M. Behera, S.K. Bhattacharyya, A.K. Minocha, R. Deoliya, S. Maiti, Recycled aggregate from C&D waste & its use in concrete - A breakthrough towards sustainability in construction sector: A review, *Constr. Build. Mater.* 68 (2014) 501-516.
- [11] M. Sandanayake, G. Zhang, S. Setunge, Estimation of environmental emissions and impacts of building construction - A decision making tool for contractors, *J. Build. Eng.* 21 (2019) 173-185.
- [12] J.M. Manso, D. Hernández, M.M. Losáñez, J.J. González, Design and elaboration of concrete mixtures using steelmaking slags, *ACI Mater. J.* 108 (6) (2011) 673-681.
- [13] J.M. Manso, J.J. Gonzalez, J.A. Polanco, Electric arc furnace slag in concrete, *J. Mater. Civ. Eng.* 16 (6) (2004) 639-645.
- [14] J.A. Fuente-Alonso, V. Ortega-López, M. Skaf, Á. Aragón, J.T. San-José, Performance of fiber-reinforced EAF slag concrete for use in pavements, *Constr. Build. Mater.* 149 (2017) 629-638.
- [15] V. Ortega-López, J.A. Fuente-Alonso, A. Santamaría, J.T. San-José, Á. Aragón, Durability studies on fiber-reinforced EAF slag concrete for pavements, *Constr. Build. Mater.* 163 (2018) 471-481.
- [16] A. Santamaría, A. Orbe, M.M. Losañez, M. Skaf, V. Ortega-Lopez, J.J. González, Self-compacting concrete incorporating electric arc-furnace steelmaking slag as aggregate, *Mater. Des.* 115 (2017) 179-193.
- [17] A. Santamaría, A. Orbe, J.T. San José, J.J. González, A study on the durability of structural concrete incorporating electric steelmaking slags, *Constr. Build. Mater.* 161 (2018) 94-111.
- [18] A. Santamaría, V. Ortega-López, M. Skaf, J.A. Chica, J.M. Manso, The study of properties and behavior of self compacting concrete containing Electric Arc Furnace Slag (EAFS) as aggregate, *Ain Shams Eng. J.* 11 (1) (2020) 231-243.
- [19] V. Ortega-López, A. García-Llona, V. Revilla-Cuesta, A. Santamaría, J.T. San-José, Fiber-reinforcement and its effects on the mechanical properties of high-workability concretes manufactured with slag as aggregate and binder, *J. Build. Eng.* 43 (2021) 102548.
- [20] A. Santamaría, A. García-Llona, V. Revilla-Cuesta, I. Piñero, V. Ortega-López, Bending tests on building beams containing electric arc furnace slag and alternative binders and manufactured with energy-saving placement techniques, *Structures* 32 (2021) 1921-1933.
- [21] A. Santamaria, F. Faleschini, G. Giacomello, K. Brunelli, J.T. San José, C. Pellegrino, M. Pasetto, Dimensional stability of electric arc furnace slag in civil engineering applications, *J. Clean. Prod.* 205 (2018) 599-609.
- [22] F. Faleschini, A. Santamaria, M.A. Zanini, J.T. San José, C. Pellegrino, Bond between steel reinforcement bars and electric arc furnace slag concrete, *Mater. Struct.* 50 (3) (2017) 170.
- [23] F. Fiol, C. Thomas, C. Muñoz, V. Ortega-López, J.M. Manso, The influence of recycled aggregates from precast elements on the mechanical properties of structural self-compacting concrete, *Constr. Build. Mater.* 182 (2018) 309-323.
- [24] F. Fiol, C. Thomas, J.M. Manso, I. López, Influence of recycled precast concrete aggregate on durability of concrete's physical processes, *Appl. Sci.* 10 (20) (2020) 7348.
- [25] F. Fiol, C. Thomas, J.M. Manso, I. López, Transport mechanisms as indicators of the durability of precast recycled concrete, *Constr. Build. Mater.* 269 (2021) 121263.

-
- [26] L. Evangelista, M. Guedes, J. De Brito, A.C. Ferro, M.F. Pereira, Physical, chemical and mineralogical properties of fine recycled aggregates made from concrete waste, *Constr. Build. Mater.* 86 (2015) 178-188.
- [27] L. Evangelista, J. De Brito, Concrete with fine recycled aggregates: A review, *Eur. J. Environ. Civ. Eng.* 18 (2) (2014) 129-172.
- [28] L. Evangelista, J. de Brito, Durability performance of concrete made with fine recycled concrete aggregates, *Cem. Concr. Compos.* 32 (1) (2010) 9-14.
- [29] L. Evangelista, J. de Brito, Mechanical behaviour of concrete made with fine recycled concrete aggregates, *Cem. Concr. Compos.* 29 (5) (2007) 397-401.
- [30] V. Revilla-Cuesta, M. Skaf, F. Faleschini, J.M. Manso, V. Ortega-López, Self-compacting concrete manufactured with recycled concrete aggregate: An overview, *J. Clean. Prod.* 262 (2020) 121362.
- [31] EFNARC, Specification Guidelines for Self-compacting Concrete, European Federation of National Associations Representing producers and applicators of specialist building products for Concrete (2002).
- [32] V. Revilla-Cuesta, V. Ortega-López, M. Skaf, J.M. Manso, Effect of fine recycled concrete aggregate on the mechanical behavior of self-compacting concrete, *Constr. Build. Mater.* 263 (2020) 120671.
- [33] V. Revilla-Cuesta, M. Skaf, A.B. Espinosa, A. Santamaría, V. Ortega-López, Statistical approach for the design of structural self-compacting concrete with fine recycled concrete aggregate, *Mathematics* 8 (12) (2020) 2190.
- [34] V. Revilla-Cuesta, M. Skaf, A. Santamaría, J.J. Hernández-Bagaces, V. Ortega-López, Temporal flowability evolution of slag-based self-compacting concrete with recycled concrete aggregate, *J. Clean. Prod.* 299 (2021) 126890.
- [35] V. Revilla-Cuesta, M. Skaf, R. Serrano-López, V. Ortega-López, Models for compressive strength estimation through non-destructive testing of highly self-compacting concrete containing recycled concrete aggregate and slag-based binder, *Constr. Build. Mater.* 280 (2021) 122454.
- [36] V. Revilla-Cuesta, M. Skaf, A. Santamaría, V. Ortega-López, J.M. Manso, Assessment of longitudinal and transversal plastic behavior of recycled aggregate self-compacting concrete: A two-way study *Constr. Build. Mater.* 292 (2021) 123426.
- [37] V. Revilla-Cuesta, M. Skaf, J.A. Chica, J.A. Fuente-Alonso, V. Ortega-López, Thermal deformability of recycled self-compacting concrete under cyclical temperature variations, *Mater. Lett.* 278 (2020) 128417.

Article 1

Self-compacting concrete manufactured with recycled concrete aggregate: an overview

Title: Self-compacting concrete with recycled concrete aggregate: an overview

Authors: Víctor Revilla-Cuesta, Marta Skaf, Flora Faleschini, Juan M. Manso, Vanesa Ortega-López

Journal: Journal of Cleaner Production

Year: 2020

Volume: 262

Article number: 121362

DOI: <https://doi.org/10.1016/j.jclepro.2020.121362>

Journal classification (2019 JCR ranking data): 19/265 (environmental sciences). First quartile (Q1), first decile (D1)

ABSTRACT

The use of different types of waste in the manufacture of concrete is increasingly common, due to unabating concerns over climate change and sustainability in the construction sector. It is now widely accepted that the optimal behavior of vibrated concrete produced with the addition of certain wastes can rival the behavior of conventional products. The manufacture of special concretes, such as self-compacting concrete, is also currently under investigation, although the state of knowledge in this field is not so well developed. In this review paper, current and past research articles on the design of self-compacting concrete with recycled concrete aggregate, both by itself and in combination with other wastes, are summarized and assessed. Research is presented into recycled concrete aggregate properties and the mix-design of the self-compacting concretes that contain them, as well as relevant results on the fresh state (workability, rheology), the hardened state (compressive strength, splitting tensile and flexural strength, modulus of elasticity, density, and porosity), durability (resistance to aggressive agents), long-term properties of concrete (shrinkage, creep), and structural elements manufactured with self-compacting concrete containing recycled concrete aggregate. The results under review reaffirm that the incorporation of recycled concrete aggregate can produce a suitable self-compacting recycled concrete, on the basis of careful designs that are essential for successful performance.

Keywords: durability; flowability; hardened state; recycled concrete aggregate; self-compacting concrete; structural elements.

1. INTRODUCTION

Emissions of CO₂ attributed to the construction sector and its enormous consumption of natural resources are both major environmental concerns at a global level [1]. Large amounts of energy are consumed by the extraction of natural aggregates [2] for use in many engineering activities, such as concrete and asphalt mixes, geotechnical activities (fillings, embankments and some types of dams), and even hydraulic activities such as trench and ditch fillings, and beds for piping systems. Finally, there is the contentious issue of high atmospheric emissions of CO₂ from manufacturing processes at cement factories, and at asphalt and concrete plants [3].

Over the past few years, this situation has been firmly noted in the construction sector and initiatives are underway to change what are in many cases considered traditional practices, seeking

to reduce environmental impacts and to mitigate climate change [4]. Following some years of economic recession in the construction industry, investment has increased, which has also prompted the emergence of various new fields of research that, in different ways, encourage more sustainable construction patterns:

- Reducing CO₂ emissions produced during the raw-material manufacturing process, usually direct atmospheric emissions from cement factories [5]. The main solutions have focused on the search for novel production technologies and materials [6].
- Controlling indirect atmospheric emissions and evaluating the carbon footprints of construction components prior to their manufacture and the machinery in use [7].
- And, the central issue in this paper, the search for different techniques to reduce the consumption of natural resources [8].

The areas where the consumption of natural resources can be reduced differ widely. The use of different wastes to replace those aggregates is progressively more extensive, especially in relation to coarse and/or fine Natural Aggregates (NA) in concrete design. Recycled aggregates from Construction and Demolition Waste (CDW) [9], roof tiles [10], rubber [11], plastics [12], and glass [13] are the most common examples of residues that can be added to concrete mixes, provided that the proportion in the mixture is carefully researched and adjusted to the properties of each residue.

Among the above-mentioned residues, CDW has the lengthiest history of use and is currently the most widely used in the manufacture of concrete based on a sustainable approach. CDW, following treatment in certified recycling plants, is an appropriate product for certain types of structural concrete. Its use is regulated in many standards such as the Spanish regulations [14] or the Italian one (DM-17/01/2018) [15] and it may be classified into three main types of materials, according to its components: crushed concrete, crushed masonry, and mixed demolition debris.

The use of crushed concrete or Recycled Concrete Aggregate (RCA) has proven to be especially suitable for high-performance concrete, resulting in countless experimental tests [16] and many reviews of conventional concrete manufactured with RCA regarding fresh state [17], compressive strength [18], mechanical behavior [19], durability [20] and fine RCA performance [21].

The use of RCA in Self Compacting Concrete (SCC) has only recently been studied, however RCA applications and the use of RCA in SCC are gaining ground, reflecting its particular advantages and a need for continued research in that area. SCC is characterized by very good flowability and workability and its main advantage is that no vibration is required when filling formwork enclosures [22]. These properties are usually assisted through the addition of plasticizers and superplasticizers [23]. Regarding SCC with RCA, there is only one review article elaborated. The review article by Santos *et al.* (2019a) [24] is the only one found to date on the topic of SCC with RCA.

This bibliographic review will firstly set out a brief description of RCA properties (average values from the aggregates used in the different articles studied) and some guidelines for the design of concrete dosages. Then, the results of the different studies will be organized into different sections, each one corresponding to a different concrete behavior: fresh state, hardened state (compressive strength, splitting tensile strength, flexural strength, and modulus of elasticity, among others), durability and long-term properties (shrinkage and creep) and finally, the behavior of structural elements.

Lastly, the subsections will be structured by the type of waste in the concrete mix. The papers that are reviewed all report studies of RCA, although the use of more than one type of waste in concrete manufacture is increasingly widespread and SCC is no exception in that regard. The main combinations include the use of RCA in combination with fly ash (FA) and silica fume (SF), among others.

2. CHARACTERIZATION OF RECYCLED CONCRETE AGGREGATE (RCA)

As is widely established, RCA properties are very variable and depend on many aspects, such as the origin of the RCA (precast elements, in-situ manufactured concrete, CDW, laboratory samples, etc.), the dosage and components of the original concrete (pumpable concrete, SCC, type of cement, etc.), and the crushing process of the original elements.

In what follows, a number of interesting studies on the properties of RCA will be highlighted.

Agrela *et al.* (2011) [25] characterized CDW with a content of concrete higher than 90%, which can be considered coarse RCA, in a study of 35 mixed recycled coarse aggregates from several CDW treatment Spanish plants. Those aggregates provided the following results (95% confidence interval):

- Saturated Surface-Dry (SSD) density (kg/dm^3): 2.40 ± 0.07
- Water absorption 24h (wt. %): 5.42 ± 1.70
- Soluble sulphate (% SO_3): 0.40
- Sulphur content (% S): 0.25

Safiuddin *et al.* (2013) [26] in their review regarding the use of the RCA for the manufacture of concrete, established the following average values for the coarse RCA, obtained from six references:

- Shape and texture: Angular with rough surface.
- SSD density (kg/dm^3): 2.1–2.5.
- Bulk density (compacted) (kg/dm^3): 1.20–1.43.
- Absorption (wt. %): 3–12.
- Pore volume (vol. %): 5.6-16.5.

In addition to the information presented above, a summary based on the different references cited throughout this article is presented in Table 1.1. In view of their high variability, 95% confidence intervals (*t*-student distribution) of these properties are presented.

Table 1.1. Average values of some RCA properties

Property	Coarse/fine RCA	Values (95% confidence interval)	References used
SSD density (kg/dm^3)	Coarse	(2.38, 2.48)	[27-51]
	Fine	(2.21, 2.39)	[28, 30, 32, 36-38, 45, 51, 52]
Water absorption (%)	Coarse	(4.53, 6.27)	[27-48, 50, 51, 53, 54]
	Fine	(7.76, 11.06)	[28, 30, 32, 36-38, 45, 51, 52]
Fines content (%)	Coarse	(0.31, 2.65)	[28, 29, 31, 44]
Los Angeles coefficient (%)	Coarse	(28.28, 36.31)	[29, 34, 38, 40, 42-44, 46, 47]

3. SELF-COMPACTING CONCRETE (SCC) REFERENCE DOSAGE

In this section, the dosages proposed by different authors are compiled for the production of conventional SCC with natural aggregates and no waste. The aim is to have a reference in the mix design of Self-Compacting Recycled Concrete (SCRC) for subsequent analysis of the incorporation of the different wastes and their effects.

It must be also emphasized that a key property of SCC is flowability. Various authors have underlined the importance of careful design, proper water to cement (w/c) ratios, and suitable types and amounts of plasticizer (or superplasticizer), to achieve good flowability [55]. Regarding the dosage of a SCC, the addition of superplasticizer is necessary, but a high content of fines is very

important as well. Correct dosing will yield a sufficiently compact cement paste that can carry all coarse aggregate particles and thereby prevent segregations. For this reason, the addition of limestone filler is generally essential.

From the references under study, an average reference dosage is obtained, which collects the quantities of coarse aggregate, fine aggregate, cement, water, limestone filler, and superplasticizer that are necessary to obtain 1 m³ of SCC, as shown in Table 1.2 (95% confidence interval). The average w/c ratio is also shown, which should be significantly increased with additions of RCA, to compensate the high water-absorption levels of the RCA and obtain optimum flowability values.

Table 1.2. Average dosage in reference SCC

Component (kg/m ³)	Values (95% confidence interval)	Average value of the interval	References used
Cement	(332.54, 409.03)	370.78	[28, 29, 31, 34, 36, 37, 41, 43, 44, 48, 51-53]
Water	(168.11, 202.49)	185.30	
Coarse aggregate	(731.44, 890.01)	810.72	
Fine aggregate	(723.95, 865.51)	794.73	
Limestone filler	(136.91, 248.04)	192.48	
Superplasticizer	(3.43, 4.33)	3.88	
	Average value: 1.0%-1.1% wt. of cement		
w/c ratio	(0.44, 0.54)	0.49	

4. FRESH STATE PERFORMANCE

As stated earlier, flowability is the main property of SCC that distinguishes it from conventional vibrated concrete. The flowability of SCC is measured in different tests, the most important of which are the slump flow, J-ring, L-box, V-funnel and sieve segregation tests. Studied in very specific cases, direct rheological parameters are a potential field of study for future investigations [52]. The values obtained in all these tests must be in line with the national regulations of each country and the regulations of others relevant bodies, such as the European Federation of National Associations Representing producers and applicators of specialist building products for Concrete (EFNARC) [56] or the specifications of the American Concrete Institute (ACI) [57].

4.1. FRESH STATE OF SCC WITH RCA

Grdic *et al.* (2010) [53], Modani and Mohitkar (2014) [58], and Kebaïli *et al.* (2015) [34] attempted to develop an SCC manufactured with coarse RCA. In the research work of Grdic *et al.* (2010) [53] and Modani and Mohitkar (2014) [58], SCC was successfully performed, although its flowability decreased as the proportion of coarse RCA increased. In contrast, Kebaïli *et al.* (2015) [34] were unsuccessful at manufacturing SCC, which they attributed to two main reasons. First, the water content was so low that it could not compensate the high absorption of the RCA. Second, the aggregate/paste ratio was too high, meaning that particles of aggregate collided against each other, hindering the flow of concrete. Both studies add weight to the fact that a carefully designed dosage is essential to achieve self-compactability.

Campos *et al.* (2018) [28] designed a concrete mixture with coarse RCA and/or fine RCA in three different combinations (0%-20%, 20%-0% and 20%-20%). The amount of superplasticizer increased with the amount of RCA. The results showed that a suitable SCC can be achieved using these quantities of coarse RCA and fine RCA, if around 9% more water is added. Their results also corroborated previous observations that fine RCA water absorption is greater than the water absorption of coarse RCA.

Carro-López *et al.* (2015; 2017) [52, 59] considered a substitution of only the fine fraction of NA in proportions of 20%, 50%, and 100%, maintaining the superplasticizer constant. When examining

the flowability of the mixes, which as is well known will decrease over time, they reached the conclusion that the greater the fine RCA content, then the faster the decrease in flowability.

Different humidity conditions of the RCA have been also analyzed. González-Taboada *et al.* (2017a; 2017b) [31, 60] designed SCC with coarse RCA (substitution percentages of 20%, 50%, and 100%) and three different situations were considered: dry aggregate and extra water (labelled M1), pre-soaked aggregate (labelled M2), and aggregate with 3% of natural moisture and extra water in the concrete mix (labelled M3). The main conclusion was that the coarse RCA was indeed suitable for the manufacture of SCC and that the best method to guarantee flowability over time was by pre-soaking (M2) the aggregates. In contrast, control over flowability with methods M1 and M3 presented serious difficulties. Although, in conclusion, M2 was the best method, the authors claimed that aggregate pre-soaking as an industrial procedure would require excessive amounts of time and may not be profitable, which explained why M3 was the most widely used option. However, in the case of SCC as a high-performance product, pre-saturation should be considered as an alternative to enhance behavior, besides profitability considerations. However, in the perspective of industrializing RCA-based SCC, the authors of this review considered it more efficient to use RCA with natural moisture and to modify the total water content of the mix, rather than by pre-soaking the aggregates.

González-Taboada *et al.* (2018a; 2018b) [61, 62] analyzed the different aspects that affect SCC flowability: the variations of water, cement and superplasticizer in the mix-design, and the characteristics of the RCA (shape coefficient, modulus of fine, content of fines...). It was concluded that small changes in these parameters affected SCRC much more than conventional vibrated concrete. The dosages of that type of concrete must be studied further and the conditions of the mixing place (e.g., ambient moisture) must be perfectly controlled.

In terms of density, Manzi *et al.* (2017) [37] stated that the fresh bulk density of SCRC was lower than that of conventional vibrated concrete and lower than the fresh bulk density of SCC manufactured with NA. They obtained a value of 2.22 kg/dm³ with a 100% coarse substitution and 2.28 kg/dm³ with a 20-40% substitution rate, compared to 2.34 kg/dm³ of the control concrete. That result was attributed to the lower density of the RCA, mainly caused by the attached mortar.

Salesa *et al.* (2017) [44] worked with a multi-recycled SCC with a percentage substitution of 100%. An initial SCRC (named RA1) was produced, which was then crushed, sieved and used to manufacture a second SCRC (RA2). A third concrete (RA3) was then manufactured from the second. The flowability tests worsened, which was explained by the increasing amounts of adhered mortar in each cycle. Some of these results are shown in Table 1.4.

Assaad (2017) [63] evaluated the effect of coarse RCA on SCC flowability, by comparing the Direct Substitution (DR) by volume and the Equivalent Mortar Volume (EMV) methods to define the dosage. Flowability decreased with the addition of RCA, but the DR method provided better results for low percentages of RCA (20-35%). No SCC was developed using the EMV method for higher coarse RCA contents, so it is not known which method had the better result. The static stability of the SCC improved with RCA and EMV method.

Omrane *et al.* (2017) [38] used a natural pozzolan in addition to RCA in substitution of cement. They observed that when RCA was used, then pozzolan percentages could be increased by up to 20%, while the pozzolan percentage could not exceed 15% with NA if requirements related to slump flow test wanted to be fulfilled [64]. The effectiveness of the natural pozzolan was greater in combination with RCA.

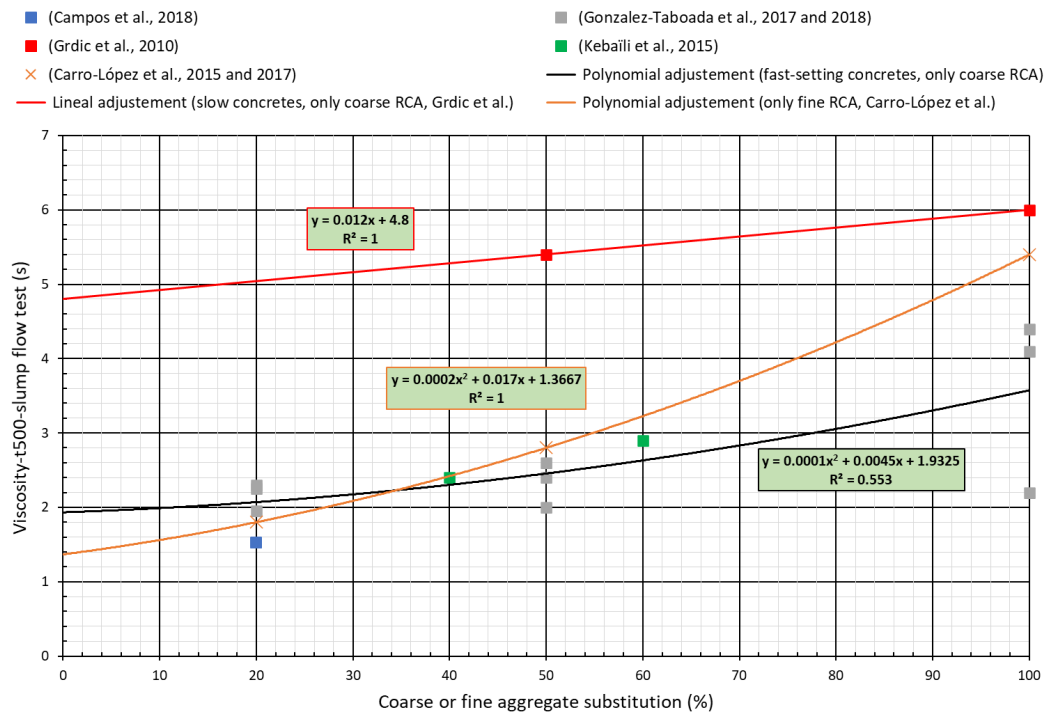


Figure 1.1. Viscosity in the t_{500} -slump flow test as a function of coarse aggregate substitution rates

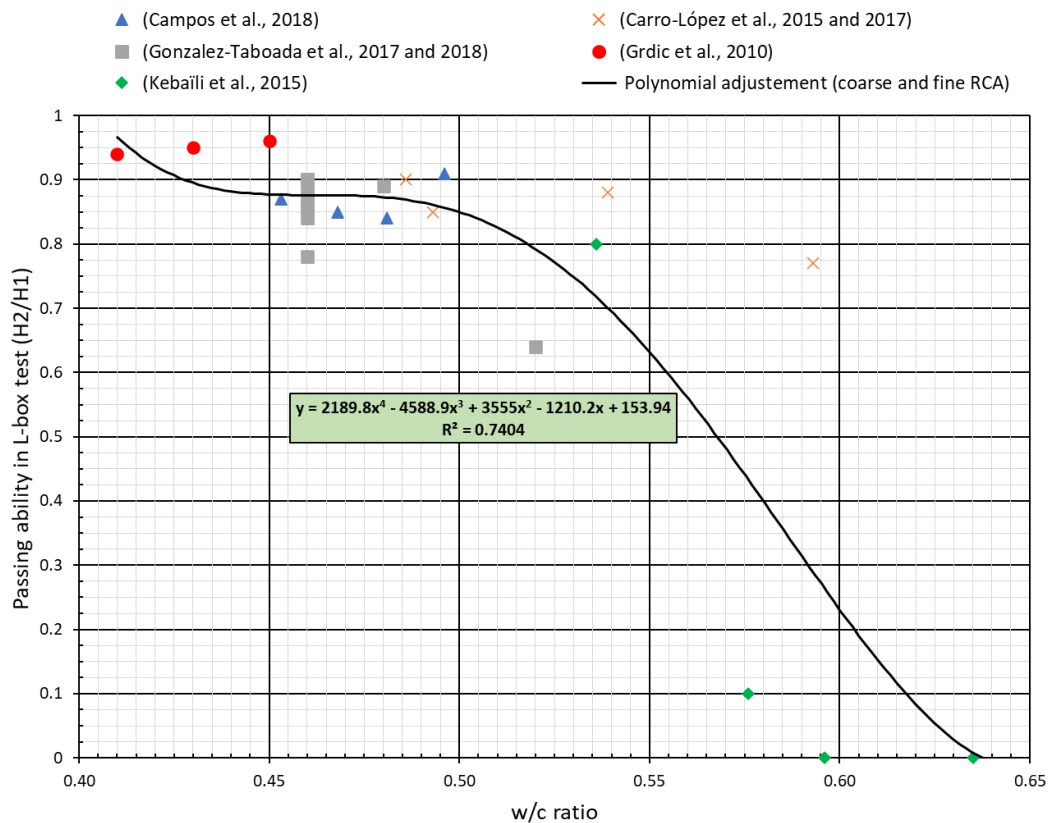


Figure 1.2. Passing ability in the L-box test as a function of the w/c ratio

Güneyisi *et al.* (2014) [65] evaluated some aggregate surface treatment methods and their effects on the properties of SCC made with RCA (100% coarse RCA replacement). Four different treatments were analyzed: submerging RCA in HCl solution for 24 h, submerging RCA in water glass ($\text{Na}_2\text{O}\cdot n\text{SiO}_2$ sodium silicate) for 30 min, submerging RCA in cement-silica fume slurry for 30 minutes, and

implementing a two-stage mixing process. All the treatments that were tested improved the flowability and the performance of the concrete compared to the control mixture. Among them, the water glass treatment appeared the most effective and was quite brief, so it could be implemented in industrial production, although consideration should also be given to the increased cost [66].

The results of some of the investigations commented in this subsection were plotted against relevant parameters, such as the percentage substitution, the w/c ratio and the percentage of superplasticizer. In Figure 1.1, the relation between RCA percentage and the slump flow t_{500} is shown, differentiating between “fast” and “slow” concretes, based on the representative differences between each one. Figure 1.2 shows the relation between passing ability in the L-box test and the w/c ratio. The values used to draw the graphs, obtained from the literature under review, are also shown in Table 1.3.

Table 1.3. Values of some in-fresh properties of SCC manufactured with only RCA

Research	Coarse RCA content (%)	Fine RCA content (%)	w/c ratio	Superplasticizer (% wt. of cement)	Viscosity t_{500} slump flow test (s)	Slump flow (mm)
Campos et al. (2018) [28]	0	0	0.45	0.47	1.17	650
	0	20	0.48	0.55	1.53	670
	20	0	0.46	0.60	1.80	690
	20	20	0.49	0.70	0.81	620
Carro-López et al. (2015; 2017) [52, 59]	0	0	0.48	0.43	1.70	830
	0	20	0.49	0.43	1.80	790
	0	50	0.53	0.43	2.80	770
	0	100	0.59	0.43	5.40	670
González-Taboada et al. (2017a; 2017b; 2018a; 2018b; 2018c) (M1/M2/M3) [31, 60-62, 67]	0	0	0.46	2.46	1.45	820
	20	0	0.46	2.46	1.95	740
	50	0	0.46	2.46	2.40	710
	100	0	0.46	2.46	4.10	680
	0	0	0.46	2.46	1.50	820
	20	0	0.46	2.46	2.25	730
	50	0	0.48	2.46	2.00	720
	100	0	0.52	2.46	2.20	750
	0	0	0.46	2.46	1.45	820
	20	0	0.46	2.46	2.30	720
	50	0	0.46	2.46	2.60	710
	100	0	0.46	2.46	4.40	660
Grdic et al. (2010) [53]	0	0	0.41	0.98	5.60	730
	50	0	0.43	0.98	5.40	730
	100	0	0.45	0.98	6.00	720
Kebaïli et al. (2015) [34]	0	0	0.53	1.05	2.50	730
	40	0	0.57	1.05	2.40	680
	60	0	0.59	1.05	2.90	600
	100	0	0.63	1.05	-	470

Table 1.3 (continued). Values of some in-fresh properties of SCC manufactured with only RCA

Research	Viscosity t_{500} J-ring (s)	Maximum diameter J-ring (mm)	Passing ability L-box H2/H1	Viscosity V-funnel (s)	Sieve segregation (%)
Campos et al. (2018) [28]	-	-	0.87	-	9.5
	-	-	0.84	-	4.6
	-	-	0.85	-	12.8
	-	-	0.91	-	12.3
Carro-López et al. (2015; 2017) [52, 59]	2.2	810	0.90	8.0	-
	2.0	750	0.85	11.0	-
	2.8	740	0.88	8.0	-
	5.4	600	0.77	11.0	-
González-Taboada et al. (2017a; 2017b; 2018a; 2018b; 2018c) (M1/M2/M3) [31, 60-62, 67]	2.5	820	0.90	23.0	14.0
	3.0	750	0.86	24.0	13.5
	3.8	700	0.88	31.0	12.0
	4.2	680	0.84	33.0	3.5
	2.5	820	0.90	24.0	14.0
	3.2	710	0.87	34.0	14.5
	4.8	660	0.89	42.0	24.5
	1.0	860	0.64	18.0	37.0
	2.5	820	0.90	23.0	14.0
	3.2	730	0.85	26.0	12.0
	3.9	690	0.86	33.0	9.0
4.5	660	0.78	22.0	4.5	
Grdic et al. (2010) [53]	-	-	0.94	-	11.7
	-	-	0.95	-	9.3
	-	-	0.98	-	5.2
Kebaïli et al. (2015) [34]	-	-	0.80	-	-
	-	-	0.10	-	-
	-	-	0.00	-	-
	-	-	0.00	-	-

Through these data, the following conclusions on SCC manufactured with RCA can be established:

- The greater the percentage of RCA substitution, the greater the viscosity of the mixture and the lower its flowability, due to the higher RCA water absorption levels, which are not usually compensated with the additional water added to the mixtures.
- The average flowability values appear to increase slightly with the amount of superplasticizer. Nevertheless, a larger amount of superplasticizer appears not to ensure better flowability by itself, due to the significant influence of other aspects, such as the water absorption and the amount of RCA.
- In principle, a higher w/c ratio should lead to greater flowability. However, increasing amounts of water are required, due to the higher water absorption of the RCA rather than the NA. Additional water can sometimes be insufficient to compensate for the extra-water absorbed by the RCA, making the effective w/c ratio lower when the RCA percentage increases. Finally, despite the increase in the w/c ratio, it can lead to lower flowability and a lower passing ability in the L-box test.

4.2. FRESH STATE OF SCC WITH RCA AND OTHER WASTES (FLY ASH, SILICA FUME, RECYCLED ASPHALT PAVEMENT AGGREGATES, RUBBER GRANULES, SLAGS)

In Table 1.4, the results from several investigations are summarized on the joint use of RCA and other wastes, namely, fly ash (FA), silica fume (SF), recycled asphalt pavement (RAP), ground granulated blast-furnace slag (GGBFS), and rubber. The results are subsequently discussed.

Table 1.4. Values of some studies on the SCC flowability tests in concretes with RCA and other wastes

Research	Waste used (replacement rate)	Coarse RCA content (%)	Fine RCA content (%)	Viscosity t_{500} slump flow (s)	Slump flow (mm)
Salesa <i>et al.</i> (2017) [44]	Multi-RCA ¹	100	0	SF1	640
		100	0	SF2	740
		100	0	SF2	710
		100	0	SF2	660
Santos <i>et al.</i> (2019b) (PC-45/PC-65) [68]	FA ² (90%)	0	0	2.5	733
		25	25	2.5	690
		50	50	2.5	688
		100	0	3	698
		0	100	2.5	685
	FA ² (34%)	0	0	2	765
		25	25	2.5	760
		50	50	2.5	700
		100	0	3	718
		0	100	2.5	683
Hu <i>et al.</i> (2017) [69]	Eco-SCC 1/12.5 mm RCA FA ² (25%)	0	0	3.9	660
		50	0	9.8	610
		100	0	6.2	559
Revathi <i>et al.</i> (2013) [43]	FA ² (56%)	0	0	3.0	750
		25	0	4.0	730
		50	0	4.0	730
		75	0	5.0	700
		100	0	5.0	710
Vinay Kumar <i>et al.</i> (2017) [51]	FA ² (33%)	0	0	1.8	710
		20	0	2.0	690
		0	20	2.0	710
		20	20	2.0	640
Tang <i>et al.</i> (2016) [48]	FA ² (35%) SF ² (6.7%)	0	0	2.9	710
		25	0	3.7	700
		50	0	3.9	720
		75	0	4.1	710
		100	0	4.3	700
Yasser Khodair (2017) [35]	RAP aggregate ³	0	0	3.0	530
		25	0	4.0	610
		50	0	5.0	640
		75	0	5.0	640
Aslani <i>et al.</i> (2018) [70]	FA ² (75%) SF ² (19%) GGBFS ² (56%)	0	0	2.0	690
		10	10	2.1	690
		20	20	2.4	650
		30	30	2.3	620
		40	40	3.0	600

¹ The RCA rate indicated in the third column "coarse RCA content" is for Multi-RCA

² Percentages respect the amount of cement added to the mix

³ The values indicated in the third column "coarse RCA content" are the sum of the percentages of RCA and RAP aggregate

Table 1.4 (continued). Values of some studies on the SCC flowability tests in concretes with RCA and other wastes

Research	Viscosity t_{500} J-ring (s)	Maximum diameter J-ring (mm)	Passing ability L-box H2/H1	Viscosity in V-funnel (s)	Segregation (%)
Salesa et al. (2017) [44]	-	-	-	-	-
	-	-	-	-	-
	-	-	-	-	-
	-	-	-	-	-
Santos et al. (2019b) (PC-45/PC-65) [68]	-	-	0.80	7.5	-
	-	-	0.80	9.0	-
	-	-	0.80	8.0	-
	-	-	0.83	7.0	-
	-	-	0.80	7.0	-
	-	-	0.81	9.0	-
	-	-	0.84	9.0	-
	-	-	0.90	8.0	-
	-	-	0.80	9.0	-
-	-	0.80	11.0	-	
Hu et al. (2017) [69]	-	584	-	-	-
	-	457	-	-	-
	-	483	-	-	-
Revathi et al. (2013) [43]	-	-	-	7.8	-
	-	-	-	7.9	-
	-	-	-	8.3	-
	-	-	-	8.8	-
	-	-	-	10.5	-
Vinay Kumar et al. (2017) [51]	-	-	0.92	8.0	5.8
	-	-	0.91	8.0	5.3
	-	-	0.97	8.0	5.3
	-	-	0.93	10.0	5.1
Tang et al. (2016) [48]	-	-	0.94	-	9.9
	-	-	0.95	-	7.7
	-	-	0.97	-	6.3
	-	-	0.92	-	6.0
	-	-	0.93	-	5.2
Yasser Khodair (2017) [35]	4.0	510	-	-	0.0
	6.0	530	-	-	0.0
	7.0	580	-	-	0.0
	7.0	580	-	-	0.0
Aslani et al. (2018) [70]	-	650	-	-	-
	-	630	-	-	-
	-	560	-	-	-
	-	530	-	-	-
	-	500	-	-	-

Research studies with different percentages of FA and RCA and RCAs of different origin have been carried out. In general, their main observations were that the joint use of RCA and FA provided SCC with appropriate in-fresh performance [36]. The behavior of SCRC was similar to the concrete with

natural filler (section 4.1) [42]. The use of FA led to a higher w/c ratio than when using only cement and natural filler [51].

Santos *et al.* (2019b) [68] developed a concrete by incorporating coarse and fine RCA at several replacement rates (25%-25%, 50%-50%, 100%-0% and 0%-100%) and FA, keeping the effective w/c ratio constant. Their results showed that an SCC could be obtained with precise and careful dosing by using an RCA with a high content of fines. Its flowability in the fresh state was similar to the flowability of non-recycled SCC.

Hu *et al.* (2017) [69] studied the in-fresh performance of an eco-efficient SCC (Eco-SCC) combining FA and RCA in 1/12.5 mm continuous granulometry. The Eco-SCC was based on an optimal gradation of the aggregate particles, so that the mixture had less need for cement paste. The addition of RCA worsened slump flow and viscosity with regard to common SCC, although the water content was increased.

Singh, R.B. and Singh, B. (2018) [71] and Kapoor *et al.* (2016) [33] analyzed the joint use of RCA, FA, SF and metakaolin in different combinations. These authors succeeded in obtaining an SCC with good in-fresh behavior, which requires a good dosage, adapted to the waste that is used, and, generally, larger amounts of superplasticizer and, more than anything, a higher w/c ratio [48].

The joint use of RCA and FA can be considered commonplace, but lately, the incorporation of new wastes in the concrete mixture is becoming more common. Some authors successfully combined RCA with other types of waste to produce SCC.

Yasser Khodair *et al.* (2017) [35] studied the performance of SCC using RCA and RAP, in joint percentages of 25%, 50%, and 75% of the total. In addition, FA and GGBFS were added to the mix: 70% FA, 70% GGBFS and 25% FA and GGBFS jointly, all of them with respect to the cement mass. The addition of RAP aggregate had no effect on the performance levels recorded for FA incorporated in concrete with RCA. Nevertheless, the use of FA and GGBFS in substitution of cement appeared to increase flowability in the slump-flow test, reaching a greater maximum diameter, although the concrete became slower, because it took more time to reach that maximum diameter.

Aslani *et al.* (2018) [70] designed a very complete study of three different mixtures in terms of aggregates substitution: one of them with only coarse and fine RCA (shown in Table 1.4), a second adding rubber granules and a third mix adding coarse and fine RAP aggregates. These wastes were used in replacement of 0% to 40% of NA. In addition, partial substitution of cement by FA, SF and GGBFS was also tested in the three mixtures. Regarding flowability, the results showed that the greater the percentage substitutions of RCA, the lower the flowability, as discussed in previous studies. Nevertheless, the joint use of fine RCA and rubber granules stabilized flowability. There again, the use of rubber granules and GGBFS in small percentage substitutions increased flowability compared to SCC manufactured with NA. A precise definition of their behavior will require a separate evaluation of the effects of each co-product.

Silva *et al.* (2016) [46] evaluated the joint use of RCA and masonry residues, the latter in partial replacement of filler. They found that the flowability of the concrete with masonry residues was equal to or even better than the flowability obtained with RCA and filler. Nevertheless, the bulk density of the concrete increased, due to the greater density of the masonry in comparison with the limestone filler. Uygunođlu *et al.* (2014) [49] compared a concrete manufactured with coarse RCA and a concrete manufactured with coarse marble waste. The latter showed better flowability, due to its more rounded shape. The irregular shape (crushed aggregate-high angularity) of the RCA hindered higher flowability values. The addition of recycling ceramic waste powder appears to result in improved slump flow if it is added in low percentages (around 10-30%) and if its granulometry has a high content of fines, less than 10 μm [72].

A general conclusion can be drawn from all the above studies: the combination of different wastes in the concrete mix yields an SCC with adequate flowability for large-scale use as long as the dosage is adjusted to the amounts of added residues, to their percentage substitution, and to the flowability requirements of the concrete. The interaction of the RCA with each of the aforementioned wastes is different and its behavior must be carefully analyzed, to obtain the dosage that will optimize the performance of the SCC.

4.3. FRESH STATE OF SCC WITH RCA AND FIBERS

It is also possible to design Fiber Reinforced Self-Compacting Concrete (FRSCC) with RCA. The properties of the hardened concrete (toughness, impact resistance, etc.) will foreseeably be improved by the addition of fibers [73], although the behavior in the fresh state will, in general, worsen.

Nalanth *et al.* (2014) [74] and Ortiz *et al.* (2017) [39] studied steel FRSCC with RCA as a replacement material. Nalanth *et al.* (2014) [74] also employed FA in substitution of cement, while Ortiz *et al.* (2017) [39] used only coarse RCA. Both studies showed that the flowability decreased as the amount of RCA increased. In addition, the decrease in flowability was greater when fibers were incorporated: the higher number of added fibers, the greater the decrease, as was expected. For instance, Nalanth *et al.* (2014) [74] observed a decrease of 2.3% in the slump flow test -with 50% RCA, compared to a reference concrete without RCA. When 0.5% vol. of fibers was incorporated, the decrease was around 2.6% compared to the same reference concrete and, with 1.5% vol. of fibers, the decrease was around 4.9%.

Mohseni *et al.* (2017) [54] and Coppola *et al.* (2005) [75] analyzed FRSCC with steel and Polypropylene (PP) fibers, obtaining similar performance for both concretes, except in the flowability test, where the addition of PP fibers yielded worse slump flows (e.g. concrete with PP fibers had a slump flow of 5.8% lower than concrete with steel fibers). That result may be due to the higher surface roughness of the PP fibers. The joint use of RCA and the fibers produced an even worse performance in the fresh state. Mohseni *et al.* (2017) [54] reported slump flows that were, respectively, 3.3% and 6.8% lower when PP fibers and when steel fibers were used with RCA, in comparison with concretes that contained the same percentages of fibers and no RCA.

5. HARDENED STATE: MECHANICAL PROPERTIES

Flowability and workability in the fresh state are the key aspects for a reliable and optimal SCC. However, the properties in the hardened state such as compressive strength, splitting tensile strength, flexural strength, and modulus of elasticity must be likewise suit the purpose for which the concrete is intended.

In Table 1.5, the values obtained for the mechanical properties in different investigations are summarized. Those values are also explored in the following sections.

5.1. COMPRESSIVE STRENGTH

The most important property of any concrete in the hardened state is its compressive strength. In this section, the effects on that parameter of adding RCA to an SCC, by itself and in combination with other co-products, will be evaluated.

5.1.1. SCC WITH RCA

Panda and Bal (2013) [40] and Pereira-De-Oliveira *et al.* (2013) [76] analyzed a concrete with percentage substitutions ranging between 0% and 40%. In both cases, the compressive strength was reduced, but Pereira-De-Oliveira *et al.* (2013) [76] registered a slight strength reduction (3%), while Panda and Bal (2013) [40] only achieved a compressive strength of 75% compared to the

reference SCC. The reduction of the compressive strength was mainly attributed to the higher RCA water absorption values, which led to a greater w/c ratio. Nevertheless, the difference between both studies is mainly attributable to the different origins of the RCA, of decisive influence on the performance and the quality of the RCA concrete.

Table 1.5. Mechanical properties of SCC

Research	Waste used (substitution rate)	Coarse/fine RCA content (%)	Compressive strength (MPa)	Splitting tensile strength (MPa)	Flexural strength (MPa)	Static modulus of elasticity (GPa)
Campos et al. (2018) [28]	RCA	0/0	51	4.9	-	31
		20/0	47	4.8	-	32
		0/20	46	4.6	-	30
		20/20	45	4.5	-	30
Fiol et al. (2018) (RAC-30/RAC-37.5/RAC-45) [29]	RCA	0/0	49	5.2	6.2	37
		20/0	50	5.1	6.3	39
		50/0	56	4.9	6.4	35
		100/0	57	4.9	5.6	34
		0/0	58	5.5	6.9	39
		20/0	60	5.2	7.6	42
		50/0	59	5.2	6.2	37
		100/0	71	5.3	6.7	36
		0/0	63	5.3	8.0	41
		20/0	64	5.2	7.8	43
Manzi et al. (2017) [37]	RCA	0/0	44	3.3	4.0	26
		13/12	45	3.2	3.8	25
		21/19	50	2.5	3.0	29
		40/0	51	3.1	4.1	27
Panda and Bal (2013) [40]	RCA	0/0	27	4.3	3.7	-
		10/0	27	3.9	3.6	-
		20/0	25	3.7	3.2	-
		30/0	24	3.4	3.1	-
		40/0	21	2.9	2.9	-
Pereira-De-Oliveira et al. (2013) [76]	RCA	0/0	54	-	-	40
		10/0	54	-	-	39
		20/0	54	-	-	39
		30/0	53	-	-	39
		40/0	53	-	-	38
Grdic et al. (2010) [53]	RCA	0	50	7.2	-	-
		50/0	48	7.1	-	-
		100/0	46	6.2	-	-
Salesa et al. (2017) [44]	Multi-RCA ¹	100/0	57	-	-	35
		100/0	59	-	-	31
		100/0	60	-	-	31
		100/0	62	-	-	30
Hu et al. (2017) [69]	Eco-SCC 1/12.5 mm RCA FA ² (25%)	0/0	41	-	-	-
		50/0	48	-	-	-
		100/0	38	-	-	-

¹ The RCA rate indicated in the third column "coarse RCA content" is for Multi-RCA

² Percentages with respect to the amount of cement added to the mix

Table 1.5 (continued). Mechanical properties of SCC

Research	Waste used (substitution rate)	Coarse/fine RCA content (%)	Compressive strength (MPa)	Splitting tensile strength (MPa)	Flexural strength (MPa)	Static modulus of elasticity (GPa)
Revathi <i>et al.</i> (2013) [43]	RCA FA ² (56%)	0/0	36	3.5	5.3	-
		25/0	35	2.9	3.5	-
		50/0	35	2.3	3.0	-
		75/0	33	2.0	2.6	-
		100/0	30	1.5	2.9	-
Vinay Kumar <i>et al.</i> (2017) [51]	RCA FA ² (33%)	0/0	43	3.3	-	-
		20/0	48	3.4	-	-
		0/20	46	3.9	-	-
		20/20	47	3.4	-	-
Santos <i>et al.</i> (2017) (PC-45/PC-65) [45]	RCA FA ² (91% for PC-45 and 34% for PC-65)	0/0	38	3.9	-	30
		25/25	36	3.5	-	29
		50/50	34	2.9	-	28
		100/0	32	2.6	-	28
		0/100	28	2.4	-	26
		0/0	74	5.5	-	46
		25/25	72	4.9	-	41
		50/50	68	4.8	-	37
		100/0	67	4.5	-	38
0/100	65	4.2	-	35		
Kou and Poon (2009) [36]	RCA FA ² (59%)	100/0	44	2.9	-	-
		100/25	45	2.7	-	-
		100/50	43	2.7	-	-
		100/75	41	2.6	-	-
		100/100	39	2.5	-	-
Tang <i>et al.</i> (2016) [48]	RCA FA ² (35%) SF ² (6.7%)	0/0	59	4.1	-	32
		25/0	64	4.9	-	30
		50/0	65	4.1	-	30
		75/0	60	3.9	-	29
		100/0	54	3.8	-	25

² Percentages with respect to the amount of cement added to the mix

Manzi *et al.* (2017) [37] evaluated low replacement rates of RCA and Fiol *et al.* (2018) [29] analyzed concrete mixtures with percentages of 50% and 100% of RCA. They both obtained compressive strength values for SCRC that were higher than non-recycled SCC (for 100% of coarse RCA, the compressive strength was around 16% greater, according to both studies). The authors explained their results in terms of higher RCA water absorption compared to NA, the constant amount of water added to all the mixes and the dry state of the aggregates. All those factors produced a lower effective w/c ratio, which favored a higher compressive strength.

The above observation was also endorsed in the study of Salesa *et al.* (2017) [44] on multi-recycled SCC and its behavior. The fact that the amount of water was the same at every stage, while the attached non-hydrated mortar content increased, led to greater absorption and higher compressive strengths of the SCC concrete mixtures of multi-recycling stages.

Table 1.5 (continued). Mechanical properties of SCC

Research	Waste used (substitution rate)	Coarse/fine RCA content (%)	Compressive strength (MPa)	Splitting tensile strength (MPa)	Flexural strength (MPa)	Static modulus of elasticity (GPa)
Gesoglu et al. (2015a) (w/b=0.3, 0% SF/ w/b=0.3, 10% SF/ w/b=0.43, 0% SF/ w/b=0.43, 10% SF) [30]	RCA GGBFS ² (25%) SF ² (0% for first and third concretes and 15% for second and fourth concretes)	0/0	78	4.3	5.4	26
		100/0	69	3.5	4.3	21
		0/100	62	3.2	4.2	20
		100/100	56	2.7	3.6	17
		0/0	81	4.5	6.5	28
		100/0	70	4.1	5.4	23
		0/100	65	3.6	4.9	21
		100/100	57	3.2	4.3	19
		0/0	67	3.5	4.8	24
		100/0	55	2.9	4.0	21
		0/100	49	2.5	3.8	18
		100/100	46	2.2	3.3	16
		0/0	72	3.8	6.3	25
		100/0	64	3.2	4.8	21
		0/100	61	2.8	4.5	19
100/100	53	2.6	3.8	17		
Aslani et al. (2018) [70]	RCA FA ² (75%) SF ² (19%) GBFS ² (56%)	0/0	25	3.2	-	-
		10/10	34	3.2	-	-
		20/20	33	3.2	-	-
		30/30	31	3.2	-	-
		40/40	34	3.2	-	-
Yasser Khodair (2017) [35]	RCA RAP aggregate ³	0/0	55	5.8	-	-
		25/0	49	5.1	-	-
		50/0	43	4.4	-	-
		75/0	38	4.0	-	-
Silva et al. (2016) [46]	RCA Masonry residue ⁴ (20%)	0/0	36	3.1	-	-
		25/0	32	2.7	-	-
		50/0	32	2.7	-	-
		75/0	33	2.4	-	-
		100/0	30	2.3	-	-

² Percentages with respect to the amount of cement added to the mix

³ Values indicated in the third column "coarse/fine RCA content" are the sum of the percentages of RCA and RAP aggregates

⁴ Percentages with respect to total amount of filler

Grdic *et al.* (2010) [53] aimed to compensate the extra RCA water absorption and to maintain a uniform effective w/c ratio for the different percentages under study (50% and 100% of the coarse fraction). They observed a decrease in the compressive strength as the RCA content increased when the mixtures were designed with a uniform effective w/c ratio.

Assaad (2017) [63] obtained SCC samples of lower compressive strengths, by adding a high content of coarse RCA, at a constant w/c ratio. The Direct Replacement (DR) method increased the strength of the mixtures.

The incorporation of low amounts of fine RCA in the mix (under 20%) appeared to have no appreciable effect on compressive strength, according to the studies of Manzi *et al.* (2017) [37], who used fine RCA percentages between 12% and 19%. Those results were corroborated by Campos *et al.* (2018) [28], who used a percentage substitution of 20% for fine and coarse RCA, and obtained a decrease in the compressive strength of only 5%, mainly attributed to the fine RCA.

Nevertheless, the same effect was more pronounced at higher substitutions, as Carro-López *et al.* (2015) [52] demonstrated with 100% percentage substitution of fine RCA and a constant w/c ratio, which reduced the compressive strength to around 40%.

According to the studies evaluated, a concrete with coarse RCA and a good compressive strength can be obtained by using a high-quality RCA and reducing the effective w/c ratio.

Other authors have analyzed the performance of SCC with RCA and some different mineral admixtures to replace part of the cement. Boudali *et al.* (2016) [27] and Omrane *et al.* (2017) [38] analyzed the addition of natural pozzolans. The results showed that the addition of this admixture, together with RCA, decreased the compressive strength more than with only RCA. Omrane *et al.* (2017) [38] showed that the substitution of 15% cement by natural pozzolan decreased concrete compressive strength by around 24%, while the joint use of 15% natural pozzolan and a blend of 50% fine and coarse RCA decreased compressive strength by around 30%, while the amount of water in each mix was maintained at a constant level.

5.1.2. SCC WITH RCA AND OTHER WASTES (FLY ASH, SILICA FUME, RECYCLED ASPHALT PAVEMENT AGGREGATES, RUBBER GRANULES, SLAGS)

In various studies, the addition of FA in substitution of cement produced a much more pronounced reduction in compressive strength than the use of RCA alone [43], both with only coarse RCA [45] and with fine and coarse RCA [36]. This latter combination of coarse RCA, fine RCA and FA produced the lowest compressive strength. The compressive strength could be recovered to some degree by adjusting the effective w/c ratio, although never as effectively as when only using RCA.

Vinay Kumar *et al.* (2017) [51] obtained higher compressive strengths than the control concrete with 33% FA in proportion to the cement mass for low RCA substitution percentages (20% coarse RCA, 20% fine RCA or 20% of both jointly). The increase in strength was around 6% and the maximum increase was linked to the use of only coarse RCA (7.3%).

The optimal packing of aggregate particles produced in an Eco-SCC was beneficial for compressive strength when RCA and FA were used [69]. It is noticeable that the compressive strength of the mixture with 50% of RCA increased around 17% with respect to the control mix.

The joint use of RCA, FA, and SF led to similar results, however, SCRC with higher strengths than the reference concrete was achieved at high replacement percentages up to 75% [48], maintaining the effective w/c ratio at a constant level [77]. The authors attributed this performance to the use of SF.

Gesoglu *et al.* (2015a) [30] analyzed an SCC manufactured with coarse and fine RCA and SF. It was observed that concrete with 10% SF increased compressive strength by approximately 10%, compared to SCC with the same percentage of RCA and no SF [33].

As indicated in subsection 4.2, Yasser Khodair *et al.* (2017) [35] and Aslani *et al.* (2018) [70] designed a concrete with several wastes: RCA, RAP aggregate, rubber granules, FA, GGBFS, and SF in many different combinations. From all these combinations, some conclusions may be drawn. Firstly, the joint use of RCA and RAP aggregates or RCA and rubber granules had the same performance as RCA alone: the higher the substitution rate, the lower the compressive strength; although this effect was sometimes compensated by additional water with a different result in each case. In contrast, GGBFS appeared to have a better effect than FA. Finally, the effect of SF appeared to be unaffected by the addition of other waste apart from RCA. Nevertheless, the strength performance is unpredictable in multiple residues combination, and, an in-depth and individual specific investigation into each combination is necessary.

Neither masonry residue [46] nor marble waste [49] appeared to affect the compressive strength of the SCC with RCA. The addition of recycled ceramic waste in powder form reduced the compressive strength, although this decrease can be compensated for by reducing the water content if this waste has a high particle content of less than 10 μm in size [72].

5.1.3. SCC WITH RCA AND FIBERS

Finally, recycled FRSCC can be analyzed. As expected, a higher compressive strength was obtained for the concrete with fibers than for the concrete without fibers. This strength increased as the proportion of fibers increased [78], and it decreased as the percentage of RCA increased [39].

In addition, Mohseni *et al.* (2017) [54] noted that the effect of steel fibers on compressive strength was far more noticeable than the effect of PP fibers, although the joint use of both fiber types yielded even higher strengths.

5.1.4. COMPRESSIVE STRENGTH CONCLUSIONS

The compressive strengths noted in the works on SCC manufactured with only RCA and with both RCA and FA are represented in Figure 1.3; the abscissa of the graph reflects the coarse RCA substitution rate. The values can also be observed in a summary of the results in Table 1.5.

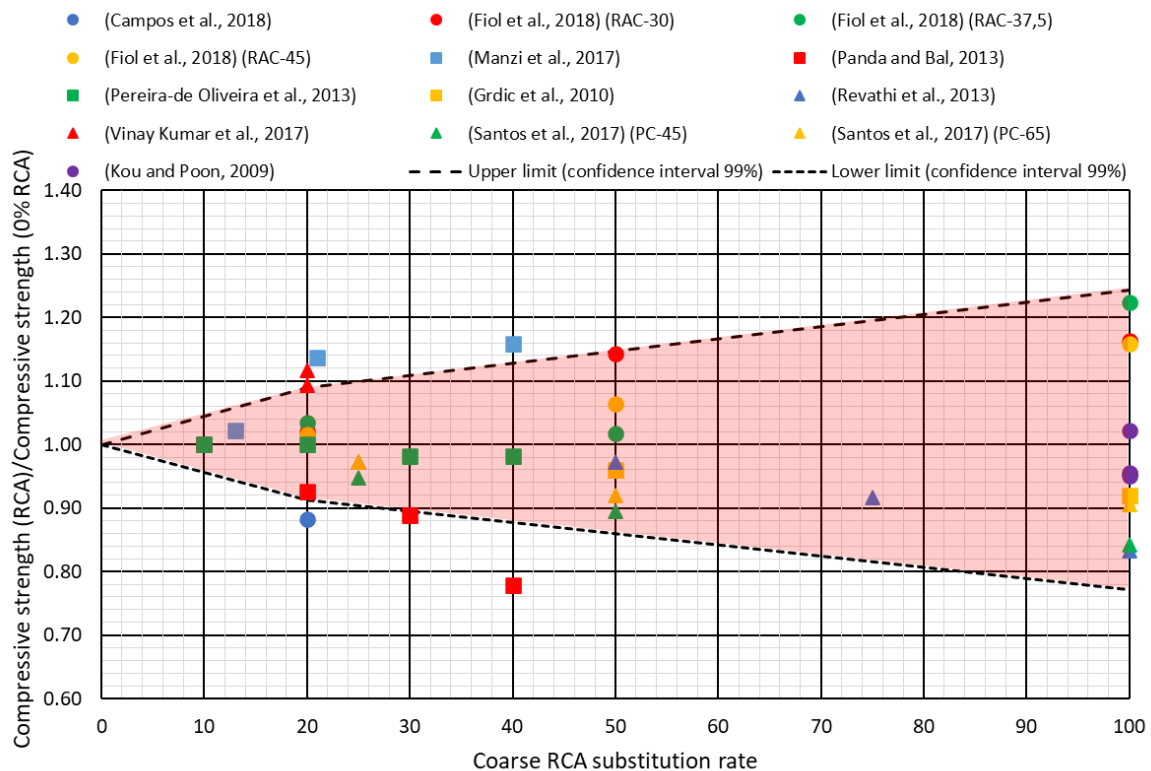


Figure 1.3. Compressive strength evolution as a function of coarse RCA substitution rates (99% confidence interval)

Some conclusions can be established from the above data that are valid for SCC manufactured with RCA and, optionally, with a reduced percentage of FA:

- A clear trend for the effect of the coarse RCA on the concrete compressive strength cannot be established. There is a high dispersion of the compressive strength values for a certain replacement rate of coarse RCA in the different studies, with values both above and below those of the reference concrete. Moreover, the higher the amount of RCA, the greater dispersion, which shows that the uncertainty increases with the RCA replacement rate. The variables that cause this dispersion are different, such as the origin and quality of the recycled

aggregate, the amount of adhered mortar and the compressive strength of the concrete of origin.

- In spite of the aforementioned dispersion, most of the values are within the limits of the confidence interval. These results show that despite the absence of a clear trend, the compressive strength of the concrete with coarse RCA can be delimited. The values that are not within that interval usually corresponded either to studies that presented low-quality RCA [40], to studies that included both coarse and fine RCA [28, 37] or to studies in which RCA and FA is used jointly [51] in which the fine fraction appeared to intensify the dispersion, increasing or decreasing the compressive strength beyond expected levels.
- The substitution of NA by RCA may be expected to decrease compressive strength. Nevertheless, an SCC of greater compressive strength than non-recycled concrete was achieved in three different studies [29, 37, 51], as can be seen from Figure 1.3. This behavior is because the w/c ratio was held constant, so the high absorption of the RCA caused a lower effective w/c ratio. The negative effect of the RCA on compressive strength can very simply be compensated by adjusting the dosage. These factors also favor the dispersion that is mentioned above.

No general conclusions can be drawn with regard to the effect of fine RCA, because the studies that evaluate its use are very scarce and, as with coarse RCA, all the results are highly dispersed. The absence of studies on the behavior of fine RCA may be due to the widely accepted fact that their effects are harmful in non-SCC, based on different studies [21] and their use is strictly limited in standards and regulations [14].

5.2. SPLITTING TENSILE STRENGTH AND FLEXURAL STRENGTH

Splitting tensile strength and flexural strength values are also affected by the replacement of NA for RCA with other waste co-products, which will be evaluated in this section.

5.2.1. SCC WITH RCA

In all studies on the use of RCA alone, the reference SCC manufactured with NA achieved the highest splitting tensile strength [53]. The higher the substitution rate, the lower the splitting tensile strength [40]. In that case, the splitting tensile strength was not related to the effective w/c ratio as much as the compressive strength [29], so that strength value could not be compensated by decreasing the effective w/c ratio [37].

Flexural strength behavior [29] appeared very similar to splitting tensile strength behavior in various studies [40]. As a property, it is rarely analyzed in the different research lines, because it is largely conditioned by the segment of the test sample that is placed under traction.

5.2.2. SCC WITH RCA AND OTHER WASTES (FLY ASH, SILICA FUME, RECYCLED ASPHALT PAVEMENT AGGREGATES, RUBBER GRANULES, SLAGS)

The behavior of concrete manufactured with both RCA and FA can be inconsistent, mainly due to weaker bonding between the RCA and the FA than between the RCA and the cement matrix.

In all the referenced studies in which RCA and FA were jointly examined [36], similar behaviors for splitting tensile strength and for compressive strength were observed: weaker strengths with higher additions of RCA [43]. However, unlike concretes with only RCA, the reduction of an effective w/c ratio in concretes with both RCA and FA appeared to compensate the overall decrease in strength as the RCA content increased [51], but only if the replacement percentage of RCA was low (less than 20%). At higher RCA rates, that reduction will no longer be compensated and when the amount of RCA increases, the strength will decrease too [45].

The behavior of concrete with combinations of either RCA, FA and SF or with RCA and SF was stable. The splitting tensile strength presented very similar performance to the compressive strength,

increasing the strength without reducing the effective w/c ratio [48], although again only at low RCA contents, no higher than 25% [30].

Revathi *et al.* (2013) [43] presented a study on coarse RCA and FA, in which they observed lower flexural strengths, due to the additions of FA, as the percentage of coarse RCA increased. For instance, the flexural strength of a concrete with 25% coarse RCA and 56% FA (as a proportion of the cement mass) decreased by around 17% in relation to the reference concrete. However, in a concrete with 100% coarse RCA, that decrease was around 59%. Gesoglu *et al.* (2015a) [30] observed the same performance in a concrete with only RCA and SF.

The influence of the other wastes on the splitting tensile strength and flexural strength values was similar to their effect on compressive strength. Masonry and marble waste appeared to have no influence [46], unlike RCA, the effects of which appeared to be fundamental [49]. Recycled ceramic waste in powder form affected compressive strength in a similar way to flexural strength [72]. In comparison with FA, slag was found to reduce any decrease in strength compared to FA [35] and multi-material SCRC showed no clear pattern of behavior in the analysis by Aslani *et al.* (2018) [70].

5.2.3. SCC WITH RCA AND FIBERS

The use of fibers can compensate the decrease in splitting tensile strength and flexural strength that is produced by the addition of RCA and, in some cases, RCA concrete can have a greater strength than the reference SCC specimen: the addition of 0.5% vol. of fibers was found to compensate the strength loss caused by increases of up to 40% in RCA content [74]. Mohseni *et al.* (2017) [54] found once again that strength improvements were better with steel rather than with PP fibers, although the joint use of both fiber types produced higher strengths. The formulas for flexural strength values included in the standards provided results that were in line with the empirical values [39].

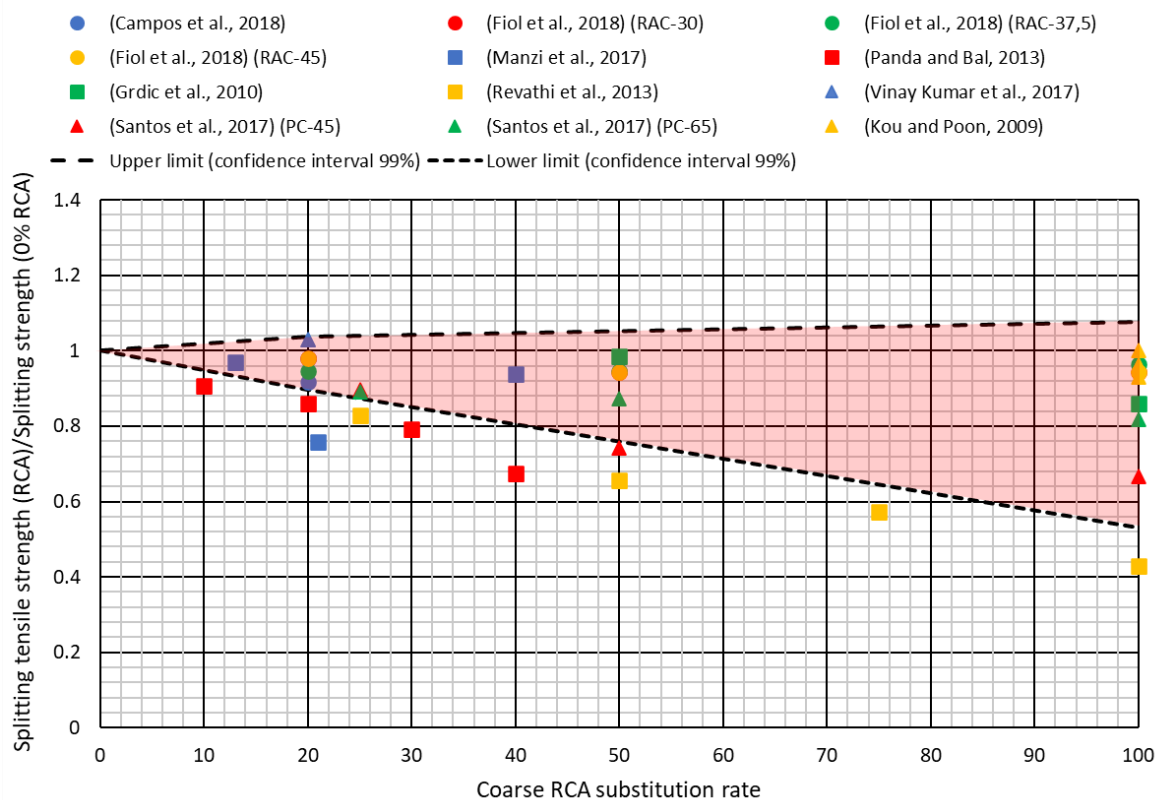


Figure 1.4. Splitting tensile strength evolution as a function of coarse RCA percentage substitutions (99% confidence interval)

5.2.4. GENERAL CONCLUSIONS

The evolution of splitting tensile strength is shown in Figure 1.4 as a function of the percentage substitution of NA by coarse RCA. Flexural strength is not represented, due to a scarcity of data, but its behavior is expected to mirror the behavior of splitting tensile strength. Table 1.5 also shows the values used in this graph.

- Firstly, a clear downward trend of splitting tensile strength can be globally observed as the percentage of RCA increases (most strength ratios between the SCRC and the reference concrete were less than one). The lower limit of the interval clearly reflects this trend.
- Secondly, the values show a high dispersion for each RCA replacement rate. Moreover, in this case, the points of the four studies below the lower limit of the confidence interval [37, 40, 43, 45] cannot all be justified with the use of fine RCA, as opposed to compressive strength.

Once again, the scarcity of studies on fine RCA means that its effect of the strength of SCC cannot be assessed. However, the detrimental effect of fine RCA on the splitting strength on non-self-compacting concretes, even more so than on their compressive strength, has been demonstrated [19].

5.3. MODULUS OF ELASTICITY

The modulus of elasticity defines the deformational behavior of concrete in the elastic zone. It is used to estimate stiffness and, consequently, stress and strain distributions within structural components should be carefully studied, bearing in mind the effects of RCA.

5.3.1. SCC MADE WITH RCA

Pereira-De-Oliveira *et al.* (2013) [76] and Fiol *et al.* (2018) [29] assessed the dynamic modulus of elasticity in an SCC manufactured with coarse RCA. Both concluded that the modulus of elasticity was lower (albeit only marginally), at higher percentages of RCA. According to Fiol *et al.* (2018) [29], the decrease was around 9% for 100% coarse RCA. The relationship between the dynamic and the static moduli, at approximately between 60% and 70%, was similar to other studies.

The performance of the static modulus of elasticity was evaluated by Fiol *et al.* (2018) [29] and Campos *et al.* (2018) [28]. It was very similar to the dynamic modulus described above, in both cases descending as the proportion of RCA increased. However, the static modulus was even higher than that of the control concrete, at low RCA percentages. In addition, the decrease in the static modulus was slightly lower at high RCA ratios than the dynamic modulus of elasticity, e.g. for 100% of RCA, the decrease was around 6% [29]. Nevertheless, Manzi *et al.* (2017) [37] obtained values that were 4% higher than those of the control concrete at 100% replacement percentages.

It can be concluded from the above that the modulus of elasticity does not depend heavily on the RCA content, but on the RCA and its properties (the quality of the RCA, roughness, amount of attached mortar...). In addition, whenever a high modulus of elasticity was obtained, it was evidence of good adhesion between the old and the new mortars.

Interestingly, the lineal relationship between the compressive strength and modulus of elasticity was maintained [79], regardless of the percentage substitution or the RCA fraction in use [80].

5.3.2. SCC WITH RCA AND OTHER WASTES (FLY ASH, SILICA FUME, RECYCLED ASPHALT PAVEMENT AGGREGATES, RUBBER GRANULES, SLAGS)

If FA is added to the mix, the decrease in the modulus of elasticity is much more noticeable, because of the worse adherence of the aggregate to the FA than to cement [45]. These authors obtained a decrease of around 15% with respect to the control concrete. The addition of SF to concrete containing RCA led to a lower decrease of the modulus of elasticity [30], so the adverse effect of

the addition of FA can be compensated by the addition of SF, leaving any decrease in the modulus of elasticity at around 10% [48].

In addition, Gesoglu *et al.* (2015a) [30] established that the modulus of elasticity in an SCC with RCA and SF continued to show a linear relationship with the compressive strength, as in the case where only RCA is used.

According to Uygunođlu *et al.* (2014) [49], the joint use of RCA and marble waste produced a much lower modulus of elasticity. The decrease was around 33%, mainly due to the marble waste, because the decrease was around 8% with only RCA. Moreover, concrete with both wastes was, in consequence, less rigid and fragile. Again, the combinations of other wastes followed no clear pattern, with different values in each case [70].

5.3.3. SCC WITH RCA AND FIBERS

Ortiz *et al.* (2017) [39] affirmed that the content, particle size, and nature of RCA have a greater impact on the value of the modulus of elasticity than on the other mechanical properties analyzed above (compressive strength, splitting tensile strength...), mainly because of the configuration of the granular skeleton. So, the addition of fibers in this case could not compensate the decrease caused by the RCA, producing only a negligible improvement.

5.4. VOLUMETRIC PROPERTIES AND OTHERS

The density of hardened SCC manufactured with RCA and, optionally, with other wastes, has been evaluated in several research works. Pereira-De-Oliveira *et al.* (2013) [76] and Fiol *et al.* (2018) [29] manufactured their concrete with only coarse RCA and, for all the substitution percentages, found that the density of the concrete decreased slightly as the substitution percentage increased, by around 0.5% for 25% RCA, and, by around 3% for 100% RCA, regardless of the compressive strength of the concrete. The addition of FA to the mixture slightly intensified the decreased density, by an additional decrease of around 1%, due to the lower specific weight of FA with respect to the cement [45]. Either masonry residue [46] or fibers at low percentages of around 0.5% [39] hardly appeared to affect this property. The concrete density was mainly dependent on the RCA.

The density is highly related to the porosity of the concrete. Fiol *et al.* (2018) [29] reported that, for a 100% substitution percentage of coarse RCA, open porosity increased by around 1.5-1.8%. In addition, Manzi *et al.* (2017) [37] observed that the higher the flowability in the fresh state, the lower the open porosity.

Ultrasonic Pulse Velocity (UPV) is, in turn, related to the measurement of both porosity and the quality of any Interfacial Transitions Zones (ITZ) present in the concrete that hinder the UPV wave propagation. It also depends on the density of the concrete. This property decreased with larger amounts of RCA. Fiol *et al.* (2018) [29] found that UPV reduction was, on average, around 4%. Other wastes combined with RCA, such as masonry [45] and marble [49], had negligible effects compared to the use of RCA by itself.

Abrasion resistance and fracture energy [79] were analyzed in a concrete with both RCA and FA [48]. Once again, their values were lower when the RCA substitution rate increased, but an increase in FA improved those properties [45]. In contrast, the use of SF, jointly with RCA, caused a more brittle behavior (low characteristic length) [30].

Velay-Lizancos *et al.* (2016; 2017) [50, 81] analyzed the influence of temperature on the compressive strength of SCC. They found that the higher the substitution percentage, the greater the difference in strength at different temperatures, with an optimum of 20 °C at all ages.

6. DURABILITY

In Table 1.6, durability and other long-term properties evaluated by the main articles in this review are shown, followed by a discussion of their results.

Table 1.6. Durability properties analyzed by different research lines

Research	Waste used	Durability properties analyzed
Grdic et al. (2010) [53]	RCA	Water absorption
Fiol et al. (2018) [29]	RCA	Water absorption
Pereira-De-Oliveira et al. (2014) [41]	RCA	Permeability
Boudali et al. (2016) [27]	RCA	Resistance to sulphate attack Compressive strength after sulphate attack (immersion-drying cycles and total immersion)
Manzi et al. (2015; 2017) [37, 84]	RCA	Creep Drying shrinkage Shrinkage
Salesa et al. (2017) [44]	Multi-RCA	Water absorption
Omrane et al. (2017) [38]	RCA Natural pozzolan	Resistance to penetration of chloride ions Resistance to sulphate attack
Santos et al. (2019b) [68]	RCA FA	Water absorption Capillary absorption Oxygen permeability Resistance to penetration of chloride ions Electrical resistivity Carbonation depth
Rajhans et al. (2018a; 2018b) [42, 85]	RCA FA	Water penetration depth Resistance to penetration of chloride ions Carbonation depth Creep Drying shrinkage
Kou and Poon (2009) [36]	RCA FA	Penetration of chloride ions Drying shrinkage
Vinay Kumar et al. (2017) [51]	RCA FA	Resistance to sulphate attack Resistance to acid attack
Singh and Singh (2016) [47]	RCA FA Metakaolin	Carbonation depth
Singh, N. and Singh, S.P. (2018) [86]	RCA SF	Carbonation depth
Yasser Khodair (2017) [35]	RCA RAP aggregate	Permeability Drying shrinkage Shrinkage
Silva et al. (2016) [46]	RCA Masonry residue	Water absorption Percentage of voids Capillarity absorption
Gesoglu et al. (2015b) [87]	RCA SF	Water absorption Water permeability Gas permeability Resistance to penetration of chloride ions
Kapoor et al. (2016; 2017; 2018) [33, 88, 89]	RCA SF Metakaolin	Water absorption Penetration of chloride ions
Mohseni et al. (2017) [54]	RCA (FRSCC)	Water absorption Penetration of chloride ions

6.1. SCC WITH RCA

It is widely acknowledged that in vibrated concretes [82], the mortar attached to the RCA has a negative effect on the water absorption of the manufactured concrete. That effect is due to the non-hydrated cement present in the attached mortar, which increases the water absorption levels of the concrete manufactured with RCA. An effect that is accentuated when using fine RCA [83].

The same behavior was observed in various studies in the case of the SCC mixes. Coarse RCA with low amounts of adhered mortar implied slightly higher water absorption values [29], while high amounts of that mortar mean the concrete will have higher water absorption values [53]. The water absorption values of multi-recycled SCC were found to be higher in accordance with the number of times it had been recycled [44].

Pereira-De-Oliveira *et al.* (2014) [41] analyzed water permeability, capillarity coefficients, and water penetration. From their results, the authors affirmed that the addition of RCA was favorable because the non-hydrated cement present in the mortar adhering to the RCA built up some barriers in the porous structure reducing the water movement. Moreover, preconditioning of aggregates (pre-soaking) originated a higher number of pores and higher water absorption by capillarity.

Omrane *et al.* (2017) [38] designed SCC manufactured with coarse and fine RCA (in equal percentages of 50%) and a natural pozzolan. Two durability characteristics were evaluated: resistance to the penetration of chloride ions (full immersion) and resistance to H₂SO₄ attack. For both tests, the concrete with higher amounts of RCA and natural pozzolan experienced lower levels of penetration of that type of ion.

Boudali *et al.* (2016) [27] evaluated the exposure of concrete samples to sulphate attack. All the tests that were performed, showed that SCRC presented a better behavior than the reference SCC. Again, this improvement was explained by the continuity of the matrix hydration reaction (due to the non-hydrated cement adhered to the aggregate), which created barriers that prevented the passage of external agents. The voids were filled by the hydrated cement, which increased the compressive strength, despite the attack of those agents.

6.2. SCC WITH RCA AND OTHER WASTES (FLY ASH, SILICA FUME, RECYCLED ASPHALT PAVEMENT AGGREGATES, RUBBER GRANULES, SLAGS)

Santos *et al.* (2019b) [68] evaluated water absorption, by both total immersion and capillarity, in mixtures with RCA and FA at different ages (28, 91 and 182 days). The water absorption level increased with increased amounts of RCA and the mixes with 100% coarse RCA and 0% fine RCA improved the behavior of the mixture with 50% of both fine and coarse RCA. Neither FA [42, 85] nor sulphate attack [51] appeared to influence water permeability.

In contrast, FA increased the effect of the fine RCA in some properties [51], such as the chloride penetration test [36]. The tests carried out by Santos *et al.* (2019b) [68] also showed a similar performance against chlorides attack. The mixes with high amounts of coarse RCA improved the performance of mixtures with low percentages of fine RCA. In addition, according to the aspects discussed in the previous section, FA seems to amplify this negative effect. In relation to oxygen permeability, this effect was not so noticeable, but it also existed. From the comments in this paragraph and in section 6.1, it can be affirmed that coarse RCA leads to a lower SCC deterioration by chloride ions than fine RCA, especially if FA is added to the mix.

Kapoor *et al.* (2017) [88] evaluated chloride ion penetration in a SCC with coarse and fine RCA, FA and 10% metakaolin as cement replacement. The resistance to chloride penetration of the mix with 100% RCA and 10% metakaolin was higher than that of the control mix (without metakaolin). In addition, the joint use of fine RCA and metakaolin reduced the initial absorption rate of water.

The electrical resistivity of SCC [68] is lowered by the addition of RCA [47]. Depending on the application, this effect may be either positive or negative.

The carbonation process of SCC jointly manufactured with RCA and FA was also assessed in various studies [90]; the results showed that the greater the percentage substitution, the deeper the carbonation depth. An observation that was attributed to the attached mortar, because the mortar adhering to RCA can have many micro cracks, voids, and pores that facilitate carbonation processes [42, 85]. In addition, the performance of coarse RCA was improved over time, with carbonation depth becoming similar to that of control concrete at 182 days, especially in mixtures with high cement content [68]. Moreover, the addition of FA appeared to produce a negative effect, increasing that penetration index. However, the effect of each waste (RCA and FA) could not be separately quantified. As a final point, the authors proposed the existence of a linear relationship between the depth of carbonation and the compressive strength, which was valid at any age, and for concretes with both RCA and FA [90].

In an SCC with no RCA, SF fills up all the pores and cracks, and has a waterproofing effect on the aggregate particles. This waterproofing effect occurs to a greater extent in concrete with RCA. It all reduces porosity and hinders water circulation [42, 85]. In addition, the improvement was notably greater as the concrete aged; from 0 to 60 days a certain improvement occurred, but from 60 to 120 days, the improvement was twice as effective [33, 91]. However, SF could not compensate all the negative effect caused by RCA [87].

Other observations suggested that the masonry residue appeared to have no influence on the durability performance of the concrete [46]. Moreover, while GGBFS is detrimental to any resistance to chloride ion penetration, RAP aggregate increased this resistance, which can be attributed to the highly viscous asphalt mortar and binder surrounding the RAP aggregate [35].

6.3. SCC WITH RCA AND FIBERS

In their study, Mohseni *et al.* (2017) [54] determined that the incorporation of fibers within the concrete mixes had no notable effect on water absorption; in contrast, fiber addition did indeed affect chloride ion penetration. The chloride ion penetration resistance of a concrete with RCA and fibers decreased when the amount of RCA increased, while in the case of concrete with RCA, but no fibers, the effect was the opposite. This contrary effect was attributed to the high conductivity of the fibers incorporated in the mixture. The effect of either steel fibers or PP fibers separately was similar, although the effect of steel fibers was slightly worse, due to their higher conductivity, and a combination of both fiber types provided the best solution.

7. LONG-TERM PROPERTIES: SHRINKAGE AND CREEP

Shrinkage and creep define the long-term deformational behavior of concrete and the effect upon those two parameters of RCA is important, due to its high water-absorption level. The main studies on these properties will be discussed in this section.

7.1. SHRINKAGE

Highly influenced by the hydration process, shrinkage is more pronounced during the first hours and days, due to the hydration reaction of the cement – known as drying shrinkage. Subsequently (around a week after the hydration), long-term shrinkage commences. Although very slight compared to the previous shrinkage process, long-term shrinkage lasts throughout the whole life of the concrete, tending towards an asymptotic value [19]. This shrinkage process is similar for SCC, although the higher content of water and the use of different kinds of superplasticizers, among other aspects [92], means that shrinkage is usually more pronounced in SCC than in conventional concrete [93].

Manzi *et al.* (2015; 2017) [37, 84] observed that the drying shrinkage experienced by all the concretes was the same regardless of the amount of coarse RCA. Kou and Poon (2009) [36] and Rajhans *et al.* (2018a; 2018b) [42, 85] found that the higher the percentage substitution of NA by coarse RCA, then the greater the water absorption and the higher the drying shrinkage of the concrete. That result contradicted the findings of Manzi *et al.* (2015; 2017) [37, 84], which may either be because the effective w/c ratio remained constant or it may be due to the addition of FA, which formed a less compact paste with more pores and voids, facilitating the absorption of water, and leading to greater shrinkage.

On the contrary, the greater the amount of fine RCA, then the greater the drying shrinkage, which could be due to the high water absorption of fine RCA [36]. After two months (long-term shrinkage), the shortening was slightly higher for the control SCC (only NA) and for the concrete with low substitution rates of RCA (25% RCA) than for concretes with high RCA percentages (50%, 75% and 100% RCA) [36]. The presence of non-hydrated cement in the mortar adhered to the aggregates caused a decrease of the effective w/c ratio, which led to less excess water and, in brief, to less shrinkage. In contrast, SF appeared to decrease shrinkage [87], an effect also produced by the addition of recycled ceramic waste in powder form of a very small size [72]. As opposed to FA and SF, which affected shrinkage, neither RAP aggregate nor slag appeared to have any effect on that property [35].

7.2. CREEP

Both creep and shrinkage behavior were very similar: very intense at first, when the effects were more pronounced, followed later on by stabilization.

However, Manzi *et al.* (2015; 2017) [37, 84] noted a remarkable long-term difference between shrinkage and creep. On the one hand, shrinkage was almost the same for all the concretes, regardless of the RCA percentage of substitution. On the other hand, the creep levels of the concretes with different RCA contents were very different, although the concretes with a higher creep were still those with a lower RCA content, as with the study on shrinkage.

The addition of FA led to a greater difference regarding creep strain between concretes with different RCA substitution rates. Separate addition of the components in the mixing process were again demonstrated to produce a concrete with better characteristics and lower creep [42, 85].

8. STRUCTURAL ELEMENTS: BEAMS AND COLUMNS

Li *et al.* (2011; 2012) [94, 95] tested the flexural strength of different beams manufactured with coarse RCA. In all cases, the performance of the RCA beams was quite similar to those made with NA. The cement and RCA bonds were good, although the use of this kind of aggregate led to a lesser stiffness and to a larger mid-span deflection [96].

Later on, Li *et al.* (2018) [97] evaluated the performance of three reinforced concrete beams under flexural testing. Each beam was manufactured with a different replacement rate of coarse RCA in the SCRC dosage: 70%, 85% and 100%. The authors found that the crack development process in the beams manufactured with RCA was the same as that of the reference concrete beam. The crack distribution of the 85%-beam was more uniform than in the 100%-beam and the 70%-beam. A result that was explained, on one hand, by the many micro-cracks and minor defects found in the coarse RCA, which meant that the 100%-beam had more cracks where there were high concentrations of RCA. On the other hand, the higher quality of the coarse NA in the 70%-beam explained why the highest number of cracks were found in the regions where the RCA was concentrated, avoiding the regions with NA.

Another interesting aspect analyzed by Li *et al.* (2018) [97] was that the plane section assumption could also be used as the basis for the theoretical calculation of SCC with RCA beams. It is

remarkable that the failure loads of the three beams were very similar: the failure load decreased slightly as the percentage substitutions increased and was consistent with the overall conclusions on the compressive strength of SCRC. Nevertheless, the real moment of failure was higher than the theoretical moment, at both high and low RCA replacement percentages, an observation that was also noted in the investigations of Jagannadha Rao *et al.* (2012) [98] and Gao *et al.* (2018) [99], thereby demonstrating the suitability of this concrete for structural use. Finally, the maximum crack width between the coarse RCA beams and the coarse NA beams manufactured with SCC appeared not to make a significant difference

Velay-Lizancos *et al.* (2018) [100] analyzed eight similar beams in flexural and shear tests. Four types of concrete were designed, with the same percentage of coarse RCA and fine RCA in each of them: M-0, with 0% coarse and fine RCA; M-20, with 20% coarse and fine RCA; M-35, with 35% coarse and fine RCA and M-50, with 50% coarse and fine RCA. The study sought to compare the results obtained experimentally in the beams with those obtained by means of two calculation methods: a traditional method, applying the expressions collected in EC-2 (2010) [101] and EHE-08 (2010) [14], and a modern Finite Element Method (FEM) [102]. As a general conclusion, it was established that traditional methods were quite valid, at low substitution percentages, that are very often used with conventional concrete. At higher percentages (over 50%), more complete methods such as the FEM should be used, due to the loss of precision of the traditional methods.

Tanaka *et al.* (2002) [103] and Zhou *et al.* (2011) [104] concluded that the performance of SCC columns with RCA and different kinds of reinforcements was similar to that of RCA vibrated concrete columns [105], because of the predominantly similar levels of compressive strength in both.

9. OTHER RELEVANT ASPECTS

Non-destructive methods (e.g., hammer rebound test) were also valid for SCC with RCA, so that in structures already built with these types of concretes, those tools can be used to determine the compressive strength “*in situ*”. The linear relationship between compressive strength and those properties could be established [106]. Models that can be used to correlate compressive strength from those indirect measures represent a field of study in which important advances are still possible.

González-Taboada *et al.* (2018c) [107] evaluated the thixotropy of SCRC or variations of its viscosity when agitated and when left to stand in the fresh state. The authors observed that the thixotropic level of change was similar in all the concretes, regardless of the RCA replacement percentage.

Finally, the thermal analysis suggested an appreciable change in thermal behavior in comparison with the reference mix without RCA. For example, Fenollera *et al.* (2015) [108] found that thermal conductivity was reduced by 15% when raising the RCA percentage from 20% to 50%.

10. CONCLUSIONS

Considering the literature on RCA and other industrial wastes reused in SCC that has been reviewed and commented upon in this paper, the following conclusions can be presented:

- The decrease in SCC flowability caused by the high water-absorption levels of RCA, compared to NA, can generally be compensated by the addition of a larger quantities of water.
- The mechanical properties of SCC present high sensitivity to dosage changes, so a decrease in the effective w/c ratio can compensate for the negative effect of the replacement of NA by RCA on these properties. This high sensitivity leads to high dispersion in the overall results, such that no clear trend of the effect of RCA on compressive strength can be

established, as shown in section 5.1.4. In section 5.2.4, the results of splitting tensile strength, a property that was less affected by the water content of the mixture, showed a clearly negative effect of RCA.

- The two previous conclusions show that the negative effect of RCA on flowability and strength can be solved by adjusting the water content. For this reason, it is necessary to define the aspect that should be optimized in the SCC with RCA, since improving one of these aspects leads to worsening of the other. The addition of RCA with other co-products sourced from industrial wastes should be studied on a case-by-case basis, due to the variety of possible behaviors.
- The effect of RCA on both the durability and the long-term behavior of SCC is unclear. Properties such as permeability and carbonation resistance are significantly worsened when RCA is used. However, other studies showed that resistance to sulphate attack or water absorption by capillarity action improved with additions of RCA. This variety may be because some SCCs have a better sealing of the voids of the RCA due to their greater flowability. It is necessary to carry out more studies, to clearly define the influence of RCA and flowability on durability properties.
- The differences between this concrete and conventional concrete in structural elements, for example, with regard to cracking patterns or the validity of FEM, were notable. Although SCC with RCA appears to be a suitable structural material for use in beams and columns, the validity of traditional structural design procedures must be checked on full-scale elements. Following that strategy, these co-products may be widely added to concrete mixes used for the construction of many common structures.

Currently, the development of a more sustainable construction sector is essential. If the pressure on natural resources is to be reduced, then the reuse of different residues is also essential, as a pathway that has to be followed. In this particular case, further research related to the combination of SCC and RCA is still needed. Nevertheless, all the research that has been reviewed represents important advances within this field that all move closer to combining waste products and especially RCA in SCC. The authors of this article wish to express their thanks to all the researchers for their studies and their important contributions to progress in this field and would urge them to continue with their valuable research.

REFERENCES

- [1] M. Sandanayake, G. Zhang, S. Setunge, Estimation of environmental emissions and impacts of building construction - A decision making tool for contractors, *J. Build. Eng.* 21 (2019) 173-185.
- [2] C.T. Marques, B.M.F. Gomes, L.L. Brandli, Consumo de água e energia em canteiros de obra: um estudo de caso do diagnóstico a ações visando à sustentabilidade diagnosis to actions aiming at sustainability, *Amb. Constr.* 17 (4) (2017) 79-90.
- [3] L.P. Thives, E. Ghisi, Asphalt mixtures emission and energy consumption: A review, *Renew. Sust. Energ. Rev.* 72 (2017) 473-484.
- [4] S.C. Bostanci, M. Limbachiya, H. Kew, Use of recycled aggregates for low carbon and cost effective concrete construction, *J. Clean. Prod.* 189 (2018) 176-196.
- [5] D.G. Carmichael, N.K. Mustaffa, X. Shen, A utility measure of attitudes to lower-emissions production in construction, *J. Clean. Prod.* 202 (2018) 23-32.
- [6] R. Maddalena, J.J. Roberts, A. Hamilton, Can Portland cement be replaced by low-carbon alternative materials? A study on the thermal properties and carbon emissions of innovative cements, *J. Clean Prod.* 186 (2018) 933-942.
- [7] E. Rossi, A. Sales, Carbon footprint of coarse aggregate in Brazilian construction, *Constr. Build. Mater.* 72 (2014) 333-339.
- [8] A.M. Braga, J.D. Silvestre, J. de Brito, Compared environmental and economic impact from cradle to gate of concrete with natural and recycled coarse aggregates, *J. Clean. Prod.* 162 (2017) 529-543.

- [9] D. Soares, J. De Brito, J. Ferreira, J. Pacheco, Use of coarse recycled aggregates from precast concrete rejects: Mechanical and durability performance, *Constr. Build. Mater.* 71 (2014) 263-272.
- [10] M. Jagadeesh, R. Bhuvanewari, B. Preethiwini, P. Magudeaswaran, Experimental study on self compacting concrete contains partially manufactured sand and recycled clay roof tile, *Int. J. Civ. Eng.* 8 (3) (2017) 599-608.
- [11] W.H. Yung, L.C. Yung, L.H. Hua, A study of the durability properties of waste tire rubber applied to self-compacting concrete, *Constr. Build. Mater.* 41 (2013) 665-672.
- [12] B. Preethiwini, S. Bharaniraja, M. Aravindhan, B.B. Pradeep, R. Jothiprasath, Comparative study on durability characteristics of high strength self compacting concrete, *Int. J. Civ. Eng.* 8 (3) (2017) 942-949.
- [13] E.E. Ali, S.H. Al-Tersawy, Recycled glass as a partial replacement for fine aggregate in self compacting concrete, *Constr. Build. Mater.* 35 (2012) 785-791.
- [14] EHE-08, Instrucción de Hormigón Estructural EHE-08, Structural Concrete Regulations, Ministerio de Fomento, Gobierno de España (2010).
- [15] DM-17/01/2018, Technical Standards for Construction, Ministry of Infrastructure and Transport, Italian Government (2018).
- [16] M. Etxeberria, E. Vázquez, A. Marí, M. Barra, Influence of amount of recycled coarse aggregates and production process on properties of recycled aggregate concrete, *Cem. Concr. Res.* 37 (5) (2007) 735-742.
- [17] R.V. Silva, J. de Brito, R.K. Dhir, Fresh-state performance of recycled aggregate concrete: A review, *Constr. Build. Mater.* 178 (2018) 19-31.
- [18] R.V. Silva, J. De Brito, R.K. Dhir, The influence of the use of recycled aggregates on the compressive strength of concrete: A review, *Eur. J. Environ. Civ. Eng.* 19 (7) (2015) 825-849.
- [19] M. Behera, S.K. Bhattacharyya, A.K. Minocha, R. Deoliya, S. Maiti, Recycled aggregate from C&D waste & its use in concrete - A breakthrough towards sustainability in construction sector: A review, *Constr. Build. Mater.* 68 (2014) 501-516.
- [20] H. Guo, C. Shi, X. Guan, J. Zhu, Y. Ding, T.C. Ling, H. Zhang, Y. Wang, Durability of recycled aggregate concrete – A review, *Cem. Concr. Comp.* 89 (2018) 251-259.
- [21] L. Evangelista, J. De Brito, Concrete with fine recycled aggregates: A review, *Eur. J. Environ. Civ. Eng.* 18 (2) (2014) 129-172.
- [22] V. Corinaldesi, G. Moriconi, The role of industrial by-products in self-compacting concrete, *Constr. Build. Mater.* 25 (8) (2011) 3181-3186.
- [23] A. Barbudo, J. De Brito, L. Evangelista, M. Bravo, F. Agrela, Influence of water-reducing admixtures on the mechanical performance of recycled concrete, *J. Clean. Prod.* 59 (2013) 93-98.
- [24] S.A. Santos, P.R. da Silva, J. de Brito, Self-compacting concrete with recycled aggregates – A literature review, 22 (2019) 349-371.
- [25] F. Agrela, M. Sánchez De Juan, J. Ayuso, V.L. Geraldes, J.R. Jiménez, Limiting properties in the characterisation of mixed recycled aggregates for use in the manufacture of concrete, *Constr. Build. Mater.* 25 (10) (2011) 3950-3955.
- [26] M. Safiuddin, U.J. Alengaram, M.M. Rahman, M.A. Salam, M.Z. Jumaat, Use of recycled concrete aggregate in concrete: A review, *J. Civ. Eng. Manag.* 19 (6) (2013) 796-810.
- [27] S. Boudali, D.E. Kerdal, K. Ayed, B. Abdulsalam, A.M. Soliman, Performance of self-compacting concrete incorporating recycled concrete fines and aggregate exposed to sulphate attack, *Constr. Build. Mater.* 124 (2016) 705-713.
- [28] R.S. Campos, M.P. Barbosa, L.L. Pimentel, G.F. Maciel, Influence of recycled aggregates on rheological and mechanical properties of self-compacting concrete, *Rev. Mat.* 23 (1) (2018) e-11964.
- [29] F. Fiol, C. Thomas, C. Muñoz, V. Ortega-López, J.M. Manso, The influence of recycled aggregates from precast elements on the mechanical properties of structural self-compacting concrete, *Constr. Build. Mater.* 182 (2018) 309-323.

- [30] M. Gesoglu, E. Güneysi, H.Ö. Öz, I. Taha, M.T. Yasemin, Failure characteristics of self-compacting concretes made with recycled aggregates, *Constr. Build. Mater.* 98 (2015) 334-344.
- [31] I. González-Taboada, B. González-Fontebo, J. Eiras-López, G. Rojo-López, Tools for the study of self-compacting recycled concrete fresh behaviour: Workability and rheology, *J. Clean. Prod.* 156 (2017) 1-18.
- [32] E. Güneysi, M. Gesoglu, Z. Algin, H. Yazici, Rheological and fresh properties of self-compacting concretes containing coarse and fine recycled concrete aggregates, *Constr. Build. Mater.* 113 (2016) 622-630.
- [33] K. Kapoor, S.P. Singh, B. Singh, Durability of self-compacting concrete made with Recycled Concrete Aggregates and mineral admixtures, *Constr. Build. Mater.* 128 (2016) 67-76.
- [34] O. Kebaili, M. Mouret, N. Arabia, F. Cassagnabere, Adverse effect of the mass substitution of natural aggregates by air-dried recycled concrete aggregates on the self-compacting ability of concrete: Evidence and analysis through an example, *J. Clean. Prod.* 87 (1) (2015) 752-761.
- [35] L. Yasser Khodair, Self-compacting concrete using recycled asphalt pavement and recycled concrete aggregate, *J. Build. Eng.* 12 (2017) 282-287.
- [36] S.C. Kou, C.S. Poon, Properties of self-compacting concrete prepared with coarse and fine recycled concrete aggregates, *Cem. Concr. Comp.* 31 (9) (2009) 622-627.
- [37] S. Manzi, C. Mazzotti, M.C. Bignozzi, Self-compacting concrete with recycled concrete aggregate: Study of the long-term properties, *Constr. Build. Mater.* 157 (2017) 582-590.
- [38] M. Omrane, S. Kenai, E.H. Kadri, A. Ait-Mokhtar, Performance and durability of self compacting concrete using recycled concrete aggregates and natural pozzolan, *J. Clean. Prod.* 165 (2017) 415-430.
- [39] J.A. Ortiz, A. de la Fuente, F. Mena Sebastia, I. Segura, A. Aguado, Steel-fibre-reinforced self-compacting concrete with 100% recycled mixed aggregates suitable for structural applications, *Constr. Build. Mater.* 156 (2017) 230-241.
- [40] K.C. Panda, P.K. Bal, Properties of self-compacting concrete using recycled coarse aggregate, Conference Paper, NUICONE 2012, 51 (2013) 159-164.
- [41] L.A. Pereira-De-Oliveira, M.C.S. Nepomuceno, J.P. Castro-Gomes, M.F.C. Vila, Permeability properties of self-Compacting concrete with coarse recycled aggregates, *Constr. Build. Mater.* 51 (2014) 113-120.
- [42] P. Rajhans, S.K. Panda, S. Nayak, Sustainability on durability of self compacting concrete from C&D waste by improving porosity and hydrated compounds: A microstructural investigation, *Constr. Build. Mater.* 174 (2018) 559-575.
- [43] P. Revathi, R.S. Selvi, S.S. Velin, Investigations on Fresh and Hardened Properties of Recycled Aggregate Self Compacting Concrete, *J. Inst. Eng. Ser. A* 94 (3) (2013) 179-185.
- [44] Á. Salesa, J.Á. Pérez-Benedicto, L.M. Esteban, R. Vicente-Vas, M. Orna-Carmona, Physico-mechanical properties of multi-recycled self-compacting concrete prepared with precast concrete rejects, *Constr. Build. Mater.* 153 (2017) 364-373.
- [45] S.A. Santos, P.R. da Silva, J. de Brito, Mechanical performance evaluation of self-compacting concrete with fine and coarse recycled aggregates from the precast industry, *Materials* 10 (8) (2017) 904.
- [46] Y.F. Silva, R.A. Robayo, P.E. Matthey, S. Delvasto, Properties of self-compacting concrete on fresh and hardened with residue of masonry and recycled concrete, *Constr. Build. Mater.* 124 (2016) 639-644.
- [47] N. Singh, S.P. Singh, Carbonation and electrical resistance of self compacting concrete made with recycled concrete aggregates and metakaolin, *Constr. Build. Mater.* 121 (2016) 400-409.
- [48] W.C. Tang, P.C. Ryan, H.Z. Cui, W. Liao, Properties of Self-Compacting Concrete with Recycled Coarse Aggregate, *Adv. Mater. Sci. Eng.* 2016 (2016) 2761294.
- [49] T. Uygunoğlu, I.B. Topçu, A.G. Çelik, Use of waste marble and recycled aggregates in self-compacting concrete for environmental sustainability, *J. Clean. Prod.* 84 (1) (2014) 691-700.

- [50] M. Velay-Lizancos, I. Martínez-Lage, M. Azenha, P. Vázquez-Burgo, Influence of temperature in the evolution of compressive strength and in its correlations with UPV in eco-concretes with recycled materials, *Constr. Build. Mater.* 124 (2016) 276-286.
- [51] B.M. Vinay Kumar, H. Ananthan, K.V.A. Balaji, Experimental studies on utilization of coarse and finer fractions of recycled concrete aggregates in self compacting concrete mixes, *J. Build. Eng.* 9 (2017) 100-108.
- [52] D. Carro-López, B. González-Fonteboa, J. De Brito, F. Martínez-Abella, I. González-Taboada, P. Silva, Study of the rheology of self-compacting concrete with fine recycled concrete aggregates, *Constr. Build. Mater.* 96 (2015) 491-501.
- [53] Z.J. Grdic, G.A. Toplicic-Curcic, I.M. Despotovic, N.S. Ristic, Properties of self-compacting concrete prepared with coarse recycled concrete aggregate, *Constr. Build. Mater.* 24 (7) (2010) 1129-1133.
- [54] E. Mohseni, R. Saadati, N. Kordbacheh, Z.S. Parpinchi, W. Tang, Engineering and microstructural assessment of fibre-reinforced self-compacting concrete containing recycled coarse aggregate, *J. Clean. Prod.* 168 (2017) 605-613.
- [55] N. Hani, O. Nawawy, K.S. Ragab, M. Kohail, The effect of different water/binder ratio and nano-silica dosage on the fresh and hardened properties of self-compacting concrete, *Constr. Build. Mater.* 165 (2018) 504-513.
- [56] EFNARC, Specification Guidelines for Self-compacting Concrete, European Federation of National Associations Representing producers and applicators of specialist building products for Concrete (2002).
- [57] ACI, 237R-07, Self-consolidating concrete, American Concrete Institute (2007).
- [58] P.O. Modani, V.M. Mohitkar, Performance of recycled aggregates in self compacting concrete, *Indian Concr. J.* 88 (10) (2014) 57-64.
- [59] D. Carro-López, B. González-Fonteboa, F. Martínez-Abella, I. González-Taboada, J. De Brito, F. Varela-Puga, Proportioning, Microstructure and Fresh Properties of Self-compacting Concrete with Recycled Sand, Conference Paper, SCESCM 2016, 171 (2017) 645-657.
- [60] I. González-Taboada, B. González-Fonteboa, F. Martínez-Abella, S. Seara-Paz, Analysis of rheological behaviour of self-compacting concrete made with recycled aggregates, *Constr. Build. Mater.* 157 (2017) 18-25.
- [61] I. González-Taboada, B. González-Fonteboa, F. Martínez-Abella, N. Roussel, Robustness of self-compacting recycled concrete: analysis of sensitivity parameters, *Mater. Struct.* 51 (1) (2018) 8.
- [62] I. González-Taboada, B. González-Fonteboa, F. Martínez-Abella, S. Seara-Paz, Evaluation of self-compacting recycled concrete robustness by statistical approach, *Constr. Build. Mater.* 176 (2018) 720-736.
- [63] J.J. Assaad, Influence of recycled aggregates on dynamic/static stability of self-consolidating concrete, *J. Sustain. Cem. Based Mater.* 6 (6) (2017) 345-365.
- [64] K. Said, M. Belkacem, D. Amina, K. El-Hadj, Effect of recycled concrete aggregates and natural pozzolana on rheology of self-compacting concrete, *Key Eng. Mater.* 600 (2014) 256-263.
- [65] E. Güneyisi, M. Gesoğlu, Z. Algin, H. Yazici, Effect of surface treatment methods on the properties of self-compacting concrete with recycled aggregates, *Constr. Build. Mater.* 64 (2014) 172-183.
- [66] H. Wang, N. Zhang, Assessment of treated recycled concrete aggregates on the properties of recycled-aggregate-self-compacting concrete, *JHIT* 48 (6) (2016) 150-156.
- [67] I. González-Taboada, B. González-Fonteboa, F. Martínez-Abella, D. Carro-López, Self-compacting recycled concrete: Relationships between empirical and rheological parameters and proposal of a workability box, *Constr. Build. Mater.* 143 (2017) 537-546.
- [68] S.A. Santos, P.R. Da Silva, J. De Brito, Durability evaluation of self-compacting concrete with recycled aggregates from the precast industry, *Mag. Concr. Res.* 71 (24) (2019) 1265-1282.

- [69] J. Hu, I. Levi Souza, F. Cortês Genarini, Engineering and environmental performance of eco-efficient self-consolidating concrete (Eco-SCC) with low powder content and recycled concrete aggregate, *J. Sustain. Cem. Based Mater.* 6 (1) (2017) 2-16.
- [70] F. Aslani, G. Ma, D.L. Yim Wan, G. Muselin, Development of high-performance self-compacting concrete using waste recycled concrete aggregates and rubber granules, *J. Clean. Prod.* 182 (2018) 553-566.
- [71] R.B. Singh, B. Singh, Rheological behaviour of different grades of self-compacting concrete containing recycled aggregates, *Constr. Build. Mater.* 161 (2018) 354-364.
- [72] L. Ferrara, P. Deegan, A. Pattarini, M. Sonebi, S. Taylor, Recycling ceramic waste powder: effects its grain-size distribution on fresh and hardened properties of cement pastes/mortars formulated from SCC mixes, *J. Sustain. Cem. Based Mater.* 8 (3) (2019) 145-160.
- [73] B. Jena, K. Sahoo, B.B. Mohanty, Comparative study on self-compacting concrete reinforced with different chopped fibers, *P. I. Civil Eng-Constr. Mat.* 171 (2) (2018) 72-84.
- [74] N. Nalanth, P.V. Venkatesan, M.S. Ravikumar, Evaluation of the fresh and hardened properties of steel fibre reinforced self-compacting concrete using recycled aggregates as a replacement material, *Adv. Civ. Eng.* 2014 (2014) 671547.
- [75] L. Coppola, T. Cerulli, D. Salvioni, Sustainable development and durability of self-compacting concretes, *Conference Paper, ICF113*, (2005) 2226-2241.
- [76] L.A. Pereira-De-Oliveira, M. Nepomuceno, M. Rangel, An eco-friendly self-compacting concrete with recycled coarse aggregates, *Inf. Constr.* 65 (EXTRA 1) (2013) 31-41.
- [77] R.B. Singh, N. Kumar, B. Singh, Effect of supplementary cementitious materials on rheology of different grades of self-compacting concrete made with recycled aggregates, *J. Adv. Concr. Technol.* 15 (9) (2017) 524-535.
- [78] N. Nalanth, P. Vincent Venkatesan, M.S. Ravikumar, Optimization of the mixture proportion of self-compacting concrete using recycled aggregates and steel fibers, 7 (2) (2014) 780-784.
- [79] A. Bordelon, V. Cervantes, J.R. Roesler, Fracture properties of concrete containing recycled concrete aggregates, *Mag. Concr. Res.* 61 (9) (2009) 665-670.
- [80] M. Safiuddin, U.J. Alengaram, M.A. Salam, M.Z. Jumaat, F.F. Jaafar, H.B. Saad, Properties of High-Workability Concrete with Recycled Concrete Aggregate, *Mater. Res.-Ibero-am. J. Mater.* 14 (2) (2011) 248-255.
- [81] M. Velay-Lizancos, J.L. Perez-Ordoñez, I. Martinez-Lage, P. Vazquez-Burgo, Analytical and genetic programming model of compressive strength of eco concretes by NDT according to curing temperature, *Constr. Build. Mater.* 144 (2017) 195-206.
- [82] K.P. Verian, W. Ashraf, Y. Cao, Properties of recycled concrete aggregate and their influence in new concrete production, *Resour. Conserv. Recycl.* 133 (2018) 30-49.
- [83] A. Yacoub, A. Djerbi, T. Fen-Chong, Water absorption in recycled sand: New experimental methods to estimate the water saturation degree and kinetic filling during mortar mixing, *Constr. Build. Mater.* 158 (2018) 464-471.
- [84] S. Manzi, C. Mazzotti, M.C. Bignozzi, Preliminary Studies on the Effect of C&DW on the Long-Term Properties of Sustainable Self-Compacting Concrete, *Conference Paper, CONCREEP 2015*, (2015) 1554-1560.
- [85] P. Rajhans, S.K. Panda, S. Nayak, Sustainable self compacting concrete from C&D waste by improving the microstructures of concrete ITZ, *Constr. Build. Mater.* 163 (2018) 557-570.
- [86] N. Singh, S.P. Singh, Carbonation resistance of self-compacting recycled aggregate concretes with silica fume, *J. Sustain. Cem. Based Mater.* 7 (4) (2018) 214-238.
- [87] M. Gesoglu, E. Güneyisi, H.Ö. Öz, M.T. Yasemin, I. Taha, Durability and Shrinkage Characteristics of Self-Compacting Concretes Containing Recycled Coarse and/or Fine Aggregates, *Adv. Mater. Sci. Eng.* 2015 (2015) 278296.
- [88] K. Kapoor, S.P. Singh, B. Singh, Permeability of self-compacting concrete made with recycled concrete aggregates and metakaolin, *J. Sustain. Cem. Based Mater.* 6 (5) (2017) 293-313.

- [89] K. Kapoor, S.P. Singh, B. Singh, Water Permeation Properties of Self Compacting Concrete Made with Coarse and Fine Recycled Concrete Aggregates, *Int. J. Civ. Eng.* 16 (1) (2018) 47-56.
- [90] N. Singh, S.P. Singh, Carbonation resistance and microstructural analysis of Low and High Volume Fly Ash Self Compacting Concrete containing Recycled Concrete Aggregates, *Constr. Build. Mater.* 127 (2016) 828-842.
- [91] K. Kapoor, S.P. Singh, B. Singh, Evaluating the durability properties of self compacting concrete made with coarse and fine recycled concrete aggregates, *Eur. J. Environ. Civ. Eng.* 2018 (2018) 17.
- [92] F. Fiol, Estudio experimental sobre propiedades mecánicas y de durabilidad de hormigones estructurales autocompactantes con áridos reciclados y su aplicación a la prefabricación, Doctoral Thesis, Universidad de Burgos (2016).
- [93] M. Bocciarelli, S. Cattaneo, R. Ferrari, A. Ostinelli, A. Terminio, Long-term behavior of self-compacting and normal vibrated concrete: Experiments and code predictions, *Constr. Build. Mater.* 168 (2018) 650-659.
- [94] J. Li, X. Qu, L. Wang, C. Zhu, Experimental research on compressive strength of self-compacting concrete with recycled coarse aggregates, *Adv. Mater. Res.* 306-307 (2011) 1084-1087.
- [95] J. Li, X. Qu, H. Chen, L. Jiang, Experimental research on mechanical performance of self-compacting reinforced concrete beam with recycled coarse aggregates, *Adv. Mater. Res.* 374-377 (2012) 1887-1890.
- [96] J. Li, L. Wang, X. Qu, L. Jang, Research on flexural behavior of coarse recycled aggregate-filled plain concrete beam, *Adv. Mater. Res.* 250-253 (2011) 379-382.
- [97] J. Li, T. Guo, S. Gao, L. Jiang, Z. Zhao, Y. Wang, Study on Effects of Different Replacement Rate on Bending Behavior of Big Recycled Aggregate Self Compacting Concrete, *IOP Conf. Ser.: Mater. Sci. Eng.* 322 (2018) 022032.
- [98] K. Jagannadha Rao, V. Bhikshma, P. Rajesh, Flexural behavior of reinforced self compacting concrete beams with recycled aggregate, *J. Struct. Eng.* 39 (4) (2012) 393-398.
- [99] S. Gao, X. Liu, J. Li, C. Wang, J. Zheng, Research on Durability of Big Recycled Aggregate Self-Compacting Concrete Beam, Conference Paper, *IOP Conf. Ser.: Mater. Sci. Eng.* 322 (2018) 032002.
- [100] M. Velay-Lizancos, P. Vazquez-Burgo, D. Restrepo, I. Martinez-Lage, Effect of fine and coarse recycled concrete aggregate on the mechanical behavior of precast reinforced beams: Comparison of FE simulations, theoretical, and experimental results on real scale beams, *Constr. Build. Mater.* 191 (2018) 1109-1119.
- [101] EC-2, Eurocode 2: Design of concrete structures. Part 1-1: General rules and rules for buildings, CEN (European Committee for Standardization) (2010).
- [102] S. Chandra Paul, B. Šavija, A.J. Babafemi, A comprehensive review on mechanical and durability properties of cement-based materials containing waste recycled glass, *J. Clean. Prod.* 198 (2018) 891-906.
- [103] H. Tanaka, H. Ogura, T. Sawamoto, M. Tsuji, Effect of aggregate on concrete strength under tri-axial load, *Zairyo/Journal Soc. Mat. Sci.* 51 (10) (2002) 1067-1072.
- [104] J. Zhou, M. Su, X. Meng, Y. Yang, Recycled self-compacting concrete-filled steel tube stub columns tests, *Journal of Shenyang Jianzhu University (Natural Science)* 27 (2) (2011) 266-271.
- [105] A.-u.-R. Khan, S. Fareed, S. M Shamaim Ali, H. Sajid, M. Mustafa, Behavior of Recycled Aggregate Reinforced Concrete Columns under Uniaxial Loading, Conference Paper, E2S2-CREATE, (2019).
- [106] N. Singh, S.P. Singh, Evaluating the performance of self compacting concretes made with recycled coarse and fine aggregates using non destructive testing techniques, *Constr. Build. Mater.* 181 (2018) 73-84.
- [107] I. González-Taboada, B. González-Fonteboa, F. Martínez-Abella, S. Seara-Paz, Thixotropy and interlayer bond strength of self-compacting recycled concrete, *Constr. Build. Mater.* 161 (2018) 479-488.
- [108] M. Fenollera, J.L. Míguez, I. Goicoechea, J. Lorenzo, Experimental study on thermal conductivity of self-compacting concrete with recycled aggregate, *Materials* 8 (7) (2015) 4457-4478.

Article 2

Effect of fine recycled concrete aggregate on the mechanical behavior of self-compacting concrete

Title: Effect of fine recycled concrete aggregate on the mechanical behavior of self-compacting concrete

Authors: Víctor Revilla-Cuesta, Vanesa Ortega-López, Marta Skaf, Juan M. Manso

Journal: Construction and Building Materials

Year: 2020

Volume: 263

Article number: 120671

DOI: <https://doi.org/10.1016/j.conbuildmat.2020.120671>

Journal classification (2019 JCR ranking data): 11/134 (engineering, civil). First quartile (Q1), first decile (D1)

ABSTRACT

The high flowability of Self-Compacting Concrete (SCC) is achieved by adding large amounts of fine aggregate. Therefore, the addition of fine Recycled Concrete Aggregate (RCA) in this type of concrete can very noticeably change its behavior. SCCs with different percentages of fine RCA (0%, 25%, 50%, 75%, and 100%) and 100% coarse RCA were manufactured in this study, to evaluate their performance, and to analyze the effect of fine RCA in an SCC when a high amount of coarse RCA is also added. Both the fresh properties (flowability, density, and air content) and their mechanical behavior (strengths, non-destructive tests, stress-strain curves, and Poisson coefficient) at different curing ages were studied. These mechanical properties were compared with the values calculated using the formulas from two of the most common structural design standards. High values of strength and modulus of elasticity were obtained up to a fine RCA content of 50%. Additionally, any increase in fine RCA increased flowability and elastic and plastic deformability of the SCC. The theoretical values overestimated the experimental ones by around 25%. From the mechanical point of view, SCC with up to 50% fine RCA could be used for structural applications, although service requirements regarding deformability recommend that its content should be limited to 25%.

Keywords: design values; flowability; mechanical performance at different curing ages; recycled concrete aggregate; self-compacting concrete; stress-strain curves.

1. INTRODUCTION

Construction sector activities are generally characterized as large-scale projects that consume vast amounts of natural resources, something that the production figures of the sector largely reflect. On average, within the European Union, around 2,700 Mt of Natural Aggregate (NA) are placed on the market each year, of which 120 million were consumed in Spain. Moreover, 16 Mt of bituminous concrete, and 22 Mm³ of hydraulic concrete were produced, in 2018, in this country [1]. High levels of resource exploitation have continued over time, leading in some areas to significant scarcities [2].

Construction and Demolition Waste (CDW) represents 34.7% of all building waste generated in Europe, over 800 Mt/year, where the countries with the highest production levels are France and Germany (227 and 207 Mt/year respectively) [3]. In Spain, with the upturn of the construction sector, CDW production exceeded 20 Mt in 2017 [3]. Demolition processes generated around 0.9 t

of CDW per m² of demolished housing, reaching 1.2 t/m² in industrial buildings, 40% of which was deposited in illegal landfill sites [4]. CDWs usually present a mixture of concrete with ceramic residues and glass and/or gypsum, which worsen their behavior as a raw material for other uses [5]. Recycled Concrete Aggregate (RCA), a particular type of CDW, is usually produced from the crushing of selected concrete elements, such as precast concrete rejects, and it demonstrates better mechanical behavior, because it contains fewer contaminants and its properties are less variable [6].

The two above-mentioned problems -scarcity of natural resources and abundance of waste- could be mitigated through a simple strategy: using waste as a raw material in different construction sector applications, in substitution of NA, among which the manufacture of hydraulic and bituminous concretes is notable [7-13]. This strategy would also help to reduce the ecological impact of quarrying as well as the carbon footprint of the construction sector [5, 14-16]. Among the various potential usages of RCA, this study is focused on its validation in the manufacture of Self-Compacting Concrete (SCC).

The total aggregate volume of concrete is 65-70%, making RCA an ideal material for applying the above strategy. In fact, the literature contains several studies of conventional concretes made with proper dosages of coarse RCA that have demonstrated a good behavior [17, 18]. The addition of fine RCA has a more harmful effect, causing a very noticeable decrease in the mechanical properties of the concretes in which it is incorporated [19]. Although there are some studies on high-performance concretes, such as SCC [20], the available bibliography is scarce, fundamentally in relation to fine RCA, a remarkable aspect, considering the importance of the fine aggregate fractions within this type of concrete [21].

The aspects commented on above are due to the particular characteristics of RCA. The coarse fraction of RCA, which is larger than 4 mm, is mainly characterized by three interrelated aspects. Firstly, the mortar adhering to the surface of the RCA means that, in comparison with the NA, its density and hardness are lower [22, 23]. Secondly, RCA has a contact surface between the aggregate and the mortar, known as the Interfacial Transition Zone (ITZ) [24], which is weaker and less dense than the ITZ of NA [22, 25]. Finally, the high water absorption levels of RCA can be due to the unhydrated cement in the attached mortar [23, 25]. The behavior of the fine RCA, less than 4 mm in size, is strongly conditioned by the mortar particles, as well as some pollutants (clay, gypsum and mica), mainly introduced during the crushing process, which cause, among other aspects, higher levels of water absorption than in the coarse fraction [26].

The addition of RCA affects not only both the fresh and the hardened behavior of the concrete, but also the estimation of compressive strength through non-destructive testing, such as the hammer rebound index and Ultrasonic Pulse Velocity (UPV), mainly due to the presence of attached mortar [27]. However, the validity of these procedures has been demonstrated in vibrated concrete with high contents of coarse RCA [28, 29], even at early ages [30]. Despite the low coarse aggregate content of SCC, non-destructive tests are also valid for this type of concrete when NA is used [31].

The aim of this study is to evaluate the effect of adding different amounts of fine RCA in an SCC with a constant amount of coarse RCA. SCC requires a high proportion of fine aggregate to reach flowability, so it is more sensitive to the effects of fine RCA. In addition, the interaction between coarse and fine RCA can influence its performance. The coarse RCA content was defined in a preliminary analysis, involving tests on the compressive strengths and the elastic moduli of mixes with 0%, 50% and 100% of coarse RCA. Based on this analysis, the amount of 100% coarse RCA was chosen for the optimum sustainability of the product. Subsequently, five different SCCs with 100% coarse RCA and fine RCA percentages of 0%, 25%, 50%, 75% and 100% were manufactured and analyzed in this study.

Firstly, the evaluation of the fresh concrete behavior of these SSCs verified their compliance with all the recommendations of the European Federation of National Associations Representing producers and applicators of specialist building products for Concrete (EFNARC) [32]. Subsequently, the temporal evolution of the mechanical properties was evaluated. Additionally, the theoretical values of these mechanical properties, estimated from their compressive strengths, were calculated and compared with the experimental values, in order to validate the calculation methods. The validity of RCA as a material for manufacturing SCC for structural usage was therefore demonstrated, in accordance with its dosage (in particular, the percentage of fine RCA), which must be selected to meet the main purpose of the concrete design (self-compactability and/or strength).

2. MATERIALS

The characteristics of the materials used in this study are described in this section. An analysis of the physical properties and the chemical composition of the RCA is also included, to evaluate its suitability for concrete manufacture.

2.1. CEMENT, WATER, FILLER AND ADMIXTURES

A conventional Portland cement CEM I 52.5 R was used, with a density of 3.12 Mg/m^3 and a clinker content of around 98%. Mix water that contained no chemical compounds with potentially adverse effects on concrete behavior was taken from the water supply of the city of Burgos, Spain.

The finest fraction of the granulometry ($< 0.063 \text{ mm}$) was provided by the addition of limestone filler with a CaCO_3 content higher than 98%. According to the manufacturer's specifications, this filler had a density of 2.77 Mg/m^3 and a water absorption rate of 0.54% over 24 h (0.37% in 10 minutes).

Two admixtures, fundamental components for providing the SCC with its characteristic self-compactability, were used, which had demonstrated good behavior in a similar study [33]. The first one, a plasticizer, enhanced concrete flowability. The second, a viscosity regulator, maintained SCC flowability over longer periods, improving the results of the in-fresh state tests. In all dosages, total additions of admixture amounted to 2.2% by weight of cement.

2.2. AGGREGATES (RCA, SILICEOUS GRAVEL AND SILICEOUS SAND)

The RCA was produced from concrete components with a characteristic strength of 45 MPa, manufactured with siliceous aggregate, which had subsequently been rejected by the prefabrication industry and crushed. Supplied in sizes between 0 and 31.5 mm from a local CDW management company, the RCA was sieved and separated into fine RCA (0/4 mm) and coarse RCA (4/12.5 mm) fractions, both of which were used in this study.

In Table 2.1, the main properties of the RCA are compared with the recommended limit values from the Spanish concrete standard EHE-08 [34]. The comparison shows that the RCA fulfilled most of the requirements, except for density and water absorption, which explains the limitation that is specified in the standard of a maximum content of 20% total coarse RCA. The chemical composition of fine RCA obtained by X-ray fluorescence (XRF) spectrometry and the X-ray diffraction (XRD) pattern are shown in Table 2.2 and Figure 2.1, respectively. The predominance of silicon oxide and calcium carbonate can be observed in its composition. The hydrated cementitious components (CSH) are not visible in the XRD test results, although the content in both aluminum and iron oxides denotes the presence of old mortar in the fine RCA.

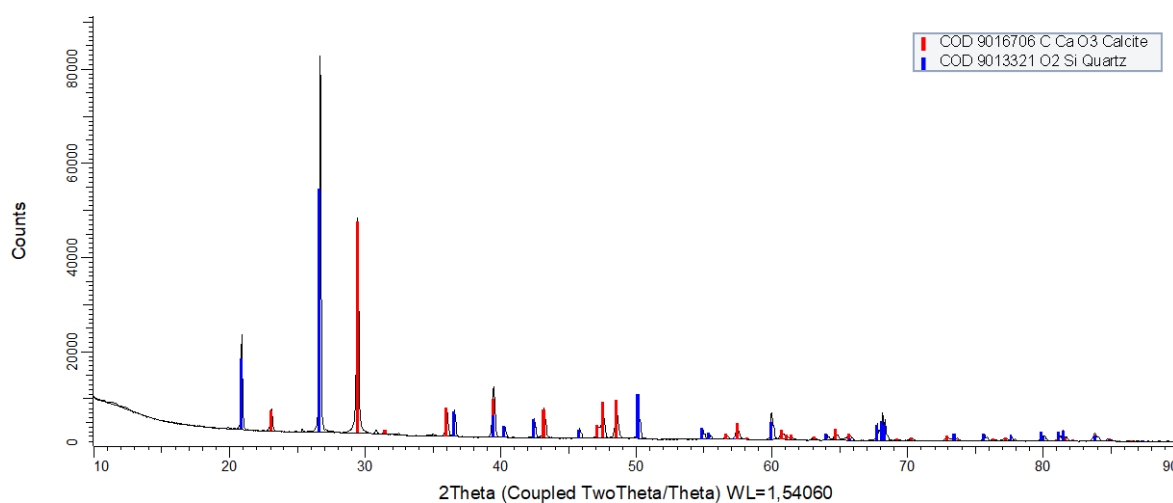
Siliceous gravel and sand were used to complete the coarse (preliminary analysis) and the fine aggregate fraction of each concrete mix. Their properties are also summarized in Table 2.1.

Table 2.1. Aggregates' physical properties

Test	Regulations [35]	Siliceous gravel	Siliceous sand	Coarse RCA	Fine RCA	EHE-08 limit [34]
Saturated-Surface-Dry (SSD) density (Mg/m ³)	EN-1097-6	2.62	2.58	2.42	2.37	≈ 2.6 kg/dm ³
Water absorption in 24h (%)	EN-1097-6	0.84	0.25	6.25	7.36	Coarse RCA content < 20%: < 7% Coarse RCA content > 20%: Combination of RCA and NA coarse fractions < 5%
Water absorption in 10 minutes (%)	-	0.66	0.18	5.28	6.03	If RCA content < 20%: < 5.5%
Fines content (%)	EN-933-1	0.11	1.82	0.17	4.83	< 1.50% (coarse fraction)
Equivalent sand (%)	EN-933-8	-	-	-	83	> 75
Bulk density (Mg/m ³)	EN-1097-3	-	-	1.26	1.23	-
Los Angeles coefficient (%) (size 10/14 mm)	EN-1097-2	-	-	35	-	< 40
Sand friability test (%) (size 0/4 mm)	UNE-146404	-	-	-	16	

Table 2.2. Chemical composition (% wt.) of fine RCA trough XRF

SiO ₂	CaO	Al ₂ O ₃	Fe ₂ O ₃	SO ₃	MgO	K ₂ O	TiO ₂	P ₂ O ₅	Others (CO ₂ ...)
50.80	20.00	3.74	1.12	1.00	0.63	0.60	0.15	0.06	21.9

**Figure 2.1.** XRD of fine RCA

The granulometric curves of all aggregates are shown in Figure 2.2. It can be seen that the fine RCA shows higher percentages of fine particles than the siliceous sand.

3. METHODOLOGY

In this section, the design of the experiment is explained. Firstly, a preliminary analysis is shown to define the coarse RCA content in the mixes. Secondly, the dosage of the SCCs with different percentages of fine RCA are defined. Thirdly, the set of tests performed on the mixes is discussed. Finally, the type of analysis of the experimental data is likewise explained.

3.1. EXPERIMENT DESIGN

Firstly, a preliminary analysis served to define the amount of coarse RCA to use in the mixes. Based on this analysis, it was decided to use 100% coarse RCA (see section 3.2). Later, the fine RCA

contents (25%, 50%, 75% and 100%), the set of tests to carry out and the number of samples in each test (application of the power method, with a significance level of 5% and a power of 20%) was defined by analyzing other similar research studies [36, 37]. In addition, testing ages were established according to the standards [34, 38, 39], in order to evaluate the effect of fine RCA over time. Therefore, age and fine RCA content were the two factors evaluated in this study.

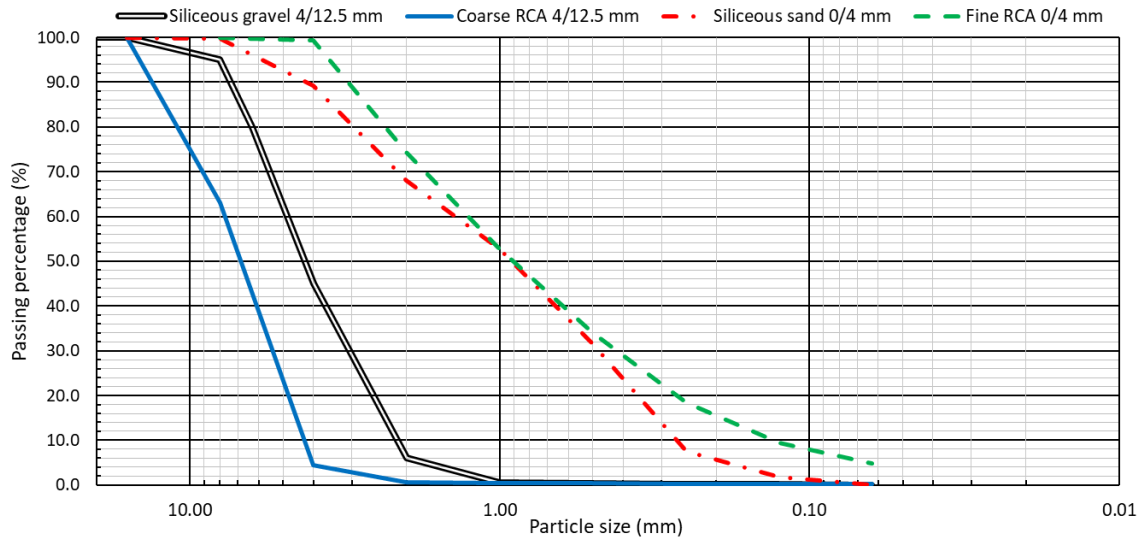


Figure 2.2. Granulometry of aggregates used

3.2. MIX DESIGN

The dosage of all mixes was defined by the specifications of EHE-08 [34], based on EC2 [39]. The overall particle size was adjusted to the Fuller curve, using the granulometric modules of the aggregates. Rather than the addition of admixtures to the mix design, the water content in the mixtures was carefully increased to achieve a proper self-compactability. That decision was taken to avoid admixture segregation that occurred when its proportion in the mix exceeded 2.2% of cement mass.

3.2.1. PRELIMINARY ANALYSIS

The optimum amount of coarse RCA to be added to the mixtures was decided after a preliminary analysis. Three mixes with 0%, 50% and 100% coarse RCA (labelled C0, C50 and C100 respectively) were used to mold 10x20-cm cylindrical samples (2 samples in each test). Their compositions are shown in Table 2.3. The compressive strength and the modulus of elasticity of the samples were tested at 7 and 28 days. The results were evaluated with a one-way ANOVA (5% significance level), which showed no significant differences between the compressive strength and the modulus of elasticity of the mixes with 50% and 100% of coarse RCA (Table 2.4). So, an amount of 100% of coarse RCA was used in the analysis of the fine RCA mix performance, in order to maximize the sustainability of the SCC designed.

3.2.2. MIXES WITH FINE RCA

Having defined the reference dosage (100% coarse RCA and 0% fine RCA), the siliceous sand 0/4 mm was progressively replaced with fine RCA by volume, in percentages of 25%, 50%, 75%, and finally 100%. As indicated above, the water content was adjusted to each mix, thereby increasing the water-to-cement (w/c) ratio and the effective w/c ratio, calculated from the water absorption rate over 10 minutes. The values for these ratios and the mix design can be seen in Table 2.5. The mixes were labelled M0, M25, M50, M75, and M100 depending on the percentage of fine RCA. In this table, the dosage of the mixtures is shown in two different ways. Firstly, in a comparative way,

by weight, with respect to the reference mix M0, so that any changes to the fine RCA and the water content may be easily observed. Secondly, the dosage of the mixtures adjusted to 1 m³ is shown, so that they may be easily reproduced. Figure 2.3 shows the overall particle size (corrected by volume) of mixes M0, M50, and M100, and their Fuller curve.

Table 2.3. Mix design of the mixes of the preliminary analysis (kg)

Mix	C0	C50	C100
Cement	300	300	300
Filler	180	180	180
Water	140	155	165
Siliceous gravel 4/12.5 mm	570	285	0
Coarse RCA 0/12.5 mm	0	265	525
Siliceous sand 0/4 mm	1,150	1,150	1,150
Admixture 1	2.20	2.20	2.20
Admixture 2	4.40	4.40	4.40

Table 2.4. Hardened properties (average values) and one-way ANOVA of the preliminary analysis

Test	Age (days)	Mixes			One-way ANOVA. Factor analyzed: coarse RCA content	
		C0	C50	C100	P-value	Homogeneous groups
Compressive strength (MPa)	7	67.6	57.8	55.7	0.0002	C50 and C100
	28	69.8	61.5	59.3	0.0082	
Modulus of elasticity (GPa)	7	39.7	35.9	34.8	0.0001	
	28	43.4	40.0	39.1	0.0002	

Table 2.5. Mix design

Mix	Comparative dosage with mixture M0 (kg)					Dosage (kg/m ³)				
	M0	M25	M50	M75	M100	M0	M25	M50	M75	M100
Cement	300	300	300	300	300	300	295	288	282	276
Filler	180	180	180	180	180	180	176	173	169	166
Water	165	187	205	230	250	165	183	198	215	232
Coarse RCA 0/12.5 mm	525	525	525	525	525	525	518	508	497	487
Fine RCA 0/4 mm	0	265	530	795	1,060	0	260	510	748	977
Siliceous sand 0/4 mm	1,150	865	575	290	0	1,150	850	555	272	0
Admixture 1	2.20	2.20	2.20	2.20	2.20	2.20	2.18	2.14	2.10	2.05
Admixture 2	4.40	4.40	4.40	4.40	4.40	4.40	4.32	4.24	4.15	4.06
Approximate volume (l)	1,000	1,018	1,038	1,060	1,083	1,000	1,000	1,000	1,000	1,000
Approximate weight (kg)	2,327	2,307	2,282	2,262	2,237	2,327	2,289	2,238	2,189	2,144
w/c	0.561	0.624	0.688	0.763	0.839	0.561	0.624	0.688	0.763	0.839
Effective w/c	0.459	0.470	0.482	0.506	0.530	0.459	0.470	0.482	0.506	0.530

3.3. EXPERIMENTAL PROCEDURE

A three-stage mixing process was performed for proper hydration of all the components, maximization of flowability, and to prevent the absorption of additive into the aggregates [40]. First, coarse RCA and fine fractions (siliceous sand 0/4 mm and/or fine RCA) were loaded in the concrete mixer bowl with half of the mix-water and mixed for 30 s. Then, the cement, filler and the rest of

the water were added, followed by another 30 s of mixing. Finally, the additive dissolved in 0.2 liters of water was added and mixed for the last 30 s. The aggregates were used under laboratory conditions, at an average temperature and humidity of 20 °C and 45%, respectively, thus adjusting the experimental procedure to the most economically advantageous methodology [41].

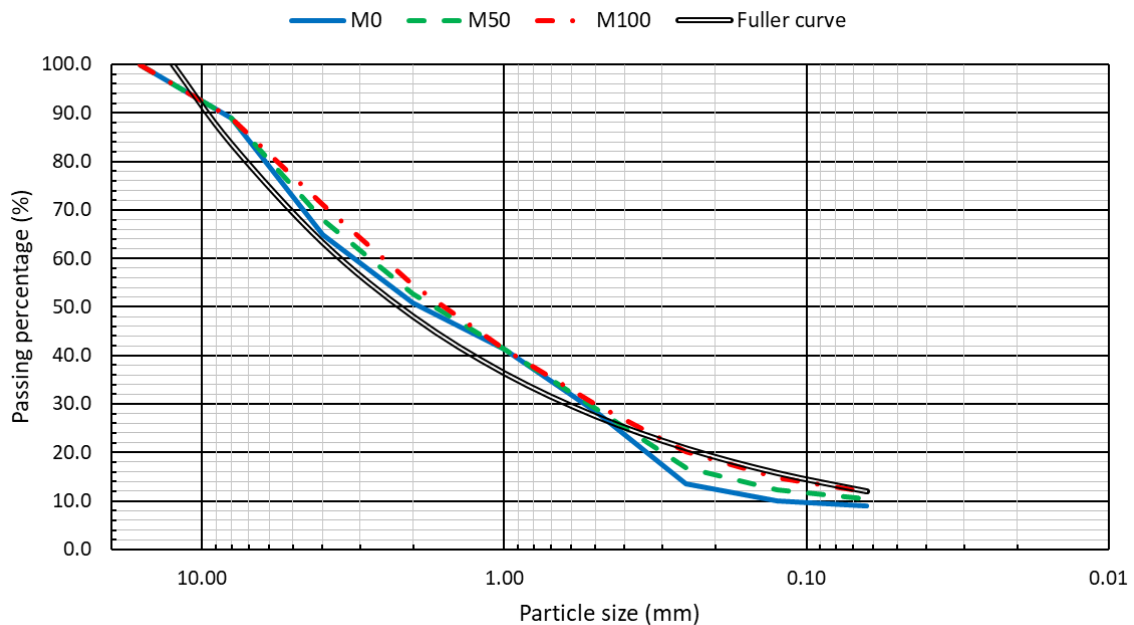


Figure 2.3. Mix design granulometry

Having completed the mixing process, in-fresh state tests, following the EFNARC recommendations, were performed [32] and the specimens were molded to carry out the hardened state tests. The tests, the standards, the age of the test, and the type and the number of test samples at each dosage are summarized in Table 2.6. The samples were held in a wet chamber at a humidity of $95 \pm 5\%$ and at temperature of 20 ± 2 °C until the time of the test. In addition, images from a Scanning Electron Microscope (SEM) were used to evaluate the quality of the ITZ in one of the worst performing specimens of mix M75.

The mechanical properties measured by these tests were evaluated both descriptively, which allows visual detection of differences in the behavior of the mixes, and by statistical analysis through one-way ANOVA at a significance level of 5%. This statistical analysis was to study the effect of each factor (age and fine RCA content) for each mechanical property under study and to establish homogeneous groups, i.e., factor values for which a certain mechanical property is significantly equal.

3.4. THEORETICAL CALCULATIONS

The experimental values of each mechanical property were compared with the theoretical values obtained from the formulas of the Spanish structural concrete standard EHE-08 [34], an adaptation of the Eurocode 2 regulation [39], based on the recommendations of the International Federation for Structural Concrete (CEB-FIP) [42].

According to EHE-08 [34], experimental compressive strengths at 28-days can be considered a medium 28-day compressive strength ($f_{c,m}$), with which the characteristic compressive strength ($f_{c,k}$) can be estimated, according to Equation 2.1. Having done so, the medium tensile strength ($f_{ct,m}$) can be determined, according to Equation 2.2, and the medium flexural strength ($f_{ct,m,fl}$), as a function of the beam height (h) in mm by applying Equation 2.3. These last two strengths were compared

with the values of splitting tensile strength and flexural strength, experimentally obtained at 28 days.

Table 2.6. Tests, regulations, and samples used for each mix

Test	Regulations [35]	Test age (days)	Number and type of sample tested per mixture
Slump flow	EN 12350-8		Sample of fresh concrete
V-funnel	EN 12350-9		
2-bar L-box	EN 12350-10		
Sieve segregation	EN 12350-11		
Fresh density	EN 12350-6		
Air content	EN 12350-7		
Compressive strength	EN 12390-3	1, 7, 28, 90	3 cylindrical samples 10x20 cm at each age
Hammer rebound index	EN 12504-2		2 cylindrical samples 10x20 cm at each age
Ultrasonic Pulse Velocity (UPV)	EN 12504-4		2 prismatic samples 10x10x40 cm at each age
Hardened density	EN 12390-7	28	2 cubic samples 10x10x10 cm
Splitting tensile strength	EN 12390-6	7, 28, 90	2 cylindrical samples 15x30 cm at each age
Flexural strength	EN 12390-5		2 prismatic samples 10x10x40 cm at each age
Static modulus of elasticity and Poisson coefficient	EN 12390-13		3 cylindrical samples 10x20 cm at each age
Stress-strain curves	-	90	2 cylindrical samples 10x20 cm
Abrasion resistance	EN 1340 EN 14157		2 cubic samples 10x10x10 cm

$$f_{c,k} = f_{c,m} - 8 \quad (2.1)$$

$$\left\{ \begin{array}{l} f_{ct,m} = 0.30 \cdot f_{c,k}^{2/3} \text{ if } f_{c,k} \leq 50 \text{ MPa} \\ f_{ct,m} = 0.58 \cdot f_{c,k}^{1/2} \text{ if } f_{c,k} > 50 \text{ MPa} \end{array} \right\} \quad (2.2)$$

$$f_{ct,m,fl} = \max \left\{ \left(1.6 - \frac{h}{1,000} \right) \cdot f_{ct,m}; f_{ct,m} \right\} \quad (2.3)$$

EHE-08 [34] specifies the formula for estimating the static concrete elasticity modulus at any age, Equation 2.4. The expression contains the following factors: curing time in days (t); the 28-day secant modulus of elasticity ($E_{c,m}$) calculated with Equation 2.5; the medium compressive concrete strength at t days ($f_{c,m}(t)$), obtained with Equation 2.6; and, the secant modulus of elasticity at t days ($E_{c,m}(t)$). The units of strength and the modulus of elasticity in all the expressions can only be introduced in Megapascals (MPa).

$$E_{c,m}(t) = \left(\frac{f_{c,m}(t)}{f_{c,m}} \right)^{0.3} \cdot E_{c,m} \quad (2.4)$$

$$E_{c,m} = 8,500 \cdot \sqrt[3]{f_{c,m}} \quad (2.5)$$

$$f_{c,m}(t) = \exp \left\{ 0.2 \cdot \left[1 - \left(\frac{28}{t} \right)^{1/2} \right] \right\} \cdot f_{c,m} \quad (2.6)$$

The structural concrete design guidelines of the American Concrete Institute (ACI) [38] contain formulas, Equation 2.7 and Equation 2.8, for calculating the tensile strength of concrete and its modulus of elasticity from its compressive strength, respectively. The variables of these equations refer to compressive strength, (f_c), tensile strength, (f_t), and the modulus of elasticity, (E). These expressions are easier to apply than those indicated above, and their validity is also analyzed in this study.

$$f_t = 0.56 \cdot f_c^{0.5} \quad (2.7)$$

$$E = 4,700 \cdot \sqrt{f_c} \quad (2.8)$$

Simple regression equations are provided, to complement this analysis, which were developed for the mechanical properties (splitting tensile strength, flexural strength, and modulus of elasticity) measured in this study. These formulas can be used as a basis for more general models taken from the literature, for accurate estimation of the properties of SCC made with RCA.

On the other hand, the value of the dynamic modulus of elasticity (E_d) at different ages of curing can be calculated from the test results with Equation 2.9 [33], using the density of the concrete (ρ), the UPV (V_t), and the Poisson coefficient (ν). All the above-mentioned properties were precisely established with the tests performed.

$$E_d = \rho \cdot V_t^2 \cdot \frac{(1 + \nu) \cdot (1 - 2 \cdot \nu)}{1 - \nu} \quad (2.9)$$

4. RESULTS AND DISCUSSION

The experimental results of the in-fresh and the hardened states, as well as the theoretical estimation of the mechanical properties from the concrete design standards are presented in this section.

4.1. FRESH PROPERTIES

It is clear from the bibliography that the addition of RCA clearly reduces the flowability of the SCC, due to its higher water absorption, resulting in a lower effective w/c ratio for any given w/c ratio without RCA [20, 33, 43]. In addition, the crushing process of the RCA produces irregular shapes, which means that the aggregate particles will not flow easily in the paste [44, 45]. Although the effective w/c ratio decreases with the coarse RCA, its irregular shaped particles have the most notable effects [33, 46]. The predominant effect of the fine RCA results from its high level of water absorption that decreases the effective w/c ratio [43]. Regarding the maximum diameter obtained in the slump-flow test, the decrease in initial flowability is as much as 36% with 100% coarse RCA and up to 19% with 100% fine RCA [43-45].

The adjustment of the water absorbed by the RCA solves the water absorption problem, preventing the effective w/c ratio from decreasing [19, 37]. Another possibility is to increase the proportion of the finest aggregate fraction (<0.125 mm), thereby increasing the volume of paste. Balanced proportions of fine and coarse aggregates are therefore fundamental for good performance of SCC [21].

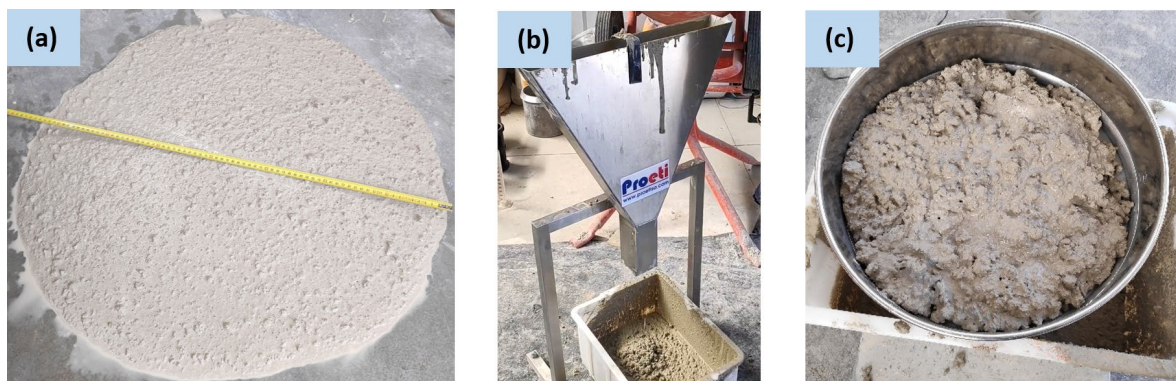


Figure 2.4. In-fresh state tests for M50 mix. (a) slump-flow; (b) V-funnel; (c) sieve segregation

In the concretes under study, the water content was adjusted by increasing the percentage of fine RCA aggregate, thereby increasing the effective w/c ratio. In addition, that increase of fine RCA

aggregate also led to an increase in the fine fraction (<0.125 mm) within the overall granulometry of the mixtures. Both aspects compensated the negative effects of RCA and even improved the slump flow and the passing ability of the SCC. Some of the in-fresh state tests are shown in Figure 2.4 and their results, presented in Table 2.7, are consistent with the above-mentioned aspects.

As reported in similar studies [43], the lower density of the RCA, compared to the NA, and the increase in water content decreased the fresh density of the SCC [46, 47]. The air content, very similar in all mixtures, mainly depended on the admixtures and the chemical reactions they produced, with no clear influence of fine RCA.

Based on the results of the in-fresh state tests and the EFNARC recommendations [32], the developed SCCs presented:

- A slump-flow class SF2 (maximum diameter between 660 and 760 mm).
- A viscosity class, according to the slump-flow test, VS2 (time to reach a diameter of 500 mm greater than 2s) and, according to the V-funnel test, VF2 (time to empty the V-funnel greater than 8s), except for the M0 mixture which was class VF1.
- A passing-ability class PA1, according to the 2-bar L-box test (blocking ratio greater than 0.80).
- A segregation-resistance class SR2 (sieve segregation less than 15%).

Table 2.7. In-fresh state test results

Test/Mix	M0	M25	M50	M75	M100
Viscosity t_{500} slump flow test (s)	3.40	3.60	4.00	4.20	4.80
Slump flow (mm)	680	695	730	740	755
Viscosity V-funnel test (s)	6.40	8.40	10.20	12.60	15.20
Passing ability L-box test H_2/H_1	0.86	0.88	0.92	0.93	0.94
Sieve segregation (%)	1.70	1.52	1.67	1.53	1.36
Air content (%)	4.80	3.75	4.35	4.00	4.15
Fresh density (Mg/m^3)	2.40	2.31	2.25	2.16	2.12

The maximum diameter in the slump-flow test increased by 11% (from 680 mm for M0 to 752 mm for M100), following the addition of 100% fine RCA, which in turn increased the effective w/c ratio by 15% (from 0.46 to 0.53). In this case, the passing ability was also increased by 9% (from 0.86 to 0.94). The fines content of the mix M25 influenced the flowability of the SCC. A fine RCA content of 25% and an effective w/c ratio of 0.47, slightly higher than 0.46 (corresponding to mix M0), led to a higher slump flow and passing ability. However, it was not possible to compensate all the negative effects of RCA by increasing the proportion of water and fines, as viscosity was negatively affected, resulting in higher slump-flow viscosity and emptying times (V-funnel test). This performance can be explained by two aspects: the irregular shapes of the coarser fine RCA particles that move more slowly within the cement paste than the rounded siliceous sand particles; and the higher proportion of cement paste, resulting from the increased volumes of fines, following the addition of RCA, leaving the SCC with a more viscous consistency.

Resistance to segregation was not negatively affected by the addition of fine RCA and was even improved by the increase of the fine RCA content. In fact, the sieve segregation of the mixture M100 (1.36%) was 25% lower than that of the mixture M0 (1.70%). Even though fine RCA had a higher content of particles smaller than NA (≤ 0.125 mm), the use of fine RCA produced higher long-term water absorption levels that reduced segregation.

4.2. HARDENED STATE BEHAVIOR

The analysis of the mechanical properties aims to evaluate the effect of fine RCA on the development of strength at different curing ages. Some of these tests, such as for splitting tensile strength, flexural strength, and modulus of elasticity, are shown in Figure 2.5.

4.2.1. DENSITY

The lower density of RCA compared to NA reduced the hardened density of the SCC, as the RCA content increased (Table 2.8), in line with the existing bibliography [33, 37, 48]. The decrease of the hardened density compared to the fresh density showed no clear trends, although it was higher in the mixtures with a higher NA content (mixture M0 showed a decrease of 4.2%, while this decrease for mixture M50 was only 0.4%), which may be due to the lower water evaporation, because of the higher water absorption of fine RCA [33].



Figure 2.5. Mechanical tests: splitting tensile strength (left); flexural strength (middle); modulus of elasticity (right)

Table 2.8. Hardened density of the mixes

Test/Mix	M0	M25	M50	M75	M100
Hardened density (Mg/m ³)	2.30	2.29	2.24	2.13	2.10
Decrease with respect to its fresh density (%)	4.2	0.9	0.4	1.4	1.0
Decrease with respect to the M0 density (%)	0	0.4	2.6	7.4	8.7

4.2.2. COMPRESSIVE STRENGTH, UPV AND HAMMER REBOUND INDEX

The addition of coarse RCA is known to reduce the compressive strength of concrete [49], although reductions of just 5 MPa for 100% coarse RCA content were obtained in some studies [45, 50]. The reduction was higher when fine RCA was added [36], and in some studies the decrease caused by 100% fine RCA in SCC reached 26% compared to the reference concrete (0% coarse and fine RCA) [20, 51]. Nevertheless, if the effective w/c ratio is reduced, the loss of strength can be compensated, especially when only coarse RCA is used [33, 46]. In the present study, as expected, the compressive strengths of the concretes under study decreased as their fine RCA content increased and with it, the w/c ratio (Table 2.5), as shown in Figure 2.6. At 28 days, the decrease in strength, with regard to the reference mixture M0 (60 MPa), was 7% for mixture M25 (56 MPa), 27% for mixture M50 (44 MPa), and 47% and 51% for mixtures M75 and M100, respectively (strengths of 31 and 30 MPa). Regarding the overall trend, mixture M25 showed a much lower than expected strength decrease, possibly due to its very similar effective w/c ratio to mix M0.

The compressive strength results showed less dispersion with higher additions of fine RCA content, although that dispersion increased at advanced ages. The strengths of the mixtures with high RCA contents were more closely limited at early ages.

The compressive strength developed at 1 and 7 days, with regard to the strength at 28 days, were in percentage terms 78% and 94% for the reference mix, M0; 60% and 90% for M50; and 47% and 86% for M100. Strength development, in percentage terms, was slower as the fine RCA content increased.

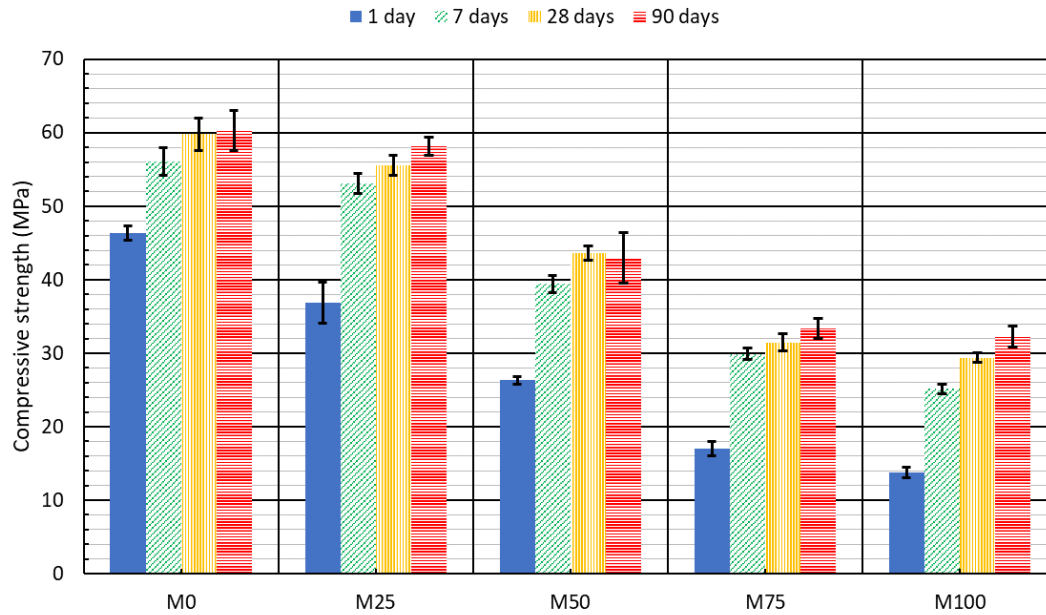


Figure 2.6. Compressive strength of the SSC mixtures

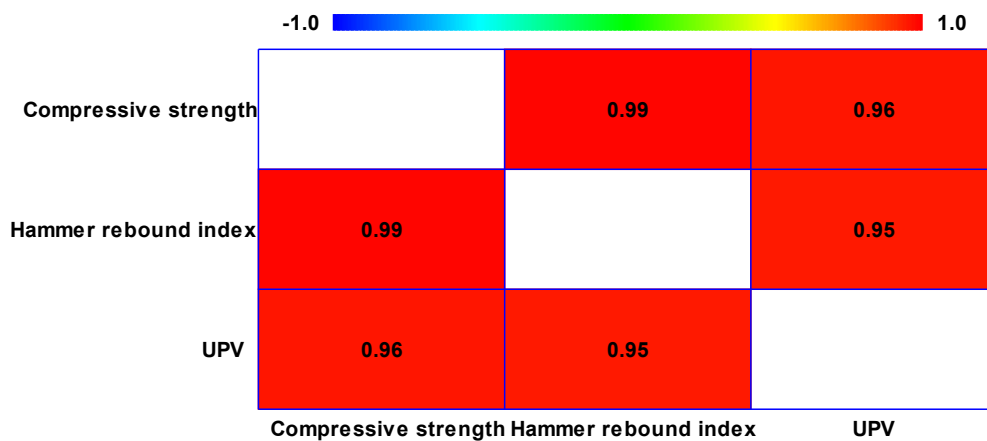


Figure 2.7. Pearson's symmetrical correlation matrix for compressive strength, hammer rebound index and UPV

Table 2.9. Exponential adjustment between UPV and hammer rebound index and compressive strength

Test/Mix		M0	M25	M50	M75	M100
UPV (km/s)	1 day	3.94	3.76	3.73	3.27	3.19
	7days	4.28	4.00	4.03	3.63	3.68
	28 days	4.32	4.20	4.09	3.80	3.71
	90 days	4.34	4.30	4.09	3.79	3.71
Exponential adjustment: compressive strength-UPV		$y=3.666 \cdot \exp(0.643x)$	$y=1.854 \cdot \exp(0.811x)$	$y=0.155 \cdot \exp(1.376x)$	$y=0.312 \cdot \exp(1.232x)$	$y=0.130 \cdot \exp(1.461x)$
Coefficient R ² UPV		0.96	0.87	0.99	0.95	0.98
Hammer rebound index	1 day	46	40	34	27	24
	7days	56	52	42	33	33
	28 days	58	54	42	39	37
	90 days	58	56	45	39	40
Exponential adjustment: compressive strength-hammer rebound index		$y=17.443 \cdot \exp(0.021z)$	$y=11.669 \cdot \exp(0.029z)$	$y=5.236 \cdot \exp(0.048z)$	$y=4.804 \cdot \exp(0.050z)$	$y=3.871 \cdot \exp(0.054z)$
Coefficient R ² hammer rebound index		0.98	0.99	0.92	0.85	0.98

The UPV and the hammer rebound tests, two conventional methods for estimating the compressive strength of non-recycled concrete, were measured at all ages. Pearson's symmetrical correlation matrix between these three properties for all mixtures and ages simultaneously is shown in Figure 2.7. A clear linear relationship between these variables can be observed, as in other similar studies [28, 52], although an individual analysis carried out in each mix showed that the exponential model had the best overall fit. Table 2.9 shows the least square exponential adjustment of compressive strength (variable "y") as a function of the UPV (variable "x") and the hammer rebound index (variable "z"). The adjustment had a coefficient R^2 higher than 0.90 in 80% of the cases. Mixture M100 had the coefficients R^2 closest to 1.00. The validity of these indirect measures was not influenced by the addition of RCA. Figure 2.8 and Figure 2.9 show this adjustment for each mixture and it may be noted that the increase in RCA content increased the curvature of the models.

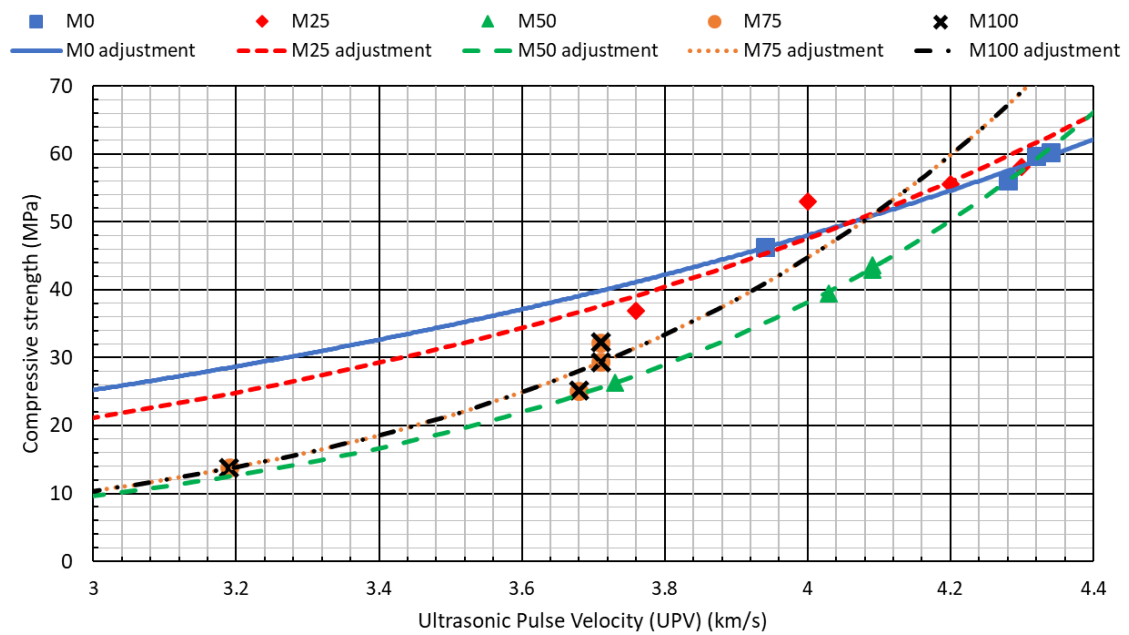


Figure 2.8. Adjustment of the compressive strength as a function of the UPV

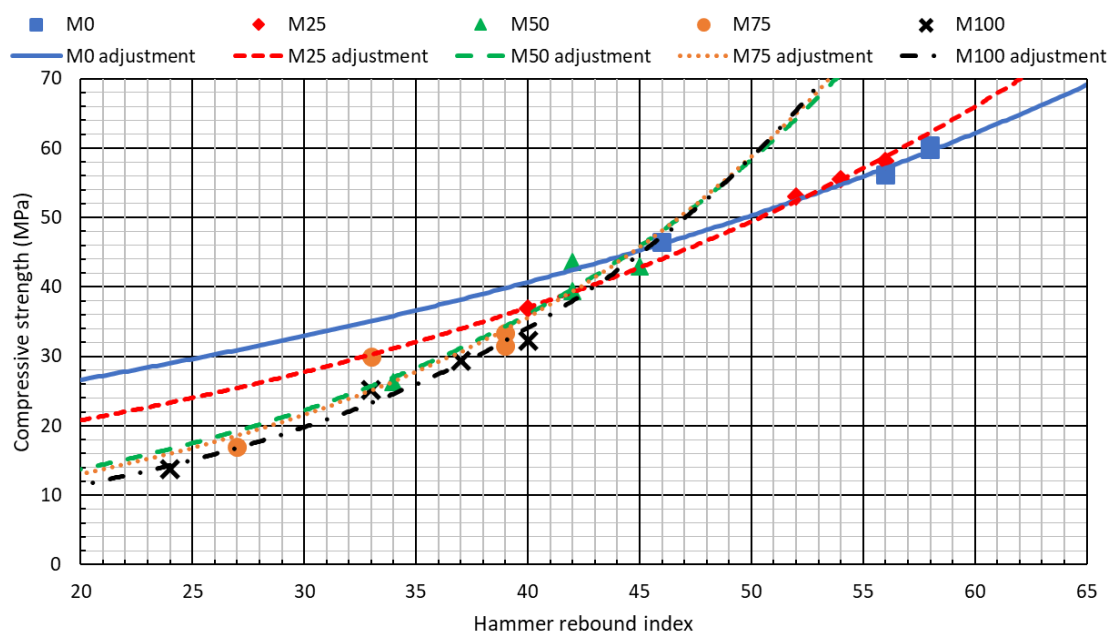


Figure 2.9. Adjustment of the compressive strength as a function of the hammer rebound index

4.2.3. SPLITTING TENSILE STRENGTH AND FLEXURAL STRENGTH

The results, obtained at 7, 28, and 90 days, showed that the addition of fine RCA decreased both the splitting tensile strength (Figure 2.10) and the flexural strength (Figure 2.11), a widely reported behavior in the literature [33, 37, 51]. The harmful effect of fine RCA can be compensated and if the dosage is correctly modified, it is possible to obtain a splitting tensile strength equal to that of the reference concrete [27]: reducing the water content, increasing the cement content, or using alternative binders such as fly ash or silica fume [53, 54].

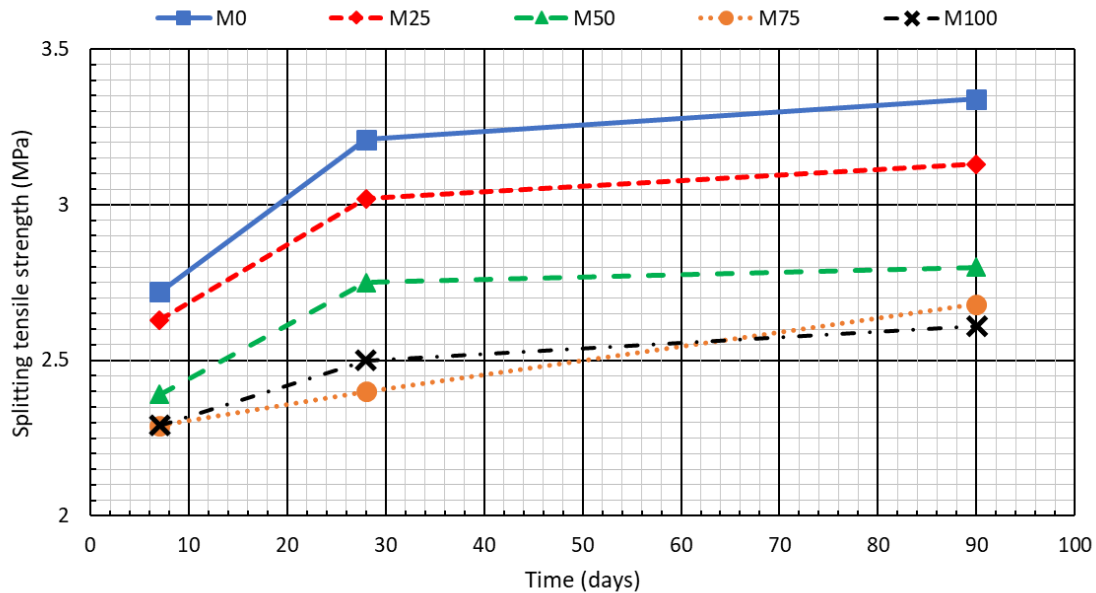


Figure 2.10. Splitting tensile strength

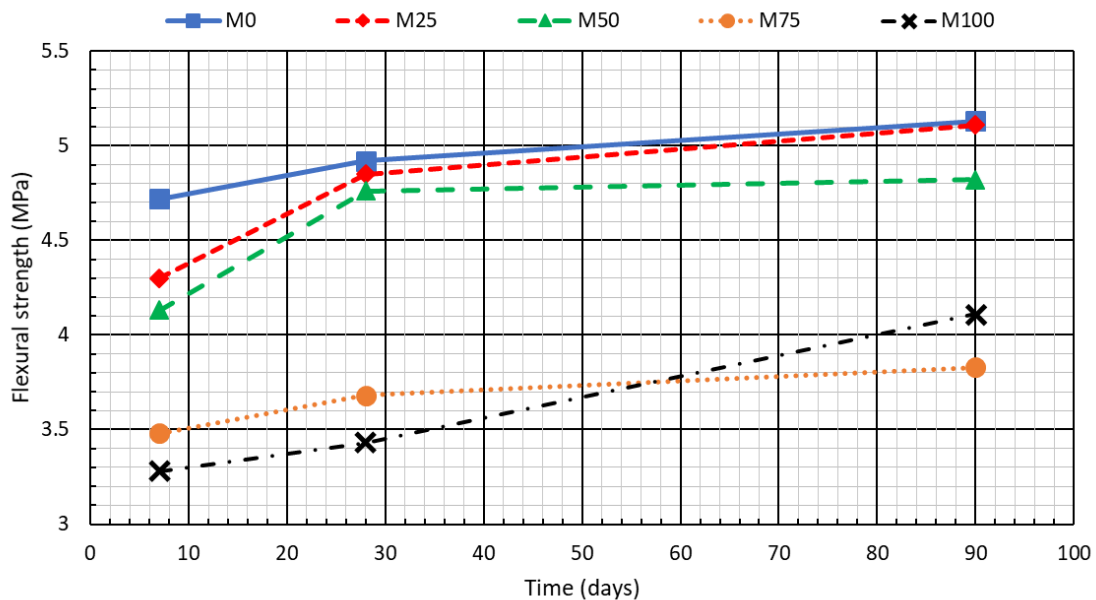


Figure 2.11. Flexural strength

In this study, the decrease was mainly observed for the flexural strength, with different behavior in two groups (fine RCA up to 50% and above 50%). Compared to M0, the decrease of the flexural strength at 28 days of the mixture M100 was 30% (3.4 versus 4.9 MPa) and was only 22% for the splitting tensile strength (2.5 versus 3.2 MPa). However, there were some exceptions, such as the

higher flexural strength of mix M100 compared to M75 at 90 days, due to the low adhesion between the cement paste and the coarse aggregate, in the mixes with high fine RCA content. It was observed that high additions of fine RCA also favored a more uniform strength over time, and a less predictable behavior.

Some studies have shown that the theoretical tensile strength value, calculated according to the EC2 [39], was lower than the experimental value in SCC made with coarse RCA, whilst the experimental value was overestimated in SCCs with high fine RCA content [37]. The theoretical tensile strength values as per EHE-08 [34], shown in Figure 2.12 and calculated with Equation 2.2, were higher than the experimentally obtained results for all the mixtures in this study, although the adjustment was improved by increasing the fine RCA content (the experimental tensile strength of M100 was higher than the theoretical value). In relation to the values estimated with Equation 2.7 from the ACI [38], it can be observed that the theoretically calculated values also overestimated the results. The SCCs with the highest fine RCA content were those that showed the least difference between both values: in M0, the theoretical value at 28 days (4.3 MPa) was 34% higher than the experimental value (3.2 MPa), while this overestimation in the mixture M100 was only 20% (3.0 versus 2.5 MPa). As the increase in compressive strength after 7 days was higher than the increase in splitting tensile strength, the adjustment was better for advanced ages. Similarly, the design values of flexural strength (Figure 2.13) also overestimated the experimental values, once again with a better fit as fine RCA was added. From all the above, it can be deduced that both the splitting tensile strength and the flexural strength were, in general, lower than expected, especially in the case of concretes with few recycled fines. The use of the equations from the standards applied to the test mixtures would imply strength overestimations of around 25%, especially with fine RCA contents up to 50%.

The standard formulas [34, 38] relate both tensile strength and flexural strength to compressive strength by means of a square or cubic root. Nevertheless, the best-fit model (coefficient R^2 of 0.86) of the splitting tensile strength (STS , in MPa) as a function of compressive strength (CS , in MPa), shown in Equation 2.10, established a polynomial relationship between both variables. In contrast, the flexural strength (FS , in MPa), Equation 2.11, with a coefficient R^2 of 0.88, has an inverse relationship with the compressive strength.

$$STS = 8.46 - 0.79 \cdot CS + 0.04 \cdot CS^2 \quad (2.10)$$

$$FS = \left(2.55 - \frac{19.26}{CS} \right)^2 \quad (2.11)$$

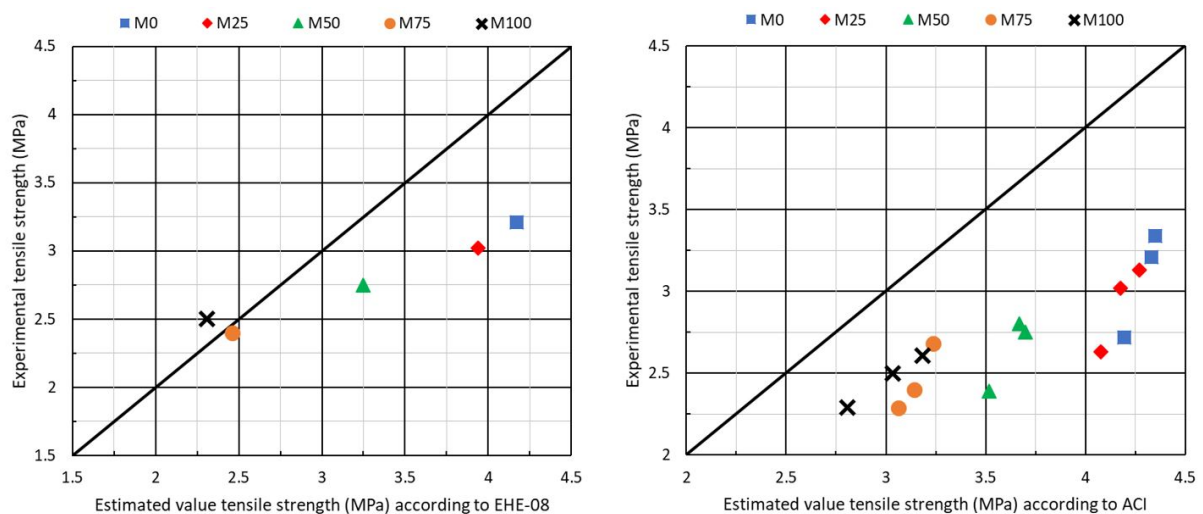


Figure 2.12. Relationship between the experimental tensile strength and the estimated value as per EHE-08 (left) and ACI (right)

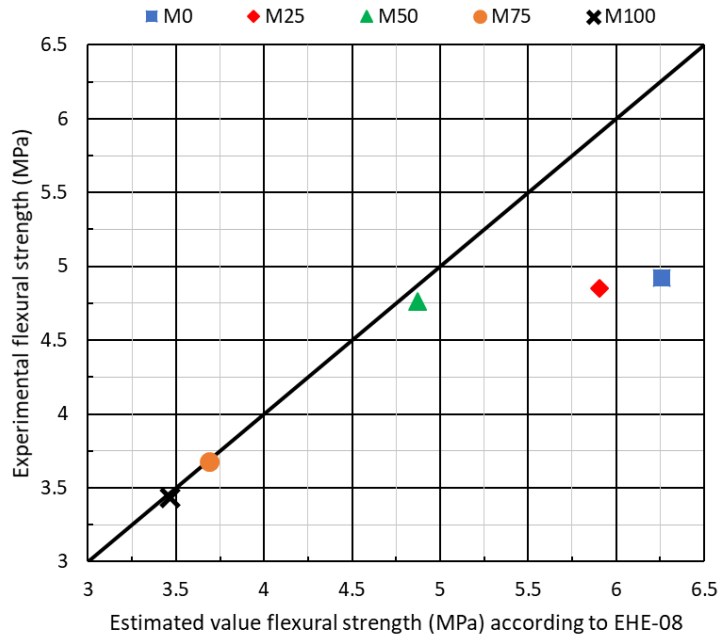


Figure 2.13. Relationship between the experimental flexural strength and the estimated value as per EHE-08

4.2.4. STATIC MODULUS OF ELASTICITY AND POISSON COEFFICIENT

The presence of adhered mortar and the ITZs, which were weak and not very dense, meant that the SCC with RCA was, in general, more deformable than the SCC with NA [25, 33], observations supported by the results from this study that are shown in Figure 2.14. A higher fine RCA content led to a lower modulus of elasticity at all ages: at 28 days, M100 presented a modulus of elasticity of 18.8 GPa, 54% lower than the mix M0 (40.6 GPa). The addition of 100% fine RCA to an SCC with 100% coarse RCA, as performed in this study, led to a greater decrease in the modulus of elasticity than when this amount of fine RCA is added to an SCC with no coarse RCA, which is around 24% [37, 51].

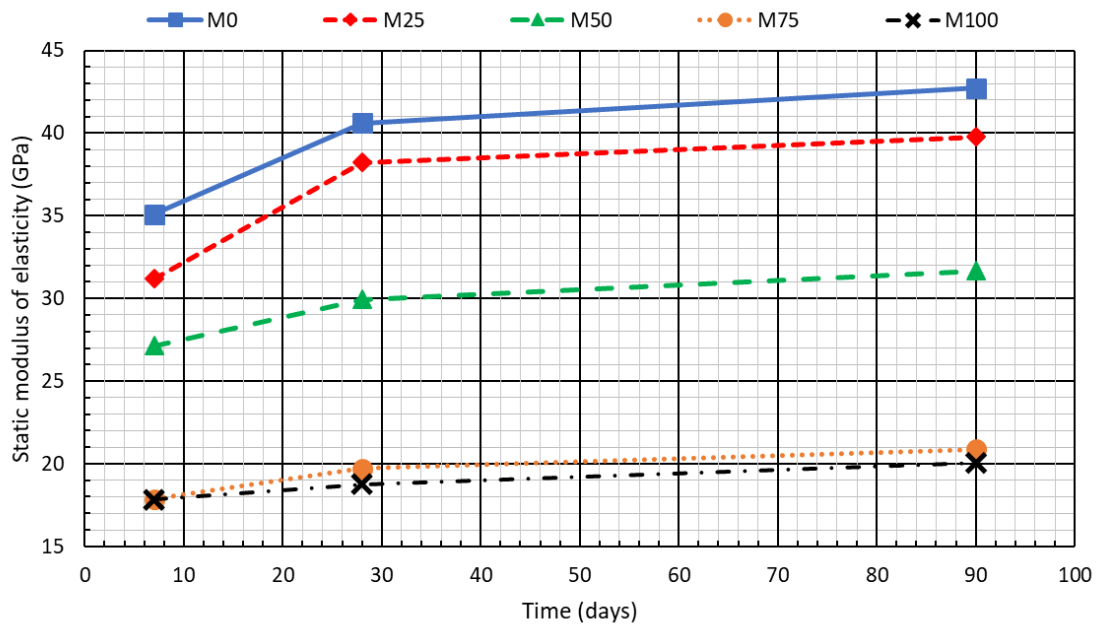


Figure 2.14. Static modulus of elasticity

The trends for the modulus of elasticity over the curing, once again showed a different behavior between the mixtures with low/medium percentages and those with high percentages of fine RCA: the mixtures with low percentages of fine RCA (M0 and M25) showed a very marked increase in the modulus of elasticity up to 28 days, while the increase in concretes with higher contents (M75 and M100) was practically uniform over time.

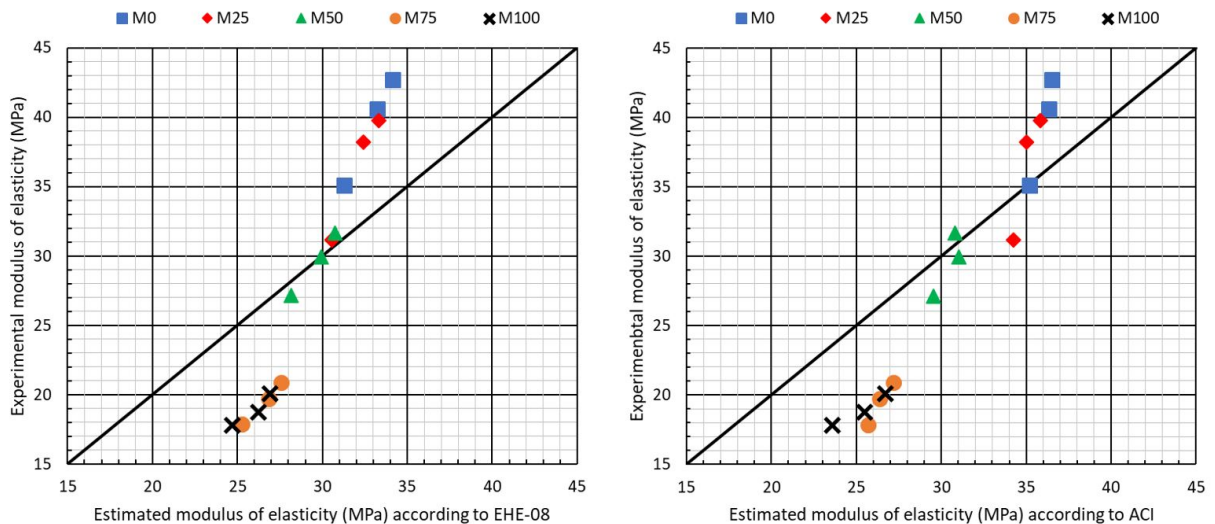


Figure 2.15. Relationship between compressive strength and modulus of elasticity according to EHE-08 (left) and ACI (right)

The adjustment of the theoretical values, obtained with Equation 2.4, to the experimental values was quite poor (Figure 2.15). In mixtures with low percentages of fine RCA (M0 and M25), the design values were lower than the experimental values (at 28 days, the design value of mixture M25 was 32.4 GPa, 15% lower than the experimental value, 38.2 GPa). The theoretical expressions overestimated the modulus of elasticity in the mixtures with high contents of fine RCA (M75 and M100), by approximately 40% at all ages of curing. Mixture M50 was in an intermediate situation: its theoretical value at 7 days (28.2 GPa) was higher than the experimental value (29.9 GPa), with the opposite situation at 90 days (theoretical value of 30.7 GPa and experimental value of 31.7 GPa). The same situation was observed for the ACI [38] formula, once again showing that mixture M50 had the best fit. These results are in line with the conclusions of other studies, which also showed that the theoretical expressions underestimated the modulus of elasticity in SCCs with low percentages of RCA and overestimated it in mixtures with high percentages of RCA [37, 55].

Equation 2.12 shows that there is an exponential relationship between the modulus of elasticity (ME , in GPa) and the logarithm of compressive strength (CS , in MPa), similar to that shown by EHE-08 [34] in Equation 2.6. Its coefficient R^2 is 0.96.

$$ME = \exp(-0.62 + 1.05 \cdot \ln(CS)) \quad (2.12)$$

Increasing percentages of fine RCA increased both the deformability of the concrete in the load direction and the volume variation under load, as shown by the lower Poisson coefficient (Figure 2.16) of the concrete with additions of fine RCA: after 28 days, the difference of the Poisson coefficient between mixtures M0 (0.20) and M100 (0.16) was 19%. This trend was similar to the one obtained in vibrated concretes with only coarse RCA [56, 57], although a constant w/c ratio appeared to prevent the Poisson coefficient from decreasing [58]. The temporal evolution of this coefficient was similar in all the mixtures: a marked decrease in the first days, less noticeable as time goes by, although M100 showed a much more remarkable decrease after 28 days than the rest of the mixtures. The conventional value of the Poisson coefficient for concrete (0.2) was higher than the experimental values, except for concretes with less than 50% fine RCA at 7 days, that had slightly higher experimental values.

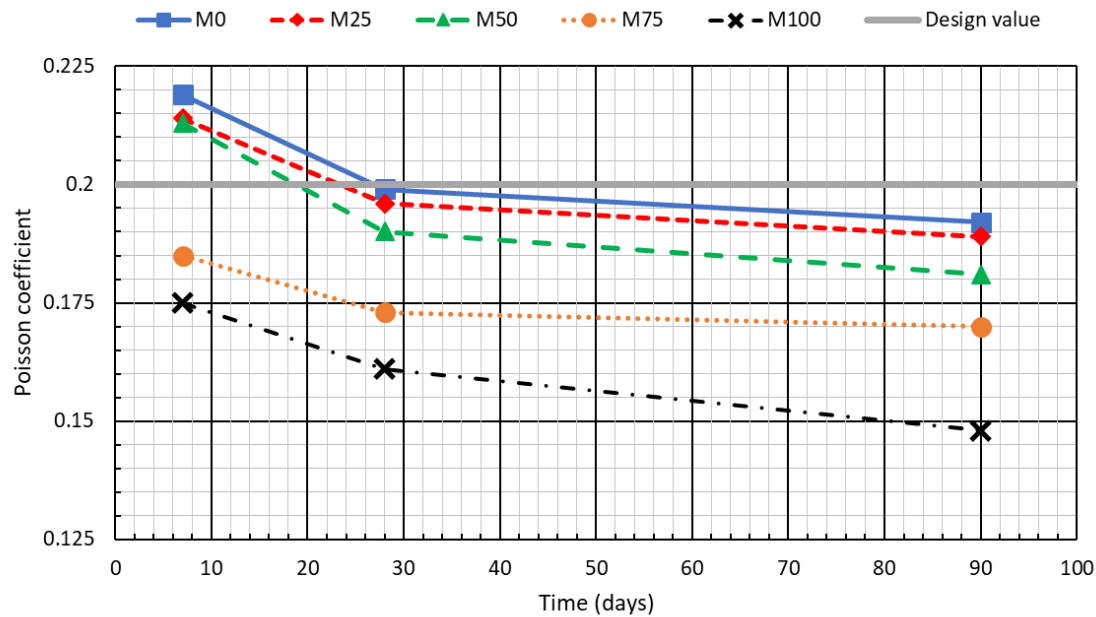


Figure 2.16. Poisson coefficient

4.2.5. STRESS-STRAIN CURVES

The stress-strain curves that are used to evaluate the plastic behavior of concrete usually show an elastic behavior at low load levels and reduced fracture strain values (theoretical value of $3,500 \mu\text{m/m}$) [34, 38, 39]. Higher fines contents will usually result in higher strain values after the ultimate strength value of the concrete is reached [59]. When this aspect was addressed in recycled concrete, it was concluded that coarse RCA reduced fracture strain [60]. No reference to this behavior was found for SCCs made with coarse and fine RCA, such as those reported in this article. Cylindrical specimens of 10 and 20 cm in diameter and height, respectively, were subjected to compressive strength tests until failure at 90 days, yielding the curves shown in Figure 2.17. The stress and strain values were recorded at a frequency of 15 Hz.

The stress-strain curves reflected the decrease, both in compressive strength (ultimate strength) and in the modulus of elasticity, as the fine RCA content increased, as previously discussed (section 4.2.2). Other relevant aspects of the structural design with this type of concrete are:

- The proportional limit (the point where linear elastic strain ends) was produced for a deformation of $720 \mu\text{m/m}$ for M0 and $580 \mu\text{m/m}$ for M100, increasing the plastic deformation with the fine RCA content.
- An increase in the fine RCA content led to a higher fracture strain: mixtures M0 and M25 showed strain values that were 18.9% lower than mixtures M75 and M100 ($3,000 \mu\text{m/m}$ versus $3,700 \mu\text{m/m}$). The strain values of mixture M50 ($3,300 \mu\text{m/m}$) were the closest to the theoretical value. Thus, the mixtures with higher fine RCA contents presented higher safety design coefficients, as they exceeded the theoretical values calculated with the formulas from the standards. This behavior was contrary to the one observed when only coarse RCA was added [60].
- The strain values corresponding to the ultimate strength increased with higher contents of fine RCA in the mixtures ($2,650 \mu\text{m/m}$ for mixture M0 and $3,250 \mu\text{m/m}$ for mixture M100). The ratios between the fracture strain and peak strain for mixtures M0 and M100 were 1.16 and 1.13, respectively, and the remaining strain after breakage increased in SCCs with low fine RCA contents. The reference specimen, mixture M0, showed the highest safety factor after failure.

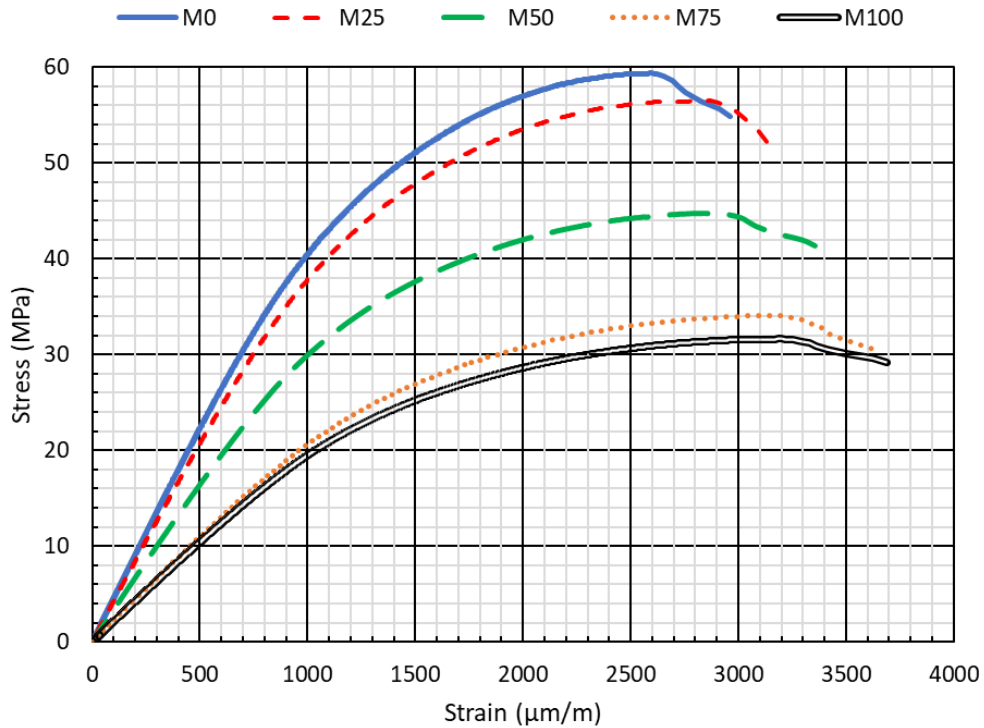


Figure 2.17. Stress-strain curves of the mixtures

4.2.6. DYNAMIC MODULUS OF ELASTICITY THROUGH THE UPV

The dynamic modulus of elasticity decreased with the addition of fine RCA. According to other studies, in mixtures with 50% coarse RCA, the decrease was approximately 4%, reaching 9% for 100% replacements [33, 61]. No other study has been found in which this property is evaluated in SCCs with fine RCA. The results of this study (Figure 2.18) showed the same overall trend as the static modulus of elasticity (Figure 2.14), both in terms of fine RCA content and its temporal evolution. The results for all properties based on the calculation of this modulus of elasticity, according to Equation 2.9, were consistent with each other.

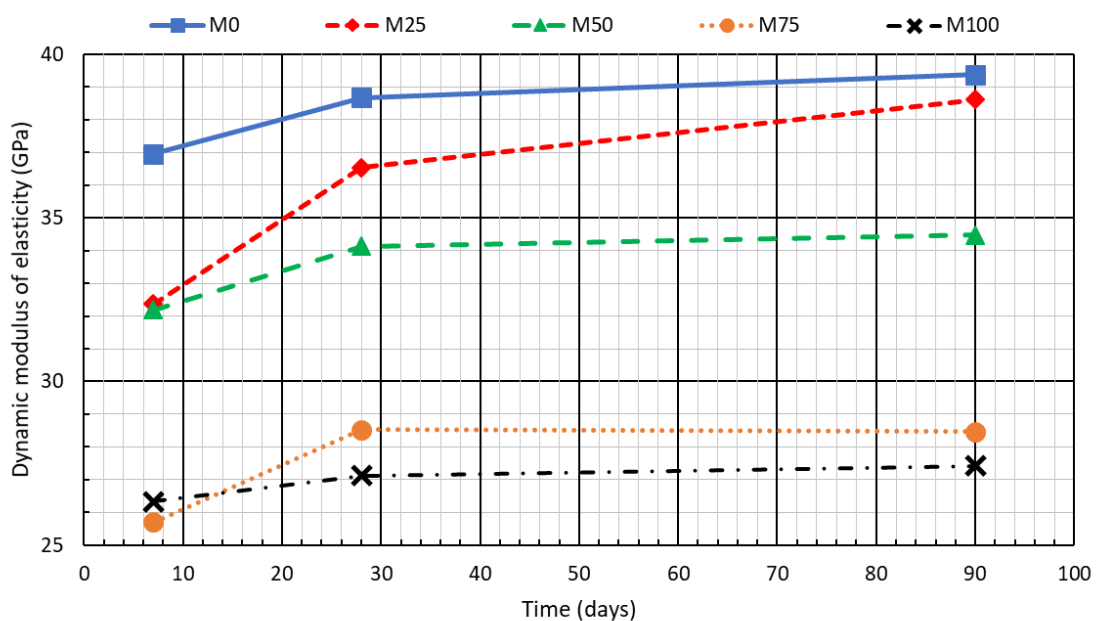


Figure 2.18. Dynamic modulus of elasticity through the UPV

Two groups of concretes may be distinguished: high and low/medium fine RCA content. Mixtures with fine RCA content of less than 50% had a lower dynamic modulus of elasticity through the UPV than the static modulus of elasticity (e.g. the values of the static and dynamic modulus of elasticity of M25 at 28 days were 38.2 and 36.5 GPa respectively). Meanwhile mixtures M75 and M100 showed higher stiffness under dynamic loading: the dynamic modulus of elasticity through the UPV of mixture M100, at 28 days, was 44.1% higher than the static modulus of elasticity (27.1 GPa versus 20.1 GPa).

4.2.7. ABRASION RESISTANCE

Resistance to abrasion was evaluated by the footprint caused by an abrasive disc on the surface of the material on cubic samples of 10x10x10 cm at 90 days (Figure 2.19), which measures the hardness of the surface cement paste [62]. According to other studies, the addition of fine RCA increased the size of the footprint [63]. Nevertheless, the use of RCA from a concrete with a strength of over 70 MPa can improve the surface resistance of the concrete [64].

In this research, the increase in fine RCA generated a cement paste with a lower surface hardness, which increased the footprint size, as shown in Figure 2.20. These results were in line with the results of the 90-day rebound index: a higher rebound index was produced in those mixtures with a smaller footprint width (mix M75 had a lower rebound index, 39, and a footprint size of 21 mm that was 27.3% larger than the M0 footprint). Once again, there were two different groups of concretes, according to the results of this test: high and low/medium fine RCA content.



Figure 2.19. Abrasion test. Left: footprint on the M50 mix. Right: sample set up in the testing machine

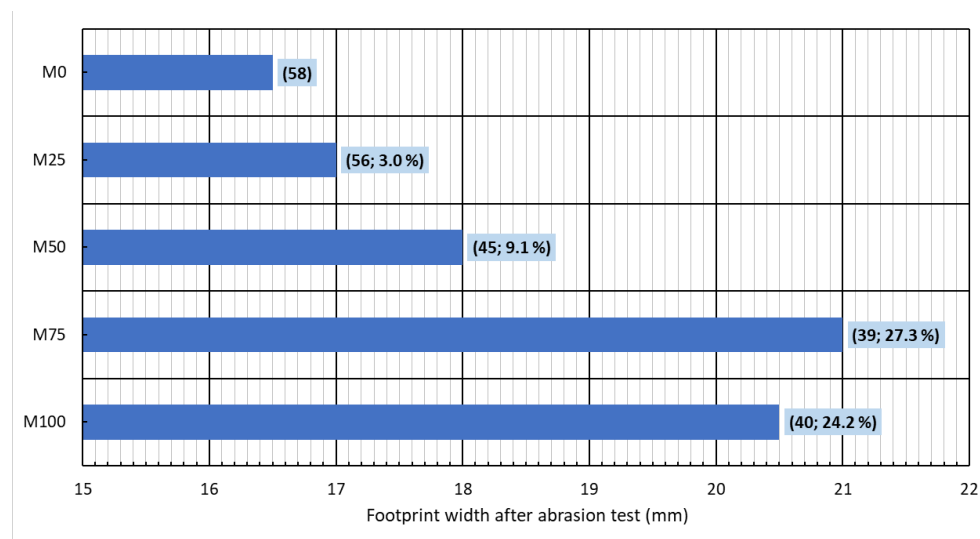


Figure 2.20. Resistance to abrasion test results. The hammer rebound index and the increase in footprint size, in relation to mixture M0, are shown between brackets

4.2.8. STATISTICAL ANALYSIS OF MECHANICAL PROPERTIES

The descriptive analysis was completed with a statistical analysis based on one-way ANOVA (Table 2.10). It showed that both age and fine RCA content significantly influenced the behavior of the mixes in all tests (p-value lower than the significance level considered, 0.05). The homogeneous groups revealed that, in general, mixes M0 and M25, as well as M75 and M100, have no significant difference in their mechanical properties regardless the age. In contrast, the mechanical properties of mixes with low fine RCA contents (M0 and M25) hardly showed significant variations between 28 and 90 days, while the mechanical properties of mixes M75 and M100, at 7, 28 and 90 days, can be considered statistically equal in several tests. Mix M50 showed an intermediate behavior.

Table 2.10. One-way ANOVA of mechanical properties

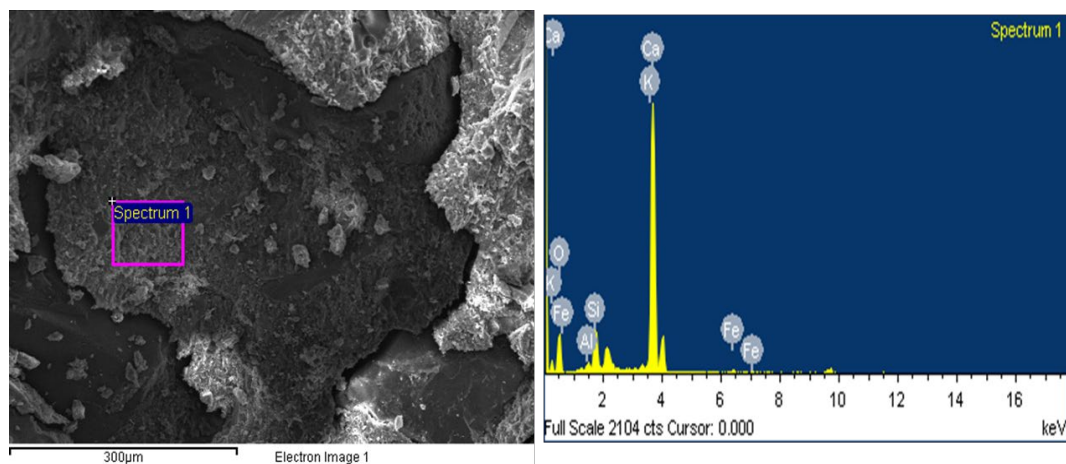
Test	Factor	Condition	P-value	Homogeneous groups
Compressive strength	Fine RCA percentage	Age of 1 day	0.0001	M75 and M100
		Age of 7 days	0.0001	M0 and M25; M75 and M100
		Age of 28 days	0.0002	M0 and M25; M75 and M100
		Age of 90 days	0.0001	M0 and M25; M75 and M100
	Age	0% fine RCA	0.0007	7, 28 and 90 days
		25% fine RCA	0.0003	7, 28 and 90 days
		50% fine RCA	0.0001	7, 28 and 90 days
		75% fine RCA	0.0002	7, 28 and 90 days
		100% fine RCA	0.0001	28 and 90 days
Splitting tensile strength	Fine RCA percentage	Age of 7 days	0.0017	M0 and M25; M50, M75 and M100
		Age of 28 days	0.0233	M75 and M100
		Age of 90 days	0.0282	M75 and M100
	Age	0% fine RCA	0.0370	None
		25% fine RCA	0.0230	None
		50% fine RCA	0.0239	28 and 90 days
		75% fine RCA	0.0351	7 and 28 days
		100% fine RCA	0.0349	28 and 90 days
Flexural strength	Fine RCA percentage	Age of 7 days	0.0173	M25 and M50; M75 and M100
		Age of 28 days	0.038	M0, M25 and M50; M75 and M100
		Age of 90 days	0.017	M0 and M25
	Age	0% fine RCA	0.0001	28 and 90 days
		25% fine RCA	0.0004	28 and 90 days
		50% fine RCA	0.0001	28 and 90 days
		75% fine RCA	0.0003	7, 28 days and 90 days
		100% fine RCA	0.0015	7 and 28 days
Static modulus of elasticity	Fine RCA percentage	Age of 7 days	0.0002	M75 and M100
		Age of 28 days	0.0001	M0 y M25; M75 y M100
		Age of 90 days	0.0002	M0 y M25; M75 y M100
	Age	0% fine RCA	0.0260	28 and 90 days
		25% fine RCA	0.0173	28 and 90 days
		50% fine RCA	0.0104	28 and 90 days
		75% fine RCA	0.0256	7, 28 and 90 days
		100% fine RCA	0.0394	7, 28 and 90 days

Table 2.10 (continued). One-way ANOVA of mechanical properties

Test	Factor	Condition	P-value	Homogeneous groups
Poisson coefficient	Fine RCA percentage	Age of 7 days	0.0083	M25 and M50
		Age of 28 days	0.0158	M0 and M25
		Age of 90 days	0.0118	M0 and M25
	Age	0% fine RCA	0.0285	None
		25% fine RCA	0.0327	None
		50% fine RCA	0.0211	None
		75% fine RCA	0.0441	28 and 90 days
		100% fine RCA	0.0303	None
Dynamic modulus of elasticity through the UPV	Fine RCA percentage	Age of 7 days	0.0023	M25 and M50; M75 and M100
		Age of 28 days	0.0016	M75 and M100
		Age of 90 days	0.0010	M0 y M25; M75 y M100
	Age	0% fine RCA	0.0344	28 and 90 days
		25% fine RCA	0.0465	None
		50% fine RCA	0.0351	28 and 90 days
		75% fine RCA	0.0222	28 and 90 days
		100% fine RCA	0.0455	7, 28 and 90 days
Abrasion resistance	Fine RCA percentage	Age of 90 days	0.0043	M0, M25 and M50; M75 and M100

4.2.9. SEM ANALYSIS

As commented in the introduction, the presence of adhered mortar in the RCA leads to the formation of an ITZ that is less dense and of poorer quality than the ITZ between the NA and the cementitious matrix [22, 25], as may be observed in the image of Figure 2.21, obtained from a low-strength M75 test specimen. In this image, two particles of siliceous aggregate of the RCA can be seen in both the lower right and left-hand-side corners; the old cementitious matrix (mortar adhered to the NA) of a darker color in the central part, corroborated by the microanalysis spectrum; and, the new cementitious matrix of a lighter color on the right-hand side and towards the upper right-hand-side corner. It is clear that the ITZ has failed due to its poor quality; the new cement paste shows low adhesion to the RCA, both with the mortar phase and the siliceous aggregate phase. This poor behavior of the ITZ, when adding large quantities of fine RCA, explained the variable behavior of the mixtures with high contents of fine RCA, especially in relation to the splitting tensile strength and the flexural strength.

**Figure 2.21.** SEM analysis of mix SA75

5. CONCLUSIONS

In this study, the physical and mechanical behavior, at different curing ages, of a Self-Compacting Concrete (SCC) manufactured with coarse and fine Recycled Concrete Aggregate (RCA) has been studied. A preliminary statistical analysis showed an acceptable mechanical behavior of the concretes manufactured with 100% of coarse RCA. Therefore, SCCs with 100% RCA in the coarse fraction and different percentages (0%, 25%, 50%, 75% and 100%) of fine RCA in substitution of Natural Aggregate (NA), 0/4 mm, were performed. The conclusions relating to the effect of the incorporation of fine RCA on these recycled SCCs are set out below:

- Increasing the mix water according to RCA water absorption was insufficient to maintain the flowability of the SCC manufactured with NA 0/4 mm when fine RCA was added. Instead, the effective water/cement ratio had to be increased. The increase in the fines content of the RCA, in comparison with NA, was favorable in the slump-flow test and the passing ability.
- All developed recycled SCCs had fresh property values within the limits of the EFNARC recommendations [32]. SCC were obtained in slump-flow class SF2, viscosity class VS2 and VF2, passage ability class PA1, and resistance to segregation class SR2.
- The mechanical properties of the SCC worsened as the percentage of fine RCA increased at all ages of curing. On the one hand, fine RCA contents of 0% and 25% allowed to obtain compressive strengths above 50 MPa (high strength concrete). On the other hand, the SCC with a high content of fine RCA (75% and 100%) showed a worsening of their mechanical properties with compressive strengths below 35 MPa. The one-way ANOVA showed that there was no significant difference between the mechanical properties for mixes with fine RCA percentages of 0% and 25%, and for 75% and 100%.
- The stress-strain curves showed that the mixtures with 75 and 100% fine RCA were much more deformable, with fracture strains of 3.7 ‰, 18.9% higher than the fracture strain of the mixture with 0% fine RCA, which had a value of 3 ‰.
- In general, recycled SCCs with high fine RCA contents showed more uniform mechanical properties over time than those with less fine RCA. According to one-way ANOVA, mixes with 0% and 25% of fine RCA showed the same strength and stiffness values at 28 and 90 days, meanwhile mixes with 75% and 100% of fine RCA had the same values at 7, 28, and 90 days.
- The adjustment of the experimental values to the theoretical design values provided by the regulations was different for each property and each recycled SCC. The theoretical values of tensile strength were higher than the experimental values, both from the European standard [34, 39, 42] and the ACI regulations [38], a fit that was improved by increasing the fine RCA content. The theoretical modulus of elasticity, calculated with both the European and the USA standard, underestimated the experimental value in mixtures with up to 25% fine RCA, while the modulus of elasticity was overestimated by percentages greater than 75%.
- Indirect measurements, such as the Ultrasonic Pulse Velocity (UPV) and the hammer rebound index yielded accurate compressive strength estimates for the concretes under analysis, with the most linear adjustment for the mixtures with low contents of fine RCA. The best statistical adjustment was obtained for the mixture with 100% fine and coarse RCA.

In view of the above, SCC of optimum flowability and with adequate mechanical behavior can be produced using high RCA contents in such a way that the SCC is valid for use in structural components. In the present study, the combination of 100% coarse RCA and a 50% fine RCA was the limit value, after which a notable worsening of the mechanical properties ensued, suggesting that the use of a fine RCA content higher than 50% in structural concretes would not be advisable

in structural applications from a mechanical point of view. Nevertheless, when service requirements are considered, the higher deformability of the SCC due to higher fine RCA contents, shown in the stress-strain curves, is a good reason for limiting the content of fine RCA to 25%.

REFERENCES

- [1] ANEFA, ANEFHOP, ASEFMA, Informes de situación económica sectorial. Sectorial economic progress reports (2018).
- [2] M. Sandanayake, G. Zhang, S. Setunge, Estimation of environmental emissions and impacts of building construction – A decision making tool for contractors, *J. Build. Eng.* 21 (2019) 173-185.
- [3] Eurostat, Waste statistics (2017).
- [4] J.I. Tertre, Construction and Demolition Waste (CDW), Conference Paper, CONAMA2016, (2016).
- [5] M. Behera, S.K. Bhattacharyya, A.K. Minocha, R. Deoliya, S. Maiti, Recycled aggregate from C&D waste & its use in concrete - A breakthrough towards sustainability in construction sector: A review, *Constr. Build. Mater.* 68 (2014) 501-516.
- [6] C. Shi, Y. Li, J. Zhang, W. Li, L. Chong, Z. Xie, Performance enhancement of recycled concrete aggregate - A review, *J. Clean. Prod.* 112 (2016) 466-472.
- [7] A. Gonzalez-Corominas, M. Etxeberria, Effects of using recycled concrete aggregates on the shrinkage of high performance concrete, *Constr. Build. Mater.* 115 (2016) 32-41.
- [8] V. Ortega-López, J.A. Fuente-Alonso, A. Santamaría, J.T. San-José, Á. Aragón, Durability studies on fiber-reinforced EAF slag concrete for pavements, *Constr. Build. Mater.* 163 (2018) 471-481.
- [9] M. Skaf, E. Pasquini, V. Revilla-Cuesta, V. Ortega-López, Performance and durability of porous asphalt mixtures manufactured exclusively with electric steel slags, *Materials* 12 (20) (2019) 3306.
- [10] A.S. Brand, J.R. Roesler, Steel furnace slag aggregate expansion and hardened concrete properties, *Cem. Concr. Compos.* 60 (2015) 1-9.
- [11] C. Pellegrino, F. Faleschini, Experimental behavior of reinforced concrete beams with electric arc furnace slag as recycled aggregate, *ACI Mater. J.* 110 (2) (2013) 197-205.
- [12] H. Qasrawi, The use of steel slag aggregate to enhance the mechanical properties of recycled aggregate concrete and retain the environment, *Constr. Build. Mater.* 54 (2014) 298-304.
- [13] A.R. Khan, S. Fareed, M.S. Khan, Use of recycled concrete aggregates in structural concrete, *Sustain. Constr. Mater. Technol.* 2 (2019).
- [14] B. Fronek, P. Bosela, N. Delatte, Steel slag aggregate used in portland cement concrete, *Transp. Res. Rec.* (2012) 37-42.
- [15] A. Santamaria, F. Faleschini, G. Giacomello, K. Brunelli, J.T. San José, C. Pellegrino, M. Pasetto, Dimensional stability of electric arc furnace slag in civil engineering applications, *J. Clean. Prod.* 205 (2018) 599-609.
- [16] I.Z. Yildirim, M. Prezzi, Chemical, mineralogical, and morphological properties of steel slag, *Adv. Civ. Eng.* 2011 (2011) 463638.
- [17] V.W.Y. Tam, M. Soomro, A.C.J. Evangelista, A review of recycled aggregate in concrete applications (2000–2017), *Constr. Build. Mater.* 172 (2018) 272-292.
- [18] C. Thomas, J. Setién, J.A. Polanco, A.I. Cimentada, C. Medina, Influence of curing conditions on recycled aggregate concrete, *Constr. Build. Mater.* 172 (2018) 618-625.
- [19] L. Evangelista, J. De Brito, Concrete with fine recycled aggregates: A review, *Eur. J. Environ. Civ. Eng.* 18 (2) (2014) 129-172.
- [20] S. Santos, P.R. da Silva, J. de Brito, Self-compacting concrete with recycled aggregates – A literature review, *J. Build. Eng.* 22 (2019) 349-371.
- [21] A.M. Matos, L. Maia, S. Nunes, P. Milheiro-Oliveira, Design of self-compacting high-performance concrete: Study of mortar phase, *Constr. Build. Mater.* 167 (2018) 617-630.
- [22] S. Nagataki, A. Gokce, T. Saeki, M. Hisada, Assessment of recycling process induced damage sensitivity of recycled concrete aggregates, *Cem. Concr. Res.* 34 (6) (2004) 965-971.

- [23] V.W.Y. Tam, K. Wang, C.M. Tam, Assessing relationships among properties of demolished concrete, recycled aggregate and recycled aggregate concrete using regression analysis, *J. Hazard. Mater.* 152 (2) (2008) 703-714.
- [24] J.T. San-José, J.M. Manso, Fiber-reinforced polymer bars embedded in a resin concrete: Study of both materials and their bond behavior, *Polym. Compos.* 27 (3) (2006) 315-322.
- [25] K.P. Verian, W. Ashraf, Y. Cao, Properties of recycled concrete aggregate and their influence in new concrete production, *Resour. Conserv. Recycl.* 133 (2018) 30-49.
- [26] A. Yacoub, A. Djerbi, T. Fen-Chong, Water absorption in recycled sand: New experimental methods to estimate the water saturation degree and kinetic filling during mortar mixing, *Constr. Build. Mater.* 158 (2018) 464-471.
- [27] V. Revilla-Cuesta, M. Skaf, F. Faleschini, J.M. Manso, V. Ortega-López, Self-compacting concrete manufactured with recycled concrete aggregate: An overview, *J. Clean. Prod.* 262 (2020) 121362.
- [28] M. Kazemi, R. Madandoust, J. de Brito, Compressive strength assessment of recycled aggregate concrete using Schmidt rebound hammer and core testing, *Constr. Build. Mater.* 224 (2019) 630-638.
- [29] B.B. Mukharjee, S.V. Barai, Influence of Nano-Silica on the properties of recycled aggregate concrete, *Constr. Build. Mater.* 55 (2014) 29-37.
- [30] R. Latif Al-Mufti, A.N. Fried, The early age non-destructive testing of concrete made with recycled concrete aggregate, *Constr. Build. Mater.* 37 (2012) 379-386.
- [31] M.C.S. Nepomuceno, L.F.A. Bernardo, Evaluation of self-compacting concrete strength with non-destructive tests for concrete structures, *Appl. Sci.* 9 (23) (2019) 5109.
- [32] EFNARC, Specification Guidelines for Self-compacting Concrete, European Federation of National Associations Representing producers and applicators of specialist building products for Concrete (2002).
- [33] F. Fiol, C. Thomas, C. Muñoz, V. Ortega-López, J.M. Manso, The influence of recycled aggregates from precast elements on the mechanical properties of structural self-compacting concrete, *Constr. Build. Mater.* 182 (2018) 309-323.
- [34] EHE-08, Instrucción de Hormigón Estructural. Structural Concrete Regulations, Ministerio de Fomento, Gobierno de España (2010).
- [35] EN-Euronorm, Rue de stassart, 36. Belgium-1050 Brussels, European Committee for Standardization.
- [36] S.C. Kou, C.S. Poon, Properties of self-compacting concrete prepared with coarse and fine recycled concrete aggregates, *Cem. Concr. Compos.* 31 (9) (2009) 622-627.
- [37] S.A. Santos, P.R. da Silva, J. de Brito, Mechanical performance evaluation of self-compacting concrete with fine and coarse recycled aggregates from the precast industry, *Materials* 10 (8) (2017) 904.
- [38] ACI-318-19, Building Code Requirements for Structural Concrete (2019).
- [39] EC-2, Eurocode 2: Design of concrete structures. Part 1-1: General rules and rules for buildings, CEN (European Committee for Standardization) (2010).
- [40] E. Güneş, M. Gesoğlu, Z. Algin, H. Yazici, Effect of surface treatment methods on the properties of self-compacting concrete with recycled aggregates, *Constr. Build. Mater.* 64 (2014) 172-183.
- [41] I. González-Taboada, B. González-Fonteboa, J. Eiras-López, G. Rojo-López, Tools for the study of self-compacting recycled concrete fresh behaviour: Workability and rheology, *J. Clean. Prod.* 156 (2017) 1-18.
- [42] CEB-FIP, Model Code 2010 (Volumes 1 and 2) (2012).
- [43] D. Carro-López, B. González-Fonteboa, J. De Brito, F. Martínez-Abella, I. González-Taboada, P. Silva, Study of the rheology of self-compacting concrete with fine recycled concrete aggregates, *Constr. Build. Mater.* 96 (2015) 491-501.

- [44] O. Kebaïli, M. Mouret, N. Arabia, F. Cassagnabere, Adverse effect of the mass substitution of natural aggregates by air-dried recycled concrete aggregates on the self-compacting ability of concrete: Evidence and analysis through an example, *J. Clean. Prod.* 87 (1) (2015) 752-761.
- [45] Z.J. Grdic, G.A. Toplicic-Curcic, I.M. Despotovic, N.S. Ristic, Properties of self-compacting concrete prepared with coarse recycled concrete aggregate, *Constr. Build. Mater.* 24 (7) (2010) 1129-1133.
- [46] S. Manzi, C. Mazzotti, M.C. Bignozzi, Self-compacting concrete with recycled concrete aggregate: Study of the long-term properties, *Constr. Build. Mater.* 157 (2017) 582-590.
- [47] T. Uygunoğlu, I.B. Topçu, A.G. Çelik, Use of waste marble and recycled aggregates in self-compacting concrete for environmental sustainability, *J. Clean. Prod.* 84 (1) (2014) 691-700.
- [48] L.A. Pereira-De-Oliveira, M.C.S. Nepomuceno, J.P. Castro-Gomes, M.F.C. Vila, Permeability properties of self-Compacting concrete with coarse recycled aggregates, *Constr. Build. Mater.* 51 (2014) 113-120.
- [49] R.V. Silva, J. De Brito, R.K. Dhir, The influence of the use of recycled aggregates on the compressive strength of concrete: A review, *Eur. J. Environ. Civ. Eng.* 19 (7) (2015) 825-849.
- [50] P. Revathi, R.S. Selvi, S.S. Velin, Investigations on Fresh and Hardened Properties of Recycled Aggregate Self Compacting Concrete, *J. Inst. Eng. Ser. A* 94 (3) (2013) 179-185.
- [51] M. Gesoglu, E. Güneyisi, H.Ö. Öz, I. Taha, M.T. Yasemin, Failure characteristics of self-compacting concretes made with recycled aggregates, *Constr. Build. Mater.* 98 (2015) 334-344.
- [52] D.B. Lad, S.A. Faroz, S. Ghosh, Fusion of Rebound Number and Ultrasonic Pulse Velocity Data for Evaluating the Concrete Strength Using Bayesian Updating, *Lect. Notes Mech. Eng.* (2020) 437-448.
- [53] B.M. Vinay Kumar, H. Ananthan, K.V.A. Balaji, Experimental studies on utilization of coarse and finer fractions of recycled concrete aggregates in self compacting concrete mixes, *J. Build. Eng.* 9 (2017) 100-108.
- [54] F. Aslani, G. Ma, D.L. Yim Wan, G. Muselin, Development of high-performance self-compacting concrete using waste recycled concrete aggregates and rubber granules, *J. Clean. Prod.* 182 (2018) 553-566.
- [55] J.A. Ortiz, A. de la Fuente, F. Mena Sebastia, I. Segura, A. Aguado, Steel-fibre-reinforced self-compacting concrete with 100% recycled mixed aggregates suitable for structural applications, *Constr. Build. Mater.* 156 (2017) 230-241.
- [56] J. Xie, W. Chen, J. Wang, C. Fang, B. Zhang, F. Liu, Coupling effects of recycled aggregate and GGBS/metakaolin on physicochemical properties of geopolymer concrete, *Constr. Build. Mater.* 226 (2019) 345-359.
- [57] B. Wu, H. Jin, Compressive fatigue behavior of compound concrete containing demolished concrete lumps, *Constr. Build. Mater.* 210 (2019) 140-156.
- [58] C. Zhou, Z. Chen, Mechanical properties of recycled concrete made with different types of coarse aggregate, *Constr. Build. Mater.* 134 (2017) 497-506.
- [59] F. Aslani, S. Nejadi, Mechanical characteristics of self-compacting concrete with and without fibres, *Mag. Concr. Res.* 65 (10) (2013) 608-622.
- [60] Y. Chen, Z. Chen, J. Xu, E.M. Lui, B. Wu, Performance evaluation of recycled aggregate concrete under multiaxial compression, *Constr. Build. Mater.* 229 (2019) 116935.
- [61] L.A. Pereira-de Oliveira, M. Nepomuceno, M. Rangel, An eco-friendly self-compacting concrete with recycled coarse aggregates, *Inf. Constr.* 65 (EXTRA 1) (2013) 31-41.
- [62] M.K. Ismail, A.A.A. Hassan, Abrasion and impact resistance of concrete before and after exposure to freezing and thawing cycles, *Constr. Build. Mater.* 215 (2019) 849-861.
- [63] D. Pedro, J. de Brito, L. Evangelista, Structural concrete with simultaneous incorporation of fine and coarse recycled concrete aggregates: Mechanical, durability and long-term properties, *Constr. Build. Mater.* 154 (2017) 294-309.
- [64] G. Duarte, M. Bravo, J. de Brito, J. Nobre, Mechanical performance of shotcrete produced with recycled coarse aggregates from concrete, *Constr. Build. Mater.* 210 (2019) 696-708.

Article 3

Statistical approach for the design of structural self-compacting concrete with fine recycled concrete aggregate

Title: Statistical approach for the design of structural self-compacting concrete with fine recycled concrete aggregate

Authors: Víctor Revilla-Cuesta, Marta Skaf, Ana B. Espinosa, Amaia Santamaría, Vanesa Ortega-López

Journal: Mathematics

Year: 2020

Volume: 8

Issue: 12

Article number: 2190

DOI: <https://doi.org/10.3390/math8122190>

Journal classification (2019 JCR ranking data): 28/325 (mathematics). First quartile (Q1), first decile (D1)

ABSTRACT

The compressive strength of recycled concrete is acknowledged to be largely conditioned by the incorporation ratio of Recycled Concrete Aggregate (RCA), although that ratio needs to be carefully assessed to optimize the design of structural applications. In this study, Self-Compacting Concrete (SCC) mixes containing 100% coarse RCA and variable amounts, between 0% and 100%, of fine RCA were manufactured and their compressive strengths were tested in the laboratory for a statistical analysis of their strength variations, which exhibited robustness and normality according to the common statistical procedures. The results of the confidence intervals, the one-factor ANalysis Of VAriance (ANOVA), and the Kruskal–Wallis test showed that an increase in fine RCA content did not necessarily result in a significant decrease in strength, although the addition of fine RCA delayed the development of the final strength. The statistical models presented in this research can be used to define the optimum incorporation ratio that would produce the highest compressive strength. Furthermore, the multiple regression models offered accurate estimations of compressive strength, considering the interaction between the incorporation ratio of fine RCA and the curing age of concrete that the two-factor ANOVA revealed. Lastly, the probability distribution predictions, obtained through a log-likelihood analysis, fitted the results better than the predictions based on current standards, which clearly underestimated the compressive strength of SCC manufactured with fine RCA and require adjustment to take full advantage of these recycled materials. This analysis could be carried out on any type of waste and concrete, which would allow one to evaluate the same aspects as in this research and ensure that the use of recycled concrete maximizes both sustainability and strength.

Keywords: analysis of variance; compressive strength prediction; characteristic compressive strength; distribution fitting; recycled concrete aggregate; recycled concrete aggregate content optimization; robustness; self-compacting concrete.

1. INTRODUCTION

The varied environmental impacts of the construction sector are often of great magnitude [1], extending to resource-intensive materials [2], widely used in this sector, such as concrete and bituminous mixtures [3]. The recovery of waste sub-products for use in construction materials is now a widely accepted solution to this problem [4], to reduce these impacts [5], and to minimize dumping in landfill sites [6]. Waste with pozzolanic properties that can substitute clinker [7] is specified in European standard EN 197-1 [8]. Replacing Natural Aggregates (NAs) with waste sub-products [9] is, likewise, a valid strategy, if the effect of each particular waste is evaluated [10] in order to get a correct mix design of the construction material [11]. The most used by-products are Recycled Concrete Aggregate (RCA) [12]; slag, both in concrete [13] and asphalt mixes [14]; rubber [15].

There are three main characteristics of RCA. Firstly, its angular shape, due to the crushing process. Secondly, the presence of adhered mortar, which causes lower wear resistance, a greater water absorption, and the appearance of Interfacial Transition Zones (ITZs) of poor quality [16]. Finally, the presence of altered and potentially contaminated cement particles within the finest fraction [17].

Self-Compacting Concrete (SCC) is a high flowability concrete in the fresh state, characterized by its slump flow and viscosity [18]. The slump-flow test measures the ease with which the concrete will pour, while the viscosity index is related to the speed of flow [19]. The addition of RCA, in general, worsens both aspects, due to its angular shape [20], which hinders the flow of aggregate particles within the paste [21], and its high water absorption, which decreases the effective water-to-cement (w/c) ratio [22]. This last aspect can be compensated by increasing the water content [23]. Another possible solution is to use RCA with a high fine particle proportion, although it implies a decrease in concrete strength [24].

The most important property of concrete in the hardened state, including SCC, is its compressive strength [25], to which most structural calculations refer [26, 27]. The standardized strength is referred to as the characteristic strength, and it can be used for a theoretical estimate of the modulus of elasticity or the tensile strength [28]. This strength is obtained through the statistical treatment of a large number of experimental data, all of which are necessary as this material is not homogeneous and can be affected, for example, by irregular aggregate distributions [28, 29]. Most of the statistical models developed to predict the compressive strength of vibrated concrete with NA show that the quantities of the mix components and the w/c ratio are the key aspects that influence this strength [30, 31]. The characteristics of the NA and their gradation have much less influence [32]. However, the characteristics and amount of waste are key factors in the compressive strength of the recycled concrete.

In principle, the replacement of NA by RCA, in any fraction, decreases the compressive strength of SCC [33], due to the presence of contaminants and ITZs with poor adhesion [34]. However, a lower water content can yield higher strengths than those obtained with NA, by decreasing the effective w/c ratio [35], although the flowability of the SCC will worsen [36]. A literature review of over 60 studies on vibrated concrete, conducted by Portuguese researchers [30], showed this trend (lower strength when increasing the RCA content). The same trend has also been observed in SCC [37].

Statistical studies of compressive strength in non-recycled SCC are very scarce and focus on the validity of Artificial Neural Networks and multivariate models that can predict compressive strength as a function of the composition of the mix [27, 38]. The acceptability of these procedures has been demonstrated, but their disadvantage is that they only evaluate strength at the standard age of 28 days [39]. In relation to recycled concrete, regardless of its type, the influence of different cement components has been statistically evaluated [40], as well as the good fit of normal probability distribution to the compressive strength if coarse RCA is used [41]. Correct statistical studies allow

one to predict both the compressive strength when a certain waste is used and the optimal amount to add of this waste. With this kind of analysis, it is possible to adapt the strength of concrete to the requirements of each structural application [42]. Nevertheless, there is a lack of research that statistically evaluates the strength behavior of recycled concrete and the effect of the waste used. Therefore, this study aims to fill this gap of knowledge in the field of concrete.

Previous research has demonstrated the good performance of coarse RCA [20, 37], so the sustainable SCC designed included 100% of coarse RCA. Therefore, the study focused on the effect of different percentages of RCA in the fine fraction (0, 25, 50, 75, and 100%). Both the flowability and the compressive strength of the mixes were analyzed. Moreover, an experimental procedure was designed to discard the effect of the water content [35] and the curing conditions [43], and then isolate the effect of the fine RCA content.

The novelty of this study lies in the extensive laboratory work carried out and the statistical analysis of the compressive strength afterwards. This analysis is quite significant and allows us to study some aspects that the traditional descriptive analysis does not cover:

- Evaluating the effect of RCA at each age and the significance of the differences in the strength of concrete made with different RCA ratios. This way, it is possible to detect whether the same performance can be expected with different waste contents, and to define the optimum ratios from the strength point of view.
- Developing models to estimate the compressive strength of SCC with RCA. The effect of the residue is different at each age and the interaction between these two parameters, age and RCA content, must be considered when developing these models.
- Analyzing if the predicted values of the compressive strength according to the existing structural design regulations are suitable for recycled SCC.

Therefore, this study allows us to obtain relevant conclusions regarding how the analysis of SCC with RCA should be carried out. This analysis includes the evaluation of the significance of the effect of RCA, the estimation of the strength, and the analysis of the existing regulations for the design of this type of concrete. These aspects are important for the generalization and standardization of the analysis of the SCC produced with RCA.

In addition to the particular conclusions reached for the material studied, another scope of this research is the development of the study procedure, which is described in detail. Therefore, it could be replicated in any type of concrete manufactured with any alternative material. With this type of analysis, the use of sustainable materials in real structures is closer.

2. MATERIALS

CEM I 52.5 R was used, according to EN 197-1 [8], in all mixtures, with a clinker content of 95% and a density of 3.12 Mg/m³. The mix water was taken from the mains water supply of the city of Burgos, Spain.

Proper use of chemical admixtures is essential to achieve self-compacting properties [44]. In this study, a plasticizer gave the concrete a high level of flowability. In addition, a viscosity regulator was also added, so that the concrete retained its flowability for longer. Previous studies of this research group have shown the validity of these admixtures in proportions between 2% and 2.2% by weight of cement [35].

The mixes were developed with three different types of aggregates:

- RCA, supplied by a local Construction and Demolition Waste (CDW) management company (IGLECAR S.L.) based in Burgos. This waste came from crushing 45 MPa strength prefabricated elements, rejected due to aesthetic manufacturing defects. The initial

granulometry, 0/31.5 mm, was sieved into three fractions: fine RCA 0/4 mm, coarse RCA 4/12.5 mm, and RCA > 12.5 mm. The first two fractions were used and the third was discarded and posteriorly re-crushed.

- Rounded siliceous sand 0/4 mm. used in the region to elaborate SCC.
- Limestone filler, with a size below 0.063 mm and high purity (CaCO₃ content above 98%), to provide the finest particle size fraction [45].

The physical properties of these aggregates, shown in Table 3.1, were in line with other similar investigations [46]: the presence of adhered mortar reduced the density and increased the water absorption of the RCA in comparison with the NA [47]. The content of particles of less than 0.125 mm in size was higher in the RCA, a very relevant aspect for the flowability of the SCC, as can be seen in Figure 3.1 and Table 3.2.

Table 3.1. Physical properties of the aggregates

Test	Regulation [8]	Coarse RCA 4/12.5 mm	Fine RCA 0/4 mm	Siliceous sand 0/4 mm	Limestone filler < 0.063 m
Saturated-Surface-Dry (SSD) density (Mg/m ³)	EN 1097-6	2.42	2.37	2.58	2.77
Water absorption 24 h (%)		6.25	7.36	0.25	0.54
Water absorption 10 min (%)		5.28	6.03	0.18	0.37

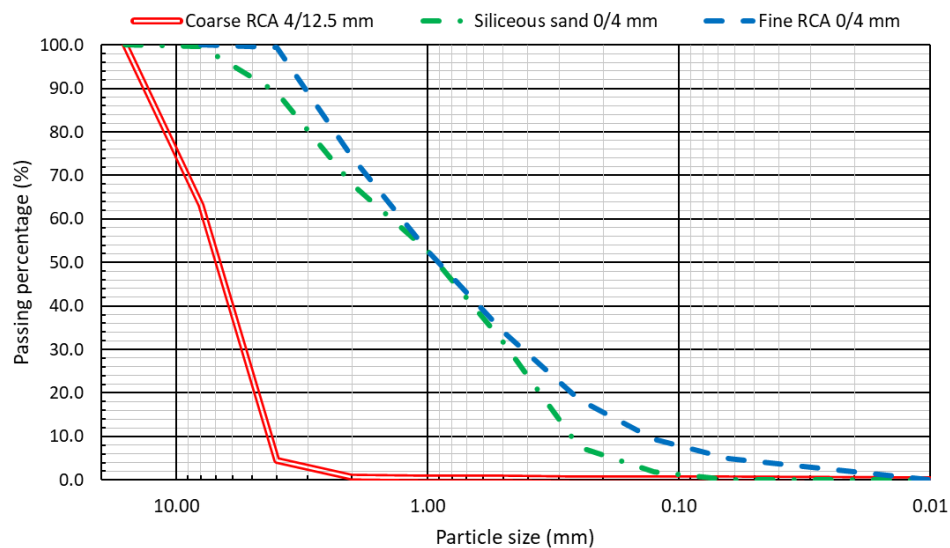


Figure 3.1. Aggregates' sieve analysis

Table 3.2. Gradation of the aggregates (EN 933-1 [8])

Size	Coarse RCA 4/12.5 mm	Siliceous sand 0/4 mm	Fine RCA 0/4 mm
16 mm	100.0	100.0	100.0
8 mm	63.1	99.7	100.0
4 mm	4.5	89.2	99.4
2 mm	0.7	68.1	74.3
1 mm	0.5	52.8	52.7
0.5 mm	0.4	31.6	34.0
0.25 mm	0.3	7.5	18.4
0.125 mm	0.2	1.8	9.4
0.063 mm	0.2	0.0	4.8
0.01 mm	0.0	0.0	0.0
Fineness modulus	6.3	3.5	3.1

3. EXPERIMENTAL PROCEDURE

As large proportions of fine aggregate are required by SCC [48], its performance is very sensitive to the presence of residues within that fraction [33]. For this reason, this study evaluated the effect of adding fine RCA on the compressive strength of SCC with 100% coarse RCA at different ages, while minimizing the influence of other variables such as water content and curing conditions. To do so, the following experimental procedure was developed:

- Having an optimal SCC with 100% NA in the fine fraction and 100% RCA in the coarse fraction, the NA content was replaced by 25, 50, 75, and 100% fine RCA. The mixtures were labelled SA0, SA25, SA50, SA75, and SA100, in which the acronym “SA” and the following number refer to “Statistical Analysis” and to the percentage of fine RCA, respectively.
- In each mix, all the aggregates, except the filler, were pre-soaked for 24 h, which managed to maintain the effective w/c ratio constant (at a value of 0.45) in all the mixes. As RCA water absorption can be very prolonged over time [49], this long pre-soaking time (24 h) was chosen to achieve complete stabilization of water absorption. Thus, the effect of the variable “water content” in the experiment was eliminated. In addition, the behavior of the RCA may be optimized with this procedure, although it requires prior preparation of the aggregates and it is not economically profitable [50].
- The mixing process consisted of a single stage, first adding the aggregates after drying their surface (SSD conditions) [50], then the cement, and finally the water with the admixtures dissolved. The concrete, 60 L per mix, was mixed in a horizontal-axis mixer for 1 min.
- When the mixing process was finished, the fresh state tests were carried out (Table 3.3) and 32 cylindrical 10 × 20 cm specimens were made for the compressive-strength test. Thirty minutes after mixing, the slump-flow test was repeated with the rest of the concrete mass, to evaluate the evolution of flowability over time [49].
- The specimens were left in their molds for 22 h under laboratory conditions: at a temperature and a humidity level of 20 °C and 60%, respectively. Subsequently they were demolded and, 23 h after the mixing process, were placed in a wet chamber (temperature of 20 ± 2 °C and humidity of 95 ± 5%), until the time of testing.
- At ages 24 ± 1 h (1 day), 168 ± 1 h (7 days), 672 ± 1 h (28 days), and 2160 ± 1 h (90 days), from the manufacturing of the mixes, 8 specimens were subjected to the compressive-strength test, EN 12390-3 [8], obtaining the data for the statistical analysis. With these precise moments of time, the effect of the variable “curing conditions” on the strength of SCC was eliminated: all the mixtures were tested at exactly the same age and after they had been in the same humidity and temperature conditions for the same time.

Some images of the most outstanding steps of the experimental plan are shown in Figure 3.2. On the other hand, the dosage of each mix is shown in Table 3.4. As the aggregate was pre-soaked, the amount of water added to each concrete mixture was the same.

Table 3.3. In-fresh state tests on each mix

Test	Regulation [8]
Slump-flow	EN 12350-8
V-funnel	EN 12350-9
2-bar L-box	EN 12350-10
Sieve segregation	EN 12350-11
Fresh density	EN 12350-6
Air content	EN 12350-7



Figure 3.2. Highlights of the experimental plan: coarse RCA pre-soaked (left), slump-flow test of mix SA50 (middle), and specimen tested for compressive strength (right)

Table 3.4. Mix design (kg/m³)

Material	SA0	SA25	SA50	SA75	SA100
Cement	300	300	300	300	300
Filler	180	180	180	180	180
Water	135	135	135	135	135
Coarse RCA 4/12.5 mm	525	525	525	525	525
Fine RCA 0/4 mm	0	265	530	795	1,060
Siliceous sand 0/4 mm	1,150	865	575	290	0
Plasticizer	2.20	2.20	2.20	2.20	2.20
Viscosity regulator	4.40	4.40	4.40	4.40	4.40
Approximate weight (kg)	2,296.6	2,276.6	2,251.6	2,231.6	2,206.6
Approximate volume (m ³)	1.00	1.00	1.00	1.00	1.00
Effective w/c ratio	0.45	0.45	0.45	0.45	0.45

4. IN-FRESH BEHAVIOR

The results of these tests (Table 3.5) were in line with expectations, as stated in the introduction: the decrease in flowability, due to the addition of RCA, can be compensated by the increase in the water content, in this case by pre-soaking [50]. Thus, only the effect of fine RCA was evaluated, with aggregate water absorption having no influence.

Table 3.5. Results of in-fresh state tests.

Test	SA0	SA25	SA50	SA75	SA100
Viscosity, t ₅₀₀ slump-flow test (s)	4.20	4.80	5.40	6.00	7.20
Slump flow (mm)	675	680	690	700	710
Viscosity, t ₅₀₀ slump-flow test after 30 min (s)	4.40	5.00	5.60	6.20	7.40
Slump flow after 30 min (mm)	650	660	665	675	680
Viscosity, V-funnel test (s)	6.60	9.00	11.20	13.80	16.20
Passing ability, L-box test H ₂ /H ₁	0.86	0.86	0.88	0.90	0.91
Sieve segregation (%)	1.65	1.51	1.32	1.07	0.85
Fresh density (Mg/m ³)	2.35	2.29	2.24	2.19	2.15
Air content (%)	3.80	3.90	4.20	3.95	4.05

A very different effect of the residue was observed in relation to slump flow and viscosity according to a descriptive analysis:

- The fine RCA slightly increased the flowability (slump-flow and L-box tests) [24]. Mixture SA100 showed a 4.7% higher slump flow than mixture SA0, and the improvement in the L-box test was 5.8%.
- The addition of fine RCA resulted in an increase in viscosity [49]. The results for mixture SA100 in the slump-flow (t_{500}) and in the V-funnel tests were, respectively, 28.6% and 70.8% higher than the results for mixture SA0.

This behavior can be explained by the content of particles smaller than 0.125 mm of fine RCA, which was higher than that of the NA (see the fineness modulus in Table 3.2, and Figure 3.1). As the entire NA fraction 0/4 mm was replaced simultaneously by fine RCA, it was not done size-by-size, the proportion of cement paste was greater when this waste was added. Therefore, the aggregate particles were evenly interspersed and dragged within the paste in the mixtures with fine RCA. This led to the increase in the slump flow [20]. However, this higher proportion of cement paste also resulted in a more viscous consistency and slower movement [33]. Sieve segregation was reduced as the fine RCA content increased due to the increase in viscosity and its higher water absorption [19].

After 30 min of the end of the mixing process, the overall decrease in slump flow was 4%, and t_{500} increased by 3%. The pre-soaking of the aggregates caused the water absorption by the aggregate to be minimal, thus favoring an optimum temporary conservation of self-compactability [50].

No clear influence of the fine RCA on the air content was observed, which was mainly controlled through the use of admixtures [51]. Nevertheless, other studies have stated that admixtures do not control the air content of the mix [52] and that it increases as the fine RCA content increases [33]. The fresh density of SCC decreased when replacing NA by RCA, due to its lower density [49].

Table 3.6. One-factor ANOVA of the fresh properties

Test	<i>p</i> -Value	Homogeneous groups
Viscosity t_{500} slump-flow test	0.0000	None
Slump flow	0.0202	SA0, SA25 and SA50; SA75 and SA100
Viscosity t_{500} slump-flow test after 30 min	0.0000	None
Slump flow after 30 min	0.0418	SA0, SA25 and SA50; SA75 and SA100
Viscosity V-funnel test	0.0000	None
Passing ability L-box test H_2/H_1	0.3827	All
Sieve segregation	0.0119	SA0 and SA25; SA75 and SA100
Fresh density	0.0281	SA75 and SA100
Air content	0.1898	All

The descriptive analysis can be completed with the one-factor ANalysis Of VAriance (ANOVA). By this statistical procedure it can be determined whether the effect of the factor (in this case, fine RCA content) is significant if the variances of the mixes are similar [53]—an aspect that is checked with two hypothesis tests explained in detail in Section 5.6. The results of this analysis are the *p*-value and the homogeneous groups. The effect of the factor will be significant when the *p*-value is lower than the chosen significance level (in this case the most usual one, 5% [41]). On the other hand, the homogeneous groups indicate the factor values that provide significantly equal results. The results obtained from the ANOVA carried out for the fresh state tests performed (all mixes exhibited a similar variance) are collected in Table 3.6 and show that:

- The behavioral differences obtained between mixtures with different percentage of fine RCA regarding the passing ability and the air content were not significant.
- Any variation in RCA content significantly affected both viscosity, which increased when adding fine RCA, and fresh density, which decreased with the addition of fine RCA. No homogeneous groups were obtained.

- Slump flow and resistance to segregation were significantly equal for 0–50% and 75–100% fine RCA contents. The increase in fines content experienced by SCC mixtures with the addition of RCA increased filling ability (slump flow) and resistance to segregation, thus compensating for the effect of the irregular shape of RCA.

5. COMPRESSIVE STRENGTH: STATISTICAL ANALYSIS AND STRENGTH PREDICTION

This section includes the statistical procedure carried out to evaluate the effect that the addition of different amounts of fine RCA will have on the compressive strength of SCC at different curing ages. Thanks to the experimental procedure designed (Section 3), the remaining variables that might potentially influence compressive strength (water content and curing conditions) were completely discarded [43]. This section includes the steps performed sequentially to obtain conclusions and which could be applied to any type of waste or concrete.

5.1. STAGES OF THE STATISTICAL ANALYSIS

Eight 10 × 20 cm cylindrical specimens were subjected to a compressive-strength test at 1, 7, 28, and 90 days (Table 3.7) for each mix. All these values were required for applying all the statistical procedures collected in this paper [41], main novelty regarding previous similar studies [54].

The statistical analysis was performed with the above values. The aspects under evaluation were:

- The robustness of the measurements (Section 5.2).
- The normality of the compressive strength (Section 5.3).
- The confidence intervals of the compressive strength and its dispersion (Section 5.4).
- The influence of the age and the percentage of fine RCA (Sections 5.5 and 5.6).
- The estimation of the compressive strength (Section 5.7).
- The determination of the characteristic strength (Section 5.8), which is the main property of concrete in any structural design.

A significance level of 5% was also used throughout this analysis ($\alpha = 0.05$), as in the analysis of the properties in the fresh state, which is very common and widely accepted in this type of studies [41].

Table 3.7. Compressive strength (MPa) values by mix and by age

Age	SA0	SA25	SA50	SA75	SA100
1 day	47.05; 47.84; 50.13; 47.76; 44.87; 48.04; 44.02; 48.62	38.36; 42.31; 35.43; 35.46; 37.48; 40.20; 40.61; 42.02	31.45; 30.64; 30.77; 32.25; 30.64; 33.28; 32.58; 33.21	21.30; 24.62; 24.35; 27.74; 25.12; 25.48; 23.88; 22.38	22.85; 22.88; 22.92; 21.82; 21.78; 21.98; 22.64; 22.24
7 days	60.32; 50.69; 55.97; 58.21; 58.13; 62.23; 59.49; 52.73	56.29; 51.96; 53.17; 54.47; 58.97; 52.73; 50.00; 55.32	45.85; 45.36; 48.29; 46.21; 40.28; 40.34; 43.71; 46.91	33.55; 34.89; 32.75; 34.11; 34.93; 34.01; 33.33; 34.99	34.29; 33.17; 32.41; 35.31; 33.83; 32.57; 35.37; 32.20
28 days	64.51; 58.77; 58.13; 62.37; 52.85; 65.91; 59.53; 65.86	56.21; 54.92; 56.59; 57.20; 55.11; 58.10; 58.07; 57.13	49.31; 52.01; 46.03; 50.66; 49.42; 50.91; 47.19; 49.43	41.30; 37.77; 36.46; 41.87; 41.19; 37.27; 40.56; 36.49	37.78; 36.78; 38.78; 38.81; 37.49; 38.26; 40.02; 35.83
90 days	56.11; 57.42; 64.35; 67.65; 48.32; 49.60; 65.24; 62.31	60.43; 55.97; 58.66; 60.37; 57.43; 63.15; 61.28; 65.74	54.23; 45.29; 51.15; 53.08; 52.33; 46.87; 55.33; 48.91	42.62; 38.27; 41.95; 37.24; 41.92; 44.48; 43.25; 45.03	39.73; 39.91; 39.05; 43.13; 42.63; 40.83; 41.67; 38.62

5.2. ROBUSTNESS

A robustness analysis will detect anomalous data, which are results that are not in harmony with the other measures. The absence of such data is fundamental to the application of any statistical procedure, as they will affect the significance of the analysis.

Two approaches were followed to assess the existence of anomalous data (outliers):

- They can be visually detected within the box and whiskers plot (outliers are the data that are not within the limits of the diagram, defined by the whiskers).
- The comparison between the traditional indicators (arithmetic mean and standard deviation) and the robust indicators (median, trimmed mean 5%, winsorized mean, winsorized standard deviation, and Sbi), which are not affected by the presence of this type of data. In the absence of anomalous data, both types of indicators have very similar values.

In this study, the existence of anomalous data would indicate inappropriate breakage of specimens and, above all, a lack of homogeneity of the RCA in use: an eventual increase in the content of fine fractions (<1 mm) would cause notably lower strengths (anomalous data).

All the indicators commented upon for each mixture, at each age are shown in Table 3.8, while Figure 3.3 shows the box and whiskers graphs at 1 and 28 days. It can be seen that the traditional and robust indicators presented very similar values, and the box and whiskers graphs showed no outliers. It can therefore be stated that the data agreed with each other and that no anomalous data were present, so all the data were incorporated in the analysis. Furthermore, the results show the great homogeneity in the compressive-strength behavior of all the mixtures that were produced, a fundamental aspect when this waste is used [33]. Therefore, the distribution of fine RCA was uniform in all of them.

Table 3.8. Both traditional and robust indicators of the compressive strength in MPa of the mixtures

Mix and age	Arithmetic mean	Median	Trimmed mean 5%	Winsorized mean	Standard deviation	Winsorized standard deviation	Sbi
SA0-1d	47.29	47.80	47.32	47.29	1.98	1.98	1.97
SA0-7d	57.22	58.17	57.31	57.22	3.89	3.89	3.86
SA0-28d	60.99	60.95	61.17	60.99	4.53	4.53	4.40
SA0-90d	58.88	59.87	58.97	58.88	7.24	7.24	7.22
SA25-1d	38.98	39.28	39.00	38.98	2.73	2.73	2.68
SA25-7d	54.11	53.82	54.07	54.11	2.78	2.78	2.70
SA25-28d	56.67	56.86	56.68	56.67	1.21	1.21	1.19
SA25-90d	60.38	60.40	60.33	60.38	3.12	3.12	3.02
SA50-1d	31.85	31.85	31.84	31.85	1.12	1.12	1.09
SA50-7d	44.62	45.61	44.66	44.62	2.96	2.96	3.00
SA50-28d	49.37	49.43	49.41	49.37	1.96	1.96	1.90
SA50-90d	50.90	51.74	50.96	50.90	3.57	3.57	3.56
SA75-1d	24.36	24.49	24.34	24.36	1.96	1.96	1.93
SA75-7d	34.07	34.06	34.09	34.07	0.83	0.83	0.80
SA75-28d	39.11	39.17	39.11	39.11	2.33	2.33	2.29
SA75-90d	41.85	42.29	41.92	41.85	2.77	2.77	2.71
SA100-1d	22.39	22.44	22.39	22.39	0.49	0.49	0.48
SA100-7d	33.64	33.50	33.63	33.64	1.26	1.26	1.25
SA100-28d	37.97	38.02	37.97	37.97	1.30	1.30	1.27
SA100-90d	40.70	40.37	40.68	40.70	1.66	1.66	1.65

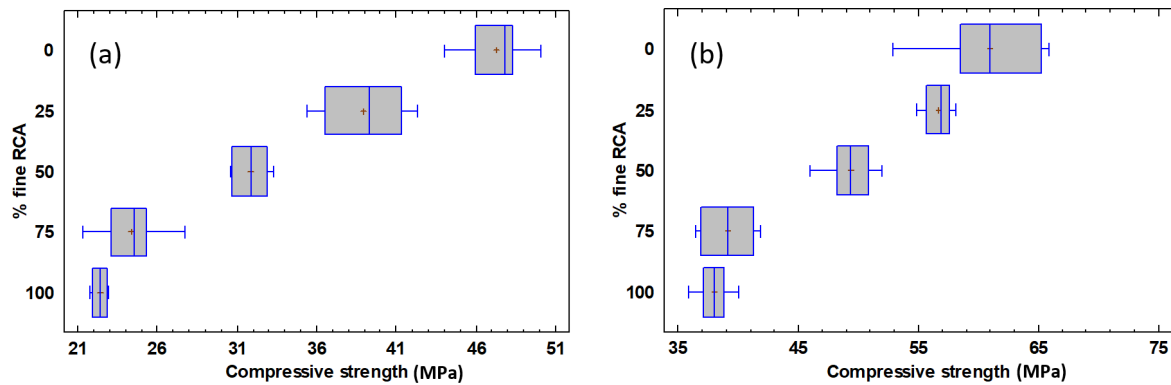


Figure 3.3. Box plot for all mixes: (a) 1 day; (b) 28 days.

5.3. NORMALITY

Data normality was validated with three hypothesis tests: the Chi-square test, the Saphiro–Wilk test, with which the histogram and the quartiles of each variable were, respectively, compared with those corresponding to a normal distribution, and the Z-asymmetry test, which evaluates the symmetry of the data. All these tests have as their null hypothesis that the data sample will follow a normal distribution, which is rejected if its p -value (Table 3.9) is lower than the significance level (in this study, 0.05).

It is known that the strength of non-recycled concrete conforms to a normal distribution [28]. If the RCA concretes also complied with this distribution, then similar calculation procedures would be applicable [28, 29].

Table 3.9. p -Value for the normality tests of the compressive strength of each mixture at each age

Mix and age	Chi-square test	Shapiro–Wilk test	Z-asymmetry test
SA0-1d	0.1247	0.5203	0.5877
SA0-7d	0.7769	0.6493	0.5339
SA0-28d	0.1247	0.4483	0.5632
SA0-90d	0.1247	0.4297	0.6801
SA25-1d	0.2570	0.3616	0.8480
SA25-7d	0.9856	0.9923	0.7139
SA25-28d	0.4815	0.4258	0.7394
SA25-90d	0.7769	0.9630	0.7219
SA50-1d	0.2570	0.1483	0.9021
SA50-7d	0.4815	0.2399	0.5156
SA50-28d	0.2570	0.6155	0.5733
SA50-90d	0.9856	0.6942	0.6539
SA75-1d	0.7769	0.9187	0.9218
SA75-7d	0.1247	0.3958	0.7797
SA75-28d	0.0245	0.0731	0.9760
SA75-90d	0.2570	0.2869	0.4457
SA100-1d	0.1247	0.1089	0.8789
SA100-7d	0.1247	0.2888	0.7316
SA100-28d	0.4815	0.9913	0.8830
SA100-90d	0.7769	0.6304	0.7558

It may be observed that the p -value of these three tests was higher than 0.05, so the compressive strength of each mixture at each age followed a normal distribution. Nevertheless, there was an

exception: at 28 days, mix SA75 presented an incompatible histogram with the normal distribution (Chi-square test) at a confidence level of 95%, although it was compatible with that distribution at a significance level of 0.01. This discrepancy was due to the concentration of the experimental results in two small intervals (around 37 MPa and 41 MPa), with no intermediate values (see Table 3.7). A significance level of 0.01 was therefore used for mixture SA75 at 28 days throughout the rest of the study.

5.4. CONFIDENCE INTERVALS

The confidence intervals for the arithmetic mean and the absolute and the relative standard deviation (Table 3.10 and Figure 3.4) inform us of the values between which a variable is found for a certain level of confidence. Thus, it can be ascertained whether, for example, an overlap is possible between the strengths obtained in the concretes with different percentages of fine RCA.

Table 3.10. Confidence intervals for mean and standard deviation of compressive strength for each mixture and age

Mix and age	Confidence interval arithmetic mean (MPa)	Confidence interval standard deviation (MPa)	Relative confidence interval of the standard deviation from the arithmetic mean (%)
SA0-1d	(45.63; 48.95)	(1.31; 4.04)	(2.77; 8.54)
SA0-7d	(53.97; 60.48)	(2.57; 7.92)	(4.49; 13.84)
SA0-28d	(57.20; 64.78)	(2.30; 9.22)	(3.77; 15.12)
SA0-90d	(52.83; 64.92)	(4.78; 14.73)	(8.12; 25.02)
SA25-1d	(36.71; 41.26)	(1.80; 5.55)	(4.62; 14.24)
SA25-7d	(51.79; 56.44)	(1.84; 5.67)	(3.40; 10.48)
SA25-28d	(55.66; 57.68)	(0.79; 2.46)	(1.39; 4.34)
SA25-90d	(57.77; 62.99)	(2.07; 6.36)	(3.43; 10.53)
SA50-1d	(30.91; 32.79)	(0.74; 2.29)	(2.32; 7.19)
SA50-7d	(42.15; 47.09)	(1.96; 6.02)	(4.39; 13.49)
SA50-28d	(47.73; 51.01)	(1.30; 3.99)	(2.63; 8.08)
SA50-90d	(47.91; 53.88)	(2.36; 7.27)	(4.64; 14.28)
SA75-1d	(22.72; 26.00)	(1.29; 3.99)	(5.30; 16.38)
SA75-7d	(33.38; 34.76)	(0.55; 1.69)	(1.61; 4.96)
SA75-28d ¹	(36.23; 41.99)	(1.37; 6.19)	(3.50; 15.83)
SA75-90d	(39.53; 44.16)	(1.83; 5.64)	(4.37; 13.48)
SA100-1d	(21.98; 22.80)	(0.32; 1.00)	(1.43; 4.47)
SA100-7d	(32.59; 34.70)	(0.84; 2.57)	(2.50; 7.64)
SA100-28d	(36.88; 39.06)	(0.86; 2.65)	(2.26; 6.98)
SA100-90d	(39.31; 42.08)	(1.10; 3.37)	(2.70; 8.28)

¹ The confidence intervals of the mixture SA75 at 28 days have been obtained for a confidence level of 99%

The arithmetic mean confidence intervals showed several relevant aspects (see Figure 3.4):

- In almost all mixtures, the 28-day and 90-day confidence intervals overlapped, with their strengths developing mainly during the first 4 weeks. The 7-day and 28-day confidence intervals also overlapped in two mixes, SA0 and SA25, showing that, in principle, the increase in the content of this residue caused a slower development of strength.
- Comparing the confidence intervals of different mixtures with each other, it was found that they overlapped in mixtures SA0 and SA25, as well as in mixtures SA75 and SA100, at 7, 28, and 90 days. Therefore, the strength of mix SA25 might be greater than the strength of mix SA0 at any of these ages, despite the higher fine RCA content of the first one. This behavior of mixture SA25 was mainly due to the higher fines content of fine RCA compared to NA (see Figure 3.1), which produced a “filler effect” that increased the expected compressive

strength of SCC. On the other hand, mixtures SA75 and SA100 also did not show a significant difference in their compressive strength. Therefore, it seems, in principle, that strength can increase, despite a small increase in fine RCA.

The standard deviation confidence intervals show the dispersion of the compressive strength. At early ages (1 and 7 days), there was no clear trend in the dispersion of results with respect to the fine RCA content, although at older ages (28 and 90 days), the dispersion decreased as the percentage of fine RCA increased. Therefore, in spite of the contaminants present in the RCA, the concretes that contain fine RCA can show a homogeneous behavior.

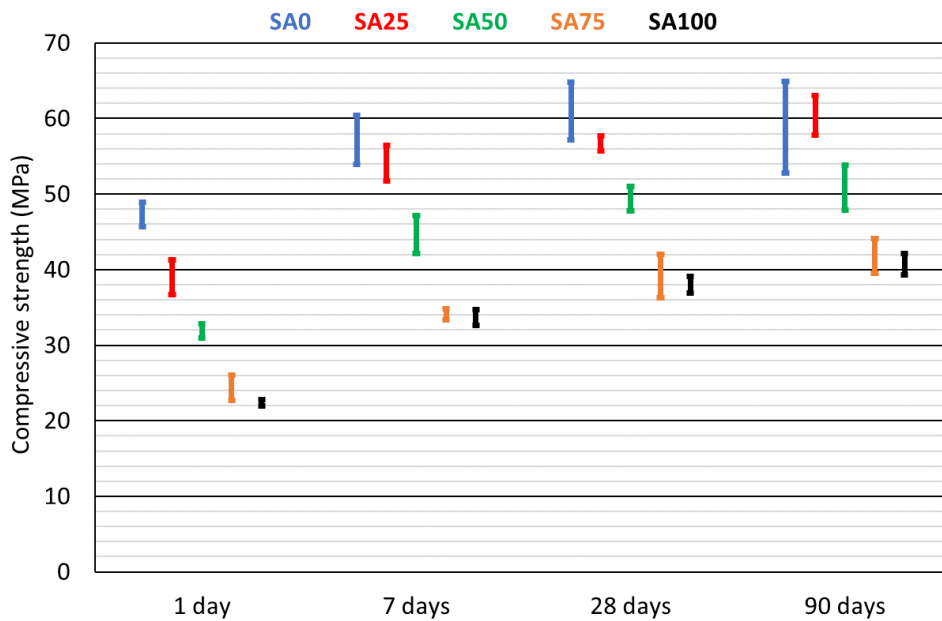


Figure 3.4. Graph of the confidence intervals of the arithmetic mean

5.5. PEARSON CORRELATIONS

A correlation between two variables is a number between -1 and 1 that shows the linearity of the relationship between them. If there are more than two variables, the correlations are obtained by pairs of variables ignoring the others. The closer the absolute value is to 1 , the greater the linearity, while if the sign is positive or negative it indicates whether the relationship is increasing (if one variable increases, so too is the other) or decreasing.

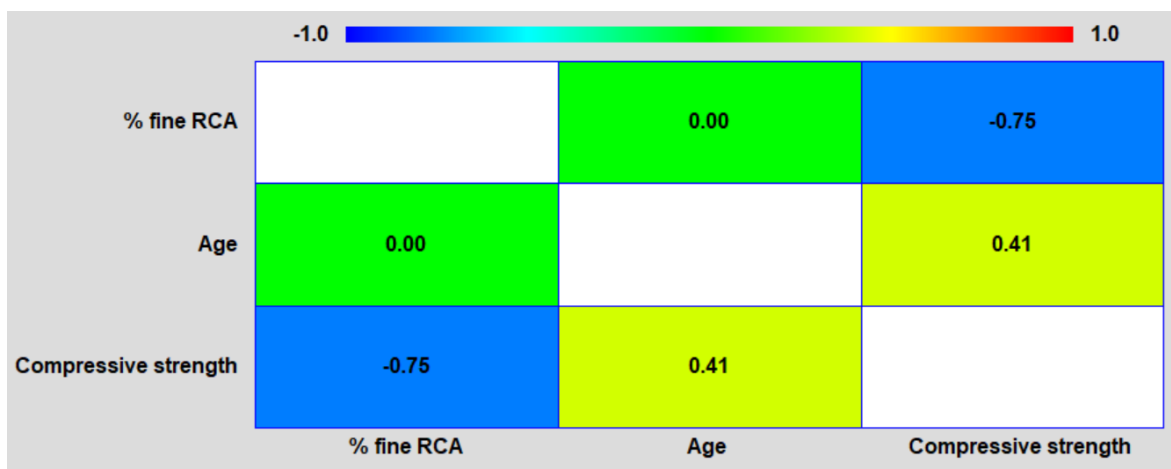


Figure 3.5. Pearson correlation matrix

In this study, the variables considered were compressive strength, age, and percentage of fine RCA. It is clear that the correlation between compressive strength and age is positive and, according to existing studies [49], is negative between this strength and the percentage of fine RCA. However, the absolute value, indicated in the correlation symmetric matrix (Figure 3.5), shows that the effect of the percentage of fine RCA on the compressive strength was 83% $((0.75-0.41)/0.41 \cdot 100)$ greater than the effect of the passing of time. The compressive strength was mainly conditioned by the residue content of the SCC.

5.6. EFFECT OF AGE AND PERCENTAGE OF FINE RCA ON COMPRESSIVE STRENGTH

The effect of each factor (age and fine RCA percentage) can be separately analyzed when the other factor takes a particular value, rather than neglecting it (as in correlations). An example would be the effect of the percentage of fine RCA at the age of 7 days or the effect of age, if the percentage of fine RCA was 50%.

The usual statistical procedure for this analysis is the one-factor ANOVA, which was also used in the statistical analysis of the fresh properties. In this case, this statistical test states as its null hypothesis that there is no effect of the factor (age or fine RCA percentage) on the variable (compressive strength), providing a p -value that indicates whether to accept or to reject the null hypothesis. ANOVA must be applied to independent measurements (in our case, each compressive strength value was from a different specimen and was therefore independent). Likewise, the variances of the variable must be significantly equal for each value of the factor under analysis, which was evaluated with two hypothesis tests, Cochran test and Bartlett test, the null hypothesis of which is that the variances are equal (Table 3.11).

These tests on the age factor showed that the variance was significantly equal in all cases except for 25% fine RCA, at a significance level of 5%. For this reason, the one-factor ANOVA with a significance level of 1% was applied, except for 25% fine RCA, for which the significance level of 5% was maintained.

Table 3.11. p -Value for both the Cochran test and the Bartlett test.

Factor analyzed	Condition	p -Value Cochran test	p -Value Bartlett test
Age	0% fine RCA	0.0262	0.0210
	25% fine RCA	0.5981	0.1360
	50% fine RCA	0.1348	0.0369
	75% fine RCA	0.2585	0.0435
	100% fine RCA	0.2547	0.0445
Fine RCA percentage	1 day	0.0629	0.0023
	7 days	0.0617	0.0021
	28 days	0.0006	0.0026
	90 days	0.0008	0.0036

For the fine RCA percentage factor, the low p -values of the Bartlett test prevented the use of the one-factor ANOVA, regardless of the level of significance. Therefore, the Kruskal–Wallis test was used, which is similar to the one-factor ANOVA, although it requires no equal variances, as it is a robust procedure. Both procedures allow homogeneous groups to be obtained, i.e., those factor values (age or fine RCA percentage) for which there is no significant difference in the value of the variable (compressive strength). In this study, the homogeneous groups would indicate at which ages the compressive strength of a mixture (specific fine RCA percentage) no longer varies and for which fine RCA percentages the compressive strength is statistically the same (at a specific age). The results of this analysis are shown in Table 3.12.

Table 3.12. Results of ANOVA analysis and Kruskal–Wallis test

Factor analyzed	Condition	ANOVA/Kruskal–Wallis <i>p</i> -value	Homogeneous groups
Age ¹	0% fine RCA	0.0001	Ages 7, 28 and 90
	25% fine RCA	0.0002	Ages 7 and 28
	50% fine RCA	0.0001	Ages 28 and 90
	75% fine RCA	0.0003	Ages 28 and 90
	100% fine RCA	0.0006	None
Fine RCA percentage ²	Age of 1 day	0.000000248	SA75 and SA100
	Age of 7 days	0.000000662	SA0 and SA25; SA75 and SA100
	Age of 28 days	0.000000492	SA0 and SA25; SA75 and SA100
	Age of 90 days	0.00000171	SA0 and SA25; SA75 and SA100

¹ One-factor ANOVA with a significance level of 1% except for 25% fine RCA, which was used at 5%

² Kruskal–Wallis test with a significance level of 5%

The results of the ANOVA/Kruskal–Wallis test were consistent with the above-mentioned studies [33] and with the correlations: both factors, age and fine RCA percentage, influenced the compressive strength. The homogeneous groups confirmed the trends shown by the confidence intervals:

- The compressive strength development of the SCC was slower as the fine RCA content increased. The compressive strength of mixture SA0 was statistically identical at 7, 28, and 90 days, while this strength for mixtures SA50 and SA75 was statistically different at 7 days and was the same at later ages (28 and 90 days). Mixture SA100 showed different strengths at all ages.
- In contrast, the factor fine RCA percentage showed that the compressive strengths of mixtures SA75 and SA100 were statistically equal, as they were in mixtures SA0 and SA25, at both 7 and 90 days. It can therefore be stated that the effect on the compressive strength of the fine RCA content can statistically be divided into three groups with the same strength: low percentage (0–25%), medium percentage (50%), and high percentage (75–100%). Therefore, according to the statistical results obtained, in this study the optimal amount of fine RCA would be 25–50% from the strength point of view, depending on the level of self-compactability and sustainability required for the mixture. Nevertheless, if the beneficial effect of the higher fines content of RCA is to be maximized, the incorporation of fine RCA in SCC should be less than 25%.

Finally, the interaction between the factors (age and percentage of fine RCA), i.e., whether the effect of one factor is different depending on the value of the other factor, can be assessed by means of a two-factor ANOVA. Since a *p*-value of 0.0034 was obtained, the interaction between both factors was significant (at any confidence level). A result indicating that no generalization is possible and that the effect of fine RCA on compressive strength should in particular be studied for each age and each fine RCA percentage, which is the approach followed in this section. This interaction also conditions the estimation of compressive strength as a function of RCA content and age, as explained in the next section.

5.7. COMPRESSIVE STRENGTH REGRESSION

Simple regression models were developed as a function of the compressive strength and its dependence on two variables: age and percentage of fine RCA. A process similar to one-factor ANOVA was performed: each mixture (different fine RCA percentages) was studied at each age, as the interaction between both factors was significant. Table 3.13 shows, for each situation, the two models with the best fit with their coefficient R². The variables used are CS (mean values of Compressive Strength, in MPa), FRP (Fine RCA Percentage, in percentage), and A (Age, in days).

These were fitted with the arithmetic mean of the compressive strength for each fine RCA percentage and age (see Table 3.8). The best-fit models are shown in Figure 3.6 (compressive strength as a function of age) and Figure 3.7 (compressive strength as a function of fine RCA percentage).

With all the above, it is observed that the simple regression provides an optimal adjustment of the compressive strength, reaching R^2 coefficients of 99%. However, four aspects should be highlighted:

- A good fit was obtained for both the age and the percentage of fine RCA, although better R^2 coefficients were obtained for the function of the age.
- The adjustment according to the percentage of fine RCA worsened with the age of the concrete: the longer the time that had elapsed since the concrete was mixed, the less reliable the estimate of its compressive strength.
- The adjustment of the compressive strength by age was robust: the best-fit model was unchanged when the percentage of fine RCA varied, only the coefficients (a , b) changed. For all mixtures, except mix SA75, the best-fit model followed Equation 3.1.

$$y = \frac{1}{a + \frac{b}{x}} \quad (3.1)$$

- When the compressive strength was fitted to the percentage of fine RCA, the best-fit model varied with age (there were three different models, for four different ages). This makes it difficult to obtain a valid overall model.

Table 3.13. Best-fit models of compressive strength as a function of the fine RCA percentage and age.

Dependent variable	Condition	Model equation ($A \geq 1$ day; $FRP = 0-100\%$)	Coefficient R^2
Age	0% fine RCA	$CS = 1/(0.0167 + 0.0045/A)$	0.9793
		$CS = \exp(4.0931 - 0.2377/A)$	0.9728
	25% fine RCA	$CS = 1/(0.0170 + 0.0087/A)$	0.9910
		$CS = \exp(4.0700 - 0.4101/A)$	0.9826
	50% fine RCA	$CS = 1/(0.0200 + 0.0115/A)$	0.9904
		$CS = \exp(3.9062 - 0.4507/A)$	0.9795
	75% fine RCA	$CS = (621.75 + 260.606 \cdot Lg(A))^{0.5}$	0.9932
		$CS = 25.2318 + 3.9337 \cdot Lg(A)$	0.9779
100% fine RCA	$CS = 1/(0.0256 + 0.0192/A)$	0.9861	
	$CS = (553.028 + 257.627 \cdot Lg(A))^{0.5}$	0.9833	
Fine RCA percentage	Age of 1 day	$CS = \exp(3.8495 - 0.0079 \cdot FRP)$	0.9830
		$CS = (229.177 - 182.027 \cdot FRP^{0.5})^{0.5}$	0.9816
	Age of 7 days	$CS = (3307.49 - 24.2083 \cdot FRP)^{0.5}$	0.9402
		$CS = 58.173 - 0.2688 \cdot FRP$	0.9396
	Age of 28 days	$CS = (3715.6 - 24.9521 \cdot FRP)^{0.5}$	0.9597
		$CS = 61.542 - 0.2544 \cdot FRP$	0.9584
	Age of 90 days	$CS = 1/(0.0158 + 0.00009 \cdot FRP)$	0.8957
		$CS = \exp(4.1303 - 0.0044 \cdot FRP)$	0.8941

It can therefore be concluded that in order to predict the compressive strength of an SCC made from fine RCA using single-variable models, the best option was to do so as a function of age (for each specific percentage of fine RCA). This approach achieves greater stability and accuracy.

Obtaining a multiple regression model is very useful, since it allows the strength of all the mixtures to be predicted (different percentages of fine RCA) at any age by means of a single expression.

Firstly, the simplest linear model was evaluated, as shown in Equation 3.2. It presented a poor fit (coefficient R^2 of 78%), which is explained by the large width of the confidence intervals of all its coefficients (Table 3.14) and the low correlation between the different variables (Figure 3.5). Therefore, and secondly, from the combination of the simple regression models with a better fit, a more complex multiple model was developed, as indicated in Equation 3.3, reaching a correlation coefficient of 96.5%. It can be seen that this model, unlike the simple regression models, has a much more complex formulation with four terms: an independent term, two terms that each depend on a variable (age and percentage of fine RCA) and a fourth summand that reflects the effect of the interaction between both variables (discussed above in the two-factor ANOVA). The variables involved in both models are the same as in the simple regression (CS , FRP , and A), whose valid ranges are $A \geq 1$ day and $FRP = 0\text{--}100\%$. Figure 3.8 shows the estimated values compared to the experimental values of both models, clearly supporting the higher precision of the second model.

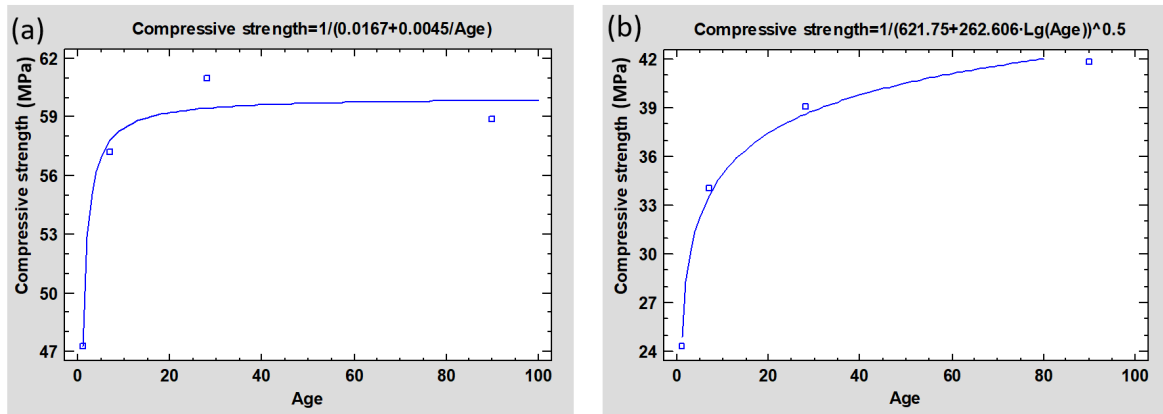


Figure 3.6. Best-fit models of compressive strength as an age function: (a) mix SA0, also valid for mixtures SA25, SA50 and SA100; (b) mix SA75

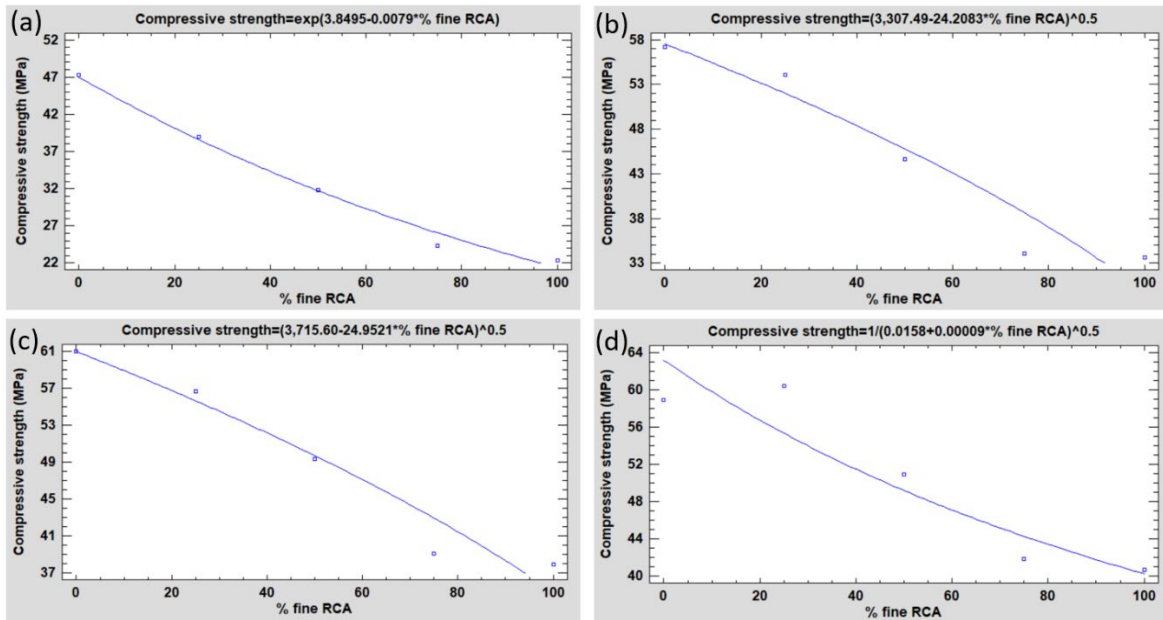


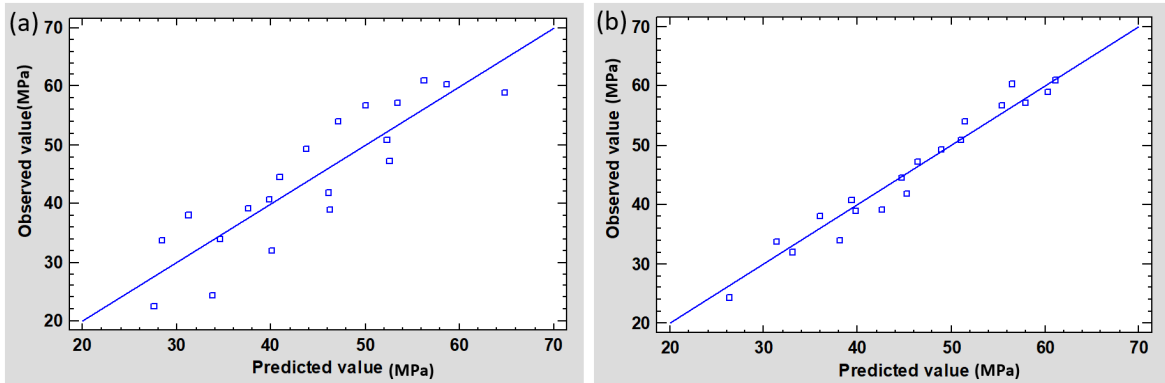
Figure 3.7. Best-fit models of compressive strength as a fine RCA percentage function: (a) 1 day; (b) 7 days; (c) 28 days; (d) 90 days.

$$CS = 52.4322 - 0.2501 \cdot FRP + 0.1378 \cdot A \quad (3.2)$$

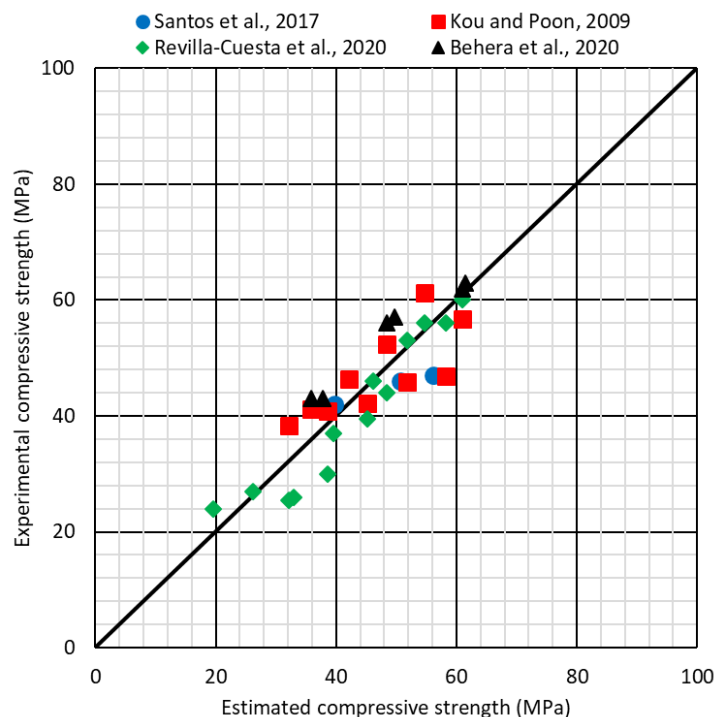
$$CS = 26.7876 + \frac{1}{0.0284 + \frac{0.0233}{A}} - 0.2657 \cdot FRP + 0.0005 \cdot A \cdot (FRP + 0.8373) \quad (3.3)$$

Table 3.14. Main results for the model obtained by multiple linear regression (Equation 3.2)

Coefficient R^2	0.7799
Confidence interval for the independent term ($\alpha = 0.05$)	(47.0884; 57.7760)
Confidence interval for FRP (fine RCA percentage) coefficient ($\alpha = 0.05$)	(-0.3277; -0.1726)
Confidence interval for A (age) coefficient ($\alpha = 0.05$)	(0.0560; 0.2156)

**Figure 3.8.** Relationship between observed values and estimated values of compressive strength: (a) linear model; (b) multiple regression proposed model

The proposed models are not intended to be general models that can be applied independently of the composition of the mixtures since, for example, the effect of adding different types or quantities of cement, variations in the w/c ratio or different compressive strength of the original concrete of the RCA have not been evaluated. Nevertheless, this model can be useful to predict the behavior of SCC with a compressive strength of 40–60 MPa at 28 days, as shown in Figure 3.9. In this figure, the results obtained are compared with the values collected in the few existing investigations in which the elaboration of SCC with RCA was approached. At most, the difference between the experimental value and the value estimated by this model is less than 5–8 MPa. In addition, the estimated value is generally lower than the experimental one. This allows us to carry out a safe estimation of the compressive strength of this type of concrete.

**Figure 3.9.** Validation of the model developed (Equation 3.3) throughout other similar studies [4, 24, 54, 55]

However, the main utility of this model is that it does allow us to establish some guidelines for the prediction of the compressive strength of recycled concrete; in this case SCC, which can serve as a starting point. On the one hand, the amount of recycled aggregate added, in this study fine RCA (coarse RCA content was 100% for all the mixes), has a significant influence on the compressive strength and must be considered. On the other hand, the effect of recycled aggregate varies with age (interaction), which makes it necessary to introduce a term in the model that reflects it. The models developed for non-recycled concrete do not reflect these aspects, as NA does not affect the behavior of concrete in this way [32].

5.8. PROBABILITY DISTRIBUTIONS FITTING: CHARACTERISTIC STRENGTH

The characteristic strength of concrete is the compressive strength value for which the probability of the actual compressive strength being lower is 5% at an age of 28 days, according to the standards [28, 29]. This strength is used in structural design and its determination is made by adjusting the experimental values to the normal probability distribution and determining the 5% percentile [41]. However, other probability distributions may be better fitted to the experimental data.

In Section 5.3, the normality of the results was evaluated, concluding that the compressive strength of each mixture at any age could be adjusted to a normal distribution, whose expression is shown in Equation 3.4. Nevertheless, a log-likelihood study indicated that the probability distribution that best fitted the experimental data was the Weibull distribution, shown in Equation 3.5, except for the mix SA100, which was the gamma distribution, shown in Equation 3.6. In the normal distribution, μ and σ are the arithmetic mean and standard deviation of the experimental data, respectively. In the Weibull and gamma distribution, k and λ are the shape and scale parameters, respectively, i.e., the parameters of distribution fitting. All these parameters for each mixture are given in Table 3.15 for the 28-day compressive strength.

- Normal distribution:

$$f(x) = \frac{1}{\sigma \cdot \sqrt{2 \cdot \pi}} \cdot \int_{-\infty}^x e^{\left(-\frac{(u-\mu)^2}{2 \cdot \sigma^2}\right)} \cdot du \quad (3.4)$$

- Weibull distribution:

$$f(x) = \frac{k}{\lambda} \cdot \left(\frac{x}{\lambda}\right)^{k-1} \cdot e^{-\left(\frac{x}{\lambda}\right)^k} \quad (3.5)$$

- Gamma distribution:

$$f(x) = \lambda \cdot e^{-\lambda \cdot x} \cdot \frac{(\lambda \cdot x)^{k-1}}{(k-1)!} \quad (3.6)$$

Table 3.15. Adjustment parameters for the probability distributions of the 28-day compressive strength

Mix	Normal Distribution	Weibull/Gamma Distribution
SA0	$\mu = 60.99; \sigma = 4.53$	$k = 17.97; \lambda = 62.89$
SA25	$\mu = 56.67; \sigma = 1.21$	$k = 59.99; \lambda = 57.20$
SA50	$\mu = 49.37; \sigma = 1.96$	$k = 32.80; \lambda = 50.21$
SA75	$\mu = 39.11; \sigma = 2.33$	$k = 21.27; \lambda = 40.14$
SA100	$\mu = 37.97; \sigma = 1.30$	$k = 964.75; \lambda = 25.41$ ¹

¹ In the mix SA100, the best-fit distribution at 28 days was the gamma distribution

It is possible to determine the characteristic compressive strength of each mixture by obtaining the 5% percentile if the probability distributions are known. Table 3.16 shows the characteristic

strength according to the normal distribution and the best-fit distribution (Weibull or gamma) for each mixture. In addition, this table also shows the normalized value according to the Spanish Instruction of Structural Concrete EHE-08 [29], calculated by approximating the value obtained to the standard series (20, 25, 30, 35, 40, 45, 50, 55, 60, 70, 80, 90, and 100 MPa). Figure 3.10 shows the calculation of the 5% percentile for each mixture in the best-fit distribution (Weibull or gamma).

Table 3.16. Characteristic compressive strength of the mixes developed

Mix	Characteristic compressive strength: normal distribution (MPa)	Characteristic compressive strength: weibull/gamma distribution (MPa)	Normalized characteristic compressive strength (MPa)
SA0	53.54	53.31	50
SA25	54.68	54.44	50
SA50	46.15	45.86	45
SA75	35.28	35.11	35
SA100	35.83	35.98	35

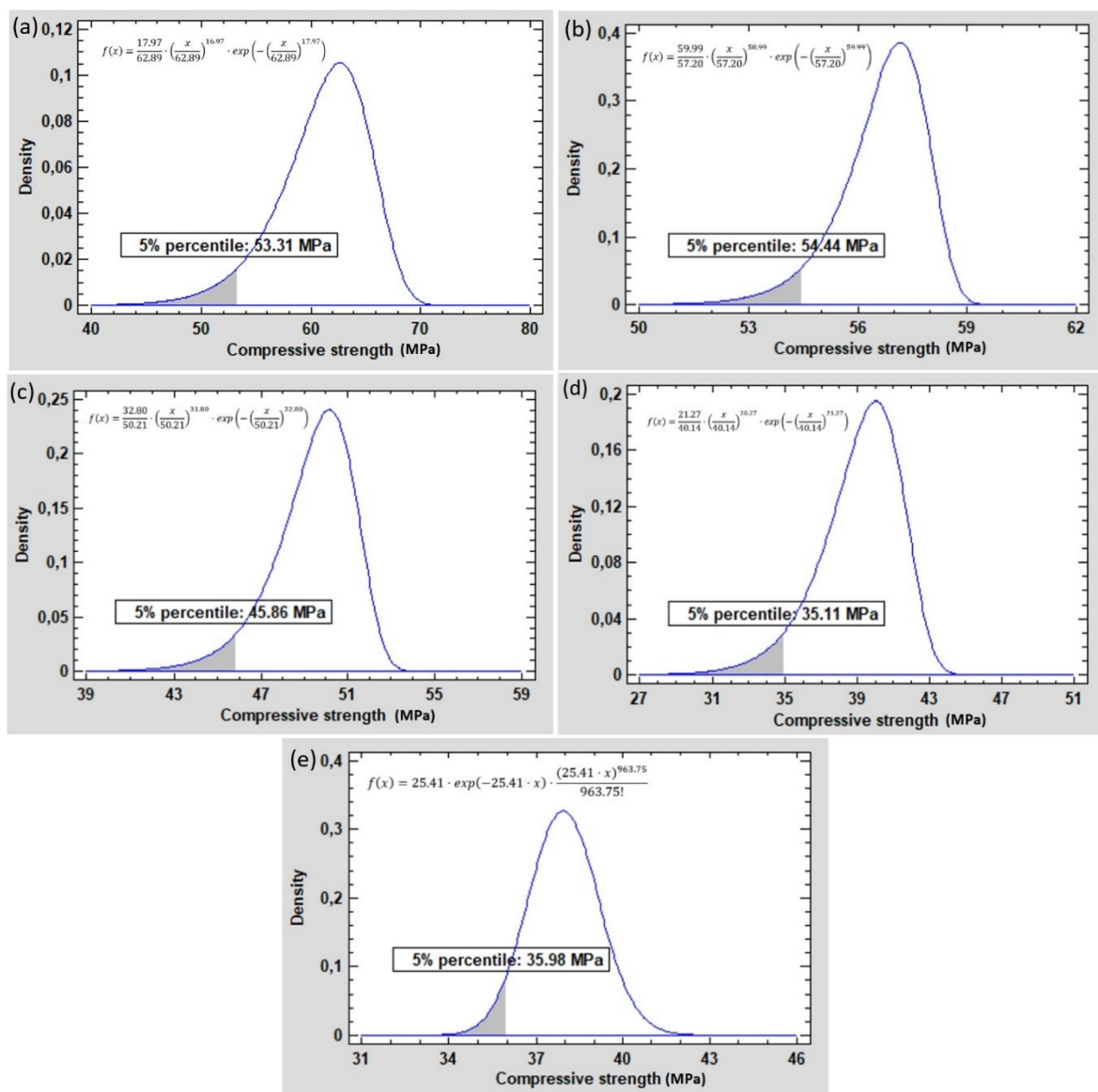


Figure 3.10. Graph of the characteristic compressive strength for the best-fit distribution (Weibull and gamma): (a) SA0; (b) SA25; (c) SA50; (d) SA75; (e) SA100

The values obtained show that mixtures with larger quantities of fine RCA can present the same characteristic strength as others with a lower fine content. Therefore, if structural calculations are to be performed, each mix developed with these sorts of recycled aggregates must be separately studied. The characteristic strength of concrete may not be affected by the increased amounts of recovered waste because, as shown in Table 3.16, mixes with 0 and 25% fine RCA had the same standardized characteristic strength, as also did mixtures incorporating 75 and 100% fine RCA.

Finally, both EC-2 [28] and EHE-08 [29] estimate characteristic compressive strength (f_{ck} , in MPa) by Equation 3.7 as a function of 28-day medium compressive strength ($f_{c,m}$, in MPa, see Table 3.8). This expression was only valid for mix SA0, underestimating the characteristic strength between 4 and 6 MPa for the rest of the mixtures that incorporate fine RCA (Table 3.17). This is due to the sharpest form of the adjusted probability distribution, so that the use of this expression would not allow us to employ all the strength capacity of these mixtures, with the consequent economic loss. This is one of the reasons why the analysis of this article is fundamental in concrete for structural use.

$$f_{ck} = f_{c,m} - 8 \quad (3.7)$$

Table 3.17. Comparison between the characteristic strength obtained by calculation and through the standards

Mix	Characteristic compressive strength: distribution fitting (MPa)	Characteristic compressive strength: Equation 3.7 (MPa)
SA0	53	53
SA25	54	49
SA50	46	41
SA75	35	31
SA100	36	30

6. CONCLUSIONS

Throughout this article, the flowability and the compressive strength of a Self-Compacting Concrete (SCC) made with Recycled Concrete Aggregate (RCA) have been analyzed. The compressive strength was also subjected to an extensive statistical analysis, which allowed us to evaluate different aspects than the traditional descriptive analysis.

Regarding the flowability, it was verified that it is possible to achieve SCC using high quantities of coarse and fine RCA (up to 100% incorporation ratios). The higher proportion of fine particles of the RCA (fine fraction), compared to Natural Aggregate (NA), resulted in higher slump flow and slower movement, which reduced the risk of segregation. Nevertheless, the most relevant conclusions are related to the statistical evaluation of compressive strength:

- The behavior of fine RCA in relation to the compressive strength of SCC was homogeneous, as no discordant breaks occurred in any mixture at any age (anomalous data). The dispersion was reduced with higher contents of fine RCA.
- The compressive strength of SCC in all the mixtures was properly fitted to a normal probability distribution, although the Weibull and gamma distributions showed the best fit. Characteristic compressive strength was underestimated when applying the standard estimation methods to mixtures with fine RCA.
- The dispersion of the compressive strength values obtained in the mixtures with RCA led the variance of the different mixtures not to be considered statistically equal. Therefore, the analysis of the effect of RCA could not be carried out using the usual procedures and required unusual robust procedures such as the Kruskal–Wallis test, which is not influenced by the variance of the mixtures.
- The addition of fine RCA, at a constant effective water-to-cement (w/c) ratio, reduced the compressive strength, being its influence greater than age. However, the addition of a larger amount of fine RCA was not always associated with a significant decrease in that

strength: mixtures with low fine RCA content (0 and 25%), and high content (75 and 100%) showed, respectively, the same strength in statistical terms. Therefore, the normalized characteristic compressive strength was also the same in each batch. Thus, according to the results of the ANalysis Of VAriance (ANOVA), the optimum RCA content in the concretes developed would be 25–50% from the strength point of view. The exact amount should be defined by the assessment of flowability, service requirements of the structure, and sustainability criteria.

- With respect to age, the addition of fine RCA delayed the development of strength: for 0% fine RCA, the compressive strength at 7, 28 and 90 days was statistically equal, while for 100% fine RCA, the strength at each age was significantly different. The interaction between age and percentage of fine RCA makes the strength behavior of each mixture different. This implies that it is not possible to establish a clear generalization of the expected behavior of concrete with RCA: the effect of each RCA content must be studied in detail at each age.
- The most accurate and simplest techniques to estimate compressive strength were simple age-dependent regression models, while the models for predicting the compressive strength as a function of the fine RCA percentage showed imprecisions at advanced ages. The multiple regression model that has been developed provided highly reliable estimations, although its formulation was more complex. The interaction between RCA content and age should be considered for an accurate estimation of compressive strength.

This statistical approach towards the analysis of the compressive strength of an SCC containing coarse and fine RCA is intended to show a useful way of both addressing the problems associated with recycled aggregate and of arriving at conclusions that facilitate its use in real structures and the prediction of its strength. This procedure could be applied to any type of waste, making the structural use of recycled concrete more feasible.

REFERENCES

- [1] M. Sandanayake, G. Zhang, S. Setunge, Estimation of environmental emissions and impacts of building construction – A decision making tool for contractors, *J. Build. Eng.* 21 (2019) 173-185.
- [2] W. Liang, B. Dai, G. Zhao, H. Wu, Assessing the performance of green mines via a hesitant fuzzy ORESTE-QUALIFLEX method, *Mathematics* 7 (9) (2019) 788.
- [3] R. Maddalena, J.J. Roberts, A. Hamilton, Can Portland cement be replaced by low-carbon alternative materials? A study on the thermal properties and carbon emissions of innovative cements, *J. Clean. Prod.* 186 (2018) 933-942.
- [4] M. Behera, S.K. Bhattacharyya, A.K. Minocha, R. Deoliya, S. Maiti, Recycled aggregate from C&D waste & its use in concrete - A breakthrough towards sustainability in construction sector: A review, *Constr. Build. Mater.* 68 (2014) 501-516.
- [5] M.S. Bidabadi, M. Akbari, O. Panahi, Optimum mix design of recycled concrete based on the fresh and hardened properties of concrete, *J. Build. Eng.* 32 (2020) 101483.
- [6] H. Yuan, W. Lu, J. Jianli Hao, The evolution of construction waste sorting on-site, *Renew. Sust. Energ. Rev.* 20 (2013) 483-490.
- [7] A. Santamaría, J.J. González, M.M. Losáñez, M. Skaf, V. Ortega-López, The design of self-compacting structural mortar containing steelmaking slags as aggregate, *Cem. Concr. Compos.* 111 (2020) 103627.
- [8] EN-Euronorm, Rue de stassart, 36. Belgium-1050 Brussels, European Committee for Standardization.
- [9] A.U.R. Khan, M.S. Khan, S. Fareed, J. Xiao, Structural Behaviour and Strength Prediction of Recycled Aggregate Concrete Beams, *Arab. J. Sci. Eng.* (2019).
- [10] B. Cantero, I.F. Sáez del Bosque, A. Matías, M.I. Sánchez de Rojas, C. Medina, Inclusion of construction and demolition waste as a coarse aggregate and a cement addition in structural concrete design, *Arch. Civ. Mech. Eng.* 19 (4) (2019) 1338-1352.

- [11] G. Lu, Z. Fan, Z. Sun, P. Liu, Z. Leng, D. Wang, M. Oeser, Improving the polishing resistance of cement mortar by using recycled ceramic, *Resour. Conserv. Recycl.* 158 (2020) 104796.
- [12] A. Gonzalez-Corominas, M. Etxeberria, I. Fernandez, Structural behaviour of prestressed concrete sleepers produced with high performance recycled aggregate concrete, *Mater. Struct.* 50 (1) (2017) 94.
- [13] F. Faleschini, M.A. Zanini, K. Toska, Seismic reliability assessment of code-conforming reinforced concrete buildings made with electric arc furnace slag aggregates, *Eng. Struct.* 195 (2019) 324-339.
- [14] M. Skaf, E. Pasquini, V. Revilla-Cuesta, V. Ortega-López, Performance and durability of porous asphalt mixtures manufactured exclusively with electric steel slags, *Materials* 12 (20) (2019) 3306.
- [15] A. Mohajerani, L. Burnett, J.V. Smith, S. Markovski, G. Rodwell, M.T. Rahman, H. Kurmus, M. Mirzababaei, A. Arulrajah, S. Horpibulsuk, F. Maghool, Recycling waste rubber tyres in construction materials and associated environmental considerations: A review, *Resour. Conserv. Recycl.* 155 (2020) 104679.
- [16] A.S. Brand, J.R. Roesler, Interfacial transition zone of cement composites with steel furnace slag aggregates, *Cem. Concr. Compos.* 86 (2018) 117-129.
- [17] V.W.Y. Tam, K. Wang, C.M. Tam, Assessing relationships among properties of demolished concrete, recycled aggregate and recycled aggregate concrete using regression analysis, *J. Hazard. Mater.* 152 (2) (2008) 703-714.
- [18] V.W.Y. Tam, M. Soomro, A.C.J. Evangelista, A review of recycled aggregate in concrete applications (2000–2017), *Constr. Build. Mater.* 172 (2018) 272-292.
- [19] R.V. Silva, J. de Brito, R.K. Dhir, Fresh-state performance of recycled aggregate concrete: A review, *Constr. Build. Mater.* 178 (2018) 19-31.
- [20] V. Revilla-Cuesta, M. Skaf, J.A. Chica, J.A. Fuente-Alonso, V. Ortega-López, Thermal deformability of recycled self-compacting concrete under cyclical temperature variations, *Mater. Lett.* 278 (2020) 128417.
- [21] V. Revilla-Cuesta, M. Skaf, F. Faleschini, J.M. Manso, V. Ortega-López, Self-compacting concrete manufactured with recycled concrete aggregate: An overview, *J. Clean. Prod.* 262 (2020) 121362.
- [22] Z.J. Grdic, G.A. Toplicic-Curcic, I.M. Despotovic, N.S. Ristic, Properties of self-compacting concrete prepared with coarse recycled concrete aggregate, *Constr. Build. Mater.* 24 (7) (2010) 1129-1133.
- [23] C. Sun, Q. Chen, J. Xiao, W. Liu, Utilization of waste concrete recycling materials in self-compacting concrete, *Resour. Conserv. Recycl.* 161 (2020) 104930.
- [24] S.C. Kou, C.S. Poon, Properties of self-compacting concrete prepared with coarse and fine recycled concrete aggregates, *Cem. Concr. Compos.* 31 (9) (2009) 622-627.
- [25] J.J. Zeng, Y.Y. Ye, W.Y. Gao, S.T. Smith, Y.C. Guo, Stress-strain behavior of polyethylene terephthalate fiber-reinforced polymer-confined normal-, high- and ultra high-strength concrete, *J. Build. Eng.* 30 (2020) 101243.
- [26] A. Santamaría, V. Ortega-López, M. Skaf, J.A. Chica, J.M. Manso, The study of properties and behavior of self compacting concrete containing Electric Arc Furnace Slag (EAFS) as aggregate, *Ain Shams Eng. J.* 11 (1) (2020) 231-243.
- [27] N. Moayyeri, S. Gharehbaghi, V. Plevris, Cost-based optimum design of reinforced concrete retaining walls considering different methods of bearing capacity computation, *Mathematics* 7 (12) (2019) 1232.
- [28] EC-2, Eurocode 2: Design of concrete structures. Part 1-1: General rules and rules for buildings, CEN (European Committee for Standardization) (2010).
- [29] EHE-08, Structural Concrete Regulations (in Spanish), Ministerio de Fomento, Gobierno de España (2010).
- [30] R.V. Silva, J. De Brito, R.K. Dhir, The influence of the use of recycled aggregates on the compressive strength of concrete: A review, *Eur. J. Environ. Civ. Eng.* 19 (7) (2015) 825-849.

- [31] V. Penadés-Plà, T. García-Segura, V. Yepes, Robust design optimization for low-cost concrete box-girder bridge, *Mathematics* 8 (3) (2020) 398.
- [32] F. Moutassem, S.E. Chidiac, Assessment of concrete compressive strength prediction models, *KSCE J. Civ. Eng.* 20 (1) (2016) 343-358.
- [33] L. Evangelista, J. De Brito, Concrete with fine recycled aggregates: A review, *Eur. J. Environ. Civ. Eng.* 18 (2) (2014) 129-172.
- [34] J.T. San-José, J.M. Manso, Fiber-reinforced polymer bars embedded in a resin concrete: Study of both materials and their bond behavior, *Polym. Compos.* 27 (3) (2006) 315-322.
- [35] F. Fiol, C. Thomas, C. Muñoz, V. Ortega-López, J.M. Manso, The influence of recycled aggregates from precast elements on the mechanical properties of structural self-compacting concrete, *Constr. Build. Mater.* 182 (2018) 309-323.
- [36] S. Manzi, C. Mazzotti, M.C. Bignozzi, Self-compacting concrete with recycled concrete aggregate: Study of the long-term properties, *Constr. Build. Mater.* 157 (2017) 582-590.
- [37] S. Santos, P.R. da Silva, J. de Brito, Self-compacting concrete with recycled aggregates – A literature review, *J. Build. Eng.* 22 (2019) 349-371.
- [38] P.G. Asteris, A. Ashrafian, M. Rezaie-Balf, Prediction of the compressive strength of self-compacting concrete using surrogate models, *Comput. Concr.* 24 (2) (2019) 137-150.
- [39] P. Saha, M.L.V. Prasad, P. RathishKumar, Predicting strength of SCC using artificial neural network and multivariable regression analysis, *Comput. Concr.* 20 (1) (2017) 31-38.
- [40] B. Abolpour, M. Mehdi Afsahi, S.G. Hosseini, Statistical analysis of the effective factors on the 28 days compressive strength and setting time of the concrete, *J. Adv. Res.* 6 (5) (2015) 699-709.
- [41] J. Xiao, J. Li, C. Zhang, On statistical characteristics of the compressive strength of recycled aggregate concrete, *Struct. Concr.* 6 (4) (2005) 149-153.
- [42] A.S. Brand, A.N. Amirkhanian, J.R. Roesler, Flexural capacity of full-depth and two-lift concrete slabs with recycled aggregates, *Transp. Res. Rec.* 2456 (2014) 64-72.
- [43] M. Velay-Lizancos, I. Martínez-Lage, M. Azenha, P. Vázquez-Burgo, Influence of temperature in the evolution of compressive strength and in its correlations with UPV in eco-concretes with recycled materials, *Constr. Build. Mater.* 124 (2016) 276-286.
- [44] M. Mazloom, A. Soltani, M. Karamloo, A. Hassanloo, A. Ranjbar, Effects of silica fume, superplasticizer dosage and type of superplasticizer on the properties of normal and selfcompacting concrete, *Adv. Mater. Res.* 7 (1) (2018) 407-434.
- [45] M.E.K. Bouarroudj, S. Remond, F. Michel, Z. Zhao, D. Bulteel, L. Courard, Use of a reference limestone fine aggregate to study the fresh and hard behavior of mortar made with recycled fine aggregate, *Mater. Struct.* 52 (1) (2019) 18.
- [46] F. Agrela, M. Sánchez De Juan, J. Ayuso, V.L. Geraldés, J.R. Jiménez, Limiting properties in the characterisation of mixed recycled aggregates for use in the manufacture of concrete, *Constr. Build. Mater.* 25 (10) (2011) 3950-3955.
- [47] M. Martín-Morales, M. Zamorano, A. Ruiz-Moyano, I. Valverde-Espinosa, Characterization of recycled aggregates construction and demolition waste for concrete production following the Spanish Structural Concrete Code EHE-08, *Constr. Build. Mater.* 25 (2) (2011) 742-748.
- [48] J. Zhang, X. An, P. Li, Research on a mix design method of self-compacting concrete based on a paste rheological threshold theory and a powder equivalence model, *Constr. Build. Mater.* 233 (2020) 117292.
- [49] D. Carro-López, B. González-Fonteboa, J. De Brito, F. Martínez-Abella, I. González-Taboada, P. Silva, Study of the rheology of self-compacting concrete with fine recycled concrete aggregates, *Constr. Build. Mater.* 96 (2015) 491-501.
- [50] I. González-Taboada, B. González-Fonteboa, J. Eiras-López, G. Rojo-López, Tools for the study of self-compacting recycled concrete fresh behaviour: Workability and rheology, *J. Clean. Prod.* 156 (2017) 1-18.

- [51] B. Łaźniewska-Piekarczyk, The methodology for assessing the impact of new generation superplasticizers on air content in self-compacting concrete, *Constr. Build. Mater.* 53 (2014) 488-502.
- [52] C. MacInnis, D. Racic, The effect of superplasticizers on the entrained air-void system in concrete, *Cem. Concr. Res.* 16 (3) (1986) 345-352.
- [53] S.I. Ishrat, Z.A. Khan, A.N. Siddiquee, I.A. Badruddin, A. Algahtani, S. Javaid, R. Gupta, Optimising parameters for expanded polystyrene based pod production using Taguchi method, *Mathematics* 7 (9) (2019) 847.
- [54] S.A. Santos, P.R. da Silva, J. de Brito, Mechanical performance evaluation of self-compacting concrete with fine and coarse recycled aggregates from the precast industry, *Materials* 10 (8) (2017) 904.
- [55] V. Revilla-Cuesta, V. Ortega-López, M. Skaf, J.M. Manso, Effect of fine recycled concrete aggregate on the mechanical behavior of self-compacting concrete, *Constr. Build. Mater.* 263 (2020) 120671.

Article 4

Temporal flowability evolution of slag-based self-compacting concrete with recycled concrete aggregate

Title: Temporal flowability evolution of slag-based self-compacting concrete with recycled concrete aggregate

Authors: Víctor Revilla-Cuesta, Marta Skaf, Amaia Santamaría, Jorge J. Hernández-Bagaces, Vanesa Ortega-López

Journal: Journal of Cleaner Production

Year: 2021

Volume: 299

Article number: 126890

DOI: <https://doi.org/10.1016/j.jclepro.2021.126890>

Journal classification (2019 JCR ranking data): 19/265 (environmental sciences). First quartile (Q1), first decile (D1)

ABSTRACT

The addition of by-products, such as recycled concrete aggregate and ground granulated blast furnace slag, modify the in-fresh flowability of ordinary self-compacting concrete both initially and over time. A detailed study is presented in this paper of 18 mixtures (SF3 slump-flow class) containing 100% coarse recycled concrete aggregate, two types of cement (CEM I or CEM III/A, the latter with 45% ground granulated blast furnace slag), different contents of fine recycled concrete aggregate (0%, 50%, or 100%), and three different aggregate powders (ultra-fine limestone powder <0.063 mm, limestone fines 0/0.5 mm, and recycled concrete aggregate 0/0.5 mm). The temporal evolution of slump flow, viscosity, and passing ability, and the values of segregation resistance, air content, fresh and hardened density, and compressive strength were evaluated in all the mixtures. The addition of fine recycled concrete aggregate and CEM III/A improved initial slump flow and passing ability by 6%, due to their higher proportion of fines. Nevertheless, the temporal loss of flowability within 60 minutes was 5.8% lower when adding natural aggregate and CEM I. Viscosity and air content increased 26% on average following additions of fine recycled concrete aggregate, unlike with additions of ground granulated blast furnace slag. Flowability and strength increased with the addition of limestone fines 0/0.5 mm. According to multi-criteria analyses, the mixtures with CEM III/A, 50% fine recycled concrete aggregate, and limestone fines 0/0.5 mm showed an optimal balance between their flowability (SF2 slump-flow class 60 minutes after the mixing process), compressive strengths (around 60 MPa), and carbon footprints.

Keywords: air content; flowability, viscosity, and passing ability evolution; ground granulated blast furnace slag; recycled concrete aggregate; self-compacting concrete; sieve segregation.

1. INTRODUCTION

Concrete is the most extensively used structural material within the construction sector and its components form recurrent design features found in many buildings and civil works. Annual concrete consumption stands at around 890 Mt in Europe alone [1]. However, this material also has some significant environmental impacts. The manufacture of 1 t (1,000 kg) of cement clinker emits 0.9 t of CO₂ into the atmosphere [2] and Natural Aggregate (NA) extracted from quarries or gravel pits usually represents between 60% and 70% of concrete volume [3]. One way of adding to the sustainability of concrete is to substitute traditional clinker for residues with pozzolanic

properties and, more recently, for alkali-activated wastes [4]. Another alternative is to replace NA with different by-products [5], such as slag [6] and construction and demolition waste [7]. The application of either strategy curtails waste generation in a consumer society where it is problematic [8], such as the 865 Mt of construction and demolition waste generated in Europe alone on an annual basis [9].

Following the initial research work of Ouchi *et al.* (2000) [10], Self-Compacting Concrete (SCC) emerged between the end of the 20th century and the beginning of the 21st century. It is one of the most sustainable types of concrete, due to its high flowability in the fresh state, in so far as no vibration is needed for its placement, which significantly reduces energy consumption [11]. High flowability is ensured through the addition of a suitable admixture and an adequate balance between the coarse, fine, and powder fractions of the aggregate. The appropriate average proportions of these components are 30% by volume of coarse aggregate and a powder content of 500 kg/m³ [12]. Proper retention of flowability over time is a key aspect of this type of concrete, so that flowability is retained while in transportation from the manufacturing plant to the site for placement [12]. It is therefore essential to adapt the mix design to the characteristics of each component, in order to produce an SCC of adequate flowability over a prolonged period of time [13]. Other problems should likewise be minimized, such as high air content, resulting mainly from the high admixture and water content that is typical of SCC [11].

Ground Granulated Blast Furnace Slag (GGBFS) is a type of slag resulting from fast cooling and subsequent grinding of blast furnace slag. Its grinding fineness is very high and its pozzolanic properties make it a good substitute for cement clinker [14]. CEM III, a standardized cement type, incorporates between 35% and 95% GGBFS in accordance with EN 197-1 [15]. This type of cement has traditionally been used for marine concrete structures submerged in seawater [16]. More recently, it has been employed in the stabilization of both clayey [17] and contaminated soils [18] and in the manufacture of road bases and sub-bases [19]. Its use in the production of SCC is not widespread [20] and its effect on the temporal flowability of SCC is yet to be studied.

Recycled Concrete Aggregate (RCA) is a by-product from the demolition of aging concrete structures [8]. However, the crushing of rejected concrete elements mainly from the precast concrete industry yields the highest quality RCA [21]. If the mix design of SCC is adjusted to the particular characteristics of this residue, mainly to its high water absorption levels [22], then RCA is a valid alternative by-product for the manufacturing of SCC [23]. If coarse RCA is used, the higher its content, the worse the temporal retention of flowability. The use of the coarse fraction of this waste at room humidity without pre-soaking worsens its in-fresh performance due to a loss of flowability, as higher levels of mix-water are slowly absorbed into the RCA [24]. Nevertheless, pre-soaking of coarse RCA yields a good temporal conservation of flowability (45 minutes after the end of the mixing process, the loss of slump flow was only around 9% for 100% coarse RCA), although it hinders any industrial usage [24]. The use of only fine RCA in SCC also hinders the temporal retention of flowability: 45 minutes after the start of the mixing process, the slump flow decreased by 8% and 28% in the mixtures with 50% and 100% fine RCA respectively [25]. In both studies, no mixing process to improve SCC flowability without pre-soaking RCA was considered, although the initial flowability of SCC with 100% coarse RCA can be maximized through adjustments to the water content and the use of two-stage mixing processes [26]. It may be mentioned that there are no studies to date on the joint use of both RCA fractions, their interaction, and their effects on SCC flowability.

The hardened properties of SCC are fundamental when defining the mix design [27], as SCC is very sensitive to the slightest variation in mix composition, such as water, cement, plasticizer content, or coarse-to-fine aggregate ratio [21]. A precise definition of the amount of coarse and fine RCA added to the mix according to their specific characteristics is therefore essential to obtain high compressive strength with no loss of flowability [13]. While concrete with a high compressive

strength of over 45 MPa was obtained with 100% coarse RCA, the addition of fine RCA had more adverse effects, even at low-level replacements of 30% [28]. Nevertheless, the optimization of the mix design with 100% coarse RCA, 50% fine RCA, and standard amounts of cement yielded an SCC with a slump flow of between 650 and 750 mm (SF2 slump-flow class) and a compressive strength of over 45 MPa [29].

The objective of this study is to ascertain whether it is possible to produce a sustainable SCC with high flowability over time and an adequate compressive strength. To do so, an SF3 slump-flow class SCC was produced, using the two by-products described in detail in this introduction: coarse and fine RCA, and GGBFS. Furthermore, the effects of various aggregate powders used as sustainable alternatives to conventional ultra-fine limestone powder (*i.e.*, limestone filler) were also analyzed. The few evaluative studies on the temporal fresh behavior of medium-flowability SCC have been limited to the effect of only one RCA fraction (coarse or fine) with no additions of sustainable binders (GGBFS) or aggregate powders to the mixtures [24, 25]. Accordingly, the novelties of this study are as follows:

- Firstly, the fresh behavior over time of SCC manufactured with both coarse and fine RCA was studied. The simultaneous use of both RCA fractions can alter the performance of SCC in comparison with the use of only one fraction.
- Secondly, the influence of GGBFS as binder and aggregate powders more sustainable than standard ultra-fine limestone powder (limestone fines 0/0.5 mm, and RCA 0/0.5 mm) on the temporal flowability of SCC was evaluated. Their interactions with RCA were also analyzed.
- Both previous aspects were applied for the first time to a highly SCC (SF3 slump-flow class), the flowability of which is very sensitive to changes in its composition [27]. The addition of each by-product therefore notably alters its fresh behavior, so that the effect of each product on SCC flowability can be measured in detail.
- Finally, a statistical model was developed from the experimental results, to predict the loss of flowability of the SCC manufactured with RCA. In addition, the results of a multi-criteria analysis confirmed the suitability of the mixtures under development. Both approaches are also new in the literature.

In this study, 18 highly SCC mixes were produced to investigate the above aspects of their flowability. All of them contained 100% coarse RCA, while different percentages of fine RCA (0%, 50%, and 100%) were added in substitution of siliceous sand. CEM III/A, with 45% GGBFS, as per EN 197-1 [15], was incorporated in half of the mixtures. The effects on SCC flowability of three different aggregate powders (ultra-fine limestone powder <0.063 mm, limestone fines 0/0.5 mm, and RCA 0/0.5 mm) were also evaluated. Lastly, a three-stage mixing process was designed to assess improvements to the temporal flowability of the SCC samples following maximization of RCA water absorption [26].

2. MATERIALS AND METHODS

The raw materials, the composition of the SCC mixtures, and the experimental procedure that yielded the final results are all presented in this section.

2.1. MATERIALS

2.1.1. BINDERS AND ADMIXTURES

Two different cements as per EN 197-1, CEM I 52.5 R and CEM III/A 42.5 N, were used. CEM I 52.5 R was chosen due to its higher fineness and, therefore, higher hydration heat and faster setting than class N cements. It had a Blaine surface of 365 m²/kg, a specific gravity of 3.12 Mg/m³, and a clinker content of around 95%. CEM III/A 42.5 N had a Blaine surface of 430 m²/kg, a specific gravity

of 3.00 Mg/m^3 , and a GGBFS content of around 45%. The chemical composition of both cements is shown in Table 4.1.

Table 4.1. X-ray fluorescence (XRF) analysis of the chemical composition (%) of cement

Cement	CaO	SiO ₂	Al ₂ O ₃	Fe ₂ O ₃	SO ₃	MgO	K ₂ O	C	TiO ₂
CEM I 52.5 R	67.8	17.1	5.7	3.1	2.4	1.7	1.3	0.5	0.4
CEM III/A 42.5 N	55.3	26.8	7.6	2.4	2.7	3.5	0.8	0.4	0.5

Two different admixtures were used to achieve self-compactability. A viscosity regulator (AD1), which reduces water demand and retains the flowability of SCC over lengthier periods of time, and a plasticizer (AD2) were added. Water was obtained from the mains public supply of the city of Burgos, northern Spain.

2.1.2. AGGREGATES

The highest proportion of aggregate in all the SCC mixes was RCA. It was transported from a local recycling plant, following the crushing of precast concrete structural elements. These elements, with compressive strengths higher than 45 MPa, had been rejected during the manufacturing process, due to aesthetic and geometric defects. The continuous grain size of the RCA received in the laboratory, 0/31.5 mm, was too large for the development of highly SCC. It was therefore sieved and separated into three different fractions: 0/4 mm (fine RCA), 4/12.5 mm (coarse RCA), and 12.5/31.5 mm. The first two fractions, with the gradations shown in Figure 4.1, were used to produce the SCC. The fine aggregate fraction of the mixes with less than 100% fine RCA were completed by adding a local siliceous sand of an equivalent grading, 0/4 mm, although with a lower content of particles smaller than 0.25 mm (see Figure 4.1).

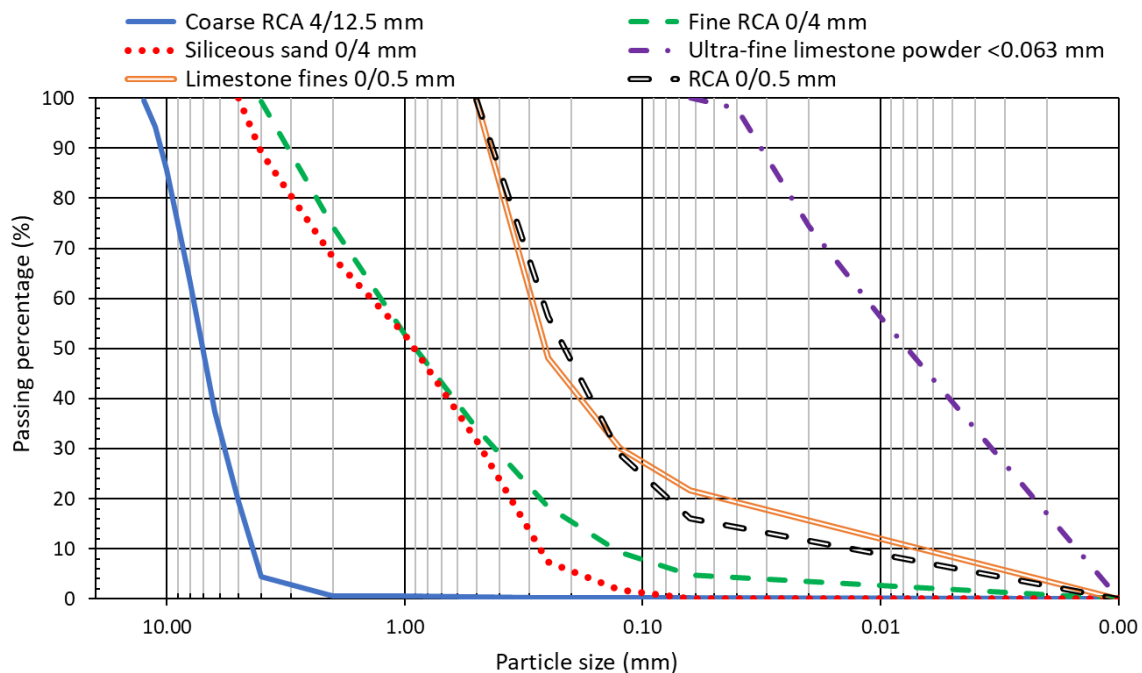


Figure 4.1. Gradation of the aggregates

Three types of aggregate powder sized less than 0.5 mm were used: ultra-fine limestone powder <0.063 mm, commercial limestone fines 0/0.5 mm, usually employed for the production of mortars, and RCA 0/0.5 mm (finely ground RCA). The last two represented sustainable alternatives to the ultra-fine limestone powder commonly in use, either because of their lower energy consumption during their manufacture, due to their larger particle size (limestone fines 0/0.5 mm), or because of their origin (RCA 0/0.5 mm). Figure 4.1 also shows the gradation curves of these materials.

The basic physical properties of all these aggregates are listed in Table 4.2: water content under environmental conditions according to EN 1097-5, density and water absorption in 24 h according to EN 1097-6, and water absorption in 10 minutes after oven drying. According to the fineness modulus of the aggregates (Table 4.2), the fine RCA 0/4 mm showed a higher fines content than siliceous sand, although, its density was lower than that of the NA, and its water absorption levels were significantly higher.

Table 4.2. Properties of the aggregates

Aggregate	Saturated-surface-dry density (Mg/m ³)	Water content (% wt.)	24 h water absorption (% wt.)	10 min water absorption (% wt.)	Fineness modulus
Coarse RCA 4/12.5 mm	2.42	0.58	6.25	5.28	6.30
Fine RCA 0/4 mm	2.37	0.73	7.36	6.03	3.11
Siliceous sand 0/4 mm	2.58	0.02	0.25	0.18	3.49
Ultra-fine limestone powder <0.063 mm	2.77	0.13	0.54	0.37	-
Limestone fines 0/0.5 mm	2.60	0.22	2.57	1.93	1.22
RCA 0/0.5 mm	2.31	0.82	7.95	6.70	1.15

Aggregate water absorption over time significantly influences SCC flowability and its temporal evolution. The water absorption levels of all the aggregates in use were determined over different periods of time (5, 10, 15, 30, 45, 60, 75, and 90 minutes), in accordance with the experimental plan (see section 2.3), for accurate determination of the water content of each mix. The aggregates for the manufacture of the SCC were stored under room-moisture conditions, without pre-soaking, with the aim of simulating the industrial manufacture of concrete. The aggregate samples used in these tests had therefore not been oven dried, thus imitating the water absorption levels of the aggregate during the mixing process. The results that are plotted in Figure 4.2 show water absorption levels for the RCA fractions that were approximately three times higher than for the limestone fines 0/0.5 mm. In addition, the water absorption of the limestone fines was less prolonged over time, increasing from practically null after minute 45, while it was around 0.03%/minute for RCA. Water absorption was higher in the finer fractions regardless of the aggregate type.

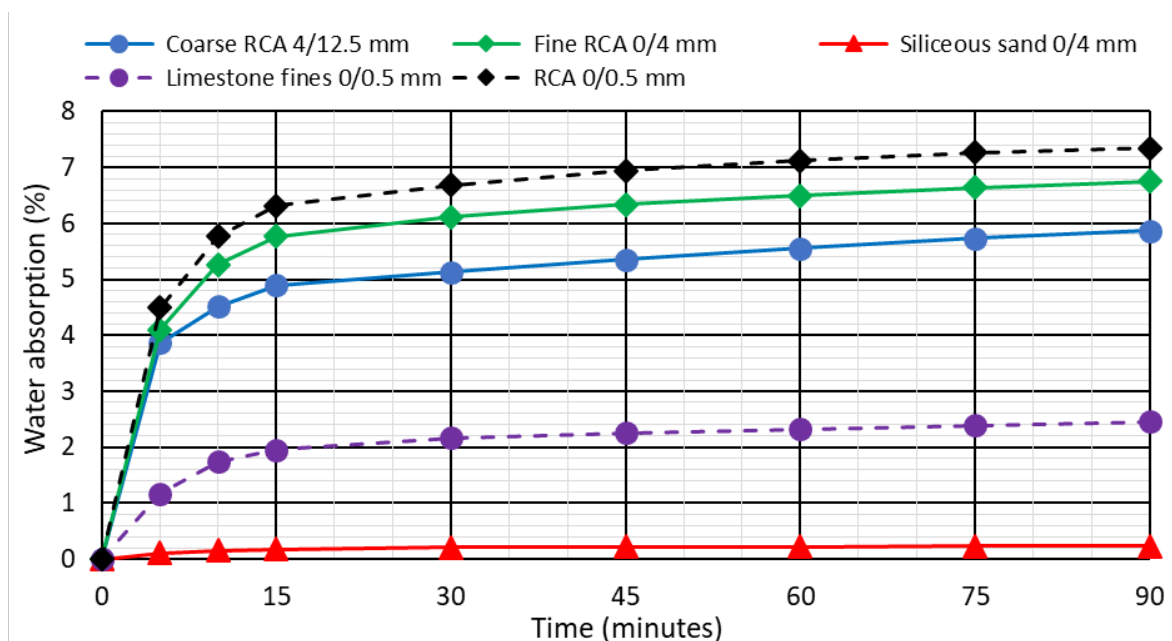


Figure 4.2. Aggregate water absorption levels over time.

2.2. MIX DESIGN

All the mixtures were designed to have a SF3 slump-flow class (slump flow between 750 and 850 mm), as defined in EFNARC (2002) [12]. The fresh behavior of all the mixes could therefore be compared between each other (same slump-flow class), and the fresh behavior of this type of SCC, usually very susceptible to changes in its composition [30], could be analyzed. An optimal fit with the Fuller curve in relation to the percentage of particles smaller than 0.25 mm (see Figure 4.3) was a pre-requisite to achieve this high slump flow. The initial proportions of the mix components, based on EC-2 (2010) [31], were empirically adapted.

All the SCC mixtures shared some aspects of this composition. On the one hand, they all incorporated 100% coarse RCA. This content was defined on the basis of the high compressive strength of the SCC that was manufactured with this amount of waste together with 100% fine NA, as demonstrated in another study by the authors [29]. On the other, the fine RCA 0/4 mm was simultaneously added in substitution of the siliceous sand 0/4 mm, a commonly used practice in the industrial manufacture of precast concrete [21]. According to the data collected in Figure 4.3 regarding the F mixes as representative examples, the replacement of siliceous sand by fine RCA increased the content of particles smaller than 0.25 mm in the mix, unlike a substitution of equal sized particles [32]. This circumstance slightly improved the initial fresh behavior of the fine RCA mixes in some tests (slump-flow and L-box tests), as shown in later sections. Hence, the temporal results of these tests are discussed on the basis of the (relative) percentile variations of these properties. Each mix composition was adjusted in three different ways, so all the mixes had different designs. All substitutions were performed with the volume correction technique.

- Firstly, the water content was adjusted to compensate for the water absorption of the RCA. The effective water-to-cement ratio remained constant in all the mixtures produced with the same type of cement (0.50 for CEM I mixtures, and 0.40 for CEM III mixtures). Its calculation involved subtracting the water absorbed into the aggregate under room-moisture conditions throughout the 15-minute mixing time from the total water content of the mix (Figure 4.4).
- Secondly, the optimal content of each aggregate powder was determined according to its percentage particle content lower than 0.25 mm. All of them yielded a SF3 slump-flow class SCC.
- Finally, the use of CEM III/A hindered the uniform dragging of the aggregate particles in the slump-flow test, due to the higher grinding fineness of CEM III/A in comparison with CEM I [33]. A reduction in the coarse RCA content used in the mixtures allowed solving this problem.

A total of 18 mixes were designed with different combinations of cement, fine RCA percentages, and aggregate powder. These mixes were labelled C-N/T:

- C represents the type of cement used: I (CEM I), or III (CEM III/A).
- N is the percentage of fine RCA added to the mix: 0, 50, or 100.
- T indicates the nature of the aggregate powder in use: F (ultra-fine limestone powder), L (limestone fines 0/0.5 mm), or R (RCA 0/0.5 mm).

The composition of the mixes is shown in Table 4.3, Table 4.4, and Table 4.5. All the mixtures had a high content of by-products as substitutes for natural materials, with the aim of maximizing the sustainability of the mixtures. The maximum RCA content in mix I-100/R represented 62% of the total volume.

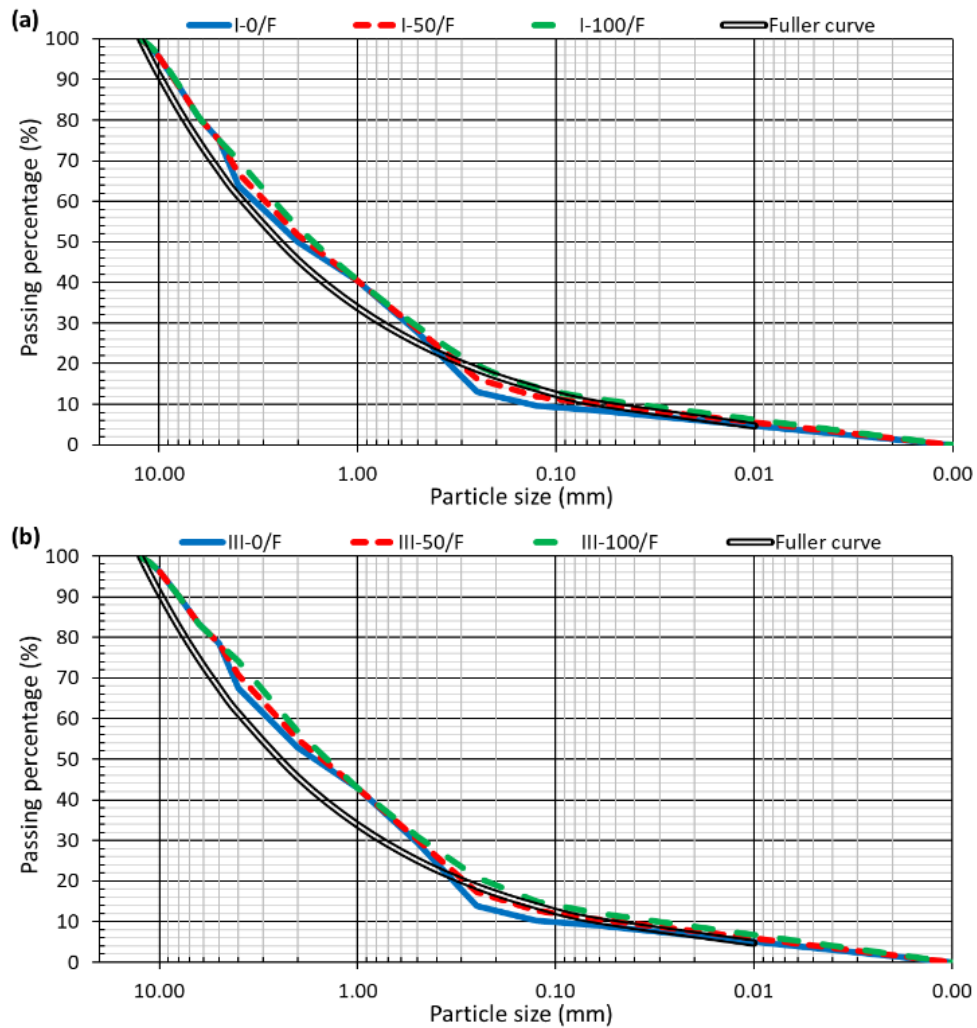


Figure 4.3. Gradation of the mixes with ultra-fine limestone powder: (a) CEM I; (b) CEM III

Table 4.3. Composition of the F mixes (kg/m³)

Material	I-0/F	I-50/F	I-100/F	III-0/F	III-50/F	III-100/F
CEM I # CEM III/A	300 # 0			0 # 425		
Ultra-fine limestone powder <0.063 mm	180					
Water	185	210	235	185	210	235
Coarse RCA 4/12.5 mm	530			430		
Fine RCA 0/4 mm	0	505	1010	0	505	1010
Siliceous sand 0/4 mm	1100	550	0	1100	550	0
AD1 # AD2	2.30 # 4.50					

Table 4.4. Composition of the L mixes (kg/m³)

Material	I-0/L	I-50/L	I-100/L	III-0/L	III-50/L	III-100/L
CEM I # CEM III/A	300 # 0			0 # 425		
Limestone fines 0/0.5 mm	335					
Water	185	210	235	185	210	235
Coarse RCA 4/12.5 mm	530			430		
Fine RCA 0/4 mm	0	435	865	0	435	865
Siliceous sand 0/4 mm	940	475	0	940	475	0
AD1 # AD2	2.30 # 4.50					

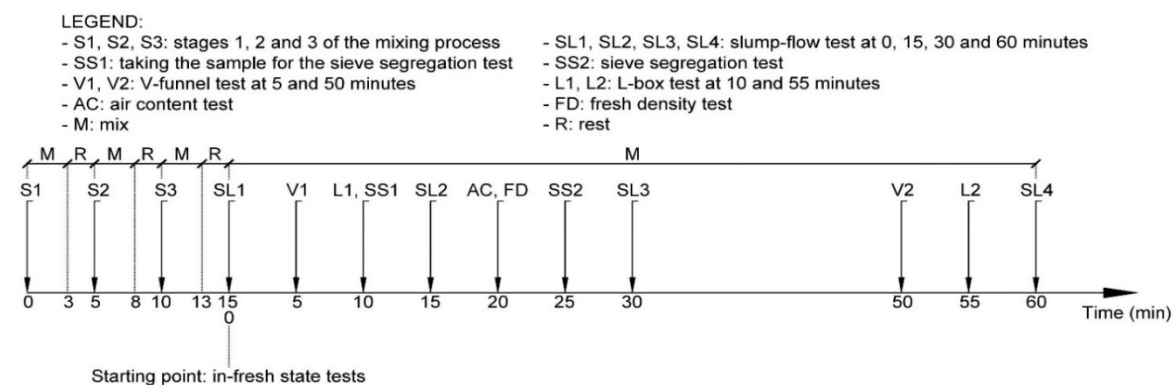
Table 4.5. Composition of the R mixes (kg/m³)

Material	I-0/R	I-50/R	I-100/R	III-0/R	III-50/R	III-100/R
CEM I # CEM III/A	300 # 0			0 # 425		
RCA 0/0.5 mm	305					
Water	200	220	245	200	220	245
Coarse RCA 4/12.5 mm	530			430		
Fine RCA 0/4 mm	0	435	865	0	435	865
Siliceous sand 0/4 mm	940	475	0	940	475	0
AD1 # AD2	2.30 # 4.50					

2.3. EXPERIMENTAL PLAN

As previously indicated, multi-stage mixing processes minimize the effects of RCA and its high water absorption levels on the fresh behavior of concrete [26]. For this reason, the components of the mix were added to the concrete mixer in three stages. In the first stage, the coarse and fine aggregate, the aggregate powder, and half of the water were added. In the second stage, the cement and the rest of the water were included. In the third stage, the admixtures were finally added. After each stage, the concrete was mixed for 3 minutes and then left to rest for 2 minutes. These times maximized the slump flow and were obtained after several attempts with mixing and resting times between 1 and 5 minutes. With this multi-stage mixing process, the aggregates absorbed water for 15 minutes before the tests in the fresh state were performed. Moreover, the hydration of the cement and the effect of the admixtures were also maximized, which also improved the flowability of the SCC [11].

After mixing, the tests in the fresh state were performed: slump-flow, V-funnel, two-bar L-box, sieve-segregation, air-content, and fresh-density tests. The slump-flow test was carried out at four different points in time to analyze its temporal evolution, while the V-funnel and the two-bar L-box tests were performed twice with an interval of 45 minutes. A strict experimental plan was defined (Figure 4.4), so that each mix could be compared with the others: each test in the fresh state was performed at the same time in all the mixes.

**Figure 4.4.** In-fresh state testing program

Apart from correct flowability, density and a compressive strength of SCC must be suitable for its use [34]. Therefore, the two aforementioned properties were determined for all the mixtures in 10x10x10-cm cubic specimens at 28 days. The specimens were manufactured between 30 and 50 minutes after the end of the mixing process.

3. RESULTS AND DISCUSSION: FRESH BEHAVIOR

The fresh-state tests were performed to evaluate the filling ability, viscosity, passing ability, and segregation resistance of the SCC. The applicable regulations for the performance of each test and

the SCC classifications according to EFNARC (2002) [12] are shown in Table 4.6. Additionally, the fresh density and the air content were determined according to the specifications of EN 12350-6 and EN 12350-7 [15], respectively. Specifications of the standardized test equipment are shown in Figure 4.5.

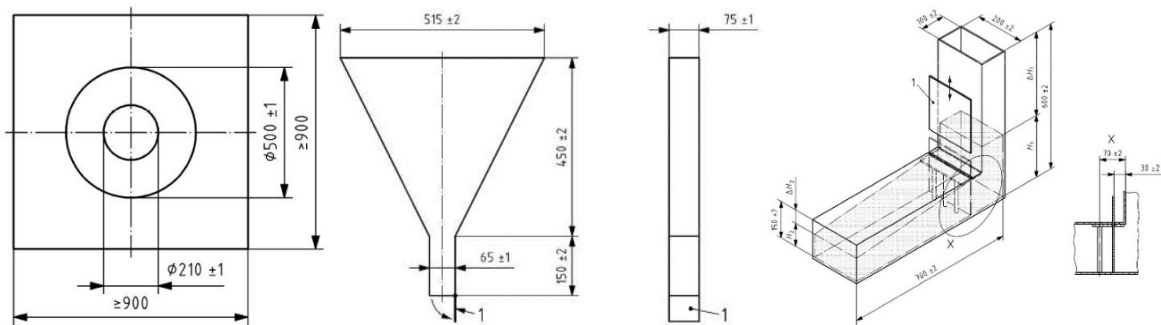


Figure 4.5. Scheme of the apparatus used in slump-flow (left), V-funnel (middle), and L-box (right) tests [15]. Dimensions in mm. Number “1” refers to the apparatus gate through which SCC flows

Table 4.6. Fresh state tests performed: regulations, and SCC classifications

Criteria	Regulations [15]	Classification according to EFNARC (2002) [12]
Filling ability, slump flow	EN 12350-8	SF1 (550-650 mm)
		SF2 (650-750 mm)
		SF3 (750-850 mm)
Viscosity according to slump-flow test	EN 12350-8	VS1 (<2 s)
		VS2 (>2 s)
Viscosity according to V-funnel test	EN 12350-9	VF1 (<8 s)
		VF2 (8-25 s)
Passing ability according to L-box test	EN 12350-10	PA1 ($H_1/H_2 > 0.80$; 2-bar L-box test)
		PA2 ($H_1/H_2 > 0.80$; 3-bar L-box test)
Resistance to segregation according to sieve-segregation test	EN 12350-11	SR1 (<20%)
		SR2 (<15%)

3.1. FILLING ABILITY AND VISCOSITY: SLUMP-FLOW TEST OVER TIME

The slump-flow test, according to EN 12350-8 [15], is fundamental in an evaluation of the filling ability of SCC without vibration [13]. In this test, the SCC is introduced into the Abrams cone, which is subsequently lifted with a vertical movement, leaving the SCC to flow freely onto a stainless-steel plate, described in Figure 4.5. The results of this test are the maximum diameter reached by the SCC, known as slump flow, and the time the SCC takes to reach a diameter of 500 mm (t_{500}), which yields a viscosity measurement of the mix. The addition of RCA with the same granulometry as NA usually results in an SCC of higher viscosity and with a lower slump flow [25], which can be compensated by adding a larger amount of water or admixtures [24]. This test was performed at 0, 15, 30, and 60 minutes after the mixing process had ended, to study the temporal evolution of the filling ability of SCC.

3.1.1. SLUMP-FLOW, SPREADING

The effects of RCA and cement type on the slump flow were similar in all series, as shown in Figure 4.6:

- The higher content of fine RCA particles smaller than 0.25 mm in comparison with siliceous sand, caused this by-product to increase the initial slump flow. It therefore compensated the other negative effects of fine RCA, such as its angular shaped particles [35]. However,

the high water absorption of the fines hindered the temporal evolution of the slump flow [36], and the slump-flow percentages gradually decreased.

- The initial slump flows of the CEM III mixtures, between 800 and 850 mm, were higher than those of the CEM I mixtures, with values between 750 and 800 mm, due to their higher fineness and lower proportion of coarse RCA. In relation to the slump flows over time, higher relative decreases at 15 and 30 minutes were noted for the CEM I mixtures. These reductions, between 3% and 10%, were similar to those obtained in SCC with only fine RCA (0% coarse RCA) when limestone aggregate powder was added [25]. Nevertheless, the decreases at 60 minutes, which averaged between 25% and 35%, were higher when CEM III was used.

The effect of each aggregate powder was different:

- The mixtures produced with CEM I and ultra-fine limestone powder (<0.063 mm) were not very sensitive to the addition of fine RCA (decreases at 60 minutes of 19.9% and 20.8% for 0% and 100% fine RCA, respectively). They also presented the highest initial slump flow of all the CEM I mixtures. Therefore, the use of good-quality cement and aggregate powder and correct hydration of the aggregates yielded an SCC with a consistent slump-flow evolution over time when adding 100% coarse and fine RCA.
- Initial slump flows similar to those of the F mixes were obtained when adding limestone fines 0/0.5 mm (L mixes), although the slump flow of those mixes decreased less over time. In addition, it was the aggregate powder that showed the best interaction with GGBFS, especially in the short term: the slump flow of mix III-0/L at 15 minutes (830 mm) was higher than the initial one (810 mm). The addition of the limestone fines produced a concrete with an optimum filling ability, which may also be observed in the initial slump flow of SCC produced with other wastes [30].
- The mixes with RCA 0/0.5 mm (R mixes) showed the lowest initial slump flows and the highest percentage decreases, due to the high water absorption of this aggregate powder [37]. Mixes III-50/R and III-100/R were the only two not to reach at least a SF1 slump-flow class at 60 minutes.

According to the results, if limestone aggregate powder is used, highly SCC produced with large quantities of alternative materials such as RCA or GGBFS can maintain its self-compactability for up to 60 minutes after the mixing process. This recycled aggregate SCC can therefore be properly poured on site at distances (in time) of 60 minutes from the point of manufacture.

3.1.2. VISCOSITY (t_{500})

Figure 4.7 shows the temporal evolution of viscosity determined with the slump-flow test (t_{500}). Although no clear trends may be detected as in the slump flow, some notable aspects are as follows:

- The viscosity of the SCC mixes with CEM I was higher than that of the mixes with CEM III for the same fine RCA content and the same type of aggregate powder. This result validates the use of GGBFS for producing SCC of acceptable initial viscosity, as observed in SCC with 100% NA [38]. However, this alternative binder induced higher relative increases in viscosity over time: 63.6% and 218.2% at 30 and 60 minutes, respectively, for mix I-0/F, and 75.0% and 325.0% for mix III-0/F.
- The increase in fine RCA content resulted in a higher viscosity at all times, probably due to the rougher surface of its particles. Nevertheless, this increase, at around 40-120%, was lower than the increase in the SCC mixes with only coarse RCA 30 minutes after the mixing process (130-160%), possibly due to the mixing process designed in this study [24].
- The lowest initial viscosity was obtained in the mixes with ultra-fine limestone powder (F mixes), due to its small particle sizes. The worst temporal results were for the R mixes, as the largest percentage decreases in the CEM I mixtures (Figure 4.7) were observed

following the addition of RCA 0/0.5 mm The highest percentage increase in viscosity was observed in the F mixes with CEM III, due perhaps to the poor interaction between those two materials [38].

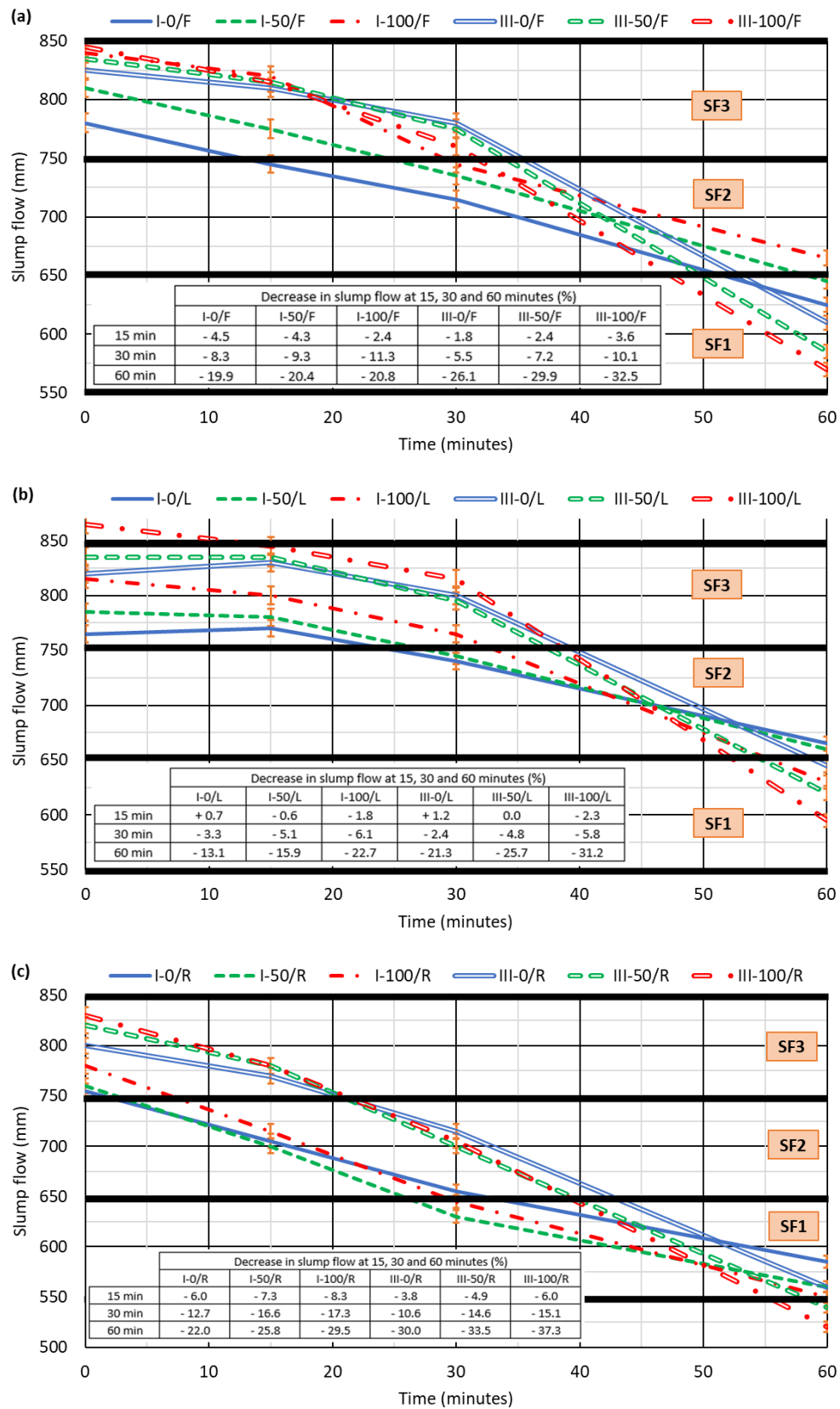


Figure 4.6. Slump-flow evolution over time: (a) F mixes; (b) L mixes; (c) R mixes

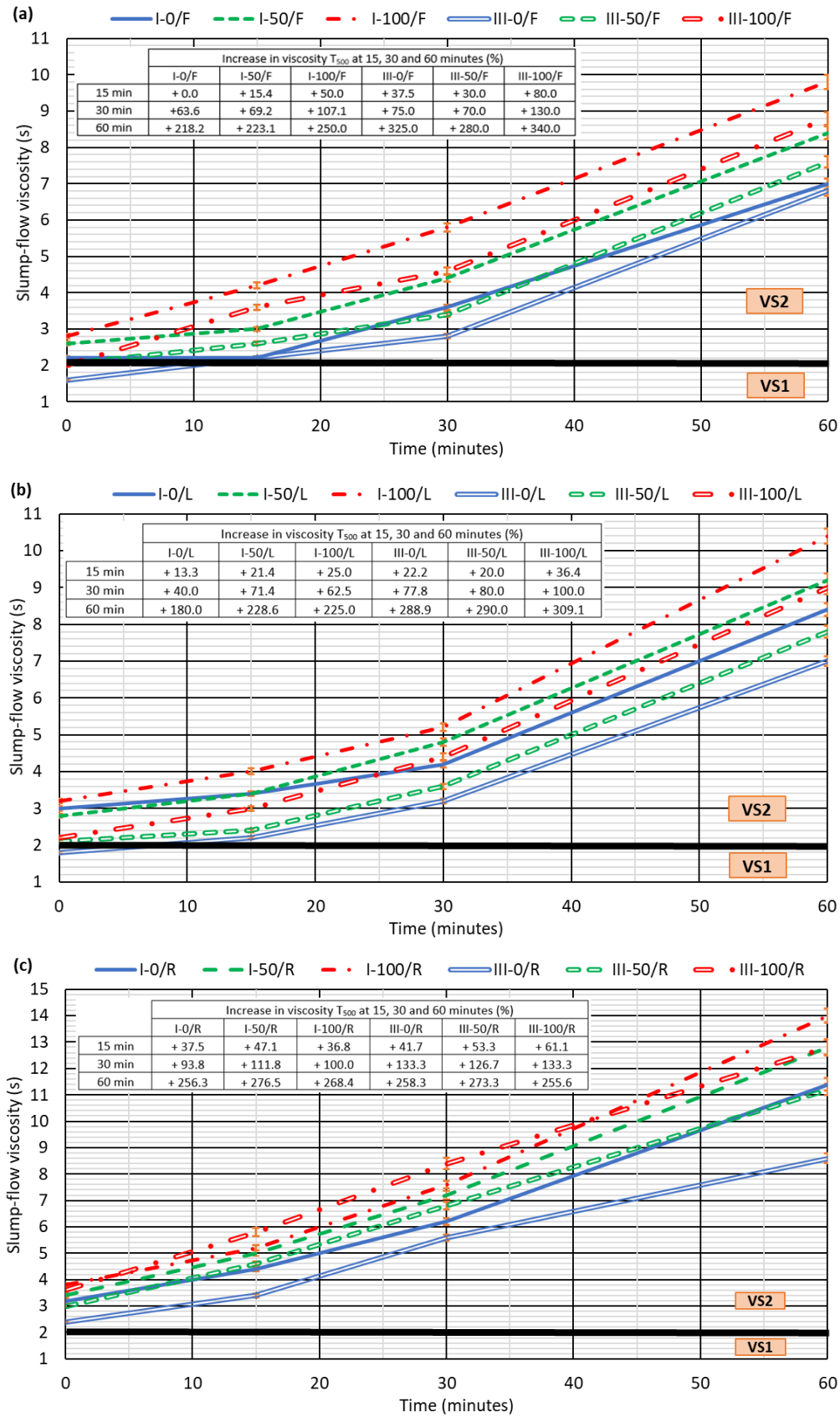


Figure 4.7. Viscosity t_{500} evolution over time: (a) F mixes; (b) L mixes; (c) R mixes

3.1.3. STATISTICAL ANALYSIS

The descriptive analyses of the two previous sections presented detailed summaries of each variation in mix composition and its effect on slump flow and viscosity. However, a one-way ANalysis Of VAriance (ANOVA) of these results might determine whether the effect of each factor (each modification in the mix composition: type of cement, fine RCA content, or nature of the aggregate powder) is significant in the results of the slump-flow test compared to the effect of all other factors at each point in time [39]. Furthermore, homogeneous groups may be identified, *i.e.*, values of a factor with the same effect on the slump flow and viscosity of the SCC. This analysis was performed at the standard significance level of 5% [29]. The results (Table 4.7) showed that if the water absorption of the RCA is maximized (a shared objective of both the mix design and the mixing process), its negative effect on the temporal evolution of SCC flowability may not be significant:

- Although the initial slump flow depended on the cement and the fine RCA content, 15 minutes after the end of the mixing process, it was more dependent on the nature of the aggregate powder.
- The temporal evolution of the viscosity also depended mainly on the aggregate powder in use. Neither the cement, nor the fine RCA content significantly influenced this behavior.

Table 4.7. One-way ANOVA for slump flow and viscosity (t_{500})

Condition	Factor	Slump flow		Viscosity	
		p -Value	Homogeneous groups	p -Value	Homogeneous groups
Time: 0 min	Cement	0.0000	None	0.0021	None
	Fine RCA percentage	0.0486	0% and 50% 50% and 100%	0.2263	0%, 50% and 100%
	Aggregate powder	0.3780	F, L and R	0.0093	F and L
Time: 15 min	Cement	0.0002	None	0.1050	CEM I and CEM III/A
	Fine RCA percentage	0.5592	0%, 50% and 100%	0.1084	0%, 50% and 100%
	Aggregate powder	0.0171	F and L L and R	0.0013	F and L
Time: 30 min	Cement	0.0031	None	0.2109	CEM I and CEM III/A
	Fine RCA percentage	0.9500	0%, 50% and 100%	0.0637	0%, 50% and 100%
	Aggregate powder	0.0002	F and L	0.0001	F and L
Time: 60 min	Cement	0.0371	None	0.1260	CEM I and CEM III/A
	Fine RCA percentage	0.6228	0%, 50% and 100%	0.2970	0%, 50% and 100%
	Aggregate powder	0.0001	F and L	0.0007	F and L

3.1.4. ADJUSTMENT MODEL

The statistical model in this section, exclusively devised by the authors of this paper, was used to predict the temporal decrease of the slump flow for each mix (see section 3.1.1).

This model depends on a variable that represents the time lapse from the beginning of the mixing process to the test time: RWA (Relative Water Absorption, %). This variable is calculated in Equation 1 as the product of the water absorption within 24 h of the fine aggregate (0/4 mm) used to prepare the mix, expressed as a percentage (WA_{24h} , %), and a coefficient, A , obtained by statistical fitting of the data from this (see the supplementary data) and other studies [24, 25]. Its values, shown in Table 4.8, reflect the percentage water absorption of the aggregate at each point in time regarding the 24-h water absorption.

$$RWA = A \cdot WA_{24h} \quad (4.1)$$

Table 4.8. Values of coefficient A

Time elapsed since the beginning of the mixing process (min)	5	10	15	30	45	60	75	90
Coefficient A	0.55	0.70	0.75	0.80	0.85	0.88	0.90	0.92

The percentage decrease in slump flow (D_{sf} , %) of the mixes may be determined with Equation 2. The R^2 coefficient was 94% for CEM I mixtures and 97% for CEM III/A mixtures:

$$D_{sf} = \left(B + \frac{C}{RWA} \right)^2 \quad \text{if CEM I is used} \quad (2)$$

$$D_{sf} = (B + C \cdot RWA^2)^2 \quad \text{if CEM III/A is used}$$

Both formulas depend on coefficients B and C:

- The formulas to calculate the coefficient B (Table 4.9) depend on the variable $WAAP$ (Water Absorption Aggregate Powder), which is the percentage 24-h water absorption of the aggregate powder. The expression to be used depends on the type of cement and the percentage of fine RCA.
- The other coefficient, C , depends on the variable $RCAP$ (Recycled Concrete Aggregate Percentage), which is the fine RCA percentage added to the mix. The formulas, shown in Table 4.10, vary according to the type of cement and the nature of the aggregate powder.

Table 4.9. Calculation of the coefficient B

% fine RCA	CEM I
0% fine RCA	$28.05 - 5.00 \cdot WAAP + 1.17 \cdot WAAP^2 - 0.07 \cdot WAAP^3$
50% fine RCA	$28.04 - 3.54 \cdot WAAP + 0.81 \cdot WAAP^2 - 0.04 \cdot WAAP^3$
100% fine RCA	$32.71 - 11.40 \cdot WAAP + 4.65 \cdot WAAP^2 - 0.41 \cdot WAAP^3$
% fine RCA	CEM III/A
0% fine RCA	$-13.50 + 3.25 \cdot WAAP - 1.51 \cdot WAAP^2 + 0.14 \cdot WAAP^3$
50% fine RCA	$-12.34 + 2.29 \cdot WAAP - 0.97 \cdot WAAP^2 + 0.09 \cdot WAAP^3$
100% fine RCA	$-13.31 + 2.05 \cdot WAAP - 0.87 \cdot WAAP^2 - 0.08 \cdot WAAP^3$

Table 4.10. Calculation of the coefficient C

Aggregate powder	CEM I
Ultra-fine limestone powder	$-4.79 - 1.31 \cdot RCAP - 0.00178 \cdot RCAP^2$
Limestone fines 0/0.5 mm	$-4.19 - 1.09 \cdot RCAP - 0.00382 \cdot RCAP^2$
RCA 0/0.5 mm	$-5.17 - 1.54 \cdot RCAP - 0.00174 \cdot RCAP^2$
Aggregate powder	CEM III/A
Ultra-fine limestone powder	$318.14 - 9.49 \cdot RCAP + 0.06312 \cdot RCAP^2$
Limestone fines 0/0.5 mm	$301.95 - 9.00 \cdot RCAP + 0.05988 \cdot RCAP^2$
RCA 0/0.5 mm	$344.08 - 10.26 \cdot RCAP + 0.06827 \cdot RCAP^2$

As shown in Figure 4.8, a global evaluation of both types of cement mixes revealed that the worst fit was associated with the R mixes, although neither over- nor underestimation exceeded an absolute value of 3%. Furthermore, the data from the few studies that have to date analyzed the temporal flowability of SCC manufactured with only one RCA fraction [24, 25] showed a reasonable fit with the model, as may be observed in Figure 4.9. In general, the results of these studies were overestimated at around an absolute value of 2-5%, which suggests that the estimations were on the safe side, although the very limited data and studies for the validation of the model must be borne in mind.

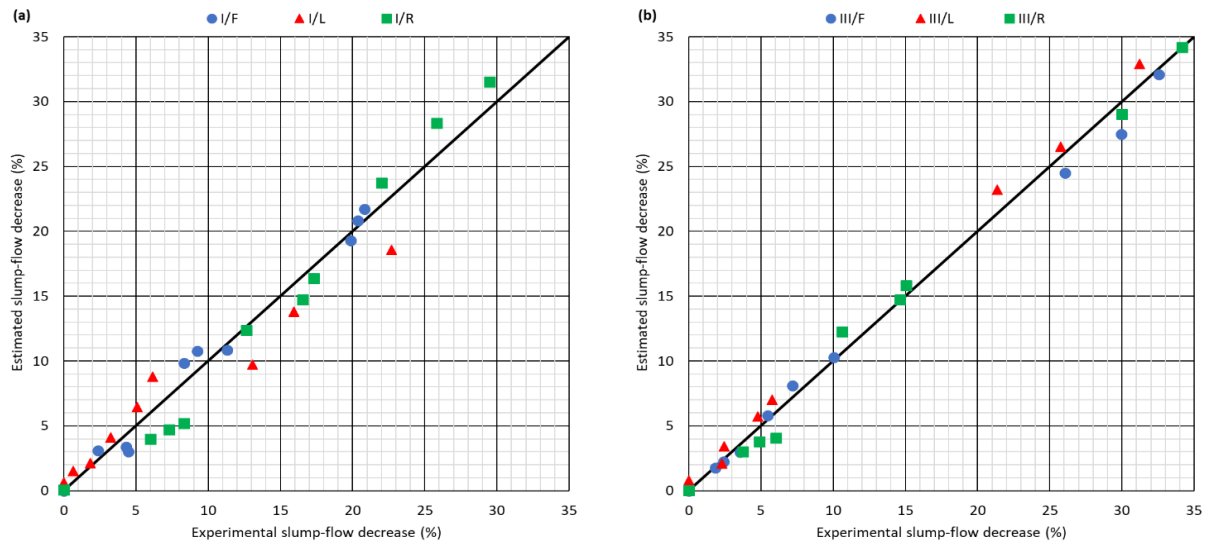


Figure 4.8. Relationship between estimated and experimental slump flow: (a) CEM I; (b) CEM III/A

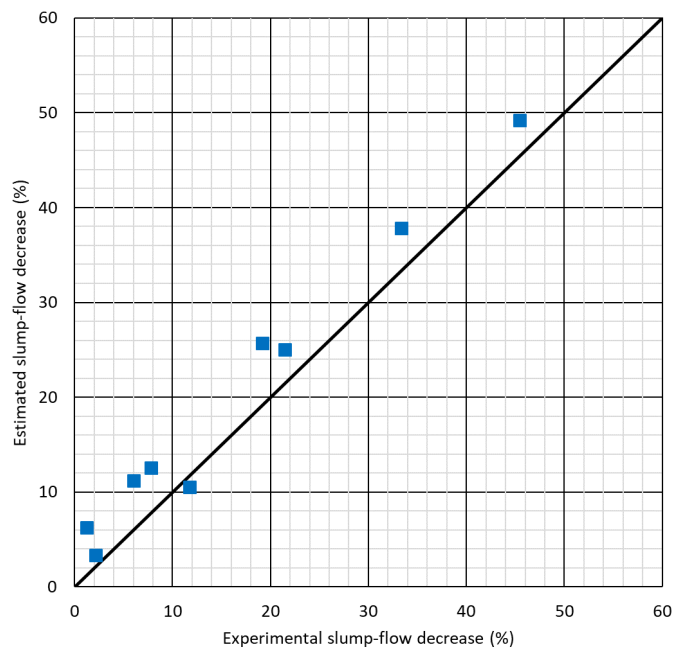


Figure 4.9. Validation of the model developed with the data from other studies

This model also reflects the global aspects on which the prediction of the evolution of the slump flow depends, some of which have already been indicated in the statistical analysis (section 3.1.3). Other factors must also be considered to predict the evolution of SCC flowability, although their effects may not be significant with regard to the slump flow of the mixes under study (one-way ANOVA, Table 4.7). These aspects are:

- Water absorption levels over time, not only of both coarse and fine aggregate as other studies have shown [13], but of all aggregate fractions, including aggregate powder (*RWA* and *WAAP* variables). In this study, *RCA* was used as a coarse aggregate in all the mixes. If the type of coarse aggregate had differed in each mix, its water absorption should have also been considered [40].
- The temporal evolution of the cement rheology [41], as the formula to be used depends on the type of cement that is used.
- The interaction of the cement with all the aggregates added to the mix, especially with the aggregate powder (formulas to calculate coefficients *B* and *C*), which explains the statistical

significance of the effect of the aggregate powder on the temporal evolution of the slump flow.

The effect of the last two aspects is clearly shown in the high decrease of slump flow between 30 and 60 minutes in all the mixes, although aggregate water absorption was fairly low within that period (see the supplementary data).

3.2. VISCOSITY: V-FUNNEL TEST

The viscosity characterization of the SCC mixtures was completed with the V-funnel test, according to EN 12350-9 [15], which was performed at 5 and at 50 minutes after the end of the mixing process. In this test, the SCC is poured into a V-shaped funnel (see Figure 4.5), and the time that SCC takes to flow through the opening of the funnel lid is measured. This test is more demanding than the slump-flow test regarding viscosity, because it forces the SCC to flow in a specific direction [27]. The results are shown in Figure 4.10. Mixes I-0/F, III-0/F, I-0/L, and III-0/L were of VF1 class. Mixes I-100/R and III-100/R (emptying time greater than 25 s) showed no compliance with the recommendations of EFNARC (2002) [12].

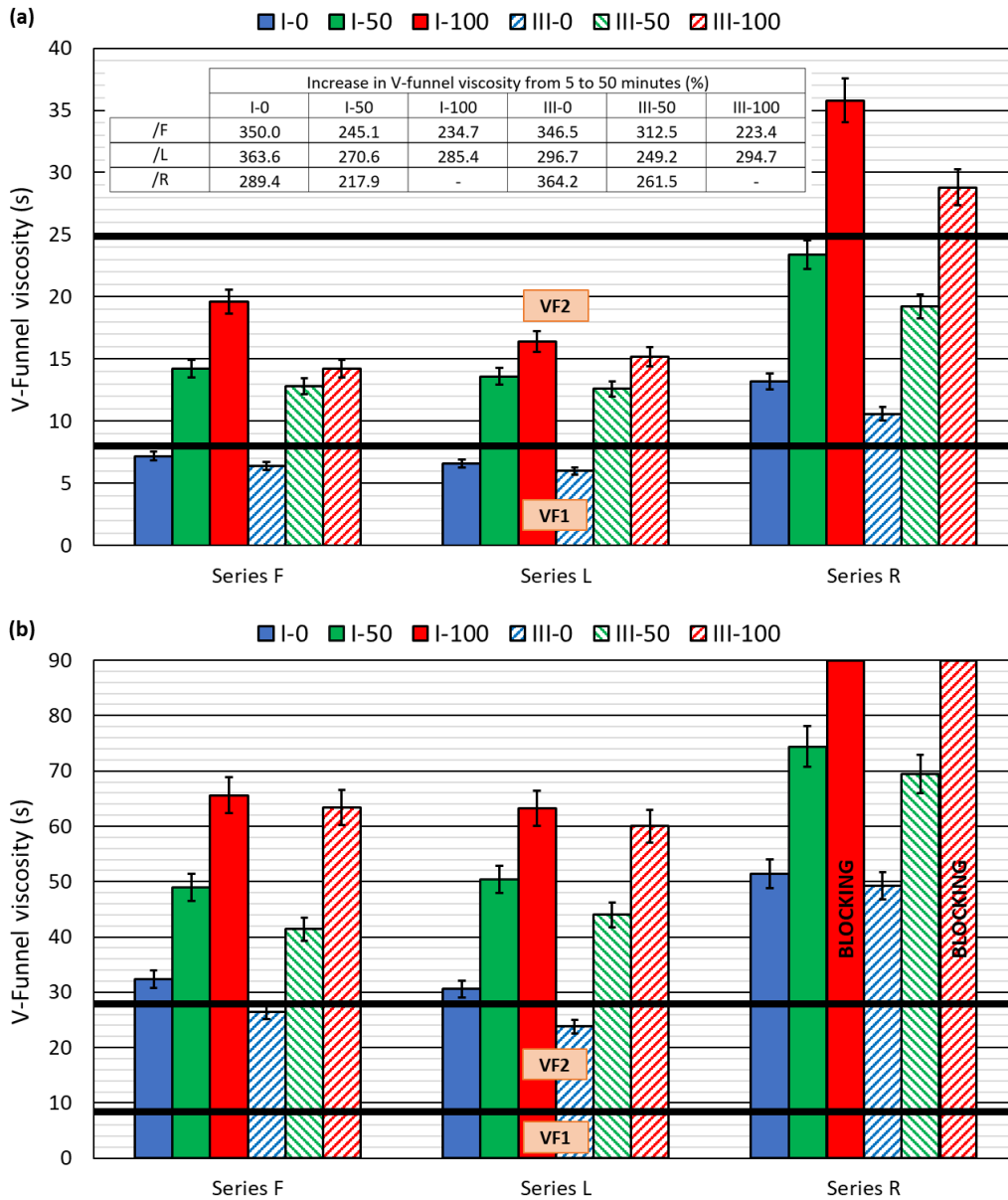


Figure 4.10. Results of V-Funnel test: (a) at 5 minutes; (b) at 50 minutes

The increase in the percentage of fine RCA increased the emptying time, due to the higher segregation within the SCC, which caused a discontinuous and irregular free-fall flow [32]. Initial viscosity improved in the CEM III mixes, mainly due to their lower proportion of coarse aggregate, an aspect that conditions this property to a greater extent [42]. Thus, compared to the viscosity of the control mix I-0/F (7.2 s), emptying times increased 172.2% for mix I-100/F (19.6 s), -11.1% for mix III-0/F (6.4 s), and 97.2% for mix III-100/F (14.2 s). The increase was 121.9% for the latter mix with respect to mix III-0/F. These increases were slightly higher than when only one RCA fraction was used: around 85% for 100% coarse RCA [24] and around 110% for 100% fine RCA [25].

As with the slump-flow test, the L mixes were also the least viscous in the V-funnel test, because the high proportion of particle sizes between 0.25-0.50 mm in this aggregate powder resulted in a very compact cement paste that dragged the larger aggregate particles more easily [43]. RCA 0/0.5 mm hindered the dragging of the coarser aggregate particles, due to their higher water absorption, their irregular shape and, especially, their lower density [25].

The emptying times at 50 minutes were, on average, 270% higher than at 5 minutes (Figure 4.10a). The effect of fine RCA was more negative than at 5 minutes and, although the behavior of CEM III improved on the behavior of CEM I, its effect was not as beneficial. CEM III mixtures again showed a greater relative increase in viscosity, which was maximum in the mixtures with 100% fine RCA. Mix III-0/L was the only mix that presented an emptying time that was shorter than 25 s (VF2 class). R mixes experienced an increase in the emptying time that was much higher than the rest of the mixes, and mixes I-100/R and III-100/R even blocked the funnel completely. Increased viscosity of SCC can hinder the pumping process. It therefore appeared reasonable to limit the fine RCA content to 50%, while the use of GGBFS hardly appeared disadvantageous when compared to conventional cement.

3.3. PASSING ABILITY: 2-BAR L-BOX TEST

In the L-box test, according to EN 12350-10 [15], the SCC is poured into the vertical zone of a L-shaped box (Figure 4.5). When the gate of the box is opened, the SCC flows into a horizontal zone through bars that simulate concrete reinforcement. The test result, known as the blocking ratio, is the ratio between the height of the SCC mass before the bars and at the end of the horizontal zone. Although SCC flows freely downwards in the V-funnel test and its movement is eventually horizontal in the L-box test, in both tests the SCC is forced to flow through an obstacle under its own weight with no other forces acting upon it. This causes similarities in the results of both tests [20]. In this study, the L-box test was performed 10 and 55 minutes after the end of the mixing process, with similar results to those obtained in the V-funnel test, although there were also some differences, mainly regarding the effect of the fine RCA (see Figure 4.11).

- The CEM III mixes yielded better blocking ratios, due to their lower coarse RCA.
- The L mixes showed the best behavior, as the limestone fines 0/0.5 mm created very compact cement pastes exerting an optimal drag force on the coarse aggregate [34]. In fact, mix III-100/L had the maximum blocking ratio after 10 minutes, 0.97. The worst results were obtained with RCA 0/0.5 mm due to its lower density, its rough form, and its high water-absorption levels [32].
- Unlike the V-funnel test, the use of fine RCA 0/4 mm, with a higher content of particles smaller than 0.25 mm compared to siliceous sand, 0/4 mm, created a cement paste with a higher dragging capacity. Its use, therefore, improved the passing ability (blocking ratio of 0.83, 0.86 and 0.91 at 10 minutes for mixes I-0/F, I-50/F, and I-100/F, respectively). The content of aggregate particles with a size of 0.25-0.50 mm is clearly fundamental to this property, as shown in other studies [42] and as found when using only coarse RCA [24].

At 55 minutes, the beneficial effect of CEM III on the passing ability was lower, and its use led to higher relative decreases. The difference in the blocking ratio between the mixes with fine RCA and

the mixes with 100% siliceous sand 0/4 mm was lower than at 10 minutes. Finally, the higher water absorption of RCA 0/0.5 mm explains the highest decrease in the blocking ratio, although limestone aggregate powders showed the worst interaction with GGBFS regarding the relative decrease of this property. According to the EFNARC (2002) [12] recommendations, both F and L mixes would be suitable for the concreting of conventional reinforced concrete elements around one hour after their manufacture.

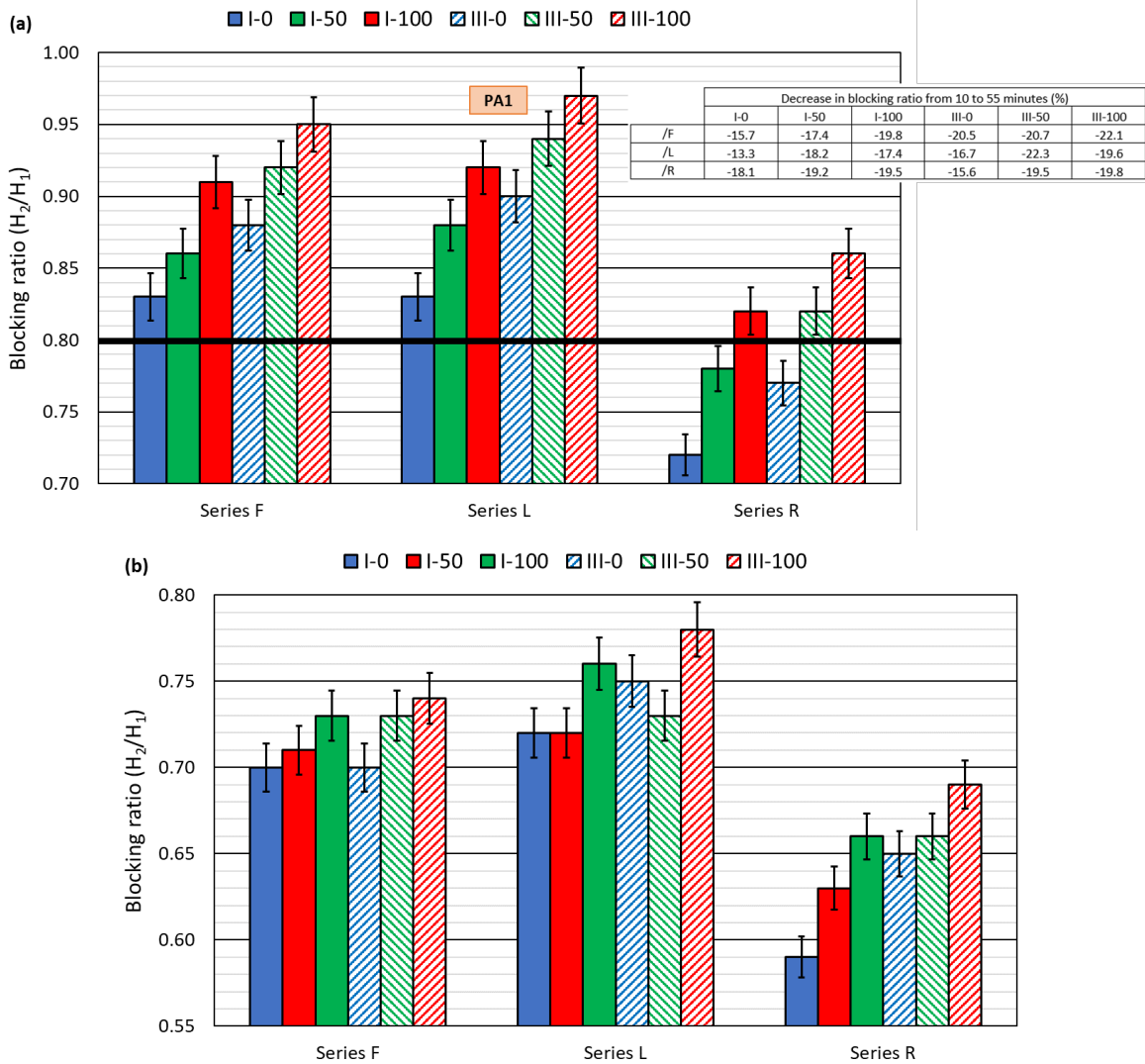


Figure 4.11. Results of 2-bar L-box test: (a) at 10 minutes; (b) at 55 minutes

3.4. SIEVE SEGREGATION

The sieve-segregation test, as per EN 12350-11 [15], assesses the adhesion of the cementitious matrix to larger aggregate particles [27]. In this test, the SCC is placed on a 5-mm-opening sieve after 15 minutes of rest, and the amount of mix that passes through it is weighed. The quotient between this mass and the total amount of SCC deposited on the sieve is called sieve segregation. Figure 4.12 shows that all mixtures had a SR2 segregation-resistance class; none exceeded 4% sieve segregation. The results were excellent for the SCC of SF3 slump-flow class, which is very sensitive to segregation. This behavior can be explained by the fast loss of flowability of SCC without mixing, thanks to the accurate amount of water added.

The higher segregation of the CEM III mixes was mainly due to their higher proportion of cement paste: the segregation of mix III-0/F was 3.57%, 93.0% higher than the segregation of mix I-0/F

(1.85%). The addition of fine RCA reduced the segregation, mainly due to the higher water absorption of this aggregate during the 15 minutes that the SCC was left to rest [13]. The same behavior was found when adding only one RCA fraction [24].

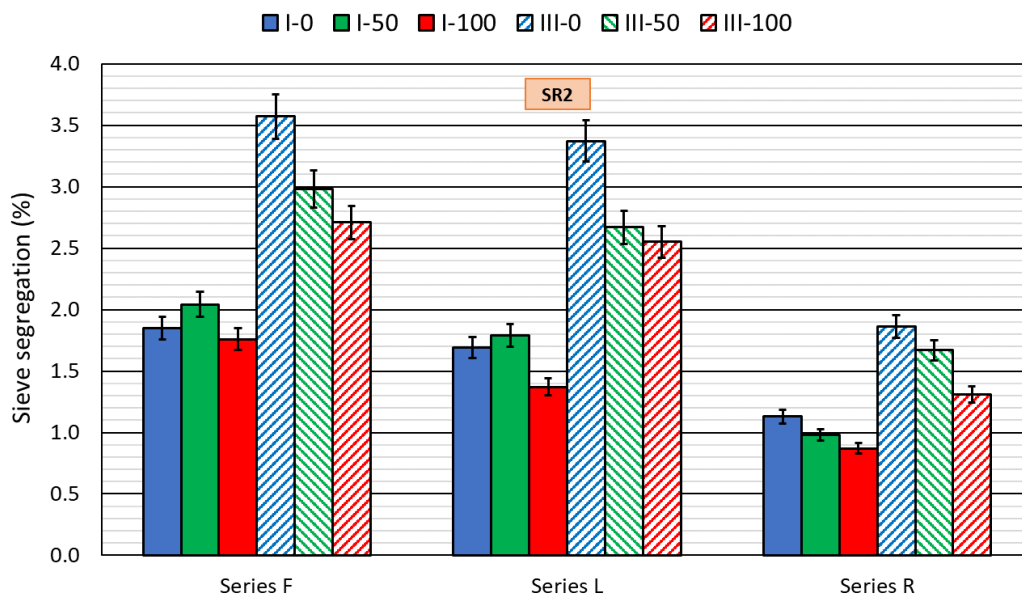


Figure 4.12. Results of sieve-segregation test

The effect of each aggregate powder mainly depended on its water absorption. The R mixes yielded the best results as they contained the aggregate powder with the highest water absorption levels (sieve segregation around 1% for mixes with CEM I and 1.5% for mixes with CEM III). The segregation of the F and L mixes was similar, although it was slightly better in mixes with limestone fines 0/0.5 mm, due to their larger particle sizes.

3.5. AIR CONTENT

The air content was determined by the pressure method according to EN 12350-7 [15]. This method consists of introducing the concrete into a micro-compressor and obtaining the value of occluded air as the difference in pressure before and after the valves are opened. The mixtures in this study were tested without vibration after having been placed inside the micro-compressor, thus reproducing the optimal placement of SCC [12]. The addition of high quantities of plasticizer to achieve self-compactability [11] and the high RCA content [27] resulted in a high air content in all the mixes, as shown in Figure 4.13: the air content was higher than 4% in 16 of the 18 mixes under study.

Since RCA is more porous than siliceous sand due to the presence of adhered mortar, the air content increased with the addition of fine RCA [40]. On the other hand, as a higher initial flowability was achieved in the mixes made with CEM III, they had a more liquid cement paste that facilitated the expulsion of air [30]. Their air content was therefore lower (for example, the air content of mixes I-100/L and III-100/L was 5.3 and 4.4%, respectively). So, the increased air content of the mixes after adding 45% GGBFS [38] was compensated by the increased flowability of the SCC.

The larger particle sizes of the aggregate powder hindered the expulsion of air [44]. The mixes with ultra-fine limestone powder showed the best results, though very close to those of the L mixes (air content of 3.9 and 4.0% for mixes I-0/F and I-0/L). The high micro-porosity of RCA 0/0.5 mm was very negative: the air content of almost all the R mixes was over 5% (maximum value in mix I-100/R, 6.6%).

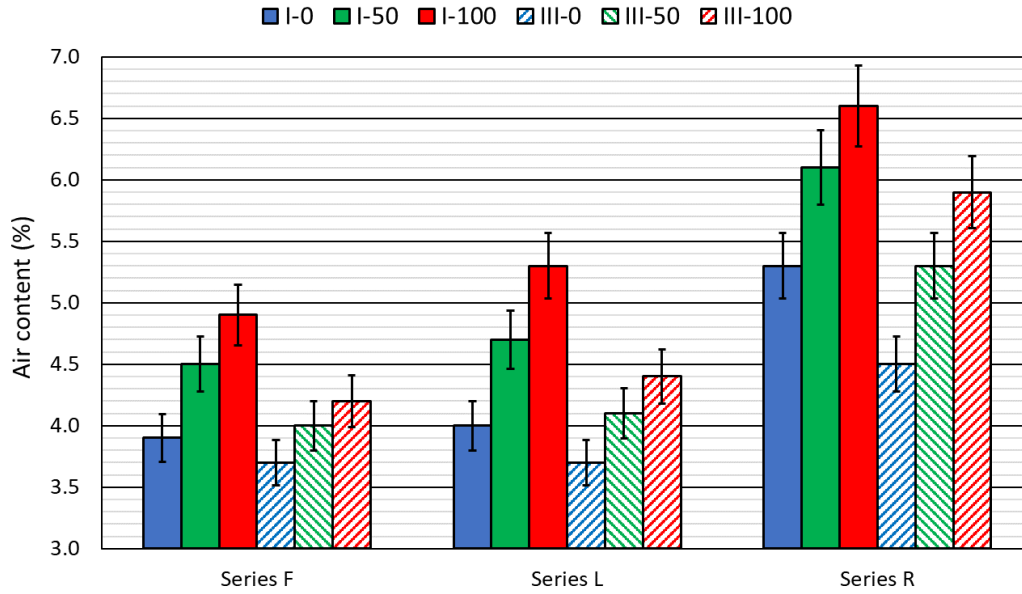


Figure 4.13. Results of air content test

3.6. FRESH DENSITY

The fresh density of concrete is determined by placing the fresh concrete in a recipient with a measured volume, as specified in EN 12350-6 [15]. The quotient between the specified concrete mass placed in the recipient and the full volume of the recipient represents the value of this property. The density of the components conditioned the fresh density of the concrete (Figure 4.14). Thus, fresh density increased with the higher cement content of CEM III that is of higher density than the aggregate, and decreased when fine RCA, less dense than fine NA, was added [21]. The densest aggregate powder, limestone fines 0/0.5 mm, produced the densest mixtures [45].

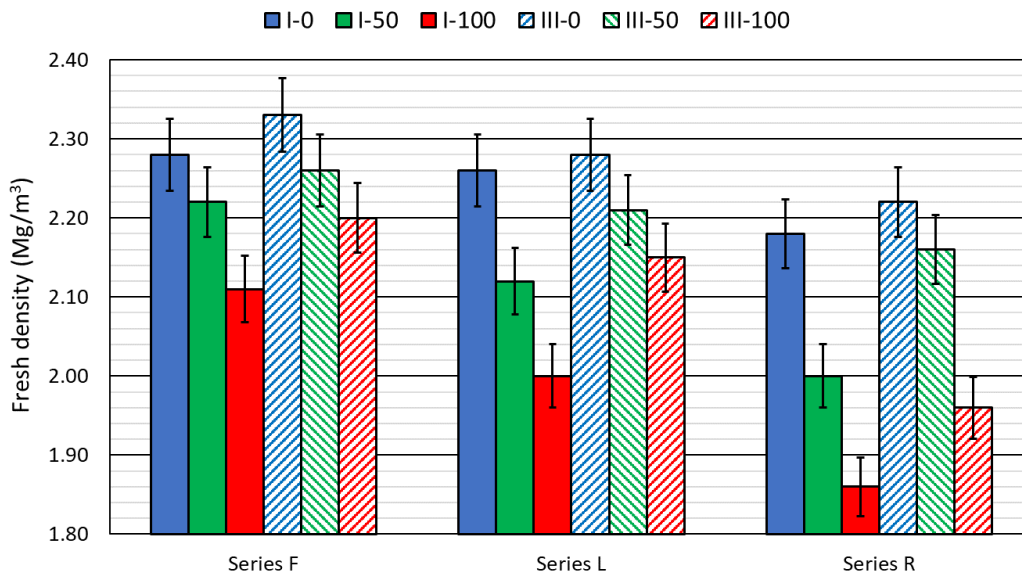


Figure 4.14. Fresh density of the mixes

However, the density of the mixes was also very sensitive to variations in the air content, as shown in Figure 4.15, which reflects the close relation between a higher air content and a lower SCC fresh density. In consequence, non-uniform variations in density across all mixture series occurred when a certain percentage of fine RCA was added, a trend also observed in vibrated concrete [40].

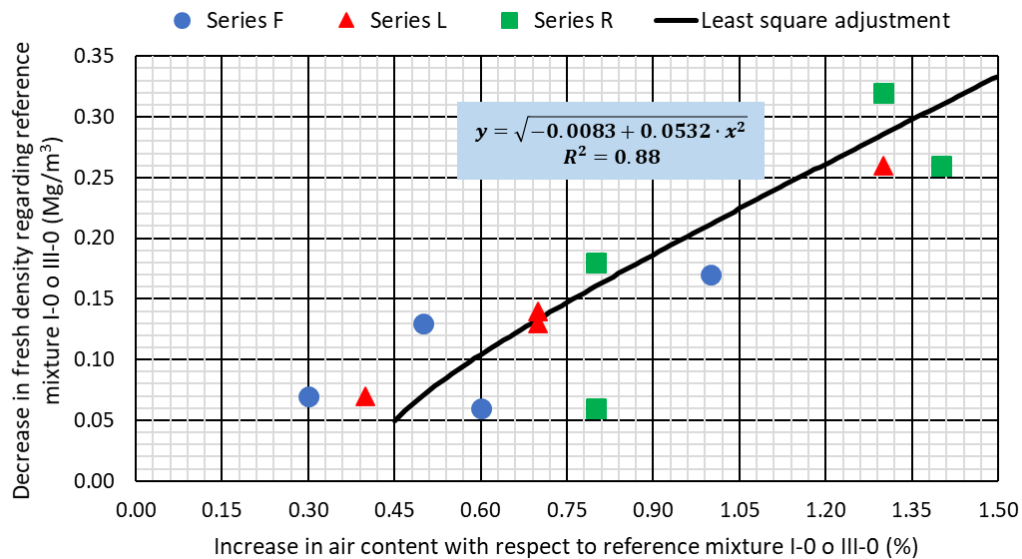


Figure 4.15. Relationship between air content increase and fresh density decrease

4. RESULTS AND DISCUSSION: HARDENED BEHAVIOR

In addition to optimum flowability, the hardened behavior of SCC must also be reasonable [27]. Accordingly, the hardened density and 28-day compressive strength of the mixtures were also evaluated on a set of 10x10x10-cm cubic specimens. These properties, along with the thermal properties, are useful for defining the validity of an SCC to be used from a functional point of view. A first approach to this thermal behavior is shown in a previous study of the authors [35]. In this study, the thermal deformability of the SCC made with RCA was evaluated under both positive and negative cyclical temperature variations. The thermal strain was continuously measured using strain gauges. It was found that the use of 100% fine RCA increased the thermal strain by 10%, while this increase was 26% for a full replacement of coarse NA with RCA. Therefore, the use of RCA, especially of the coarse fraction, implies higher stresses in SCC due to temperature changes, which should be considered when RCA is used in structural SCC.

4.1. HARDENED DENSITY

Among the different concrete density tests of EN 12390-7 [15], in this study the real density was determined, in terms of the hydrostatic equilibrium or weight difference. The hardened density was lower than the fresh density, due to the evaporation of the water released in a delayed way from the aggregate after mixing or not absorbed by the mix components [22]. Figure 4.16 shows the results of real density (and the decrease in comparison with the fresh density) of all the mixes. The results reproduced the fresh density behavior (section 3.6): the use of CEM III increased the density, and the addition of fine RCA and RCA 0/0.5 mm, of lower density than fine NA and limestone aggregate powder, respectively, reduced it.

The release of water from the aggregate and the amount of water not absorbed in the mix components conditioned the variation between the real and the fresh densities. On the one hand, the high water absorption of RCA led to a higher delayed release of water after mixing, which increased the water evaporation, the mass loss, and the density reduction [46]. On the other, the use of fine RCA and aggregate powders with irregular shapes, such as limestone fines 0/0.5 mm and RCA 0/0.5 mm, also augmented this decrease in density. The distribution of water within the concrete was less uniform when using these aggregates, resulting in higher water evaporation [29]. Finally, CEM III, which produced more fluid mixes, also slightly increased this density variation.

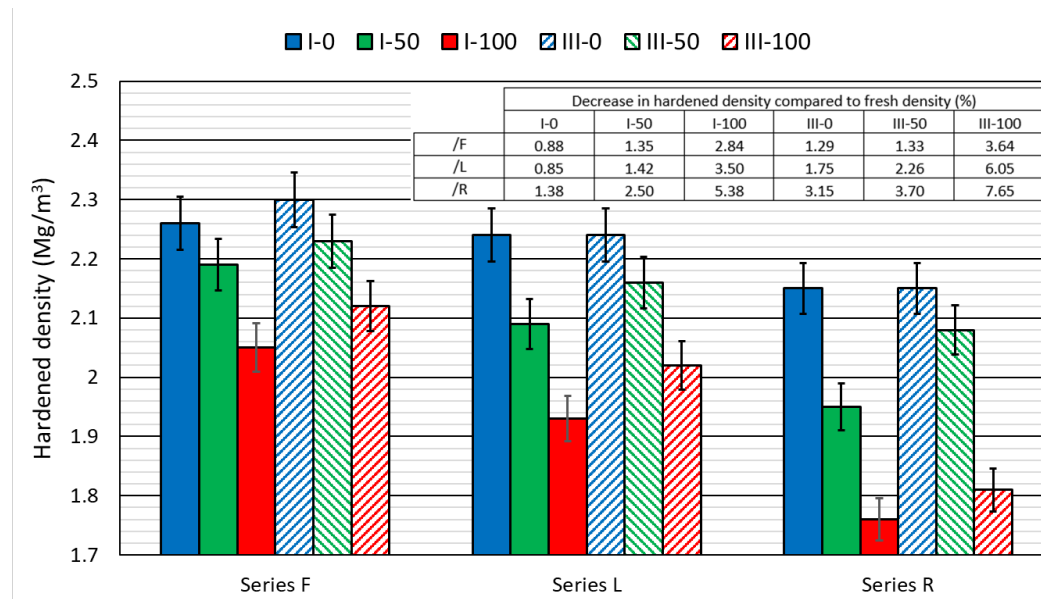


Figure 4.16. Hardened density of the mixes and their lower real density in comparison with their fresh density

4.2. COMPRESSIVE STRENGTH

The compressive strength of concrete, as per EN 12390-3 [15], is determined by applying a compressive force to a standardized specimen at a rate between 0.4 and 0.8 MPa/s. The use of RCA decreases the compressive strength of the concrete [28], although its addition can still produce high-strength SCC [27], as shown in some of the mixes in this study (third column of Table 4.12). Therefore, some of the SCC mixes might also be valid for structural use from the point of view of their strength, thus increasing the sustainability of commonly used SCC. Some relevant aspects were observed:

- The higher cement content of the CEM III mixes balanced the lower strength expected from using GGBFS [47], and even increased the strength: mixes III-0/F and III-0/L (55 and 62 MPa respectively) had 9.2 and 17.0% higher strengths than mixes I-0/F and I-0/L (50.5 and 53 MPa), respectively.
- The addition of fine RCA instead of siliceous sand decreased the compressive strength, mainly when using CEM I. The decrease between mixes with 0 and 50% fine RCA was lower than between mixes with 50 and 100% fine RCA: the respective strengths of mixes I-50/F and I-100/F were 8.2 and 35.9% lower than that of mix I-0/F. This non-proportional decrease was due to the filler effect of the high fines content of fine RCA, which was all the more outstanding when adding low or medium contents of RCA [48].
- Limestone fines 0/0.5 mm provided mixtures of higher strength than ultra-fine limestone powder. Mixes III-0/L and III-50/L exceeded compressive strengths of 55 MPa. The R mixes presented the lowest strength (average loss close to 20%), although the usual value of 30 MPa when using 300 kg/m³ of cement was achieved in all mixes except in mix I-100/R (lowest density, highest air content).

Fragments of mix III-50/L were examined under a Scanning Electron Microscope (SEM) to complete the analysis, as shown in Figure 4.17. A micrometer-scale siliceous sand particle belonging to an RCA particle can be observed. This particle of siliceous sand and the mortar adhering to it, of a darker color than the new cementitious matrix, were broken during the test. Good adhesion between the RCA and the cementitious matrix in the interfacial transition zones was detected as the aggregate broke, reflecting the high compressive strength of this mix.

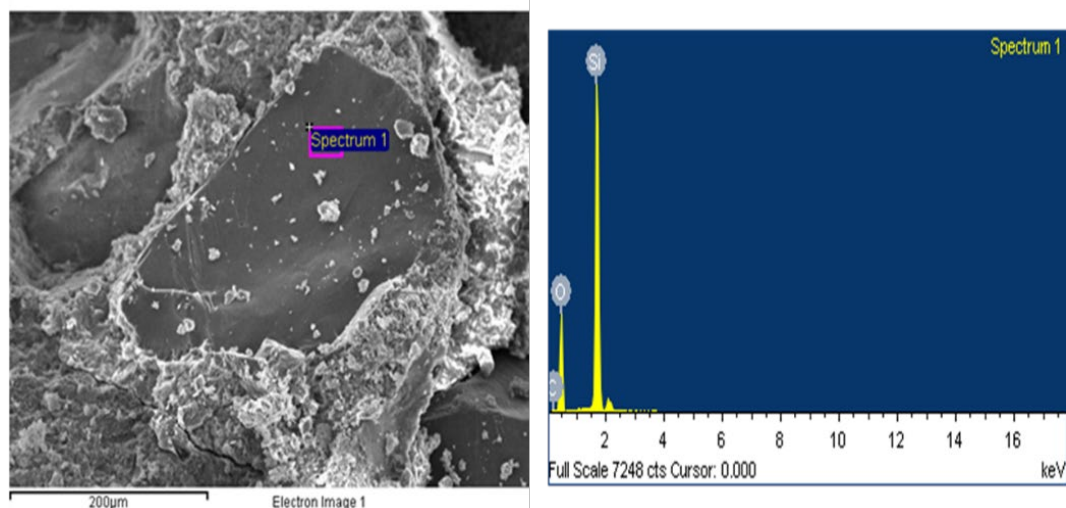


Figure 4.17. SEM analysis of mix III-50/L

The Spanish Structural Concrete Code, EHE-08 (2010) [49], and Eurocode 2 (EC-2) [31] likewise define lightweight concrete as concrete with a density between 1.2 and 2.0 Mg/m³ and a minimum compressive strength of 25 MPa. Mixes I-100/L and III-100/R fulfilled these requirements, and could be treated as lightweight concretes, highlighting a potential field of application for RCA [50].

5. RESULTS AND DISCUSSION: CARBON FOOTPRINT

The calculation of the carbon footprint of the mixes was limited to the contributions of the different raw materials used in their manufacture. The production and transport of concrete can be considered similar in all mixes. Therefore, these factors were omitted, as they are irrelevant for a comparative analysis of the carbon footprint [51]. Table 4.11 shows the carbon footprint of the raw materials of the SCC mixes under study, which were obtained through a life cycle assessment performed by Yang *et al.* (2015) [52] for the binders, admixtures, and water, Rebello *et al.* (2015) [45] for the aggregate powders, and Hossain *et al.* (2016) [53] for the NA and RCA.

Table 4.11. Carbon footprint of raw materials

Material	Carbon footprint (kg CO ₂ eq/kg)	References considered
CEM I	0.9310	[52]
GGBFS	0.0265	
Water	0.0002	
Admixtures	0.0005	
Ultra-fine limestone powder	0.0157	[45]
Limestone fines 0/0.5 mm	0.0069	
RCA 0/0.5 mm	0.0033	
Coarse NA 4/12.5 mm	0.0075	[53]
Coarse RCA 4/12.5 mm	0.0030	
Siliceous sand 0/4 mm	0.0026	
Fine RCA 0/4 mm	0.0011	

The carbon footprints (fourth column of Table 4.12) were calculated from the mix design (section 2.2) and the data in Table 4.11. These values show that the use of coarse RCA reduced the carbon footprint by 0.93%, while the decrease due to fine RCA was only 0.50-0.60%. In contrast, neither the addition of limestone fines 0/0.5 mm nor RCA 0/0.5 mm in substitution of ultra-fine limestone powder notably reduced the carbon footprint, because those additions also required higher amounts of aggregate powder to be added to the mix. Nevertheless, the high GGBFS content of

CEM III/A reduced the carbon footprint by 19.5%, thereby increasing the sustainability of SCC more than any other alternative material.

6. GLOBAL OVERVIEW

Table 4.12 summarizes the most relevant aspects of the mixtures. As indicated in previous sections, the best temporal conservation was obtained in mixes produced with CEM I, although they had lower compressive strengths and higher carbon footprints. The use of up to 50% fine RCA yielded adequate results, while limestone fines 0/0.5 mm were the aggregate powder with the best performance. These three criteria (loss of flowability, compressive strength, and carbon footprint), all with the same weight, were used to determine the best mix through a multi-criteria analysis. The TOPSIS (Technique for Order Preference by Similarity to Ideal Solution) algorithm was chosen because it is often used for these sorts of problems. Rashid et al. (2020) [54] described its implementation process in their study. Mixes III-0/L and III-50/L had the best ranking according to this analysis (Table 4.12), which demonstrates the suitability of GGBFS and 50% fine RCA to produce sustainable highly SCC.

Table 4.12. Global overview of SCC mixes. Choice of the best mix

Mix	Loss of flowability (slump flow) at 60 min (%)	Compressive strength ¹ (MPa)	Carbon footprint ² (kg CO ₂ eq/m ³)	Ranking according to TOPSIS algorithm
I-0/F	- 19.9	50.5 ± 1.9	286.4 (-0.93)	5
I-50/F	- 20.4	46.3 ± 1.2	285.5 (-1.23)	7
I-100/F	- 20.8	32.3 ± 3.6	284.6 (-1.53)	11
III-0/F	- 26.1	55.1 ± 3.2	230.0 (-20.43)	6
III-50/F	- 29.9	47.7 ± 3.8	229.1 (-20.73)	9
III-100/F	- 32.5	37.1 ± 2.3	228.3 (-21.03)	16
I-0/L	- 13.1	53.0 ± 2.4	285.7 (-1.17)	3
I-50/L	- 15.9	50.5 ± 1.6	285.0 (-1.42)	4
I-100/L	- 22.7	34.0 ± 2.3	284.2 (-1.68)	13
III-0/L	- 21.3	62.0 ± 1.2	229.3 (-20.67)	1
III-50/L	- 25.7	59.8 ± 3.1	228.6 (-20.92)	2
III-100/L	- 31.2	43.9 ± 1.6	227.8 (-21.19)	12
I-0/R	- 22.0	42.3 ± 2.4	284.4 (-1.62)	8
I-50/R	-25.8	34.5 ± 0.7	283.7 (-1.87)	14
I-100/R	- 29.5	19.0 ± 4.0	282.9 (-2.13)	18
III-0/R	- 30.0	45.9 ± 2.9	228.0 (-21.12)	10
III-50/R	- 33.5	39.6 ± 2.2	227.3 (-21.38)	15
III-100/R	- 37.3	31.8 ± 3.5	226.5 (-21.64)	17

¹ Mean value and standard deviation

² The percentage decreases of the carbon footprint regarding conventional highly SCC (CEM I, 100% NA, and ultra-fine limestone powder) are shown in brackets

7. CONCLUSIONS

The effect of the simultaneous addition of different types of waste on the temporal flowability of Self-Compacting Concrete (SCC) has been evaluated in this paper. More specifically, the use of Ground Granulated Blast Furnace Slag (GGBFS) and large amounts of both coarse and fine Recycled Concrete Aggregate (RCA), as well as different types of aggregate powder have all been analyzed. Through 18 SCC mixtures with different composition, it has been demonstrated that if the mix design is adapted to the particular characteristics of the components of the SCC, a sustainable SCC may be obtained with a high initial flowability, an SF3 slump-flow class [12], and at least an SF1

slump-flow class 60 minutes after the end of the mixing process. Nevertheless, other relevant conclusions can be drawn from the aspects addressed in the article:

- Both GGBFS and fine RCA improved the filling ability at the initial moment, although hindered its temporal conservation. The use of limestone fines 0/0.5 mm allowed obtaining SCC with a better performance in the fresh state over time than conventional ultra-fine limestone powder.
- A statistical adjustment based on the aggregates' water absorption (coarse, fine, and aggregate powder) allowed accurately predicting the temporal decrease of flowability of SCC. This statistical analysis also showed that this temporal conservation depended on the rheology of the cement, and the interaction between the type of cement and the aggregate added to the mix. An optimal hydration of the RCA during the mixing process led this waste not to condition the slump flow of SCC.
- The effect of the different components on the flow of SCC depended on the type of flow imposed. In free-fall flow (V-funnel test), the addition of fine RCA and aggregate powder of larger particle sizes favored a segregated and discontinuous flow. On the other hand, in horizontal flow (L-box test), the increase in the fines content following the addition of fine RCA to SCC mixes improved their passing ability. The lower coarse aggregate content of CEM III mixtures improved both properties. Regardless of the mix composition, the temporal conservation of viscosity and passing ability was poor.
- The addition of any RCA fraction increased the air content of the mixtures. An increase in the flowability of the mix without increasing its admixture or water content allowed reducing this increase of air content, although it caused a higher decrease of density from the fresh to the hardened state.

Overall, the mixes with CEM III/A, 100% coarse RCA, 50% fine RCA, and limestone fines 0/0.5 mm demonstrated the best global behavior (flowability, compressive strength, and carbon footprint) according to the multi-criteria analysis. These results have underlined the feasibility of using these components to produce SCC that can be placed on site up to 60 minutes after the mixing process, which represents a significant advance for the use of recycled aggregate SCC. Nevertheless, further detailed study of their mechanical and thermal behavior in the hardened state is still required to guarantee its successful use.

REFERENCES

- [1] ERMCO, Ready-mixed concrete industry statistics, European Ready-Mixed Concrete Organization (2019).
- [2] R. Maddalena, J.J. Roberts, A. Hamilton, Can Portland cement be replaced by low-carbon alternative materials? A study on the thermal properties and carbon emissions of innovative cements, *J. Clean. Prod.* 186 (2018) 933-942.
- [3] ANEFA, Sectorial economic progress reports (in Spanish) (2019).
- [4] M.M.A. Elahi, M.M. Hossain, M.R. Karim, M.F.M. Zain, C. Shearer, A review on alkali-activated binders: Materials composition and fresh properties of concrete, *Constr. Build. Mater.* 260 (2020) 119788.
- [5] N. Gupta, R. Siddique, R. Belarbi, Sustainable and Greener Self-Compacting Concrete incorporating Industrial By-Products: A Review, *J. Clean. Prod.* (2020) 124803.
- [6] N.H. Roslan, M. Ismail, N.H.A. Khalid, B. Muhammad, Properties of concrete containing electric arc furnace steel slag and steel sludge, *J. Build. Eng.* 28 (2020) 101060.
- [7] A. Gonzalez-Corominas, M. Etxeberria, C.S. Poon, Influence of the Quality of Recycled Aggregates on the Mechanical and Durability Properties of High Performance Concrete, *Waste Biomass Valor.* 8 (5) (2017) 1421-1432.
- [8] A.R. Khan, S. Fareed, M.S. Khan, Use of recycled concrete aggregates in structural concrete, *Sustain. Constr. Mater. Technol.* 2 (2019).

- [9] Eurostat, Waste statistics (2019).
- [10] M. Ouchi, M. Hibino, T. Sugamata, H. Okamura, Quantitative evaluation method for the effect of superplasticizer in self-compacting concrete, *Trans. Jpn. Concr. Inst.* 22 (2000) 15-20.
- [11] F. Huang, H. Li, Z. Yi, Z. Wang, Y. Xie, The rheological properties of self-compacting concrete containing superplasticizer and air-entraining agent, *Constr. Build. Mater.* 166 (2018) 833-838.
- [12] EFNARC, Specification Guidelines for Self-compacting Concrete, European Federation of National Associations Representing producers and applicators of specialist building products for Concrete (2002).
- [13] S.A. Santos, P.R. da Silva, J. de Brito, Self-compacting concrete with recycled aggregates – A literature review, *J. Build. Eng.* 22 (2019) 349-371.
- [14] M.E. Parron-Rubio, F. Perez-García, A. Gonzalez-Herrera, M.D. Rubio-Cintas, Concrete properties comparison when substituting a 25% cement with slag from different provenances, *Materials* 11 (6) (2018) 1029.
- [15] EN-Euronorm, Rue de stassart, 36. Belgium-1050 Brussels, European Committee for Standardization.
- [16] J. Pacheco, R.B. Polder, Critical chloride concentrations in reinforced concrete specimens with ordinary Portland and blast furnace slag cement, *Heron* 61 (2) (2016) 99-119.
- [17] Y.J. Du, J. Wu, Y.L. Bo, N.J. Jiang, Effects of acid rain on physical, mechanical and chemical properties of GGBS–MgO-solidified/stabilized Pb-contaminated clayey soil, *Acta Geotech.* 15 (4) (2020) 923-932.
- [18] H.L. Wu, F. Jin, Y.L. Bo, Y.J. Du, J.X. Zheng, Leaching and microstructural properties of lead contaminated kaolin stabilized by GGBS–MgO in semi-dynamic leaching tests, *Constr. Build. Mater.* 172 (2018) 626-634.
- [19] Z. Abdollahnejad, T. Luukkonen, M. Mastali, C. Giosue, O. Favoni, M.L. Ruello, P. Kinnunen, M. Illikainen, Microstructural Analysis and Strength Development of One-Part Alkali-Activated Slag/Ceramic Binders Under Different Curing Regimes, *Waste Biomass Valoris.* 11 (6) (2020) 3081-3096.
- [20] A.S. Reddy, P.R. Kumar, P.A. Raj, Development of Sustainable Performance Index (SPI) for Self-Compacting Concretes, *J. Build. Eng.* 27 (2020) 100974.
- [21] F. Fiol, C. Thomas, C. Muñoz, V. Ortega-López, J.M. Manso, The influence of recycled aggregates from precast elements on the mechanical properties of structural self-compacting concrete, *Constr. Build. Mater.* 182 (2018) 309-323.
- [22] J. Sainz-Aja, I. Carrascal, J.A. Polanco, C. Thomas, I. Sosa, J. Casado, S. Diego, Self-compacting recycled aggregate concrete using out-of-service railway superstructure wastes, *J. Clean. Prod.* 230 (2019) 945-955.
- [23] Á. Salesa, J.Á. Pérez-Benedicto, L.M. Esteban, R. Vicente-Vas, M. Orna-Carmona, Physico-mechanical properties of multi-recycled self-compacting concrete prepared with precast concrete rejects, *Constr. Build. Mater.* 153 (2017) 364-373.
- [24] I. González-Taboada, B. González-Fonteboa, J. Eiras-López, G. Rojo-López, Tools for the study of self-compacting recycled concrete fresh behaviour: Workability and rheology, *J. Clean. Prod.* 156 (2017) 1-18.
- [25] D. Carro-López, B. González-Fonteboa, J. De Brito, F. Martínez-Abella, I. González-Taboada, P. Silva, Study of the rheology of self-compacting concrete with fine recycled concrete aggregates, *Constr. Build. Mater.* 96 (2015) 491-501.
- [26] E. Güneş, M. Gesoğlu, Z. Algin, H. Yazici, Effect of surface treatment methods on the properties of self-compacting concrete with recycled aggregates, *Constr. Build. Mater.* 64 (2014) 172-183.
- [27] V. Revilla-Cuesta, M. Skaf, F. Faleschini, J.M. Manso, V. Ortega-López, Self-compacting concrete manufactured with recycled concrete aggregate: An overview, *J. Clean. Prod.* 262 (2020) 121362.
- [28] R.V. Silva, J. De Brito, R.K. Dhir, The influence of the use of recycled aggregates on the compressive strength of concrete: A review, *Eur. J. Environ. Civ. Eng.* 19 (7) (2015) 825-849.

- [29] V. Revilla-Cuesta, V. Ortega-López, M. Skaf, J.M. Manso, Effect of fine recycled concrete aggregate on the mechanical behavior of self-compacting concrete, *Constr. Build. Mater.* 263 (2020) 120671.
- [30] A. Santamaría, V. Ortega-López, M. Skaf, J.A. Chica, J.M. Manso, The study of properties and behavior of self compacting concrete containing Electric Arc Furnace Slag (EAFS) as aggregate, *Ain Shams Eng. J.* 11 (1) (2020) 231-243.
- [31] EC-2, Eurocode 2: Design of concrete structures. Part 1-1: General rules and rules for buildings, CEN (European Committee for Standardization) (2010).
- [32] S.A. Santos, P.R. da Silva, J. de Brito, Durability evaluation of self-compacting concrete with recycled aggregates from the precast industry, *Mag. Concr. Res.* 71 (24) (2019) 1265-1282.
- [33] J. Dai, Q. Wang, C. Xie, Y. Xue, Y. Duan, X. Cui, The effect of fineness on the hydration activity index of ground granulated blast furnace slag, *Materials* 12 (18) (2019) 2984.
- [34] A. Santamaría, J.J. González, M.M. Losañez, M. Skaf, V. Ortega-López, The design of self-compacting structural mortar containing steelmaking slags as aggregate, *Cem. Concr. Compos.* 111 (2020) 103627.
- [35] V. Revilla-Cuesta, M. Skaf, J.A. Chica, J.A. Fuente-Alonso, V. Ortega-López, Thermal deformability of recycled self-compacting concrete under cyclical temperature variations, *Mater. Lett.* 278 (2020) 128417.
- [36] I. González-Taboada, B. González-Fonteboa, F. Martínez-Abella, S. Seara-Paz, Analysis of rheological behaviour of self-compacting concrete made with recycled aggregates, *Constr. Build. Mater.* 157 (2017) 18-25.
- [37] S. Pan, D. Chen, X. Chen, G. Ge, D. Su, C. Liu, Experimental study on the workability and stability of steel slag self-compacting concrete, *Appl. Sci.* 10 (4) (2020) 1291.
- [38] H. Salehi, M. Mazloom, Opposite effects of ground granulated blast-furnace slag and silica fume on the fracture behavior of self-compacting lightweight concrete, *Constr. Build. Mater.* 222 (2019) 622-632.
- [39] B. Cantero, I.F. Sáez del Bosque, A. Matías, M.I. Sánchez de Rojas, C. Medina, Inclusion of construction and demolition waste as a coarse aggregate and a cement addition in structural concrete design, *Arch. Civ. Mech. Eng.* 19 (4) (2019) 1338-1352.
- [40] R.V. Silva, J. de Brito, R.K. Dhir, Fresh-state performance of recycled aggregate concrete: A review, *Constr. Build. Mater.* 178 (2018) 19-31.
- [41] W. Zuo, W. She, W. Li, P. Wang, Q. Tian, W. Xu, Effects of fineness and substitution ratio of limestone powder on yield stress of cement suspensions, *Mater. Struct.* 52 (4) (2019) 74.
- [42] A. Santamaría, A. Orbe, M.M. Losañez, M. Skaf, V. Ortega-Lopez, J.J. González, Self-compacting concrete incorporating electric arc-furnace steelmaking slag as aggregate, *Mater. Des.* 115 (2017) 179-193.
- [43] P. Danish, G. Mohan Ganesh, Study on self compacting concrete: A state-of-art-of-review, *Int. J. Appl. Eng. Res.* 10 (93 Special issue) (2015) 74-78.
- [44] P. Matar, J. Barhoun, Effects of waterproofing admixture on the compressive strength and permeability of recycled aggregate concrete, *J. Build. Eng.* 32 (2020) 101521.
- [45] T.A. Rebello, R. Zulcão, J.L. Calmon, R.F. Gonçalves, Comparative life cycle assessment of ornamental stone processing waste recycling, sand, clay and limestone filler, *Waste Manage. Res.* 37 (2) (2019) 186-195.
- [46] A. Gonzalez-Corominas, M. Etxeberria, Effects of using recycled concrete aggregates on the shrinkage of high performance concrete, *Constr. Build. Mater.* 115 (2016) 32-41.
- [47] K.H. Yang, Y.H. Hwang, Y. Lee, J.H. Mun, Feasibility test and evaluation models to develop sustainable insulation concrete using foam and bottom ash aggregates, *Constr. Build. Mater.* 225 (2019) 620-632.
- [48] B.M. Vinay Kumar, H. Ananthan, K.V.A. Balaji, Experimental studies on utilization of coarse and finer fractions of recycled concrete aggregates in self compacting concrete mixes, *J. Build. Eng.* 9 (2017) 100-108.

- [49] EHE-08, Structural Concrete Regulations (in Spanish), Ministerio de Fomento, Gobierno de España (2010).
- [50] A. Wongsas, A. Siriwattanakarn, P. Nuaklong, V. Sata, P. Sukontasukkul, P. Chindaprasirt, Use of recycled aggregates in pressed fly ash geopolymer concrete, *Environ. Prog. Sustainable Energy* 39 (2) (2020) e13327.
- [51] W. Song, J. Yi, H. Wu, X. He, Q. Song, J. Yin, Effect of carbon fiber on mechanical properties and dimensional stability of concrete incorporated with granulated-blast furnace slag, *J. Clean. Prod.* 238 (2019) 117819.
- [52] K.H. Yang, Y.B. Jung, M.S. Cho, S.H. Tae, Effect of supplementary cementitious materials on reduction of CO₂ emissions from concrete, *J. Clean. Prod.* 103 (2015) 774-783.
- [53] M.U. Hossain, C.S. Poon, I.M.C. Lo, J.C.P. Cheng, Comparative environmental evaluation of aggregate production from recycled waste materials and virgin sources by LCA, *Resour. Conserv. Recycl.* 109 (2016) 67-77.
- [54] K. Rashid, M.U. Rehman, J. de Brito, H. Ghafoor, Multi-criteria optimization of recycled aggregate concrete mixes, *J. Clean. Prod.* 276 (2020) 124316.

Article 5

Models for compressive strength estimation through non-destructive testing of highly self-compacting concrete containing recycled concrete aggregate and slag-based binder

Title: Models for compressive strength estimation through non-destructive testing of highly self-compacting concrete containing recycled concrete aggregate and slag-based binder

Authors: Víctor Revilla-Cuesta, Marta Skaf, Roberto Serrano-López, Vanesa Ortega-López

Journal: Construction and Building Materials

Year: 2021

Volume: 280

Article number: 122454

DOI: <https://doi.org/10.1016/j.conbuildmat.2021.122454>

Journal classification (2019 JCR ranking data): 11/134 (engineering, civil). First quartile (Q1), first decile (D1)

ABSTRACT

Indirect estimation of compressive strength through non-destructive testing is key to monitoring the strength of structural concretes used in construction and rehabilitation works. However, no models are available to perform this estimation in highly Self-Compacting Concrete (SCC) with Recycled Concrete Aggregate (RCA). To fill this gap, two indirect measures were tested in this paper, the hammer rebound index and Ultrasonic Pulse Velocity (UPV), to predict the compressive strength of highly SCC. To do so, 24 SCC mixes were developed with different aggregate powders, binders, such as Ground Granulated Blast Furnace Slag (GGBFS), and contents of fine RCA. Compressive strength, and both indirect measures of all mixtures were determined at 1, 7, 28, and 90 days. The development of specific models for highly SCC responded to the inappropriateness of conventional models that are not adapted to its high fines content. Modelling as a function of either UPV or the hammer rebound index yielded accurate predictions, although the UPV model proved more sensitive to compositional changes and presented higher uncertainty. The best predictions were modelled by combining both indirect measures. The models provided safe and accurate indirect estimations of the compressive strength of high flowability SCC in real structures.

Keywords: compressive strength; ground granulated blast furnace slag; hammer rebound index; non-destructive testing; recycled concrete aggregate; self-compacting concrete; structural health monitoring; ultrasonic pulse velocity.

1. INTRODUCTION

Traditionally, non-destructive tests have been used to estimate the compressive strength of concrete [1] in rehabilitation works [2], and for the estimation and monitoring of concrete strength during construction and throughout the lifecycle of the structure [3]. The oldest and the most common methods are the so-called indirect measures: the hammer rebound index, which is based on the surface hardness of the concrete [4], and Ultrasonic Pulse Velocity (UPV) analysis, which depends on the microstructure of the material [5]. Although the use of such semi-destructive methods as penetration resistance [6] and core tests [7] are increasingly widespread,

indirect measures are still very useful on site, due to their greater simplicity and quicker execution.

The hammer rebound index test was developed in the 1940s and has been widely used ever since, because of its low cost and ease of use [8]. This test only requires a Schmidt rebound hammer, whose operation is shown in Figure 5.1 [9]. When the hammer is moved towards the plunger, which has been previously placed in contact with a concrete surface, preferably at a right angle, a spring attached to the plunger is simultaneously tensed. The energy of the spring is released at the end of the plunger and a calibrated weight is pushed upwards. The distance this mass is displaced, dependent upon the recoil energy of the spring, represents the hammer rebound index value [10]. The validity of this method for the estimation of compressive strength was first demonstrated over half a century ago [11]. Nevertheless it has since been noted that its results will depend on the aggregate properties [4] and their natural source [12], so that its validation will therefore be dependent on statistical models [1].

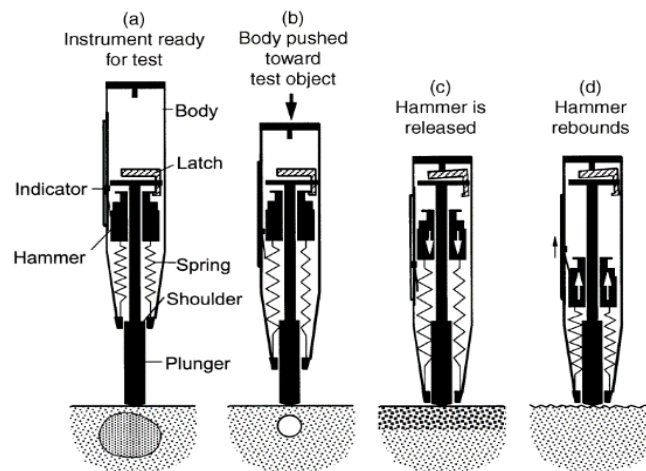


Figure 5.1. Operation of the Schmidt rebound hammer [9]

UPV analysis also emerged in the 1950s [13], although its main advances occurred at the end of the century [14]. UPV is measured by an ultrasonic device, which determines the time (μs) that an ultrasonic signal at a frequency of 1 kHz takes to reach the receiving transducer, from the transmitting transducer [15]. The direct method of performing this measurement is the most common, in which the two transducers are positioned opposite each other (Figure 5.2). Both the propagation of internal damage within concrete [16], and its porosity [17] can be evaluated with the UPV test. In addition, it is highly conditioned by the stiffness of the material, so it correlates with the compressive strength and the modulus of elasticity of the concrete [18]. The statistical adjustment of the model is also essential for accurate and safe use [5].

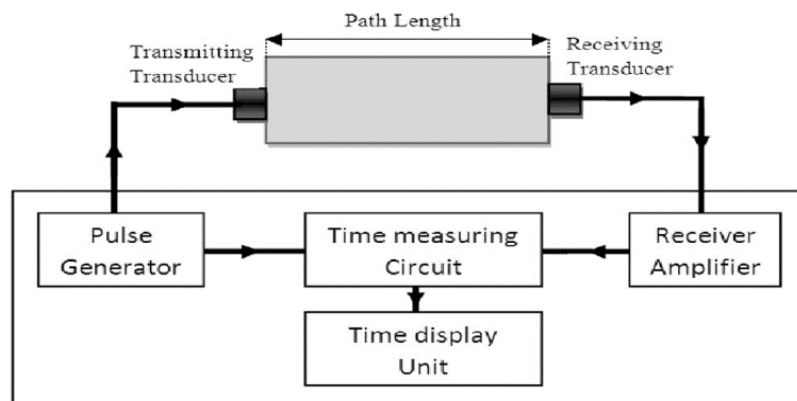


Figure 5.2. UPV device set up for direct measurements [15]

Even though these indirect measures have long been employed, their progress in relation to their use and application in construction has been remarkable since 2000 [19]. Some new trends in this field include their successful use at evaluating the compressive strength of concrete at early ages [20, 21], to study the spatial variability of concrete strength [22, 23], especially in beams [24], and high-precision detection of micro-cracking within the damaged concrete [2, 25], especially with UPV analysis [26]. In addition, there is also a field of research regarding their applicability in concretes made with alternative materials [27, 28], and in non-conventional concretes, such as high performance fiber-reinforced concrete [29] and Self-Compacting Concrete (SCC) [30].

Among the new trends in concretes with special applications, SCC is perhaps the most prominent nowadays [31], due to its high flowability in the fresh state, which facilitates placement without vibration [32]. On the other hand, the use of wastes for the production of concrete, including SCC [33], has also been increasing over recent years, as a sustainability improvement strategy within the construction sector [34]. Among the different residues that can be recovered as aggregate for concrete production, such as bricks [35], siderurgic slags [36], and construction and demolition waste [37], Recycled Concrete Aggregate (RCA) stands out [38], due to its mechanical properties [39].

The results of the literature [40], backed up by our own past experience [41], have confirmed that the use of coarse RCA, compared to fine RCA, results in a lesser decrease in the compressive strength of concrete. The few studies on the non-destructive testing of concretes containing RCA have therefore generally been focused on the validity of concrete manufactured with only coarse RCA. In this regard, a relevant conclusion is that the addition of coarse RCA alters the standard benchmarking of indirect measurements and their relationships with compressive strength [42, 43]. Nevertheless, they have successfully predicted the behavior of the concrete manufactured with this waste even at 1 day [21], despite the fact that the addition of RCA sometimes delays the development of concrete strength [41]. Finally, it has also been stated that the joint use of two non-destructive methods provides greater security for the estimation of the strength of concrete containing coarse RCA [44], due to the variability of the properties of this recycled aggregate [45]. It is especially significant that the validation of non-destructive testing in concrete manufactured with fine RCA is practically non-existent, as the nature of the finest aggregate fractions affects the accuracy of the concrete strength estimation through indirect measurements [43]. One study concluded that the UPV values were lower when the fine fraction of RCA was used, compared to concrete manufactured with natural aggregates [46], and another one found that linear equations were suitable to predict the compressive strength [47], although it was not checked whether other models provided a more precise fit.

SCC is characterized by a large content of fines and water [48] and therefore a large proportion of cement paste [32] to achieve proper flowability. The accuracy of non-destructive testing in this particular material, has been demonstrated in some studies [30, 47]. Their main conclusion was that the pre-established ratios between compressive strength and the indirect measures, suitable for conventional concretes, were not applicable. Despite that conclusion, no precise general relationships have up until now been established between indirect measurements and the compressive strength of SCC.

As observed above, the validity of the indirect measures on SCC containing RCA has many shortcomings, especially when used in the fine fraction, which has a particular impact in the case of the SCC. The main objective of this research work is to establish whether the compressive strength of SCC containing high amounts of both coarse and fine RCA can be accurately estimated by both the hammer rebound index and UPV analysis. Moreover, among the various possible SCC flowabilities, an SF3 slump-flow class [49] (very high flowability) was chosen, due to its extreme proportion of fines and powder compared to vibrated concrete [50], which can to a greater extent alter the validity of indirect measures to predict compressive strength.

Furthermore, this research is part of a larger project for the evaluation of different aspects of recycled self-compacting concretes (100% coarse RCA), and it is linked to other novel aspects such as the effect of the addition of alternative binders, in this case Ground Granulated Blast Furnace Slag (GGBFS), and different types of aggregate powder. In the present paper, this aspect is leveraged, to test the consistency of the indirect measures regardless of any change in the composition of the SCC mixtures.

The final purpose of this paper is to develop models that can be used to estimate the compressive strength of SCC containing RCA with similar levels of reliability to conventional concrete, so that the strength monitoring by non-destructive testing of this material is possible in any structure. In doing so, the authors aim to promote the actual use of SCC containing RCA.

The compressive strength, the hammer rebound index, and the UPV of 24 SCC mixtures were determined at 1, 7, 28, and 90 days for the evaluation and the analysis of all the aspects addressed above, in order to analyze all the aspects addressed. These mixes were manufactured with 100% coarse RCA, and 0%, 50%, or 100% fine RCA, as well as two different types of cement (CEM I and CEM III/A, this last one with around 45% of GGBFS) and four different types of aggregate powder (limestone filler, two sizes of limestone fines, and RCA).

1.1. NOVELTY OF THE STUDY

In view of the above discussion throughout the introduction, this study presents the following novelties:

- Firstly, it demonstrates the validity of indirect measures (hammer rebound index and UPV) to estimate the compressive strength of SF3 class SCC. This type of concrete, with a highly particular mix design, has never before been subjected to this type of analysis.
- Secondly, it evaluates the effect of several combinations of fine RCA content, type of binder, and aggregate powder in the relationship between compressive strength and indirect measures in highly SCC. These components are of immense importance in the behavior of SCC, due to its high content of fine particles, and therefore condition the validity of the indirect measurements. Studies on SF2 class SCC have to date only focused on coarse RCA content.
- Finally, this study is the first one that provides suitable models to estimate the compressive strength of SCC through non-destructive testing regardless of its composition.

2. MATERIALS AND METHODS

The raw materials and the experimental procedure used to obtain the results are detailed in this section, before moving on to the presentation of the experimental results.

2.1. MATERIALS

The main characteristics of the raw materials (cement, aggregates, admixtures, and water) used for the manufacture of SCC are set out below.

2.1.1. CEMENT, WATER, AND ADMIXTURES

Both CEM I 52.5 R (density 3.12 Mg/m³) and CEM III/A 42.5 N (density 3 Mg/m³), from among the various cement types specified in standard EN 197-1 [51], were used. The main difference between them was the presence of Ground Granulated Blast Furnace Slag (GGBFS) in the CEM III/A (content around 45%). Water was used from the mains water supply of Burgos, northwestern Spain, where the experiment was performed. Two admixtures were used to optimize the SCC: a

viscosity regulator, referred to here as "Adx1", that retains long-term flowability, and a plasticizer water reducer, "Adx2".

2.1.2. NATURAL AND RECYCLED AGGREGATES

The SCCs developed in this study contained high volumes of RCA: 100% of the coarse fraction (4/12 mm) and 0%, 50%, or 100% of the fine fraction (0/4 mm). The RCA consisted of crushed precast concrete elements at a local waste treatment company, rejected due to aesthetic defects. Its average strength was 45 MPa. They were received in the laboratory with a continuous grain size of 0/31.5 mm, which was separated by sieving into three different fractions (0/4, 4/12.5, and 12.5/31.5 mm), the first two of which were used in this study. The fine aggregate content was completed by the addition of siliceous sand 0/4 mm, usually used for SCC production in the region.

Limestone filler is generally used as aggregate powder in the manufacture of SCC [45]. Nevertheless, in this study, four aggregate powders were compared in terms of their performance: limestone filler < 0.063 mm, commercial limestone fines 0/1 mm, limestone fines 0/0.5 mm, and RCA 0/0.5 mm. The last two materials were graded by sieving limestone fines 0/1 mm and RCA 0/4 mm, respectively.

Table 5.1. Density and water absorption of the aggregates

Aggregate	Saturated-Surface-Dry (SSD) Density (Mg/m ³)	15 min water absorption (%)	45 min water absorption (%)	24 h water absorption (%)
Coarse RCA 4/12.5 mm	2.42	5.33	5.65	6.25
Fine RCA 0/4 mm	2.37	6.18	6.74	7.36
Siliceous sand 0/4 mm	2.58	0.18	0.22	0.25
Limestone fines 0/1 mm	2.62	1.88	2.12	2.53
Limestone fines 0/0.5 mm	2.60	1.99	2.31	2.57
RCA 0/0.5 mm	2.31	6.82	7.34	7.95
Limestone filler < 0.063 mm	2.77	-	-	0.54

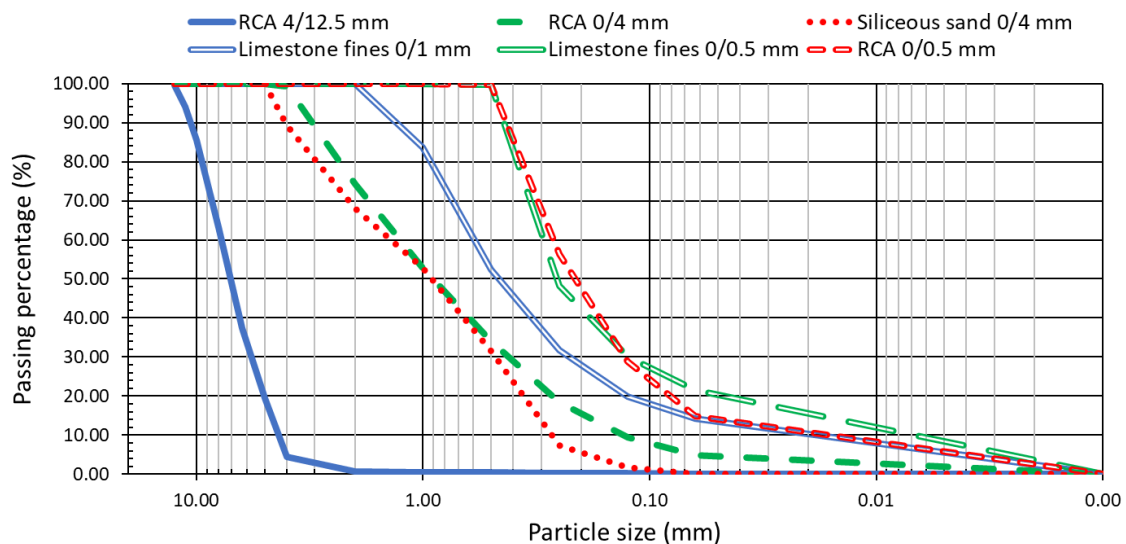


Figure 5.3. Aggregate size distribution

The density and water absorption of these aggregates, as per EN 1097-6 [51], are shown in Table 1. Two aspects of the test should be considered, regarding the determination of aggregate water absorption. Firstly, water absorption in 15 and 45 minutes was determined without prior drying of the aggregates in an oven, so the results could be assimilated to the water absorption of the

aggregate during mixing. Secondly, the fine RCA was continuously moved during the drying process to avoid the onset of setting during this test. From a comparison of the results, it can be observed that, as expected, RCA had a lower density and higher water absorption than NA [41]. Finally, the granulometry curves of all these aggregates are shown in Figure 5.3.

2.2. MIX DESIGN

A total of 24 different mixtures were prepared from combinations of the different types of cement, the aggregate powder, and the fine RCA percentages. All the aggregates were used under environmental conditions (they were stored in the laboratory throughout the study), to assimilate the mixing of the SCC to the most common method used in concrete plants [52]. An SF3 slump-flow class (maximum diameter between 750 and 850 mm) [49] in all mixtures was obtained with the following design criteria:

- First, the overall particle size, especially of the finest fractions (size less than 0.250 mm), was adjusted to the Fuller curve to reach self-compactability. This is shown in Figure 5.4 for mixtures made with CEM I and 50% fine RCA.
- The initial water content was defined according to EFNARC recommendations [49] and empirically adjusted in trial mixtures with 100% coarse RCA and 0% fine RCA before producing the final mixtures. An effective water-to cement ratio of 0.50 in mixes with CEM I and 0.40 in mixes with CEM III was established. These amounts of water were adjusted in each mix with fine RCA (0/4 mm and/or 0/0.5 mm) to maintain the effective water-to-cement ratio constant. To that end, the additional water incorporated in each mixture corresponded to the results of the water absorption test of the RCA in 15 minutes (see Table 1), which was the mixing time (see section 2.3).
- Furthermore, the coarse RCA was reduced in the mixtures with CEM III/A, to enhance flowability, as the highly ground fineness of CEM III/A hindered the drag force of the larger aggregate particles.

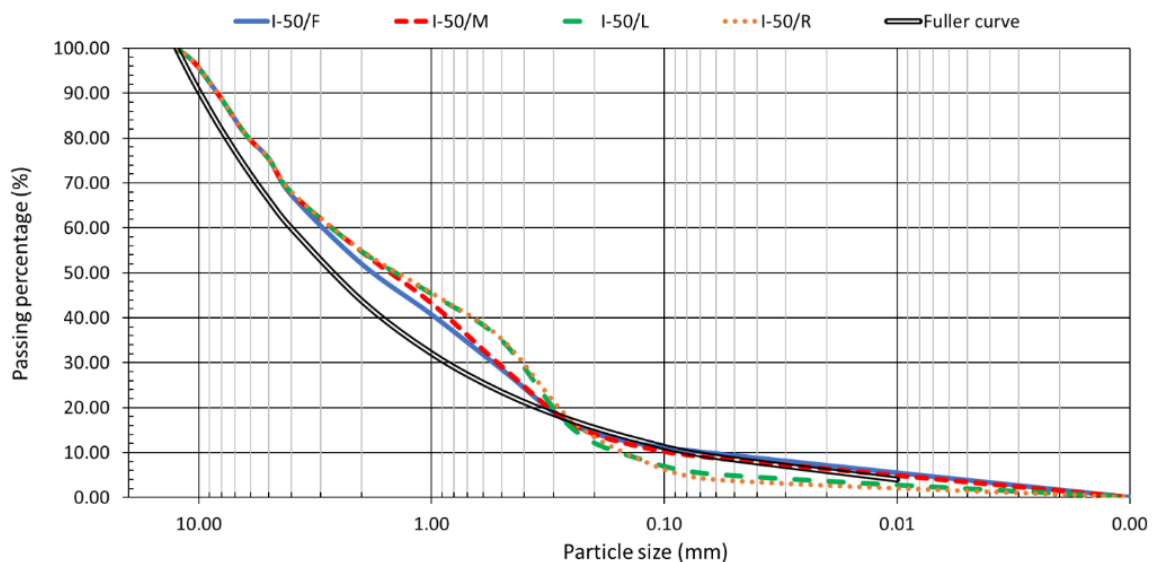


Figure 5.4. Joint granulometry of the mixes with 50% fine RCA and CEM I

All these aspects led to the development of the mix design that is shown in Table 5.2. The mixtures were labelled C-N/T, which means:

- *C* refers to the type of cement used: I (CEM I) or III (CEM III/A).
- *N* refers to the percentage of RCA 0/4 mm incorporated in the mixture: 0%, 50%, or 100%.

- *T* refers to the type of aggregate powder: F (limestone filler), M (mix of limestone filler and limestone fines 0/1 mm), L (limestone fines 0/0.5 mm), and R (RCA 0/0.5 mm). The use of only limestone fines 0/1 mm as aggregate powder was insufficient to reach an SF3 slump-flow class and had to be combined with limestone filler.

Table 5.2. Mix design (weights in kg)

Material	Mixtures with CEM I			Mixtures with CEM III/A		
CEM I	300			0		
CEM III/A	0			425		
RCA 4/12.5 mm	530			430		
Adx1	2.30					
Adx2	4.50					
	I-0/F	I-50/F	I-100/F	III-0/F	III-50/F	III-100/F
Limestone filler < 0.063 mm	180					
Water	185	210	235	185	210	235
RCA 0/4 mm	0	505	1010	0	505	1010
NA 0/4 mm	1100	550	0	1100	550	0
	I-0/M	I-50/M	I-100/M	III-0/M	III-50/M	III-100/M
Limestone filler < 0.063 mm	115					
Limestone fines 0/1 mm	225					
Water	185	210	235	185	210	235
RCA 0/4 mm	0	435	865	0	435	865
NA 0/4 mm	940	475	0	940	475	0
	I-0/L	I-50/L	I-100/L	III-0/L	III-50/L	III-100/L
Limestone fines 0/0.5 mm	335					
Water	185	210	235	185	210	235
RCA 0/4 mm	0	435	865	0	435	865
NA 0/4 mm	940	475	0	940	475	0
	I-0/R	I-50/R	I-100/R	III-0/R	III-50/R	III-100/R
RCA 0/0.5 mm	305					
Water	200	220	245	200	220	245
RCA 0/4 mm	0	435	865	0	435	865
NA 0/4 mm	940	475	0	940	475	0

2.3. EXPERIMENTAL PROCEDURE

Staged mixing processes are useful for maximizing both component hydration and, therefore, SCC flowability levels [53]. They are especially useful when aggregates with high water absorption are incorporated, such as fine RCA [54]. Hence, in this research, the components of the mixtures were added in three different stages during the mixing process. Each stage was followed by 3 minutes of mixing and 2 minutes of inactivity. These durations were determined after testing different mixing and inactivity times between 1 and 5 minutes, to maximize flowability [52]. The total duration of this mixing process was 15 minutes and the stages were as follows:

- Stage 1: addition of the aggregates (coarse RCA, siliceous sand and/or fine RCA, and aggregate powder) and half of the water.
- Stage 2: addition of cement and remaining water.
- Stage 3: addition of admixtures.

Having completed this process, the self-compactability over time of the mixes (initial class SF3) was checked with the slump-flow test at 0 and at 30 minutes, and 12 cubic 10x10x10-cm specimens were produced for each mixture.

The specimens were stored in a moist room (95±5% humidity and 20±2 °C temperature) to achieve optimum strength development. Three days before each age testing, the specimens were exposed to the laboratory environment (60±5% humidity and 20 ± 2 °C temperature), to obtain a completely dry concrete surface [2]. The real conditions of the structure when its compressive strength is indirectly estimated were thereby simulated [3].

The hammer rebound index, the UPV analysis, and the compressive strength of 3 test specimens were determined at 1, 7, 28, and 90 days. The results at each age and mix were obtained as the arithmetic mean of these values. The testing of all SCCs at four different ages meant that this study covered a wide range of strengths. The hardened density was also determined at 28 days.

The experimental plan and its link to the results, discussed in section 3, are shown in the flowchart of Figure 5.5.

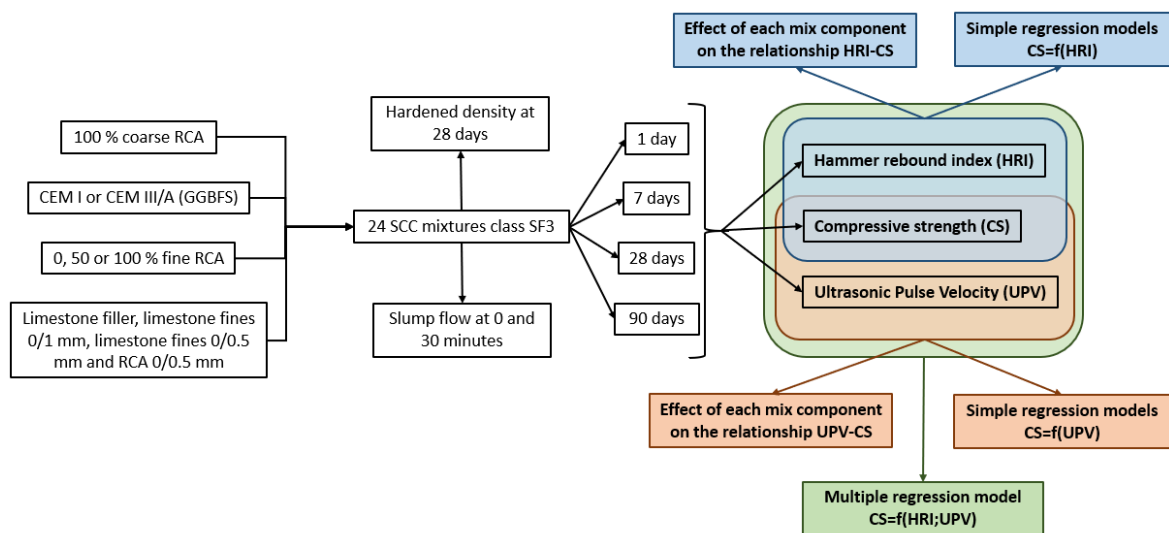


Figure 5.5. Flowchart of the study: experimental plan versus experimental results

2.4. RELATIONSHIP BETWEEN INDIRECT MEASUREMENTS AND COMPRESSIVE STRENGTH IN CONVENTIONAL CONCRETES

In this study, a Schmidt hammer type N was used for the measurement of the hammer rebound index. The compressive strength of the non-recycled vibrated concrete can be estimated from Table 5.3 [55] as a function of the rebound index obtained with this type of Schmidt hammer. The values within this table were obtained by statistical fitting of large data volumes, a fundamental aspect for the validity of these models [56], as stated in the introduction.

There is no one standard calibrated UPV model. However, the relationships shown below are generally established between the UPV and the compressive strength values [13], although the hammer rebound index is generally recommended to complement the UPV values [5].

- Low-strength concrete: 2.5-3.2 km/s.
- Medium-strength concrete: 3.2-3.7 km/s.
- High-strength concrete: 3.7-4.2 km/s.
- Very high-strength concrete: > 4.2 km/s.

Table 5.3. Estimation of compressive strength as a function of the hammer rebound index on cubic specimens in vibrated concrete manufactured with NA

Hammer rebound index	Concrete age: 7 days		Concrete age: > 7 days	
	W_m^1	W_{min}^2	W_m^1	W_{min}^2
20	9.9	5.3	11.9	7.3
21	11.1	6.3	12.9	8.1
22	12.4	7.4	14.2	9.2
23	13.6	8.4	15.4	10.2
24	14.9	9.6	16.6	11.3
25	16.3	10.8	18.0	12.5
26	17.7	12.0	19.2	13.5
27	19.1	13.2	20.6	14.7
28	20.6	14.6	22.1	16.1
29	22.1	16.0	23.4	17.4
30	23.6	17.5	24.9	18.7
31	25.2	18.9	26.4	20.1
32	26.9	20.5	28.0	21.6
33	28.5	22.1	29.4	23.0
34	30.1	23.5	30.9	24.3
35	31.8	25.1	32.5	25.8
36	33.5	26.8	34.1	27.4
37	35.3	28.4	35.8	28.9
38	37.0	30.1	37.4	30.5
39	38.7	31.8	39.0	32.1
40	40.5	33.4	40.8	33.7
41	42.4	35.2	42.6	35.4
42	44.1	37.0	44.2	37.1
43	46.0	38.7	46.1	38.8
44	47.9	40.6	47.9	40.6
45	49.7	42.4	49.7	42.4
46	51.6	44.2	51.6	44.2
47	53.5	46.1	53.5	46.1
48	55.4	48.0	55.4	48.0
49	57.3	49.8	57.3	49.8
50	59.2	51.7	59.2	51.7

¹ W_m : most likely compressive strength value (MPa)

² W_{min} : minimum expected compressive strength value (MPa)

3. RESULTS AND DISCUSSION

In this section the fresh performance of the SCCs designed are presented. Then, the results of compressive strength, the hammer rebound index, and UPV, as well as the relationships between these variables are analyzed.

3.1. IN-FRESH PERFORMANCE: SLUMP-FLOW TEST

The slump flow, EN 12350-8 [51], of each mix, obtained at 0 and at 30 minutes after the mixing process had ended, is shown in Figure 5.6 to an accuracy of ± 5 mm. As has been indicated in the mix design section, an SF3 slump-flow class [49] at 0 minutes was imposed as a design criterion. On the other hand, 30 minutes later, most of the mixes were of class SF2 (maximum diameter

between 650 and 750 mm), except for mixes I-50/R and I-100/R, which did not reach the value of 650 mm (slump-flow class SF1). The behavior of these two mixes was mainly due to the high water absorption of the RCA, which was used in these mixes as fine aggregate and aggregate powder

The three variables introduced in the composition of the mixtures (type of cement, fine RCA content, and nature of the aggregate powder) influenced the slump-flow evolution in a different way:

- In mixtures with CEM III/A, the lower coarse aggregate proportion (see section 2.2) eased the dragging of all the components of the mixture by the cement paste [57], which in turn led to a higher slump flow at both moments in time.
- The high fines proportion of the fine RCA, compared to siliceous sand, increased the initial slump flow. Nevertheless, the high water absorption worsened its temporary conservation, as other researchers had previously observed [54].
- In relation to the different types of aggregate powder, the use of limestone filler caused a higher initial slump flow (F-mixes). However, a lower temporal slump-flow loss was obtained with the use of limestone fines 0/0.5 mm (L-mixes). The high water absorption levels of the RCA filler (see Table 1) resulted in the worst behavior, obtained for the R-mixes, as has also been observed by other authors [58], regardless of the type of cement or the percentage of fine RCA. The pre-soaking of the RCA could have improved this behavior by reducing the water absorption of this waste after the mixing process [52].

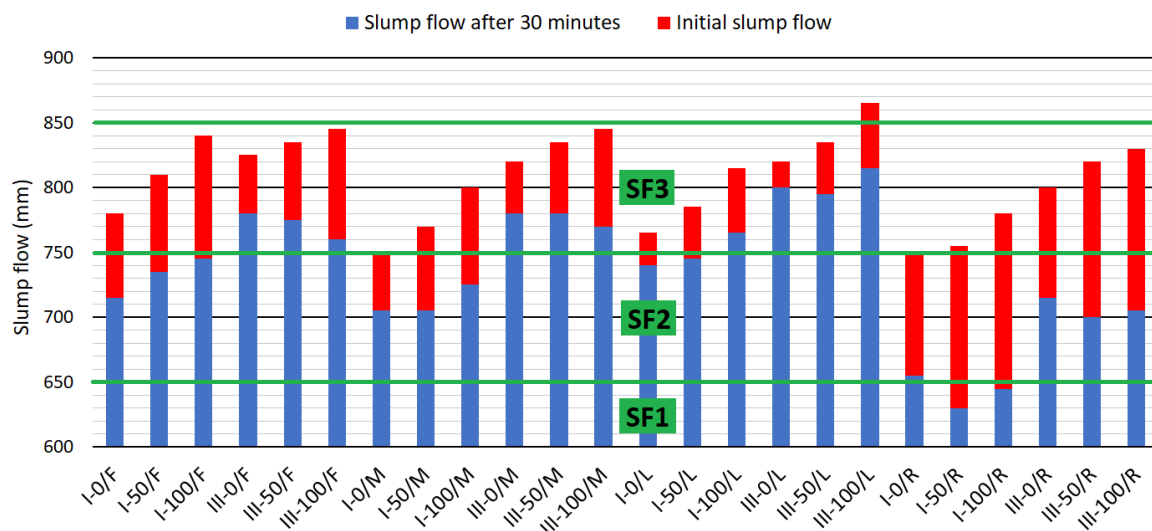


Figure 5.6. Slump flow 0 and 30 minutes after the end of the mixing process

The parameter t_{500} (time to reach a slump flow greater than 500 mm), also obtained in the slump-flow test, was used to evaluate the viscosity of the SCCs. In this study, these values were obtained to an accuracy of ± 0.2 s. As may be observed in Figure 5.7, all the concrete mixtures presented an initial viscosity of class VS2 (time to reach a slump flow of 500 mm higher than 2 s), although mixtures III-0/F and III-0/L were of class VS1 (values of 1.6 and 1.8 s, respectively). After 30 minutes, all mixtures were class VS2, clearly showing the effects of all the changes within the composition:

- CEM III/A, which incorporated GGBFS, reduced the initial viscosity. However, the mixes with CEM III/A had a greater temporal increase in viscosity than mixes with CEM I. This fact is due to the properties of GGBFS that usually hinder the temporary preservation of viscosity [59].

- The addition of fine RCA increased the viscosity both initially and at 30-minutes. Mixtures with 100% fine RCA were the most viscous. These observations are in line with the conclusions reached in studies on the effect of fine RCA on the temporal evolution of the rheology of the SCC [60].
- The aggregate powder influenced the viscosity of the mixtures in the same way as in the slump flow. Initially, the mixtures with limestone filler were the least viscous. However, due to the electrostatic charge that the limestone filler acquires during its manufacture [61], the smallest temporary increase in viscosity was in the L-mixes. According to this, the M-mixes showed an intermediate behavior. Finally, the irregular shape of the RCA filler [62] and its high water absorption [58] resulted in the highest initial viscosity and the largest temporary increase in the R-mixes.

These slump-flow and viscosity results show that a careful design of the mixture means that the concretes can achieve a high initial workability, even if RCA (in the coarse, fine, and powder fractions) and GGBFS are simultaneously used [63]. However, the addition of these by-products complicate the temporary conservation of SCC flowability levels [54, 64]. Moreover, their adverse effects appeared to increase when they were jointly used. From the results, it can be concluded that concrete mixtures with 50% fine RCA optimized their slump flow, and viscosity simultaneously, as well as their temporary conservation, regardless of the binder or the natural aggregate powder in use. These optimum amounts of RCA are in accordance with the results of other authors [33], whose recommendations were never to exceed an RCA content of 50% in the fine fraction when the whole coarse fraction is RCA [65].

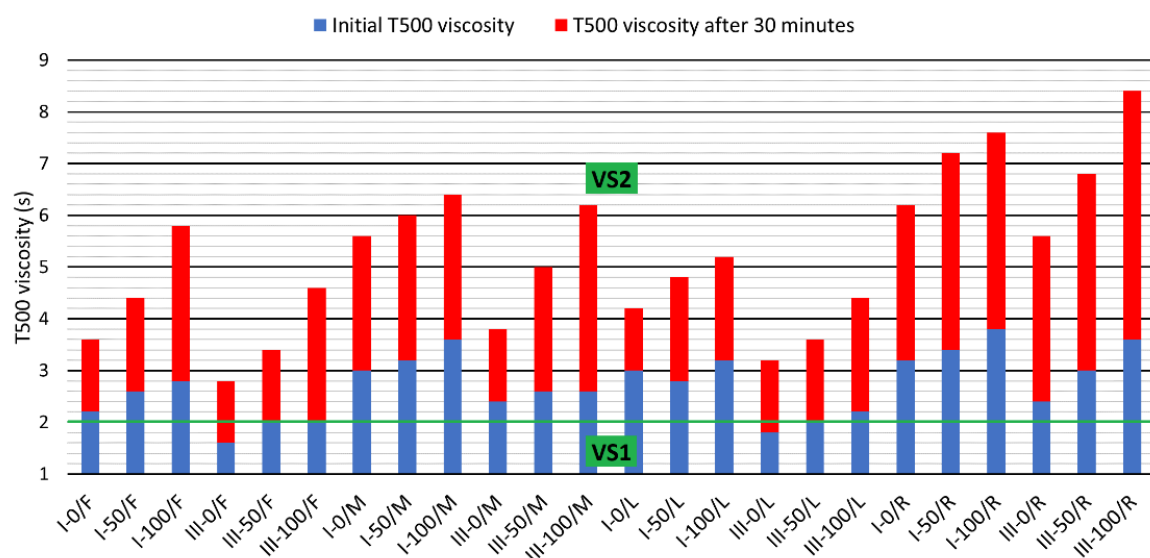


Figure 5.7. t_{500} Viscosity at 0 and at 30 minutes after the end of the mixing process

3.2. HARDENED DENSITY

The hardened density of each mix, determined according to EN 12390-7 [51], is shown in Table 5.4. These values showed the expected trends. Firstly, the hardened density of concrete was reduced when RCA, regardless of its fraction, was used, due to its lower density compared to NA, a widely reported aspect in the literature [54]. Secondly, the increase of the amount of mix water when RCA was added also favored the decrease of the hardened density [41]. Finally, the hardened density increased in mixtures with CEM III/A, due to their higher content of cement, which is denser than coarse RCA.

Table 5.4. Hardened density of the mixes (Mg/m³)

	/F	/M	/L	/R
I-0	2.26	2.24	2.24	2.15
I-50	2.19	2.17	2.09	1.95
I-100	2.05	1.97	1.93	1.76
III-0	2.30	2.27	2.24	2.15
III-50	2.23	2.21	2.16	2.08
III-100	2.12	2.07	2.02	1.81

3.3. COMPRESSIVE STRENGTH

SCC flowability and strength are very sensitive to changes in the mix composition, even more so if by-products are incorporated [45]. Therefore, it is essential to obtain a balance between flowability and strength through a correct mix design [66]. In this study, the main objective was to achieve SCCs with a SF3 slump-flow class, so the amount of water was adapted when the fine RCA content increased, to compensate its high water absorption and to maintain high flowability of the SCC, but at the same time to achieve a suitable compressive strength [41]. As a result of both the fine RCA addition and the increase of the water content [41], the compressive strength decreased at all ages (1, 7, 28, and 90 days) when this waste was used, as shown in Figure 5.8. The addition of 50% fine RCA caused a decrease in strength of around 2-7 MPa at 90 days, compared to mixtures without this by-product. This decrease was 10-20 MPa for mixes with 100% fine RCA. Therefore, the decrease in strength was not proportional to the amount of fine RCA that was added [33], which could be due to the adjustment of the water content of the mixture, which differed for each fine RCA content [39].

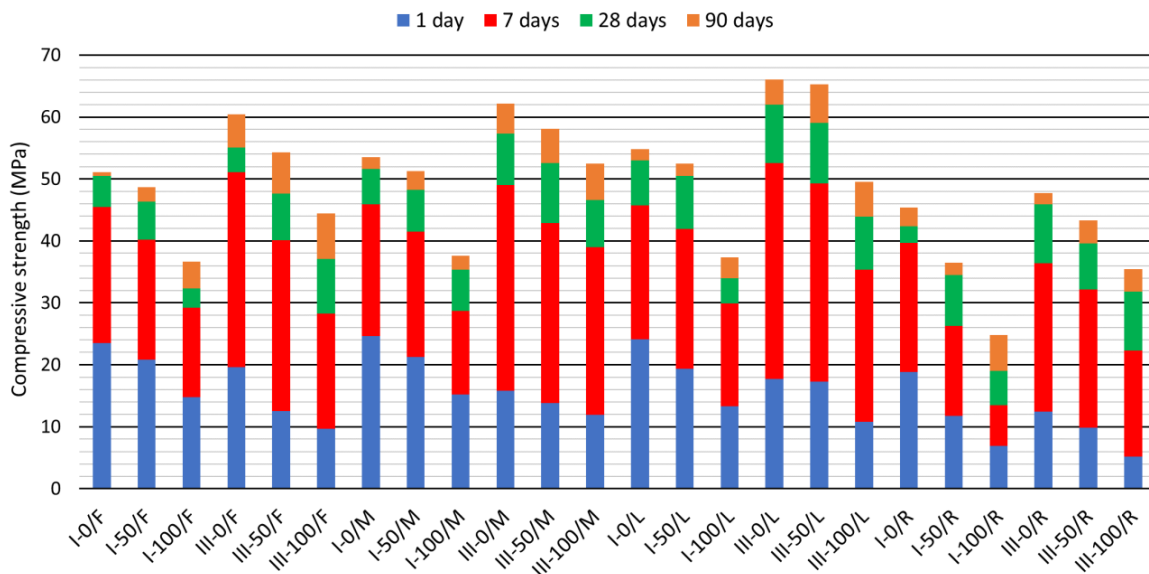


Figure 5.8. Compressive strength at 1, 7, 28, and 90 days on cubic specimens

The use of GGBFS, rather than causing a decrease, led to an increase in strength, despite the lower clinker content of the mixes (assuming a clinker content of 95% for CEM I and 55% for CEM III/A, according to EN 197-1 [51], the clinker content in mixtures with CEM I was 285 kg/m³, and only 235 kg/m³ in mixtures with CEM III/A). These results demonstrated the good behavior of GGBFS as a binder [67], even when it was combined with coarse and fine RCA [63].

The mixtures with the same type of cement and fine RCA content, but with different natural aggregate powders (limestone filler, mix of limestone filler and limestone fines 0/1 mm, or limestone fines 0/0.5 mm), had very similar strengths at 90 days, and showed trends with regard

to the fine RCA content that have also been observed in other studies [65]. However, the values obtained in the L-mixes were slightly higher. The use of RCA 0/0.5 mm provided the worst results, although mixtures I-0/R, III-0/R, and III-50/R had final strengths of over 45 MPa. Mixture I-100/R was the only one not to reach a compressive strength of 30 MPa at 90 days.

In addition to the compressive strength values that were obtained, it is possible to analyze the effect of each mix component on the temporal evolution of this strength (Figure 5.9). The mixtures manufactured with CEM III/A presented a higher final strength (Figure 5.8), although they showed a slower temporal evolution. This effect of the GGBFS is reported by both standards, such as EN 197-1 [51], and studies that evaluated the effect of the joint use of RCA and GGBFS [59]. Moreover, the addition of fine RCA also delayed the acquisition of strength [41]. Thus, the mixtures containing CEM I, natural aggregate powder, and 100% siliceous sand 0/4 mm developed 83-89% of their strength at 7 days. Nevertheless, the same mixtures, but with 100% fine RCA developed only 76-80% of their final strength. This effect was more notable when fine RCA and GGBFS were simultaneously used: mixes with CEM III/A and 100% fine RCA had developed only 63-74% of their final strength at 7 days. The use of RCA 0/0.5 mm further delayed the development of strength: at 7 days, mixture I-100/R presented only 54% of its strength at 90 days.

From all aspects addressed in this section, a clear conclusion can be obtained: the addition of 50% fine RCA (in mixtures with 100% coarse RCA) resulted in minimal decreases in strength. In addition, the flowability of these mixtures was adequate (see section 3.1). Therefore, the authors of this article considered that the most suitable fine RCA content in this study was 50%. The addition of GGBFS to these mixtures was also adequate, because this alternative binder yielded high compressive strengths.

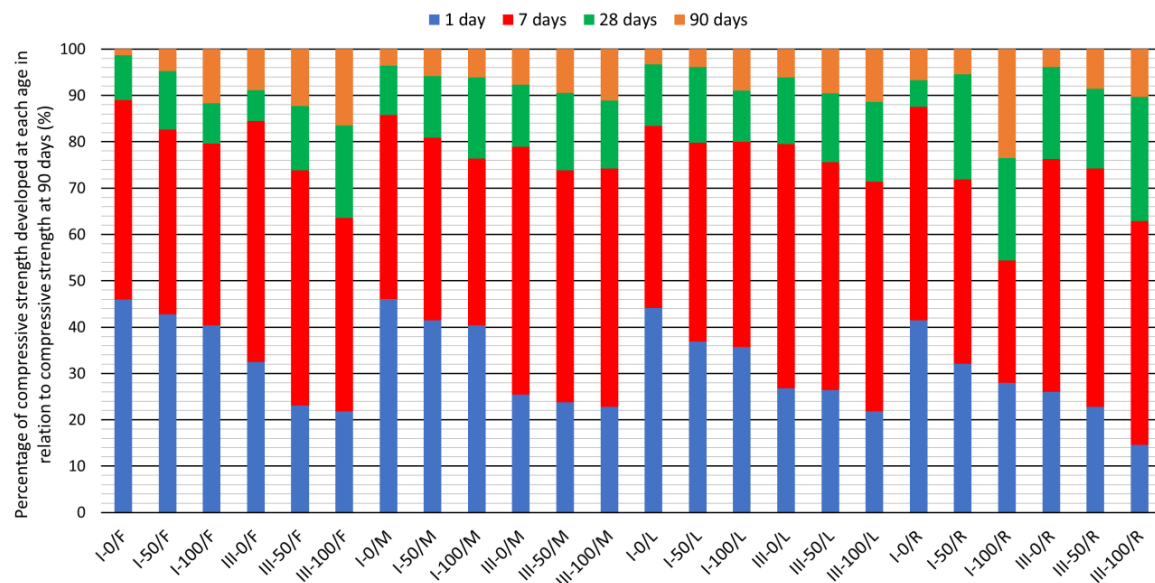


Figure 5.9. Percentage compressive strengths at 1, 7, 28, and 90 days

3.4. HAMMER REBOUND INDEX

Similar to the compressive strength, the hammer rebound index was determined at 1, 7, 28, and 90 days for all mixes. The hammer rebound index of each specimen was obtained as the median of nine determinations, according to EN 12504-2 [51]. The overall result of each mixture at each age was the arithmetic mean of three test specimens (Table 5.5). Therefore, a total of 2,592 hammer rebound tests were performed, considering all the specimens, ages, and mixtures.

The increase in compressive strength resulted, as expected, in an increase in the hammer rebound index [47]. The increase in the hammer rebound index of the SCC produced with GGBFS

was higher than expected in view of the trends shown by the models developed for non-recycled concrete (see Table 5.3). In the mixes produced with GGBFS, the surface hardness depended mainly on the binder instead of the coarse aggregate. Therefore, the hydration process of the binder led to higher increases of the hammer rebound index.

Furthermore, the value of the hammer rebound index at each age depended on the type of binder in use. Mixes with CEM I developed almost all its compressive strength at 28 days, so the results at 28 and 90 days were very similar. Nevertheless, mixes with CEM III/A underwent a higher evolution of the hammer rebound index, because of its slower strength development. Finally, the addition of RCA, with a lower surface hardness than NA, also caused the hammer rebound index to decrease [44] regardless of whether it was added as fine aggregate or aggregate powder.

Table 5.5. Hammer rebound index values at 1; 7; 28; 90 days

	/F	/M	/L	/R
I-0	25; 34; 39; 40	25; 35; 39; 42	24; 33; 41; 42	17; 28; 29; 32
I-50	23; 30; 34; 37	23; 31; 34; 41	20; 31; 40; 41	12; 22; 26; 28
I-100	19; 26; 28; 32	20; 26; 29; 31	18; 26; 29; 30	10; 12; 18; 21
III-0	20; 39; 42; 45	17; 36; 42; 46	18; 40; 46; 48	11; 28; 31; 32
III-50	17; 31; 33; 41	15; 31; 40; 43	17; 38; 45; 48	10; 26; 28; 30
III-100	14; 25; 30; 32	15; 31; 33; 40	13; 27; 32; 34	10; 20; 26; 27

3.4.1. MODEL OF THE RELATIONSHIP BETWEEN THE HAMMER REBOUND INDEX AND COMPRESSIVE STRENGTH IN CONVENTIONAL CONCRETES

As explained in section 2.4, the model shown in Table 5.3 was obtained for vibrated concrete made with NA [55]. The compressive strengths of the cubic concrete specimens of this study were estimated with that model as a function of the hammer rebound index, and the results are shown in Figure 5.10. This figure is a comparative graph between the observed value of compressive strength results, shown in figure 9, and the estimated strength at different ages through the hammer rebound index, using the model given in Table 5.3. The bisector indicates the points at which the observed strength was equal to the estimated strength. If the points are above this bisector, the observed values were greater than the estimated ones.

The first general observation on the basis of this figure is that, using this conventional model (Table 5.3), the compressive strength was, in all cases, underestimated. The high content of fine aggregate and aggregate powder required to produce a SF3 class SCC [45] showed that it had a lower surface hardness than expected and, therefore, the hammer rebound indexes were also lower. This effect was generally greater in mixtures made with CEM III/A, due to their lower amount of coarse aggregate. Moreover, the existing model underestimated the compressive strength by approximately 15 MPa (30-40%), for observed compressive strengths of 20-50 MPa. When the observed strength was higher than 50 MPa, the strength underestimations of the model were around 10 MPa (15-20%). Most of the mixes with compressive strengths of between 20 and 50 MPa incorporated fine RCA and/or RCA filler. Hence, it appeared that RCA increased this underestimation, due to its lower hardness compared to NA [44]. From these results, it can be concluded that the models developed for vibrated concrete were not valid for SF3 class SCC, so in the next section the development of new models for this type of concrete will be studied. The final aim will be to obtain a single model valid for recycled SCC of high-flowability regardless of its composition.

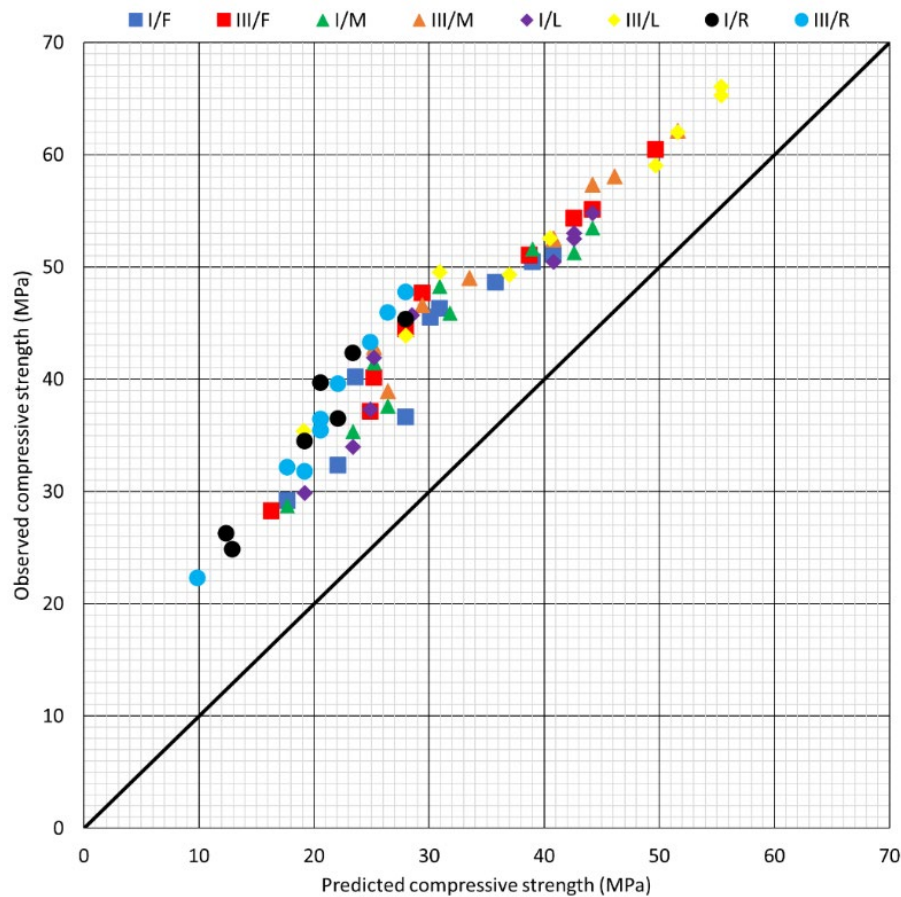


Figure 5.10. Relationship between the predicted compressive strength with the hammer rebound index, according to Table 5.3, and the experimental results of compressive strength

3.4.2. DEVELOPMENT OF A NEW MODEL FOR THE RELATIONSHIP BETWEEN THE HAMMER REBOUND INDEX AND COMPRESSIVE STRENGTH

In view of the results set out in the previous section, a particular model is needed to estimate compressive strength as a function of the hammer rebound index in SF3 class SCCs containing RCA. Firstly, the two best-fit models for the relationship between both variables (*CS*, Compressive Strength, in MPa; and *HRI*, Hammer Rebound Index) are presented in Table 5.6, distinguishing between the different variations introduced in the composition of the mixtures (type of cement, fine RCA content, and nature of the aggregate powder).

It can be seen that an optimal adjustment was obtained, with coefficients R^2 of over 95% in almost all cases. Therefore, the compressive strength of the SCC can be accurately estimated by the hammer rebound index regardless of its composition, as other studies have suggested in relation to the coarse and fine RCA content [47]. On the other hand, it is also possible to analyze the effect that each change in the composition of the mixture has on the relationship between these two variables:

- Modification of the type of cement or fine RCA content (up to percentages of 50%) led to no change in the nature of the models with the best fit, which means that models with the same expression were obtained, according to Equation 5.1. The only difference between them was the value of the coefficients (a , b).

$$CS = \sqrt{a + b \cdot HRI^2} \quad (5.1)$$

- Nevertheless, the addition of 100% fine RCA or the use of a different aggregate powder resulted in a different formulation of the best-fit model in each case. It can therefore be stated that the surface hardness of the SF3 class SCC was mainly affected by changes to the finer aggregate fractions [43], as other studies have stated for SCC of lower flowability [47]. In consequence, the relationship between compressive strength and the hammer rebound index was changed.

Table 5.6. Adjustment of compressive strength (MPa) as a function of the hammer rebound index

Mixes		Model expression	Coefficient R ² (%)
Mixes with the same type of cement	Mixes with CEM I	$CS = \sqrt{-270.40 + 1.86 \cdot HRI^2}$	94.38
		$CS = -10.00 + 1.56 \cdot HRI$	94.08
	Mixes with CEM III/A	$CS = \sqrt{-178.11 + 1.93 \cdot HRI^2}$	97.93
		$CS = -8.62 + 1.57 \cdot HRI$	97.64
Mixes with the same fine RCA content	Mixes with 0% RCA 0/4 mm	$CS = \sqrt{-197.39 + 1.90 \cdot HRI^2}$	96.06
		$CS = -7.66 + 1.53 \cdot HRI$	95.39
	Mixes with 50% RCA 0/4 mm	$CS = \sqrt{-185.55 + 1.86 \cdot HRI^2}$	96.21
		$CS = -8.03 + 1.53 \cdot HRI$	95.92
	Mixes with 100% RCA 0/4 mm	$CS = (-2.55 + 1.58 \cdot \sqrt{HRI})^2$	95.49
		$CS = (1.00 + 0.17 \cdot HRI)^2$	95.37
Mixes with the same aggregate powder	Mixes with limestone filler	$CS = (-8.57 + 4.30 \cdot \ln(HRI))^2$	97.30
		$CS = -63.45 + 18.41 \cdot \sqrt{HRI}$	96.95
	Mixes with limestone filler and limestone fines 0/1 mm	$CS = (-2.52 + 1.55 \cdot \sqrt{HRI})^2$	96.83
		$CS = \exp(-1.50 + 1.49 \cdot HRI)$	96.78
	Mixes with limestone fines 0/0.5 mm	$CS = \sqrt{-305.51 + 1.94 \cdot HRI^2}$	97.95
		$CS = -10.59 + 1.59 \cdot HRI$	97.79
	Mixes with RCA 0/0.5 mm	$CS = 5.37 + 0.04 \cdot HRI^2$	98.44
		$CS = -9.62 + 1.71 \cdot HRI$	97.64

Another relevant aspect shown in Table 5.6 is that, although the linear model (Equation 5.2) is not the best-fit model in any case, it is the model with the second better fit in 6 out of the 9 cases under study. A result that shows why previous attempts to relate the compressive strength and rebound rate in SCC to RCA, by considering exclusively linear equations, approximated this relationship quite accurately [47]. However, the accuracy of this estimate can be more precise by using equations with a slightly more complex formulation [21].

$$CS = a + b \cdot HRI \quad (5.2)$$

Notwithstanding the above, it is clear that a global model (without differentiating between the changes in the composition of the mixtures) that relates the indirect measure to compressive strength is needed. Each indirect measure could therefore be quickly and easily applied to real structures, thereby encouraging the use of recycled SF3 class SCC in building and civil works. In this study, the development of a global model was performed by fitting all the data (compressive strength and hammer rebound index of the 24 mixtures at the 4 testing ages) by simple regression. On the other hand, obtaining a single model may involve specific goodness-of-fit problems, i.e., even though its overall fit is correct, there may be some range of the independent variable for which the estimate is imprecise. For this reason, it is advisable to achieve greater accuracy by using at least two models.

According to the previous paragraph, Equation 5.3 and Equation 5.4 show the two best-fit global models (coefficients R^2 around 96%) for the relationship between compressive strength and the hammer rebound indexes of the mixes of this study. In these models, the specific goodness-of-fit problems indicated above can be clearly observed. Despite the fact that model 1 had the best overall fit, its fit was worse than for model 2 in the hammer rebound indexes between 10 and 15 and higher than 45. Therefore, although whenever possible the best-fit model should be used, it is recommended to employ model 2 for hammer rebound indexes lower than 15. Both models are plotted in Figure 5.11. These models have the same expressions (with different coefficients) as those obtained in most cases by individual analysis (Table 5.6): Equation 5.1 and Equation 5.2. It shows that the adjustment of large volumes of data can filter out the influence of the mixture composition (mainly the different nature of the aggregate powder or the high fine RCA content) on this relationship. Therefore, the hammer rebound index can be successfully used to estimate the compressive strength of SF3 class SCC containing RCA, regardless of changes to its composition, with only one model.

$$CS = \sqrt{-247.45 + 1.92 \cdot HRI^2}, \quad \text{if } 15 < HRI < 45 \quad (5.3)$$

$$CS = -9.53 + 1.57 \cdot HRI, \quad \text{if } 10 < HRI < 15 \text{ and } 45 < HRI < 50 \quad (5.4)$$

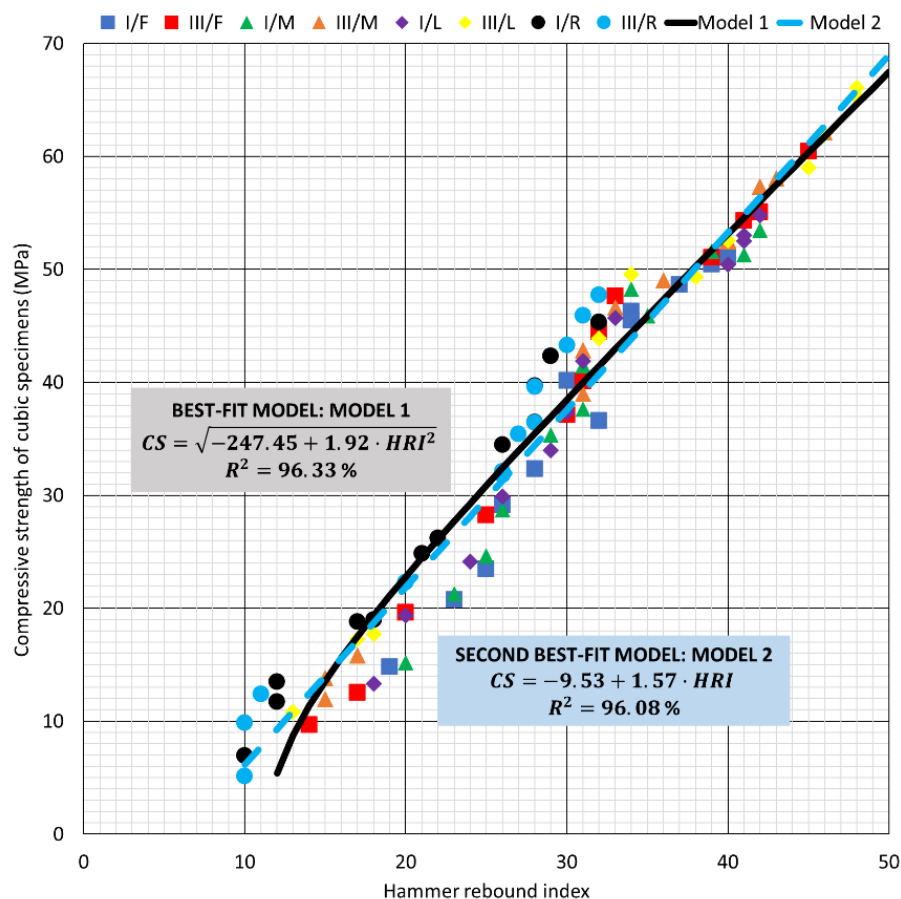


Figure 5.11. Global models with the best fit for the relationship between compressive strength and the hammer rebound index

As previously indicated, each global model that is represented (see Figure 5.11) better fits a different compressive strength range, so the optimal choice is a statistical combination of both (Equation 5.3 and Equation 5.4, Figure 5.11) in a single model, so that the estimation will be as accurate as possible. In relation to this model, it is possible to go even further. If it is provided in table form it can be used immediately, with no need for mathematical operations (equations), which favors its quick use. For this reason and with the objective of assimilating the way of

working on this type of concrete to that of conventional concrete (see Table 5.3), Table 5.7 shows the global combined model in table form. It collects both the most probable compressive strength on cubic specimens (W_m), and the minimum expected compressive strength at a 95% confidence level (W_{min}) as a function of the hammer rebound index.

Table 5.7. Global model for the estimation of the compressive strength on cubic specimens as a function of the hammer rebound index

Hammer rebound index	W_m^1	W_{min}^2	Hammer rebound index	W_m^1	W_{min}^2
10	6.2	0.0	31	39.6	33.6
11	7.7	1.0	32	41.1	35.2
12	9.3	1.9	33	42.6	36.8
13	10.9	2.9	34	44.1	38.5
14	12.5	3.9	35	45.6	40.1
15	14.0	4.8	36	47.2	41.7
16	15.6	5.8	37	48.7	43.3
17	17.3	6.8	38	50.2	44.8
18	19.0	7.7	39	51.7	46.4
19	20.7	8.7	40	53.2	48.0
20	22.3	12.5	41	54.7	49.5
21	24.0	15.0	42	56.2	51.1
22	25.6	17.3	43	57.7	52.6
23	27.1	19.3	44	59.2	54.2
24	28.7	21.3	45	60.7	55.7
25	30.3	23.2	46	62.2	57.3
26	31.9	25.0	47	63.7	58.8
27	33.4	26.8	48	65.2	60.3
28	34.9	28.5	49	66.7	61.9
29	36.5	30.2	50	68.2	63.4
30	38.0	31.9			

¹ W_m : most likely compressive strength value (MPa)

² W_{min} : minimum expected compressive strength value (MPa)

In general, as can be observed in Figure 5.12, the estimation of compressive strength using Table 5.7 is accurate. The worst fitting zone corresponded to an estimated compressive strength of 35-45 MPa, in which the observed compressive strength was underestimated by around 6 MPa. When the observed strength was overestimated, this strength was always higher than the minimum expected strength shown in Table 5.7. It demonstrates the validity of this model, with which the estimation is not only accurate, but also safe. Therefore, this model can be considered a first general approach to the use of the hammer rebound index for the estimation of compressive strength in real structures manufactured with recycled highly SCC.

3.5. UPV

The propagation speed (v) of an elastic wave in a continuous medium can be predicted by Equation 5.5 (E , modulus of elasticity; ρ , density). In this relationship, the dependence on the Poisson coefficient (ν) is a function of the boundary conditions [5]. However, it is also known that in a porous media such as concrete, the validity of this formulation can be uncertain, especially due to the capillary-type of porosity with singular pore-size distribution within both the matrix and the aggregates [41].

$$v = \sqrt{E/\rho} \cdot f(v) \quad (5.5)$$

Additionally, attempts to correlate the modulus of elasticity with the compressive strength is a classic problem in the field of concrete [56]. In view of the constraints of the literature [43, 47], the authors of this study decided to study the direct correlation between the UPV values and the compressive strength of highly SCC.

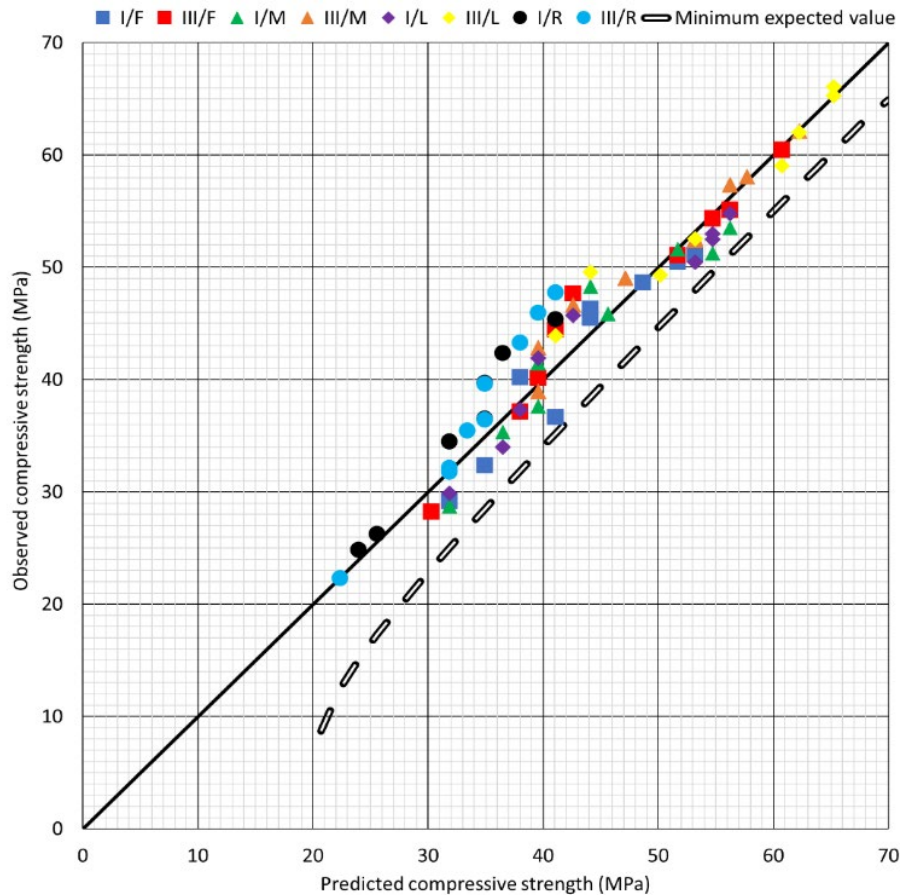


Figure 5.12. Comparison between the predicted compressive strength with the hammer rebound index global model (Table 5.7) and the observed compressive strength

UPV determination was performed according to EN 12504-4 [51]. The direct method was used (see Figure 5.2). The UPV value for each specimen was obtained as the arithmetic mean of the UPV in the three spatial directions (X, Y and Z-axis). In addition, the overall result for each mix and age was the arithmetic mean of the UPV values of three specimens. In total, considering all the specimens, ages, and mixes, 864 UPV measures were taken. The overall results obtained are shown in Table 5.8, according to which the UPV test results were higher than expected, which led to an overestimation of the compressive strength (see intervals of section 2.4): UPV values greater than 4.2 km/s were obtained when none of the mixtures that were developed could be considered very high-strength concrete.

The UPV values clearly reflected the high compressive strength provided by CEM III/A at all ages. In fact, the results for mixtures with GGBFS were 5-10% higher than those of mixtures with CEM I. Nevertheless, this indirect measure did not accurately reflect the evolution of compressive strength at advanced ages in some cases, mainly when RCA 0/4 or 0/0.5 mm was incorporated. For instance, mixture III-50/R developed around 10% of its compressive strength between 28 and 90 days (see Figure 5.9) and the UPV increased only 0.07 km/s.

Table 5.8. UPV (km/s) at 1; 7; 28; 90 days

	/F	/M	/L	/R
I-0	3.28; 4.03; 4.12; 4.15	3.41; 4.05; 4.17; 4.11	3.45; 4.02; 4.22; 4.33	3.00; 3.90; 3.95; 4.02
I-50	3.17; 3.96; 4.05; 4.08	3.20; 3.95; 4.10; 4.17	3.07; 4.00; 4.09; 4.18	2.72; 3.35; 3.87; 3.94
I-100	2.81; 3.53; 3.71; 3.87	2.92; 3.46; 3.82; 3.90	2.77; 3.59; 3.82; 3.89	2.55; 2.77; 2.98; 3.33
III-0	3.09; 4.17; 4.30; 4.57	2.94; 4.10; 4.48; 4.61	2.77; 4.21; 4.63; 4.77	2.82; 3.83; 4.03; 4.07
III-50	2.74; 3.98; 4.07; 4.28	2.90; 3.98; 4.21; 4.49	2.74; 4.11; 4.53; 4.71	2.77; 3.75; 3.94; 4.01
III-100	2.65; 3.47; 3.90; 4.02	2.72; 3.81; 4.05; 4.19	2.67; 3.89; 3.99; 4.09	2.43; 3.21; 3.68; 3.89

3.5.1. RELATIONSHIP BETWEEN UPV AND DENSITY

Very early [18] and more recent studies [30] have shown that an increase in the hardened density of concrete facilitates the propagation of ultrasonic pulses. In this study, the necessary reduction of the coarse aggregate content to obtain an SF3 slump-flow class resulted in a lower number of discontinuities within the concrete matrix, which affected this relationship [8].

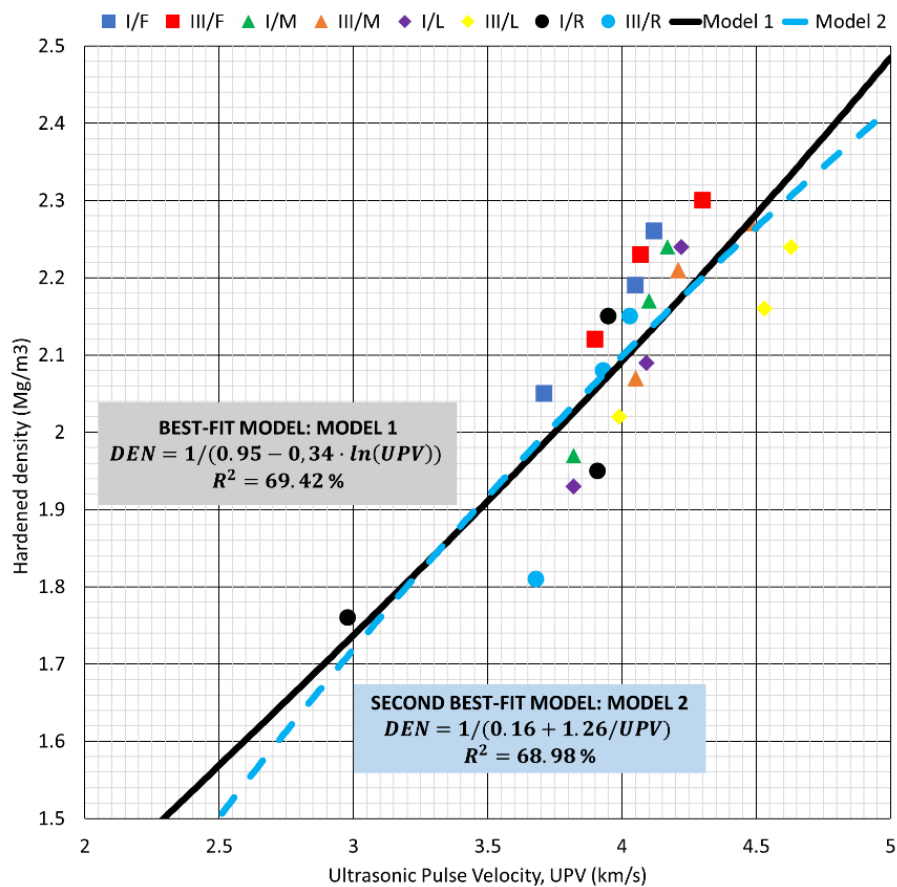


Figure 5.13. Global models with better fits for the relationship between hardened density and UPV

In Figure 5.13, the best-fit simple regression models (Equation 5.6 and Equation 5.7) between hardened density (DEN , in Mg/m^3) and UPV (km/s) are represented. Firstly, it can be seen that these models have a highly complex formulation and show a proportionally inverse relationship between both variables. Furthermore, a coefficient R^2 of only 69% was obtained, which makes the relationship between hardened density and UPV unclear. This performance is mainly due to the existence of a large number of mixes of different densities (2-2.3 Mg/m^3), but with a very similar UPV (3.8-4.2 km/s). It therefore appears that the high fines content of the SF3 class SCC created a very uniform medium for the propagation of ultrasonic waves [8], favoring similar UPV readings, despite the variation in density.

$$DEN = \frac{1}{0.95 - 0.34 \cdot \ln(UPV)} \quad (5.6)$$

$$DEN = \frac{1}{0.16 + \frac{1.26}{UPV}} \quad (5.7)$$

3.5.2. RELATIONSHIP BETWEEN UPV AND COMPRESSIVE STRENGTH

Despite the imprecise relationship between the hardened density and the UPV, the relationship obtained between this indirect measurement and compressive strength was highly accurate, as can be seen in Table 5.9. In this table, an analysis is shown of the relationship between compressive strength (CS, in MPa) and UPV (km/s) with distinctions between modifications in the composition of the mixtures. All the developed models presented an optimum fit (coefficients R^2 greater than 97% in all cases). Nevertheless, the formulation of the models with the best fit was altered with each change in the composition of the mixes. Therefore, it is clear that the equations that establish the relationship between compressive strength and UPV are highly sensitive to the nature of the materials used in the mixture [68]. In each particular case it can be defined with high precision, although the formulation of the equation is different. This performance shows the need to evaluate different mix compositions and formulations for an accurate definition of this relationship [45], as has been done in this study. Hence, a linear equation cannot be taken as valid to describe this relationship accurately without an extensive analysis [47].

Table 5.9. Compressive strength (MPa) as a function of UPV (km/s)

Mixes		Model expression	Coefficient R^2 (%)
Mixes with the same kind of cement	Mixes with CEM I	$CS = (0.87 + 0.36 \cdot UPV^2)^2$	97.23
		$CS = (-3.41 + 2.50 \cdot UPV)^2$	97.05
	Mixes with CEM III/A	$CS = -15.69 + 3.70 \cdot UPV^2$	98.19
		$CS = (-11.61 + 9.10 \cdot \sqrt{UPV})^2$	97.92
Mixes with the same RCA 0/4 mm content	Mixes with 0% RCA 0/4 mm	$CS = -15.23 + 3.72 \cdot UPV^2$	97.64
		$CS = (-11.38 + 9.02 \cdot \sqrt{UPV})^2$	97.63
	Mixes with 50% RCA 0/4 mm	$CS = (-3.08 + 2.41 \cdot UPV)^2$	96.94
		$CS = (-11.53 + 9.06 \cdot \sqrt{UPV})^2$	96.79
	Mixes with 100% RCA 0/4 mm	$CS = (-4.85 + 8.17 \cdot \ln(UPV))^2$	97.54
		$CS = (-11.57 + 9.04 \cdot \sqrt{UPV})^2$	97.52
Mixes with the same aggregate powder	Mixes with limestone filler	$CS = \exp(6.58 - 11.21/UPV)$	98.84
		$CS = \exp(-0.77 + 3.27 \cdot \ln(UPV))$	98.73
	Mixes with limestone filler and limestone fines 0/1 mm	$CS = \exp(6.68 - 11.58/UPV)$	99.03
		$CS = \exp(-0.80 + 3.30 \cdot \ln(UPV))$	98.73
	Mixes with limestone fines 0/0.5 mm	$CS = (-2.42 + 2.25 \cdot UPV)^2$	97.03
		$CS = -13.48 + 3.57 \cdot UPV^2$	97.01
	Mixes with RCA 0/0.5 mm	$CS = (13.19 - 27.10/UPV)^2$	97.21
		$CS = (-5.10 + 8.34 \cdot \ln(UPV))^2$	97.05

Due to the absence of a best-fit model with the same formulation in various mixtures, the development of a global model that relates compressive strength to UPV is essential, for an easy description of the relationship between these two variables. In addition, this model would have the advantages discussed above (see section 3.4). Figure 5.14 shows that it is possible to obtain a

highly accurate overall model (coefficients R^2 of 97%), if a large volume of data is processed, despite the high sensitivity of the relationship between compressive strength and UPV to changes in the mix design. The two best-fit models for the relationship between these two variables are shown in Equation 5.8 and Equation 5.9, respectively. These models were obtained as indicated in section 3.4: all available data were fitted by simple regression. Once again, two models were used to avoid specific goodness-of-fit problems and to achieve greater accuracy. However, Figure 5.14 also shows a problem of these global models that was not present when using the hammer rebound index: a very narrow range of UPV (3.9-4.2 km/s) is related to a very wide compressive strength interval (32-52 MPa). Hence, slight variations in the measured UPV lead to a considerable over- or underestimation of compressive strength.

$$CS = (-11.76 + 9.17 \cdot \sqrt{UPV})^2, \text{ if } 2.0 < UPV < 2.7 \text{ and } 4.4 < UPV < 5.0 \quad (5.8)$$

$$CS = (-3.22 + 2.45 \cdot UPV)^2, \text{ if } 2.7 < UPV < 4.4 \quad (5.9)$$

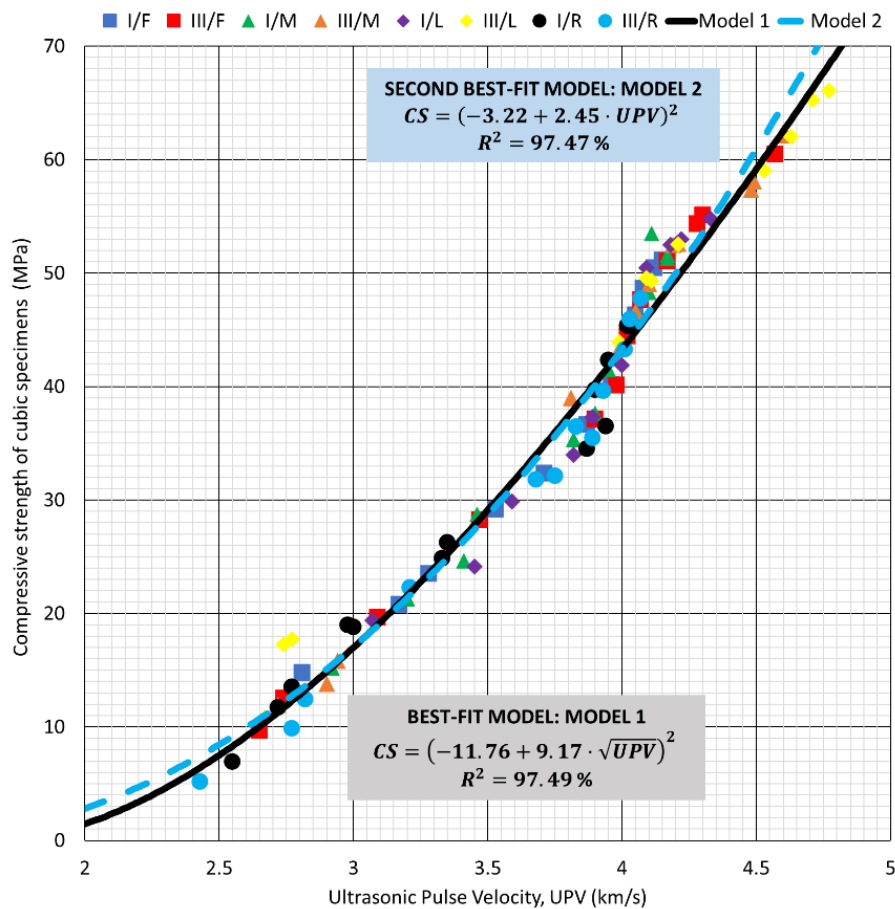


Figure 5.14. Global models with the best fit for the relationship between compressive strength and UPV

As in the hammer rebound index, Table 5.10 shows the most likely (W_m) and the least likely (W_{min}) compressive strengths of a set of cubic specimens as a function of the UPV test results. These results were obtained by the joint treatment of both models (Equation 5.8 and Equation 5.9), also shown in Figure 5.14, and mean that the procedures can be homogenized, facilitating the use of these models in real works. The comparison between the observed compressive strength and the one estimated by this model is graphically represented in Figure 5.15. The estimate for this indirect measure was also accurate and there was no observed strength below the minimum expected value. However, the UPV model had a wider safety interval than the hammer rebound index model, due to the different problems that have previously been discussed, mainly the high influence of the mix components, and the slight variation of the UPV value for compressive

strengths between 32 and 52 MPa. It meant that the compressive strength estimation was more uncertain when UPV was used. Nevertheless, the UPV compressive-strength estimate was lower than the estimate based on the hammer rebound index, which showed that this non-destructive testing could be also used to estimate the compressive strength of concrete at early ages [20].

Table 5.10. Global model for the estimation of the compressive strength on cubic specimens as a function of UPV (km/s)

UPV	W_m^1	W_{min}^2	UPV	W_m^1	W_{min}^2
2.00	2.1	1.0	3.55	30.2	25.4
2.05	2.6	1.3	3.60	31.6	26.6
2.10	3.0	1.6	3.65	33.0	27.9
2.15	3.5	2.0	3.70	34.4	29.2
2.20	4.0	2.4	3.75	35.8	30.5
2.25	4.6	2.8	3.80	37.2	31.9
2.30	5.2	3.3	3.85	38.7	33.2
2.35	5.9	3.8	3.90	40.2	34.6
2.40	6.5	4.4	3.95	41.7	36.0
2.45	7.2	4.9	4.00	43.3	37.5
2.50	8.0	5.5	4.05	44.9	38.9
2.55	8.7	6.2	4.10	46.5	40.4
2.60	9.5	6.9	4.15	48.1	41.9
2.65	10.4	7.6	4.20	49.7	43.5
2.70	11.2	8.3	4.25	51.4	45.0
2.75	12.1	9.1	4.30	53.1	46.6
2.80	13.0	9.9	4.35	54.8	48.2
2.85	14.0	10.8	4.40	56.5	49.8
2.90	15.0	11.6	4.45	58.3	51.4
2.95	16.0	12.5	4.50	60.0	53.1
3.00	17.0	13.4	4.55	61.8	54.8
3.05	18.1	14.4	4.60	63.7	56.5
3.10	19.2	15.4	4.65	65.5	58.2
3.15	20.3	16.4	4.70	67.4	60.0
3.20	21.5	17.4	4.75	69.3	61.7
3.25	22.6	18.5	4.80	71.2	63.5
3.30	23.8	19.6	4.85	73.1	65.3
3.35	25.1	20.7	4.90	75.0	67.2
3.40	26.3	21.8	4.95	77.0	69.0
3.45	27.6	23.0	5.00	79.0	70.9
3.50	28.9	24.2			

¹ W_m : most likely compressive strength value (MPa)

² W_{min} : minimum expected compressive strength value (MPa)

3.6. JOINT USE OF THE HAMMER REBOUND INDEX AND THE UPV

The highly accurate models described in the previous sections, to predict compressive strength through the hammer rebound index or UPV analysis of a SF3 class SCC, mean that the composition effect of the mix may be disregarded for the prediction of SCC strength [69]. Nevertheless, the use of a single indirect measure can lead to incorrect strength estimations, due to a wide variety of reasons, from poor calibration of the device used to occasional irregularities within the concrete [2]. The best solution to this problem is to use models with two variables

(hammer rebound index, and UPV) to estimate the strength, although they have the disadvantage of complexity and their implementation is difficult [1].

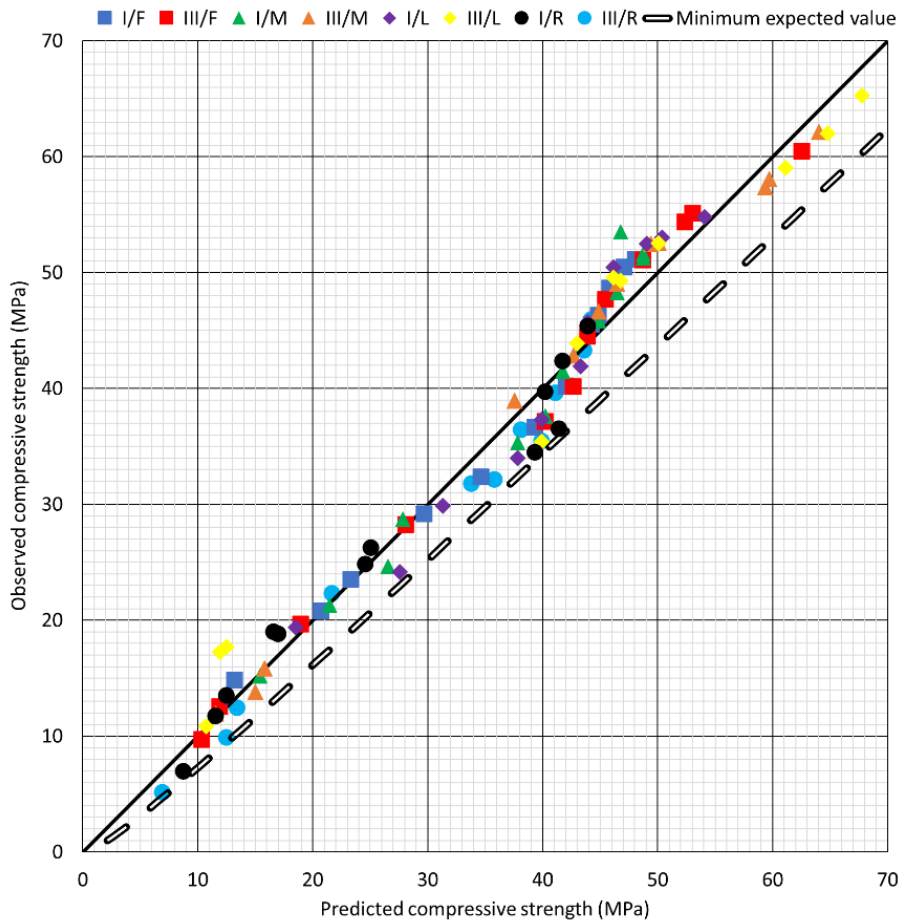


Figure 5.15. Comparison between predicted compressive strength through UPV global model (Table 5.10) and observed compressive strength

In this study, among the many existing functions that combine the effect of the hammer rebound index and UPV to estimate compressive strength, intuition appeared preferable to complex mathematic analyses. On the other hand, the validity of the simplest possible regression model, the linear equation, for this relationship is shown in both Table 5.6 and Table 5.9 (in Table 5.6, six over nine linear functions; and, in Table 5.9, six over nine quasi-linear functions). Moreover, the Pearson matrix (Figure 5.16) showed a high linear correlation between both indirect measurements under study and the compressive strength. Therefore, a multiple quasi-linear regression model (Equation 5.10) with a first-power interaction term by adjusting all available data was defined to estimate compressive strength (*CS*, in MPa) through the introduction of the hammer rebound index values (*HRI*, values from 10 to 60 units) and the UPV values (from 2.5 to 5.5 km/s). This model showed a high precision, with a coefficient R^2 of 98.50%.

$$CS = -30.94 + 0.16 \cdot HRI + 12.86 \cdot UPV + 0.13 \cdot HRI \cdot UPV \quad (5.10)$$

Although this model is quite simple, Figure 5.17 shows that the combination of both non-destructive testing offers a precise and safe way of estimating compressive strength. The difference between the most overestimated experimental strength and the corresponding estimated strength is not even 4 MPa, an acceptable margin for structural calculations with the conventional safety coefficients [70]. This high precision is due to the fact that the estimation errors of one indirect measurement are compensated by the other. This model clearly improves

the precision of other similar models performed up to date for recycled concrete, which combine indirect measures and semi-destructive methods [44].

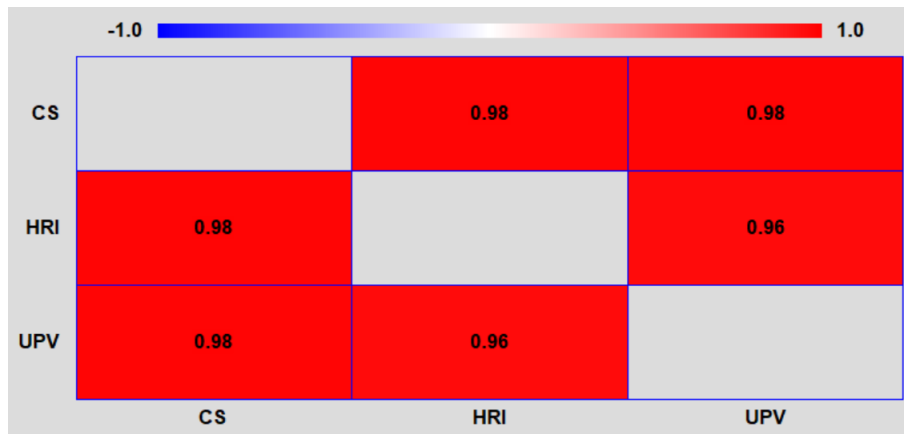


Figure 5.16. Pearson product-moment correlations between hammer rebound index (HRI), the UPV, and compressive strength (CS)

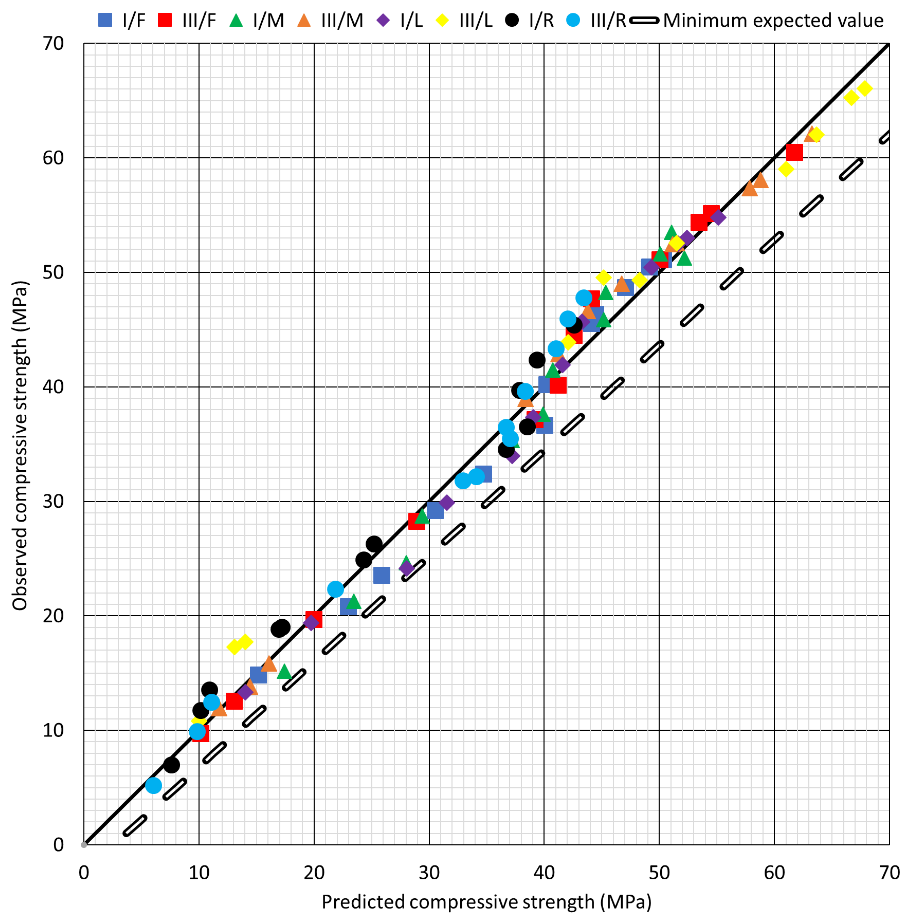


Figure 5.17. Comparison between predicted compressive strength through the two-variable model and observed compressive strength

Finally, Equation 5.11 yields the minimum expected value of compressive strength of this two-variable model. In this equation, $meCS$ is the minimum expected compressive strength, in MPa, and CS is the estimated compressive strength, in MPa, calculated by Equation 5.10.

$$meCS = 0.92 \cdot CS - 3.15 \tag{5.11}$$

3.7. VALIDATION OF THE MODELS DEVELOPED

The desirable validation of a model with data obtained from other studies is, in this case, difficult, because this is the first study in which the suitability of indirect measures has been studied in SF3 class SCC, as indicated in section 1.1. To date, this aspect has neither been analyzed in many studies on SCC of class SF2 (slump flow between 650 and 750 mm), nor there is a general model for this type of SCC. Moreover, fresh and hardened properties of SCC are very sensitive to changes in its composition [31], so any variation in its flowability could significantly affect the accuracy of the estimated compressive strength.

The global model represented in Equation 5.10 and Equation 5.11 was tested with data obtained from existing research works that studied both indirect measures in SF2 class SCC [30, 47, 71-73]. The comparison between the observed values of the referenced studies and those calculated by the model is shown in Figure 5.18. As expected, the fit of data from other studies was less accurate than the data with which the model was developed. Nevertheless, the adjustment for SF2 class SCC is considered correct, since the average deviation in absolute value of the predicted compressive strength compared to the observed one was only 5.5%.

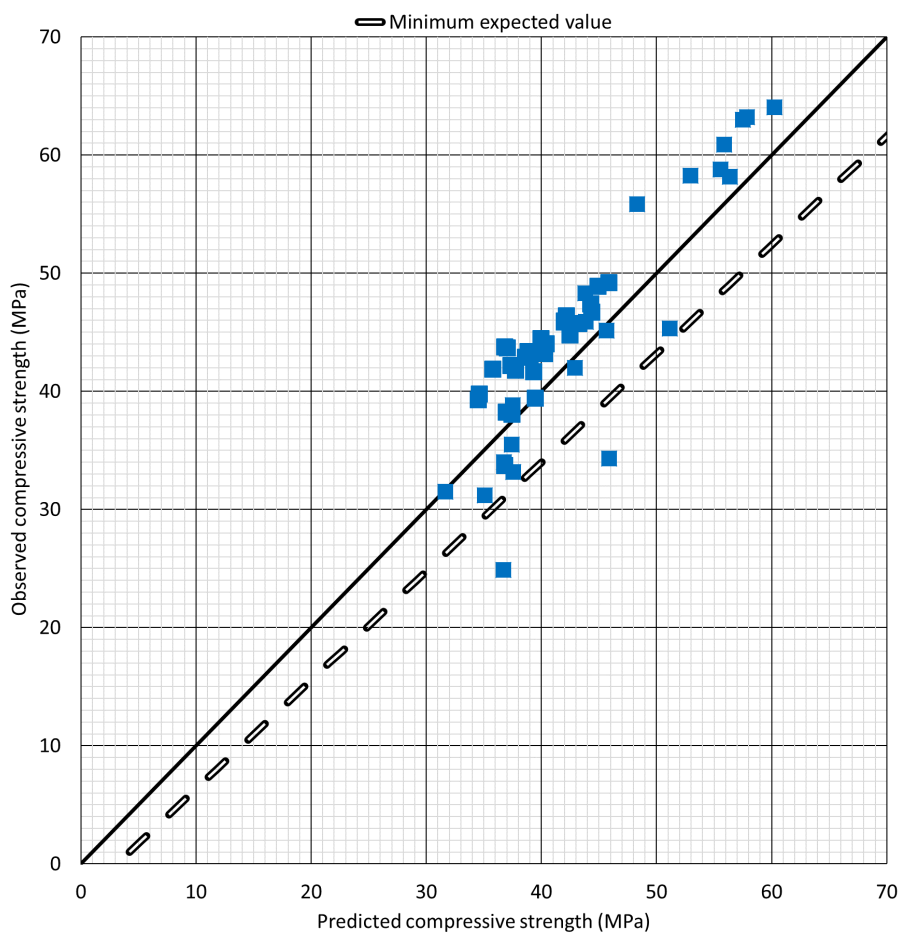


Figure 5.18. Validation of the proposed model

Two aspects of the validation should be highlighted:

- Firstly, it can be seen that the compressive strength was, in most cases, underestimated by the model. This underestimate was due to the lower flowability of the SCC, generally linked to the increase in its compressive strength [41]. Thus, SF2 class SCC yielded slightly higher compressive strengths (around 2-6 MPa in the samples under study) for similar values of indirect measurements.

- On the other hand, the cases in which the compressive strength was overestimated corresponded to SCC mixtures with a very high content of RCA and alternative binders (in particular, fly ash), which can in some cases lead to a sharp decrease in strength [58]. Nevertheless, 90% of the mixes under study were above the minimum expected value, which shows that the safety margin provided by the model is adequate.

From this study, it can be inferred that the use of the developed models in SF2 class SCC can be considered safe for medium-strength SCC mixtures with a moderate content of by-products.

3.8. USE OF THE MODELS

Throughout this paper, several models for estimating the compressive strength through non-destructive testing of a highly SCC have been provided. The proposed models can be used in two different ways:

- On the one hand, the equations obtained for a particular composition of SCC (type of cement, fine RCA content, and aggregate powder nature) can be employed, which are shown in Table 5.6 and Table 5.9. Each SCC mixture will usually fulfill one condition regarding each of its components, that is, six models could be used. Despite the accuracy of the models and their coefficient R^2 , they can have specific goodness-of-fit problems, as explained in section 3.4.2. The authors therefore recommend that the arithmetic mean of the results of the six equations be calculated for safe and precise estimations and to compensate for potential deviations.
- On the other hand, compressive strength can be estimated through the global models that have been developed (Table 5.7, Table 5.10, Equation 5.11 and Equation 5.12). This option is recommended by the authors, because specific goodness-of-fit problems were minimized during their development, and the minimum expected values of compressive strength were calculated. In addition, these models are not dependent on the composition of the SCC. Finally, the models are easier to use: the value of the hammer rebound index and/or the UPV of the mixture is introduced in the model directly, which quickly provides both the most likely, and the minimum expected compressive strength.

4. CONCLUSIONS

In this paper, the possibility of estimating the compressive strength through the hammer rebound index and the Ultrasonic Pulse Velocity (UPV) of highly Self-Compacting Concrete (SCC) that incorporates large amounts of Recycled Concrete Aggregate (RCA) has been assessed.

A total of 24 SF3 class SCCs were developed to perform this study, with different types of cement (CEM I or CEM III/A), fine RCA contents, and types of aggregate powder. The hammer rebound index, UPV, and the compressive strength of all mixtures were determined at 1, 7, 28, and 90 days.

From the investigation, it was concluded that the mixtures manufactured with 50% fine RCA optimized flowability, and compressive strength simultaneously. Furthermore, the compressive strength could be increased by the addition of CEM III/A, with around 45% of GGBFS, due to the necessary replacement of coarse aggregate by binder that was performed in these mixes to achieve SF3 class SCC. This change also led the surface hardness of these mixtures to depend more on the added binder, which produced higher increases in the hammer rebound index than in conventional concretes. On the other hand, the use of this alternative binder delayed the development of strength over time, which meant that the UPV values were not proportionate to the rise in compressive strength at advanced ages. Finally, the joint use of fine RCA and CEM III/A also yielded suitable in-fresh and hardened behaviors.

On the other hand, indirect, accurate, and safe estimation of the compressive strength of highly SCC, regardless of the mix composition, has been developed and verified with the data from other studies. High precision models were obtained (Table 5.7, Table 5.10, Equation 5.11 and Equation 5.12).

From the aspects discussed throughout this article, the main conclusions drawn are:

- The existing models for estimating the compressive strength in non-recycled vibrated concrete through non-destructive testing were not valid for SF3 class SCC. The hammer rebound index underestimated the strength, while the use of the UPV test led to an overestimation. These discrepancies were attributed to the high content of the fine aggregate fractions that were required to achieve such high levels of flowability.
- The model designed in this study to estimate compressive strength as a function of the hammer rebound index presented a robust formulation that was not affected by variations in the composition of the mixtures, except for the nature of the aggregate powder. The relationship between the compressive strength and the UPV was much more sensitive, as it was affected by any minimal change of the materials used in the mix.
- The safety interval provided by the UPV model designed in this study was slightly higher than when the hammer rebound index was used to estimate compressive strength. This result indicates that the prediction of compressive strength of SF3 class SCCs using the UPV model has a higher uncertainty, and small changes to the value of this indirect measure can imply large differences in the estimated strength.
- The estimation of compressive strength from one single indirect measurement, the hammer rebound or the UPV, yielded robust predictions. However, the combined use of both, by means of a simple quasi-linear equation, yielded estimations of greater precision.

In short, this study has provided robust models for predicting the compressive strength through indirect measurements (hammer rebound index or/and UPV) for SF3 class SCCs. These models promote the use of recycled concretes in real structures, by providing a tool with which to monitor their strength during their construction and lifecycle through non-destructive testing. Moreover, the models and procedures explained in this article can be used as a basis for the development of similar models for other recycled and/or non-conventional types of concrete. This study has, therefore, opened up a very interesting future line of research.

REFERENCES

- [1] R. Jones, The non-destructive testing of concrete, *Mag. Concr. Res.* 1 (2) (1949) 67-78.
- [2] A. Aseem, W. Latif Baloch, R.A. Khushnood, A. Mushtaq, Structural health assessment of fire damaged building using non-destructive testing and micro-graphical forensic analysis: A case study, *Case Stud. Constr. Mater.* 11 (2019) e00258.
- [3] U. Dolinar, G. Trtnik, G. Turk, T. Hozjan, The feasibility of estimation of mechanical properties of limestone concrete after fire using nondestructive methods, *Constr. Build. Mater.* 228 (2019) 116786.
- [4] G.W. Greene, Test hammer provides new method of evaluating hardened concrete, *ACI J. Proc.* 51 (11) (1954) 249-256.
- [5] R. Jones, The ultrasonic testing of concrete, *Ultrasonics* 1 (2) (1963) 78-82.
- [6] K.C. Hover, Case studies of non-destructive test results and core strengths at age of 3-days, *Constr. Build. Mater.* 227 (2019) 116672.
- [7] H. Qasrawi, Effect of the position of core on the strength of concrete of columns in existing structures, *J. Build. Eng.* 25 (2019) 100812.
- [8] J.H. Bungey, S.G. Millard, M.G. Grantham, *Testing of Concrete in Structures*, London: Taylor & Francis, 2006 p. 352. (2006).
- [9] ACI-228.1R-19, In-place methods to estimate concrete strength (2019).

-
- [10] D.J. Victor, Evaluation of hardened field concrete with rebound hammer, *ACI Mater. J.* 37 (11) (1963) 407-411.
- [11] J. Kolek, An appreciation of the Schmidt rebound hammer, *Mag. Concr. Res.* 10 (28) (1958) 27-36.
- [12] W.E. Grieb, Use of Swiss hammer for establishing the compressive strength of hardened concrete, *Public Roads* 201 (1958) 1-14.
- [13] K. Wesche, Possibilities for the application of ultrasounds in concrete testing, *Bautechnik* 32 (1955) 151-155.
- [14] S. Popovics, J.S. Popovics, Critique of the ultrasonic pulse velocity method for testing concrete, *Proceedings of Nondestructive Testing of Concrete Elements and Structures*, Publ by ASCE, New York, NY, United States San Antonio, TX, USA, 1992, pp. 94-103.
- [15] ASTM-C597-16, Standard test method for pulse velocity through concrete (2016).
- [16] S.F. Selleck, E.N. Landis, M.L. Peterson, S.P. Shah, J.D. Achenbach, Ultrasonic investigation of concrete with distributed damage, *ACI Mater. J.* 95 (1) (1998) 27-36.
- [17] W. Punurai, J. Jarzynski, J. Qu, K.E. Kurtis, L.J. Jacobs, Characterization of entrained air voids in cement paste with scattered ultrasound, *NDT E. Int.* 39 (6) (2006) 514-524.
- [18] J.R. Leslie, W.J. Cheesman, An ultrasonic method of studying deterioration and cracking in concrete structure, *J. Am. Concr. Inst.* 46 (1949) 17-36.
- [19] G. Barluenga, J. Puentes, I. Palomar, C. Guardia, Methodology for monitoring Cement Based Materials at Early Age combining NDT techniques, *Constr. Build. Mater.* 193 (2018) 373-383.
- [20] M. Benaicha, O. Jalbaud, X. Roguiez, A. Hafidi Alaoui, Y. Burtschell, Prediction of Self-Compacting Concrete homogeneity by ultrasonic velocity, *Alexandria Eng. J.* 54 (4) (2015) 1181-1191.
- [21] R. Latif Al-Mufti, A.N. Fried, The early age non-destructive testing of concrete made with recycled concrete aggregate, *Constr. Build. Mater.* 37 (2012) 379-386.
- [22] N.T. Nguyen, Z.-M. Sbartai, J.-F. Lataste, D. Breyse, F. Bos, Assessing the spatial variability of concrete structures using NDT techniques – Laboratory tests and case study, *Constr. Build. Mater.* 49 (2013) 240-250.
- [23] A.M. Ley-Hernandez, D. Feys, J.A. Hartell, Effect of dynamic segregation of self-consolidating concrete on homogeneity of long pre-cast beams, *Mater. Struct.* 52 (1) (2019) 4.
- [24] T. Xu, J. Li, Assessing the spatial variability of the concrete by the rebound hammer test and compression test of drilled cores, *Constr. Build. Mater.* 188 (2018) 820-832.
- [25] Y. Boukari, D. Bulteel, P. Rivard, N.E. Abriak, Combining nonlinear acoustics and physico-chemical analysis of aggregates to improve alkali-silica reaction monitoring, *Cem. Concr. Res.* 67 (2015) 44-51.
- [26] H. Sasanipour, F. Aslani, Effect of specimen shape, silica fume, and curing age on durability properties of self-compacting concrete incorporating coarse recycled concrete aggregates, *Constr. Build. Mater.* 228 (2019) 117054.
- [27] G. Washer, P. Fuchs, B.A. Graybeal, J.L. Hartmann, Ultrasonic Testing of Reactive Powder Concrete, *IEEE Trans. Ultrason. Ferroelectr. Freq. Control* 51 (2) (2004) 193-201.
- [28] P.N. Hiremath, S.C. Yaragal, Performance evaluation of reactive powder concrete with polypropylene fibers at elevated temperatures, *Constr. Build. Mater.* 169 (2018) 499-512.
- [29] M. Benaicha, O. Jalbaud, A. Hafidi Alaoui, Y. Burtschell, Correlation between the mechanical behavior and the ultrasonic velocity of fiber-reinforced concrete, *Constr. Build. Mater.* 101 (2015) 702-709.
- [30] M.C.S. Nepomuceno, L.F.A. Bernardo, Evaluation of self-compacting concrete strength with non-destructive tests for concrete structures, *Appl. Sci.* 9 (23) (2019) 5109.
- [31] S. Santos, P.R. da Silva, J. de Brito, Self-compacting concrete with recycled aggregates – A literature review, *J. Build. Eng.* 22 (2019) 349-371.

- [32] A. Santamaría, J.J. González, M.M. Losáñez, M. Skaf, V. Ortega-López, The design of self-compacting structural mortar containing steelmaking slags as aggregate, *Cem. Concr. Compos.* 111 (2020) 103627.
- [33] S.A. Santos, P.R. da Silva, J. de Brito, Mechanical performance evaluation of self-compacting concrete with fine and coarse recycled aggregates from the precast industry, *Materials* 10 (8) (2017) 904.
- [34] A. Singh, Z. Duan, J. Xiao, Q. Liu, Incorporating recycled aggregates in self-compacting concrete: a review, *J. Sustain. Cem. Based Mater.* 9 (3) (2019) 165-189.
- [35] F. Debieb, S. Kenai, The use of coarse and fine crushed bricks as aggregate in concrete, *Constr. Build. Mater.* 22 (5) (2008) 886-893.
- [36] C. Pellegrino, F. Faleschini, Experimental behavior of reinforced concrete beams with electric arc furnace slag as recycled aggregate, *ACI Mater. J.* 110 (2) (2013) 197-205.
- [37] M. Etxeberria, A. Gonzalez-Corominas, The assessment of ceramic and mixed recycled aggregates for high strength and low shrinkage concretes, *Mater. Struct.* 51 (5) (2018) 129.
- [38] A.R. Khan, S. Fareed, M.S. Khan, Use of recycled concrete aggregates in structural concrete, *Sustain. Constr. Mater. Technol.* 2 (2019).
- [39] D. Pedro, J. de Brito, L. Evangelista, Durability performance of high-performance concrete made with recycled aggregates, fly ash and densified silica fume, *Cem. Concr. Compos.* 93 (2018) 63-74.
- [40] C. Shi, Y. Li, J. Zhang, W. Li, L. Chong, Z. Xie, Performance enhancement of recycled concrete aggregate - A review, *J. Clean. Prod.* 112 (2016) 466-472.
- [41] F. Fiol, C. Thomas, C. Muñoz, V. Ortega-López, J.M. Manso, The influence of recycled aggregates from precast elements on the mechanical properties of structural self-compacting concrete, *Constr. Build. Mater.* 182 (2018) 309-323.
- [42] H.S. Gökçe, O. Şimşek, The effects of waste concrete properties on recycled aggregate concrete properties, *Mag. Concr. Res.* 65 (14) (2013) 844-854.
- [43] B.B. Mukharjee, S.V. Barai, Influence of Nano-Silica on the properties of recycled aggregate concrete, *Constr. Build. Mater.* 55 (2014) 29-37.
- [44] M. Kazemi, R. Madandoust, J. de Brito, Compressive strength assessment of recycled aggregate concrete using Schmidt rebound hammer and core testing, *Constr. Build. Mater.* 224 (2019) 630-638.
- [45] V. Revilla-Cuesta, M. Skaf, F. Faleschini, J.M. Manso, V. Ortega-López, Self-compacting concrete manufactured with recycled concrete aggregate: An overview, *J. Clean. Prod.* 262 (2020) 121362.
- [46] R. Sri Ravindrajah, Y.H. Loo, C.T. Tam, Strength evaluation of recycled-aggregate concrete by in-situ tests, *Mater. Struct.* 21 (4) (1988) 289-295.
- [47] N. Singh, S.P. Singh, Evaluating the performance of self compacting concretes made with recycled coarse and fine aggregates using non destructive testing techniques, *Constr. Build. Mater.* 181 (2018) 73-84.
- [48] P. Kumar, N. Singh, Influence of recycled concrete aggregates and Coal Bottom Ash on various properties of high volume fly ash-self compacting concrete, *J. Build. Eng.* 32 (2020) 101491.
- [49] EFNARC, Specification Guidelines for Self-compacting Concrete, European Federation of National Associations Representing producers and applicators of specialist building products for Concrete (2002).
- [50] F. Van Der Vurst, S. Grünewald, D. Feys, K. Lesage, L. Vandewalle, J. Vantomme, G. De Schutter, Effect of the mix design on the robustness of fresh self-compacting concrete, *Cem. Concr. Compos.* 82 (2017) 190-201.
- [51] EN-Euronorm, Rue de stassart, 36. Belgium-1050 Brussels, European Committee for Standardization (2020).

- [52] I. González-Taboada, B. González-Fonteboa, J. Eiras-López, G. Rojo-López, Tools for the study of self-compacting recycled concrete fresh behaviour: Workability and rheology, *J. Clean. Prod.* 156 (2017) 1-18.
- [53] E. Güneyisi, M. Gesoğlu, Z. Algin, H. Yazici, Effect of surface treatment methods on the properties of self-compacting concrete with recycled aggregates, *Constr. Build. Mater.* 64 (2014) 172-183.
- [54] D. Carro-López, B. González-Fonteboa, J. De Brito, F. Martínez-Abella, I. González-Taboada, P. Silva, Study of the rheology of self-compacting concrete with fine recycled concrete aggregates, *Constr. Build. Mater.* 96 (2015) 491-501.7102.
- [55] Proceq, Sclerometer types N and NR: instructions for use (2020).
- [56] I. Facadaru, Non-destructive testing of concrete in Romania., *Non-Destructive Testing 2* (1) (1969) 48.
- [57] H. Okamura, M. Ouchi, Self-compacting concrete, *J. Adv. Concr. Technol.* 1 (2003) 5-15.
- [58] C. Sun, Q. Chen, J. Xiao, W. Liu, Utilization of waste concrete recycling materials in self-compacting concrete, *Resour. Conserv. Recycl.* 161 (2020) 104930.
- [59] H. Salehi, M. Mazloom, Opposite effects of ground granulated blast-furnace slag and silica fume on the fracture behavior of self-compacting lightweight concrete, *Constr. Build. Mater.* 222 (2019) 622-632.
- [60] I. González-Taboada, B. González-Fonteboa, F. Martínez-Abella, S. Seara-Paz, Analysis of rheological behaviour of self-compacting concrete made with recycled aggregates, *Constr. Build. Mater.* 157 (2017) 18-25.
- [61] T.A. Rebello, R. Zulcão, J.L. Calmon, R.F. Gonçalves, Comparative life cycle assessment of ornamental stone processing waste recycling, sand, clay and limestone filler, *Waste Manage. Res.* 37 (2) (2019) 186-195.
- [62] Z. Duan, A. Singh, J. Xiao, S. Hou, Combined use of recycled powder and recycled coarse aggregate derived from construction and demolition waste in self-compacting concrete, *Constr. Build. Mater.* 254 (2020) 119323.
- [63] O.K. Djelloul, B. Menadi, G. Wardeh, S. Kenai, Performance of self-compacting concrete made with coarse and fine recycled concrete aggregates and ground granulated blast-furnace slag, *Adv. Concr. Constr.* 6 (2) (2018) 103-121.
- [64] W.C. Jau, C.T. Yang, Development of a modified concrete rheometer to measure the rheological behavior of conventional and self-consolidating concretes, *Cem. Concr. Compos.* 32 (6) (2010) 450-460.
- [65] S.C. Kou, C.S. Poon, Properties of self-compacting concrete prepared with coarse and fine recycled concrete aggregates, *Cem. Concr. Compos.* 31 (9) (2009) 622-627.
- [66] A. Santamaría, V. Ortega-López, M. Skaf, J.A. Chica, J.M. Manso, The study of properties and behavior of self compacting concrete containing Electric Arc Furnace Slag (EAFS) as aggregate, *Ain Shams Eng. J.* 11 (1) (2020) 231-243.
- [67] R. Feiz, J. Ammenberg, L. Baas, M. Eklund, A. Helgstrand, R. Marshall, Improving the CO2 performance of cement, part I: Utilizing life-cycle assessment and key performance indicators to assess development within the cement industry, *J. Clean. Prod.* 98 (2015) 272-281.
- [68] D. Breyse, X. Romão, M. Alwash, Z.M. Sbartai, V.A.M. Luprano, Risk evaluation on concrete strength assessment with NDT technique and conditional coring approach, *J. Build. Eng.* 32 (2020) 101541.
- [69] F. Moutassem, S.E. Chidiac, Assessment of concrete compressive strength prediction models, *KSCE J. Civ. Eng.* 20 (1) (2016) 343-358.
- [70] A.S. Brand, A.N. Amirkhanian, J.R. Roesler, Flexural capacity of full-depth and two-lift concrete slabs with recycled aggregates, *Transp. Res. Rec.* 2456 (2014) 64-72.
- [71] C.K. Mahapatra, S.V. Barai, Sustainable self compacting hybrid fiber reinforced concrete using waste materials, *Struct. Concr.* 20 (2) (2019) 756-765.

[72] V. Revilla-Cuesta, V. Ortega-López, M. Skaf, J.M. Manso, Effect of fine recycled concrete aggregate on the mechanical behavior of self-compacting concrete, *Constr. Build. Mater.* 263 (2020) 120671.

[73] L. Rojas-Henao, J. Fernández-Gómez, J.C. López-Agüí, Rebound hammer, pulse velocity, and core tests in self-consolidating concrete, *ACI Mater. J.* 109 (2) (2012) 235-243.

Article 6

Assessment of longitudinal and transversal plastic behavior of recycled aggregate self-compacting concrete: a two-way study

Title: Assessment of longitudinal and transversal plastic behavior of recycled aggregate self-compacting concrete: a two-way study

Authors: Víctor Revilla-Cuesta, Marta Skaf, Amaia Santamaría, Vanesa Ortega-López, Juan M. Manso

Journal: Construction and Building Materials

Year: 2021

Volume: 292

Article number: 123426

DOI: <https://doi.org/10.1016/j.conbuildmat.2021.123426>

Journal classification (2019 JCR ranking data): 11/134 (engineering, civil). First quartile (Q1), first decile (D1)

ABSTRACT

Plastic strain behavior in the transversal direction to the axis of loading has often been underestimated in concrete design and its strength performance. However, as this article demonstrates, it is fundamental to define the viability of using concrete of a certain composition in real applications. In this study, 15 Self-Compacting Concrete (SCC) mixtures produced with Recycled Concrete Aggregate (RCA) and Ground Granulated Blast Furnace Slag (GGBFS) were subjected to a monotonic-load test and a 5-cycle loading/unloading test with increasing maximum loads. Continuous monitoring of the applied loads and the SCC strain was performed. In the transversal direction, these tests caused the appearance of a yield step, cracking by vertical splitting, and higher levels of deformability than in the longitudinal direction. It was concluded that the RCA content of SCC should be defined according to serviceability conditions when used in compressed elements, to safeguard against failure due to transversal plastic strain.

Keywords: loading/unloading test; longitudinal and transversal strain; plastic behavior; recycled concrete aggregate; self-compacting concrete; stress-strain curves.

1. INTRODUCTION

Concrete is not a continuous medium, due to the heterogeneity and lack of dislocations caused by its composition (cement, water, aggregate, and air) [1]. Its variable composition implies a mechanical performance in the hardened state of varying degrees of complexity [2, 3]. Furthermore, its workability is also of relevance in the fresh state and must be considered during the design process [4]. Self-Compacting Concrete (SCC) is one of the most outstanding concretes with regard to ease of placement, because it needs no vibration to fill formwork, due to its high flowability [5]. This type of concrete also shows a high mechanical strength when correctly designed [6]. The good strength behavior of SCC and the fact that no vibration is needed for its placement reduces energy consumption and significantly facilitates the filling of formwork [7, 8], advantages that explain its ongoing study within the construction and building sector [9].

Concrete has a high stiffness that limits any internal strain, so its plastic behavior under compressive loading is not a widely studied field [10]. Likewise, internal strain causes cracking within concrete, which hinders the measurement of its strain when loading [11]. Nevertheless, the classical stress-strain curve of concrete is well-known: it initially shows an elastic linear section characterized by its modulus of elasticity [12] and, subsequently, a curved region of plastic deformation, with no clear separation between both zones [13]. Hence, a yielding region appears, in which the strain increases with a low variation in stress [14]. Although variations in concrete mix compositions will hardly modify the general pattern of behavior, they can cause specific modifications. For example, increasing the fines content will increase concrete workability [5] and the yield region of the curve [13]. Another example is the addition of fibers to concrete, which sew its cracks and increase the ultimate failure strain of the material [15, 16]. On the other hand, the application of compressive stress causes tension within concrete in the transversal direction (circumferential or tangential), perpendicular to the direction of load application. The strain behavior of concrete in this direction in the elastic regime is defined by the Poisson's coefficient [8]. A value of 0.2 is assumed to be the conventional Poisson's coefficient to apply to concrete [3, 17]. The authors of this research work have found no study that assesses the plastic behavior of non-confined concrete in the transversal direction.

The use of wastes as substitutes for cement clinker [18] and Natural Aggregate (NA) [19] to manufacture concrete is a major research line that aims to increase the sustainability of the construction sector [20]. Among the residues that have been validated as hydraulic binders [8], Ground Granulated Blast Furnace Slag (GGBFS) is one of the most outstanding [21]. Although previously used for soil stabilization [22], in recent years it has been used in the development of medium-strength concretes [23]. Steel slag [24] and construction and demolition waste [25] are examples of valid wastes for the optimal replacement of NA in different proportions [26], although in this study the behavior of Recycled Concrete Aggregate (RCA) is evaluated. This by-product, obtained by crushing rejected concrete precast components [27], has been used to develop concretes with good workability and strength [28]. In addition, it has even been used in recent years in non-conventional concretes, such as SCC [29].

Studies related to the addition of by-products to concrete, including SCC, have mainly been focused on their workability and mechanical properties [30] and on the behavior of structural elements [31]. However, the effect of these alternative materials on the plastic behavior of hardened concrete has not been studied in detail. It is known that the addition of GGBFS as a substitute for cement clinker decreases the modulus of elasticity of concrete [32]. Concerning RCA, only the influence of the coarse fraction on the stress-strain behavior of concrete in the longitudinal direction has been evaluated so far. Its usage reduces the strain levels upon fracture [33] and increases the cracking tendency of concrete [34]. Furthermore, it has been observed that pre-treatment of this waste can also alter the plastic behavior of concrete [35]: the use of coarse carbonated RCA decreases compressive strength, but increases strain at the maximum point of the stress-strain curve [36]. These aspects are specific alterations to plastic behavior, since the general shape of the stress-strain curve undergoes no significant change whenever the concrete composition is slightly modified [37].

In general, the stress-strain behavior of concrete under a plastic regime, in both the longitudinal and transversal directions, has hardly been studied. Furthermore, studies of concrete plastic behavior in the transversal direction have mainly been limited to concrete elements subjected to lateral confinement [38], regardless of whether NA or some type of waste was used in their manufacture [39, 40]. The energy that can be released from concrete depends on these boundary conditions [41], which also limit its transversal deformability [42]. In that regard, this confinement improves the performance of recycled concrete more than the performance of concrete manufactured with NA [33, 43]. The authors of this paper have found no other study that presents an analysis of transversal plastic behavior without confinement in any type of concrete. Hence, the objective of this study is to perform a detailed examination of the plastic performance of non-

confined self-compacting concrete, which was chosen because it can be used in any structural application that demands high workability in the fresh state [6]. The additional inclusion of GGBFS and coarse and fine RCA enhances the global sustainability of these structural concretes. All these aspects are part of a broader research project conducted by the same research group, which addresses the behavior of SCC produced with these wastes/by-products.

A total of 15 self-compacting concrete mixes were produced with and without GGBFS and coarse RCA, and with different percentages and fractions of fine RCA. All mixtures were subjected to two tests for detailed evaluation of their strength and deformability [44]. On the one hand, a monotonic-load test was performed in which the load increased at a constant rate and, on the other hand, a low-cycle alternating load test, in which the specimens were subjected to successive loading/unloading cycles of increasing magnitude. In both tests, the load applied, and the longitudinal and transversal strain levels of the SCC were continuously monitored.

2. MATERIALS AND METHODS

In this section, an explanation is provided for each raw material in use, the composition of the different mixtures under study, and the experimental procedure developed for the analysis of the main aspects.

2.1. MATERIALS

Two different types of cement were used according to EN 197-1 [45]: CEM I 52.5 R, with a density of 3.1 Mg/m^3 and a clinker content of 98%, and a sustainable CEM III/A 42.5 N, with a density of 3 Mg/m^3 , and a content of around 45% GGBFS. Mains water was supplied from the urban water supply of Burgos, Spain, where the investigation took place. Two admixtures were used to achieve an optimum self-compactability of the mixtures: a viscosity regulator and a plasticizer, labelled A1 and A2 (admixtures 1 and 2), respectively.

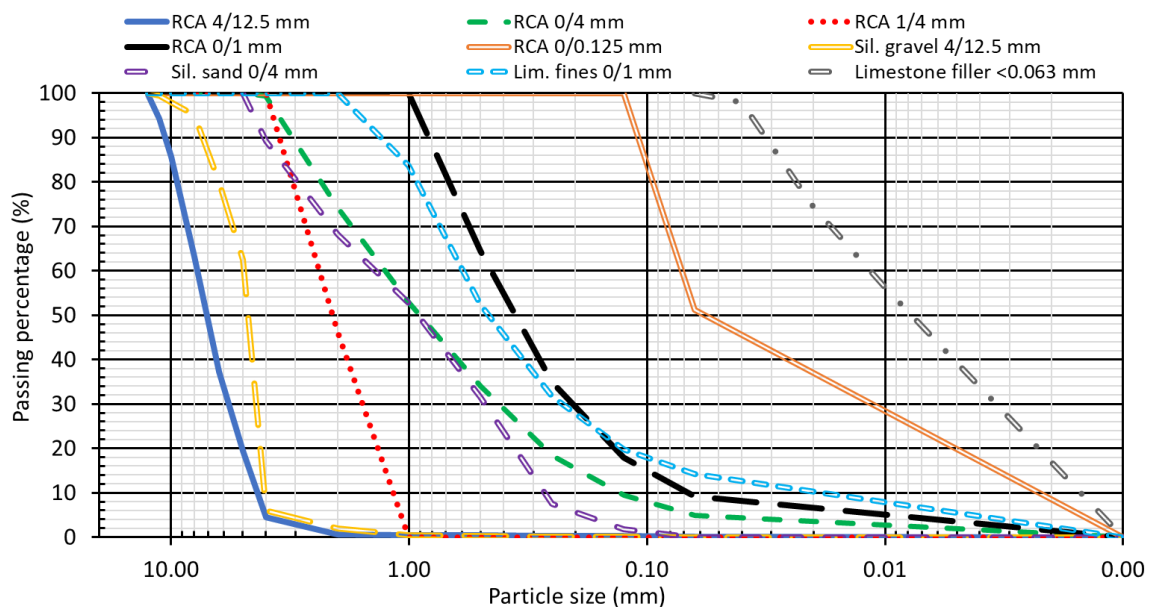


Figure 6.1. Aggregate gradation

In addition to GGBFS, some SCC samples incorporated RCA. This material was obtained by crushing rejected precast elements with a characteristic strength of 45 MPa. Its original granulometry, 0/31.5 mm, was separated into several fractions (4/12.5, 0/4, 1/4, 0/1, and 0/0.125 mm) by sieving, to obtain a maximum aggregate size suitable for SCC production (12.5 mm), and to study the effect of each RCA fraction in detail. When the coarse, fine and powder fractions of the mixtures were not 100% RCA, siliceous gravel (4/12.5 mm) and/or sand (0/4 mm), limestone fines 0/1 mm and

limestone filler (<0.063 mm) were added. The density and water absorption levels (EN 1097-6 [45]) of all the aggregates are shown in Table 6.1 and their gradation curves are depicted in Figure 6.1.

Table 6.1. Physical properties of aggregates

Aggregate	Saturated-surface-dry density (Mg/m ³)	15 min water absorption (%)	24 h water absorption (%)
RCA 4/12.5 mm	2.42	5.33	6.25
RCA 0/4 mm	2.37	6.18	7.36
RCA 1/4 mm	2.38	5.75	6.94
RCA 0/1 mm	2.36	6.76	7.47
RCA 0/0.125 mm	2.29	6.93	8.09
Siliceous gravel 4/12.5 mm	2.62	0.71	0.84
Siliceous sand 0/4 mm	2.58	0.18	0.25
Limestone fines 0/1 mm	2.62	1.88	2.53
Limestone filler < 0.063 mm	2.77	-	0.54

2.2. MIXES DESIGN

Firstly, three self-compacting reference mixes labelled ICM, IIICM1 and IIIICM2 were developed, in which the slump-flow design was between 700 and 850 mm (EN 12350-8 [45]). This flowability was achieved by adjusting the content of particles under 0.25 mm in accordance with the Fuller curve (see Figure 6.2). These mixtures were produced with 100% NA in all fractions and with a range of cement types and amounts. Mix ICM was manufactured with CEM I, and mix IIICM1 with CEM III/A. In these two control mixes, the amount of cement was the same (300 kg/m³). The cement content of mix IIIICM2 was increased by 40% to provide a similar 28-day compressive strength to mixes ICM and IIIICM2, as GGBFS provides lower strength than conventional cement clinker [46]. Furthermore, the admixtures proportion was in all cases the same: 2.3 kg/m³ of A1 and 4.5 kg/m³ of A2, respectively.

Table 6.2. Composition of batch 1 mixes (kg per cubic meter)

Material	ICM	I50N	I50R ¹	IIIICM1	III50N	III50R ¹
CEM I	300			0		
CEM III/A	0			300		
Water	170	200	225	170	200	225
Limestone fines 0/1 mm	225	430	0	225	430	0
Limestone filler < 0.063 mm	115		0	115		0
RCA 0/1 mm	0		385	0		385
RCA 0/0.125 mm	0		95	0		95
RCA 4/12.5 mm	0	530		0	530	
NA 4/12.5 mm	575	0		575	0	
RCA 1/4 mm	0	205		0	205	
NA 0/4 mm	940	475		940	475	

¹Although these mixtures were labelled *R*, part of the aggregate fraction 0/1 mm was siliceous sand 0/4 mm

After developing the reference mixtures, twelve concrete mixes with RCA were designed, in which 100% coarse NA (size 4/12.5 mm) was replaced by RCA. Subsequently, different fine RCA contents and fractions (0/4, 1/4, 0/1, and 0/0.125 mm) were progressively added (in partial or total substitution of the fine NA and aggregate powder of the reference mixes), as explained below, due to the singularly high fine aggregate (size 0/4 mm) content of SCC, and due to its high sensitivity to changes in this aggregate fraction, particularly the aggregate powder [5]. Detailed in section 3.2,

the mechanical tests of the mixtures yielded successful and coherent results that supported these progressive substitutions.

Table 6.3. Composition of batch 2 mixes (kg per cubic meter)

Material	ICM	I0	I50	I100	I100R
CEM I	300				
Water	170	185	210	235	255
Limestone fines 0/1 mm	225				0
Limestone filler < 0.063 mm	115				0
RCA 0/1 mm	0				200
RCA 0/0.125 mm	0				95
RCA 4/12.5 mm	0	530			
NA 4/12.5 mm	575	0			
RCA 0/4 mm	0		435	865	
NA 0/4 mm	940		475	0	

Table 6.4. Composition of batch 3 mixes (kg per cubic meter)

Material	IIICM2	III0	III50	III100	III100R
CEM III/A	425				
Water	170	185	210	235	255
Limestone fines 0/1 mm	225				0
Limestone filler < 0.063 mm	115				0
RCA 0/1 mm	0				200
RCA 0/0.125 mm	0				95
RCA 4/12.5 mm	0	430			
NA 4/12.5 mm	440	0			
RCA 0/4 mm	0		435	865	
NA 0/4 mm	940		475	0	

Finally, the “effective water-to-cement” ratio remained constant in all mixtures (0.50 in mixes with CEM I and 0.40 in mixes with CEM III/A), by increasing the water content to meet the water absorption (see Table 6.1) of the RCA after 15 minutes [30], which was the mixing time (see section 2.3).

The RCA mixes were labelled either *I* (CEM I) or *III* (CEM III/A) followed by the substitution percentage of NA 0/4 mm by RCA 0/4 mm. In addition, the letter *N* or *R* was added to some of the labels, depending on whether the aggregates smaller than 1 mm were either NA or RCA. The compositions of all the mixtures, once divided into the three batches detailed below, are shown in Table 6.2, Table 6.3 and Table 6.4, in which the different quantities are given in kg of each component per cubic meter of concrete.

- Batch 1. In this batch, the effects of both CEM I and CEM III/A, used in the same amounts, were assessed. The reference mix *par excellence* in this research work was ICM, although mixture ICM1 can also be considered a “partial reference” with regard to mixtures III50N, and III50R. First, the volume of the coarse fraction (4/12.5 mm) of NA was completely substituted by RCA 4/12.5 mm. Subsequently, 50% of fine NA 1/4 mm by volume was replaced with RCA of the same gradation (1/4 mm), in accordance with the results of a previous study of this research group [47], in which 50% fine NA was advanced as the maximum RCA replacement ratio for suitable mechanical behavior. The aggregate fraction 0/1 mm of these mixes was entirely NA. These two mixes were labelled I50N and III50N. Finally, as shown in Table 6.2, the aggregate fraction 0/1 mm of mixes I50N and III50N was

replaced with RCA, thereby defining mixes I50R and III50R. This particular combination of RCA fractions maintained the self-compactability of concrete mixtures and, at the same time, meant that the effects of RCA 1/4 mm could be separately analyzed from the effects of RCA sized lower than 1 mm. This aspect was studied because RCA 0/1 and 0/0.125 mm are usually the RCA fractions that more than any others weaken concrete strength [48].

- Batch 2. In this batch, the reference mix, ICM, manufactured with type-I cement, and the full replacement of coarse NA with RCA were maintained. In addition, amounts of 0%, 50%, and 100% fine NA 0/4 mm were substituted by fine RCA 0/4 mm, resulting in mixes I0, I50, and I100. These replacement ratios of fine NA were also defined according to the performance observed in a previous study of this research group [47]. Additionally, the effect of adding RCA as aggregate powder was studied in mixture I100R, in which limestone fines 0/1 mm and limestone filler were replaced by RCA. The joint gradation of the batch 2 mixtures is shown in Figure 6.2.
- Batch 3. This group includes all the mixes manufactured with CEM III/A, but with a higher content of cement, as previously explained. The reference mix was labelled IIICM2. Subsequently, mixes III0, III50, III100 and III100R were designed in the same way as the batch 2 mixes.

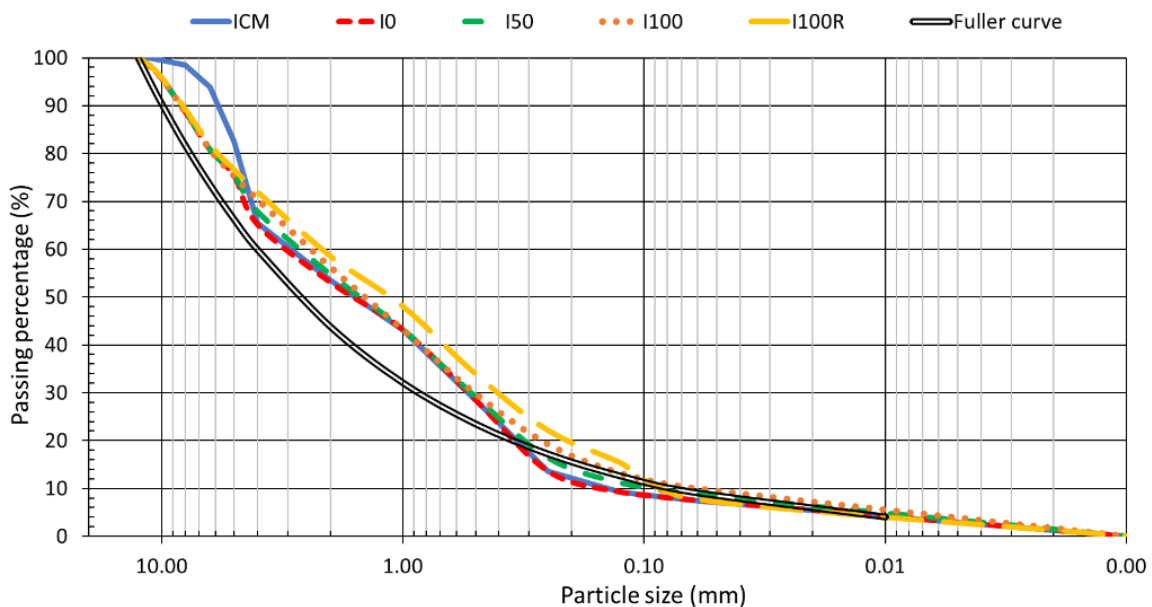


Figure 6.2. Joint gradation of the batch 2 mixes

2.3. MIXING AND TESTING

When an aggregate with high water absorption is used to produce concrete, staged mixing processes will maximize its water absorption and the workability of the concrete [49]. The mixing process that was performed therefore had three different stages: addition of the aggregate and half of the water; addition of the cement and the rest of water; and addition of the admixtures. After each stage, the concrete was mixed for 3 minutes and then left to rest for 2 minutes. These times were defined after different trials with mixing and resting times of between 1 and 5 minutes. Subsequently, the slump flow was checked (EN 12350-8 [45]) and six 10x20-cm cylindrical specimens were produced and placed in a moist room (humidity $95\pm 5\%$ and temperature $20\pm 2\text{ }^\circ\text{C}$) until the performance of the following tests:

- Determination of compressive strength (EN 12390-3 [45]), modulus of elasticity, and the Poisson's coefficient (EN 12390-13 [45]) of all mixtures at 28 days on 2 specimens.

- Monotonic-load test, similar to standard compressive-strength tests, which consisted of the progressive displacement of the head frame at a constant rate.
- Loading/unloading test of increasing magnitude to evaluate the evolution of the stiffness of the mixtures. These last two tests were performed on two specimens after 90 days of curing, a point in time when many concrete structures are already in service [31].

In the second and third tests, the load applied and the effects of both longitudinal and transversal strain on the concrete were continuously recorded. The recording of the strain was done by six strain gauges, three in the longitudinal (vertical) direction and three in the transversal (circumferential or tangential) direction, evenly distributed around the perimeter of the specimen in the central zone of its shaft. 2 LVDTs set to measure loading piston displacement completed the measurements in the longitudinal direction. The applied load was measured with a calibrated load cell. A diagram of the test set up is shown in Figure 6.3.

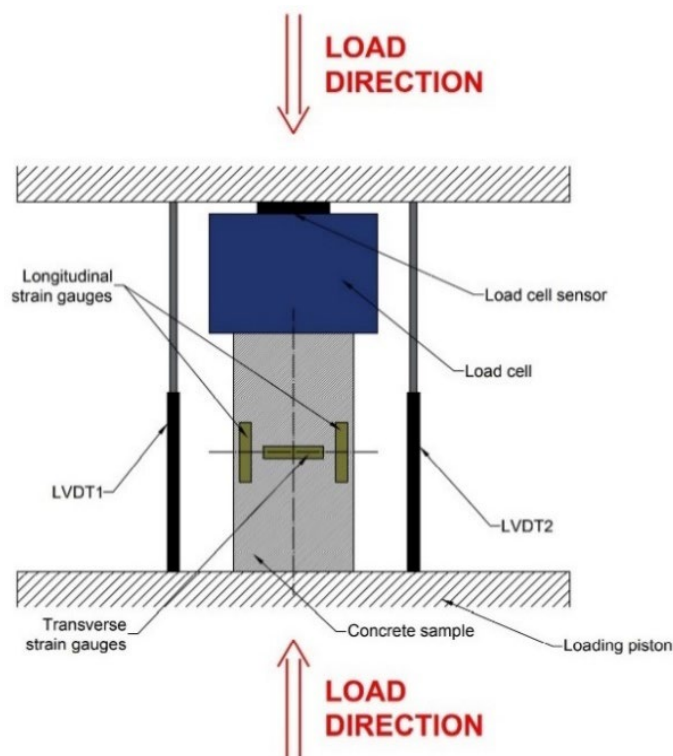


Figure 6.3. Assembly diagram for data recording

3. RESULTS AND DISCUSSION

In this section, the results of the different tests indicated in the experimental plan are reported.

3.1. FRESH BEHAVIOR: SLUMP-FLOW TEST

All the mixtures had the defined target slump flow at the beginning of the study, between 700 and 850 mm, as shown in Figure 6.4. All changes made to the composition of the mixtures modified the slump flow:

- CEM III/A has a higher grinding fineness than CEM I, which hinders the uniform dragging of aggregate particles in SCC [32]. Therefore, when the quantity of both cements remained constant, the use of CEM III/A reduced the slump flow (batch 1 mixtures). However, the decrease of the coarse aggregate content improved the slump flow of the CEM III/A mixtures in comparison with the CEM I mixtures (batches 2 and 3) [50].
- The irregular shape of coarse RCA compared to siliceous gravel [13] decreased the slump flow of the mixtures when it was incorporated.

- Finally, the higher content of particles smaller than 0.25 mm of RCA 0/4 mm compared to siliceous sand (see Figure 6.1) yielded a more compact cement paste that dragged the aggregate particles more easily [5]. Therefore, the higher the content of RCA 0/4 mm, the higher the slump flow, although it was reduced with the use of RCA as aggregate powder (mixes I50R, III50R, I100R, and III100R), possibly due to its more irregular shape compared to limestone fines 0/1 mm and filler.

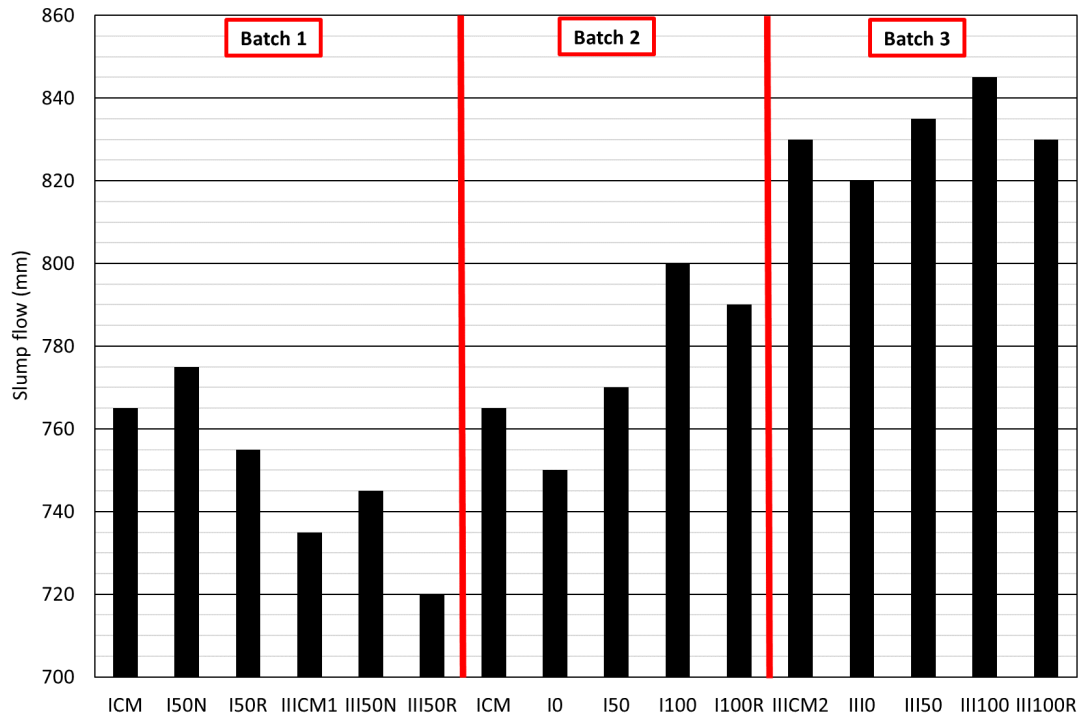


Figure 6.4. Slump flow of the mixes

3.2. COMPRESSIVE STRENGTH AND ELASTIC PROPERTIES

Compressive strength, modulus of elasticity and the Poisson's coefficient values at 28 and 90 days of all the mixtures of the three batches are shown in Figure 6.5. The compressive strengths and the moduli of elasticity, as well as their temporal increase (from 28 to 90 days) [47], decreased with the addition of all RCA fractions in all the batches [2]. Regarding the absolute values of both properties, the inclusion of coarse RCA rather than coarse NA signified a notable loss of concrete strength (IO and III0 versus ICM, and IIICM2, respectively), due to weaker Interfacial Transition Zones (ITZ) [2]. The partial substitution of fine NA by fine RCA caused even greater loss of strength (50N and I50 versus ICM; III50N versus IIICM1; and III50 versus IIICM2), due to the presence of mortar particles in this RCA fraction, as well as increased adherence problems between the aggregate and the cementitious matrix [47]. The total replacement of NA with RCA increased this damage even more (I100 and III100 versus I50 and III50, respectively). Finally, the effects of RCA aggregate powder additions (I50R versus I50N; III50R versus III50N; I100R versus I100; and III100R versus III100) could be qualified as dramatic, as the compressive strength of mixes I50R, III50R, I100R and III100R never even reached the minimal value for structural concrete (20 MPa) [3, 17]. The smaller the RCA fraction that was used, the more damaging its effect on the mechanical behavior of concrete [51]. The use of CEM III/A in higher amounts (batch 3 mixes) hardly modified the effect of RCA, although it yielded higher compressive strengths than those of batch 2 mixes, despite the similar compressive strengths of the reference mixes (ICM and IIICM2). The higher cement content could have partially compensated the negative effects of the RCA [52].

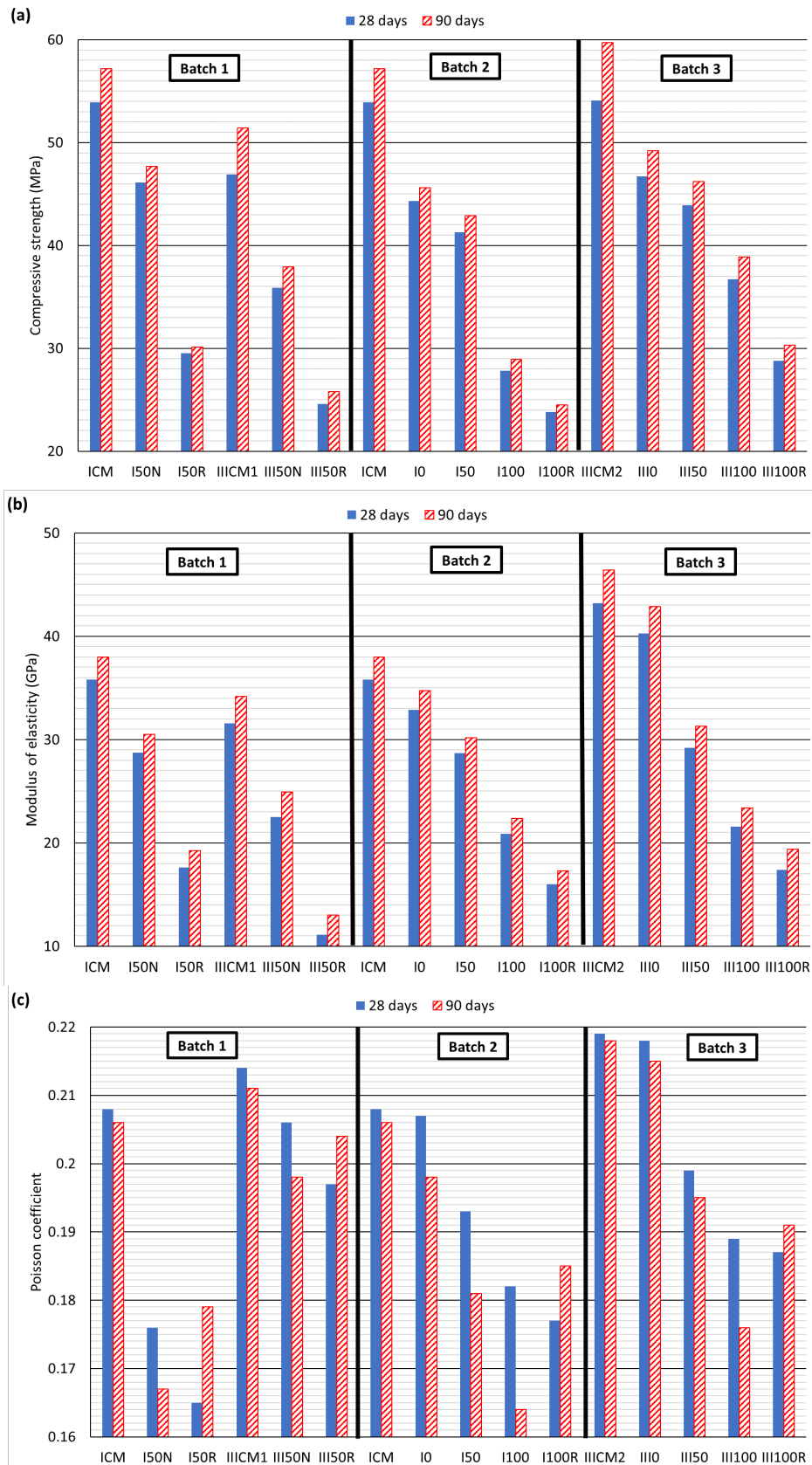


Figure 6.5. Temporal evolution of (a) compressive strength; (b) modulus of elasticity; (c) Poisson's coefficient

The temporal increase was greater when CEM III/A was used, because of its slower development of strength [46]. However, as has been stated, the growing presence of RCA reduced this temporal increase. Thus, the compressive-strength increase in both absolute and percentage terms was 3.3

(5.8%) and 5.6 (9.4%) MPa for reference mixes ICM and IICM2, respectively; 1.3 (2.9%) and 2.5 (5.1%) MPa for mixes IO and III0; and only 0.7 (2.8%) and 1.7 (4.9%) MPa for mixtures I100R and III100R.

The addition of any RCA fraction decreased the Poisson's coefficient at 28 days, while the use of CEM III/A increased it. Furthermore, this coefficient generally decreased over time, especially when using CEM I (a decrease from 28 to 90 days of 5.1 and 4.3% for mixes I50N and IO respectively, and only 3.9 and 1.4% for mixes III50N and III0) and RCA 0/4 mm (decrease from 28 to 90 days of 9.9 and 6.9% for mixes I100 and III100). However, the addition of the finest RCA fractions (0/1 and 0/0.125 mm) increased the value of this coefficient over time, possibly due to the increase of transversal deformability that resulted from the delayed release of water absorbed by these RCA fractions during mixing [49].

3.3. MONOTONIC-LOAD TEST

The monotonic-load test and the compressive-strength test were performed in similar ways, although the applied load and both longitudinal and transversal concrete strain levels were continuously recorded during the former test. Previous trials demonstrated that undesired sudden failure of the specimens, which might hinder strain measurements [37], was avoided by setting the load application rate at 1 kN/s. This rate was lower than the standard recommendation in ASTM C39 [53], 2.2 kN/s, but no problem was detected during the performance of the test. Data were recorded at a frequency of 20 Hz.

3.3.1. LONGITUDINAL DIRECTION

The stress-strain curves using conventional engineering variables for compressive tests underlined the aspects indicated in the introduction, as shown in Figure 6.6 (right-hand-side curves): a linear elastic section followed by a plastic curved zone with no clear separation between both [3, 17]. A quasi-linear elastic region probably existed after the proportionality limit before the plain yielding region was reached. The main values of this curve for all the mixtures are shown in Table 6.5: the modulus of elasticity, the limit of proportionality, the point of maximum stress (thereafter peak point) and the strain at final fracture.

The addition of 100% coarse RCA not only decreased the strength and the modulus of elasticity of the mixtures, as explained in section 3.2 [48], but also the strain at peak point and fracture point by around 12% (mixture IO versus ICM, and mixture III0 versus IICM2), as has also been shown in other studies [33].

The addition of fine RCA decreased the stiffness and strength of SCC and increased its plastic deformability [54]. On the one hand, the higher the amounts of RCA fractions, the greater the deformability of the mix at peak point and at fracture point. On the other, the replacement of CEM I by CEM III/A caused a similar effect to fine RCA, although the increase in the total binder content (batch 3 mixtures) decreased that deformability.

The expressions and values in current concrete standards approximate the main results of the stress-strain curve. These expressions and values provide safe estimates for conventional concretes.

- The peak strain can be calculated by Equation 6.1 of the model code of the International Federation for Structural Concrete (CEB-FIP) [55], in which $f_{c,m}$ and ε_0 are, respectively, the stress (MPa) and the peak strain (‰) measurements. Both in EC2 [3] and in ACI 318-19 [17], this value is estimated at 2,000 $\mu\epsilon$.

$$\varepsilon_0 = 0.7 \cdot f_{c,m}^{0.31} \quad (6.1)$$

- Strain at fracture is estimated at 3,000 $\mu\epsilon$, according to ACI 318-19 [17], and at 3,500 $\mu\epsilon$, according to EC2 [3].

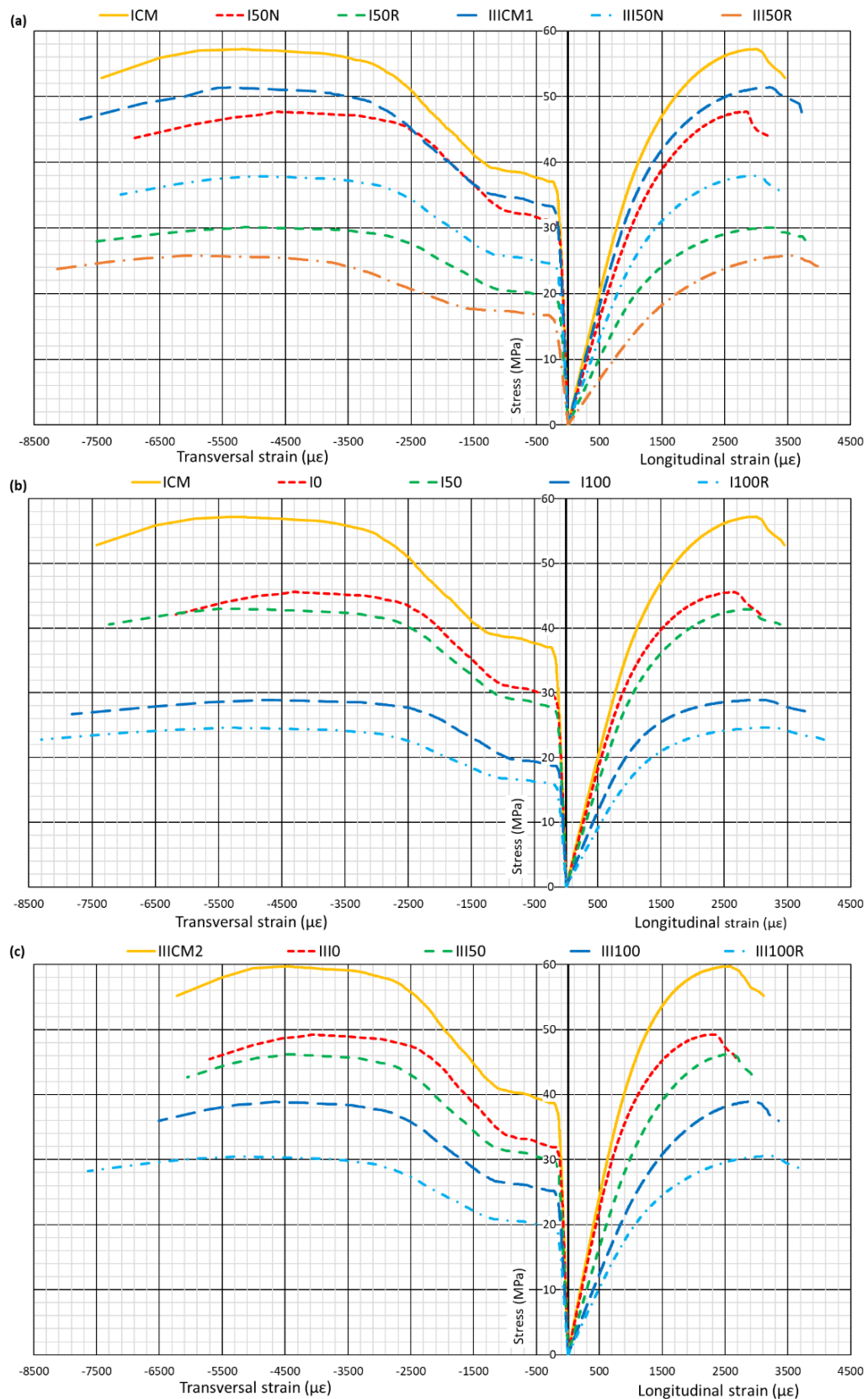


Figure 6.6. Stress-strain curves in the longitudinal and transversal directions in the monotonic-load test: (a) batch 1; (b) batch 2; (c) batch 3

Table 6.5. Main values of stress-strain curves in the longitudinal direction. For the proportional limit and the strain at fracture, the ratio (%) to the peak point appears between brackets

Batch	Mix	ELASTIC BEHAVIOR		
		Modulus of elasticity (GPa)	Proportional limit	
			Stress (MPa)	Strain ($\mu\epsilon$)
Batch 1	ICM	39.6	33.2 (58.0)	873 (29.1)
	I50N	31.8	27.9 (58.5)	915 (32.1)
	I50R	20.1	16.8 (55.8)	875 (26.7)
	IIICM1	35.6	30.0 (58.4)	877 (27.2)
	III50N	26.0	22.6 (59.6)	908 (30.2)
	III50R	13.6	15.3 (59.3)	1,177 (32.4)
Batch 2	ICM	39.6	33.2 (58.0)	873 (29.1)
	I0	36.2	25.9 (56.8)	746 (28.1)
	I50	31.5	25.7 (59.9)	851 (29.1)
	I100	23.3	17.4 (60.2)	777 (24.9)
	I100R	18.0	13.8 (56.1)	798 (24.4)
Batch 3	IIICM2	48.4	35.8 (60.0)	771 (29.8)
	III0	44.7	28.3 (57.5)	660 (28.4)
	III50	32.6	27.5 (59.5)	879 (33.6)
	III100	24.4	22.5 (57.8)	962 (32.4)
	III100R	20.2	18.4 (60.3)	948 (29.2)

Table 6.5 (continued). Main values of stress-strain curves in the longitudinal direction. For the proportional limit and the strain at fracture, the ratio (%) to the peak point appears between brackets

Batch	Mix	PLASTIC BEHAVIOR		
		Peak point		Strain at fracture ($\mu\epsilon$)
		Stress/compressive strength (MPa)	Strain ($\mu\epsilon$)	
Batch 1	ICM	57.2	2,996	3,452 (115.2)
	I50N	47.7	2,847	3,228 (113.4)
	I50R	30.1	3,277	3,808 (116.2)
	IIICM1	51.4	3,220	3,754 (116.6)
	III50N	37.9	3,003	3,454 (115.0)
	III50R	25.8	3,632	4,125 (113.6)
Batch 2	ICM	57.2	2,996	3,452 (115.2)
	I0	45.6	2,659	3,073 (115.6)
	I50	42.9	2,923	3,386 (115.8)
	I100	28.9	3,115	3,925 (126.0)
	I100R	24.6	3,272	4,071 (124.4)
Batch 3	IIICM2	59.7	2,589	3,111 (120.2)
	III0	49.2	2,324	2,685 (115.5)
	III50	46.2	2,616	2,952 (112.8)
	III100	38.9	2,967	3,352 (113.0)
	III100R	30.5	3,247	3,762 (115.9)

Table 6.6. Comparison between experimental and theoretical values in the longitudinal direction

Batch	Mix	MODULUS OF ELASTICITY (GPa), ASTM C469M-14	STRAIN AT PEAK POINT ($\mu\epsilon$)			FINAL STRAIN AT FRACTURE ($\mu\epsilon$)		
			Theoretical value		Experimental value	Theoretical value		Experimental value
			CEB-FIP [55]	ACI 318-19 [17], EC2 [3]		EC2 [3]	ACI 318-19 [17]	
Batch 1	ICM	39.6	2,454	2,000	2,996	3,500	3,000	3,452
	I50N	31.8	2,320		2,847			3,228
	I50R	20.1	2,011		3,277			3,808
	IIICM1	35.6	2,374		3,220			3,754
	III50N	26.0	2,160		3,003			3,454
	III50R	13.6	1,917		3,632			4,125
Batch 2	ICM	39.6	2,454		2,996			3,452
	I0	36.2	2,288		2,659			3,073
	I50	31.5	2,245		2,923			3,386
	I100	23.3	1,986		3,115			3,925
	I100R	18.0	1,889		3,272			4,071
Batch 3	IIICM2	48.4	2,487		2,589			3,111
	IIIO	44.7	2,342		2,324			2,685
	III50	32.6	2,297		2,616			2,952
	III100	24.4	2,178		2,967			3,352
	III100R	20.2	2,019	3,247	3,762			

The theoretical values of both peak strain and strain at fracture of ACI 318-19 were lower than the experimental values, thus providing a reliable estimate. However, mixtures I50R, IIICM1, III50R, I100, I100R, and III100R (6 of the 15 mixes, all with by-products) reached a higher strain than 3,500 $\mu\epsilon$ at fracture, a value defined by EC2. Finally, the trend shown by Equation 6.1 of the CEB-FIP for peak strain was only fulfilled in mixes with 100% fine NA (ICM, I0, IIICM1, IIICM2, and IIIO), as the loss of compressive strength, due to the addition of fine RCA, increased rather than reduced the peak strain. Table 6.6 depicts a comparison of these deformation values.

3.3.2. TRANSVERSAL DIRECTION

The curves of longitudinal stress versus transversal strain are shown in Figure 6.6 (left-hand-side curves), and their most representative values appear in Table 6.7. These curves initially presented a linear elastic zone with a high slope with no observable microstructural damage to the material. The Poisson's coefficient was around 0.2 units, the precise values of which are shown in Table 6.7 (columns of elastic behavior). This linear elastic region ended at a variable transversal strain of 150-185 $\mu\epsilon$ (except mix III50R, Table 6.7) and a stress value practically equal to the proportional limit in the longitudinal direction that is specified in Table 6.5; hence, both measurements showed an equally coherent proportional limit. The geometric evolution could be qualified as "barreling", due to the barrel shape of a centered bulge and a constraint in both bases, as shown in Figure 6.7a.

Subsequently, a short region with a decreasing slope (between the proportional limit and the start point of yield step, see Figure 6.6) occurred, showing a stress increase of 3-4 MPa and a strain increase of 30-50 $\mu\epsilon$. This region approximately represents the "start of global yielding", focused on the start of micro-structural damage (micro-cracking) in the perimeter region of the zone with the highest bulge (center of the specimen, Figure 6.7b), in which the tensile transversal strain began to exceed the threshold strain that the material can withstand.

Table 6.7. Characteristic values of stress-strain behavior in the transversal direction. The values between brackets are the percentage ratios (%) in relation to the peak point

Batch	Mix	ELASTIC BEHAVIOR				
		Poisson's coefficient	Proportional limit		Start point of yield step	
			Stress (MPa)	Strain ($\mu\epsilon$)	Stress (MPa)	Strain ($\mu\epsilon$)
Batch 1	ICM	0.206	33.2 (58.0)	180 (3.5)	37.1 (64.9)	204 (3.9)
	I50N	0.167	27.8 (58.3)	152 (3.3)	30.3 (63.5)	192 (4.2)
	I50R	0.179	17.0 (56.5)	158 (3.1)	19.6 (65.1)	195 (3.9)
	IIICM1	0.211	29.9 (58.2)	184 (3.4)	33.8 (65.8)	213 (4.0)
	III50N	0.198	22.5 (59.4)	179 (3.6)	24.4 (64.4)	201 (4.1)
	III50R	0.204	15.4 (59.7)	202 (3.4)	16.5 (64.0)	234 (3.9)
Batch 2	ICM	0.206	33.2 (58.0)	180 (3.5)	37.1 (64.9)	204 (3.9)
	IO	0.197	25.8 (56.6)	146 (3.4)	29.7 (65.1)	181 (4.2)
	I50	0.181	25.8 (60.1)	155 (3.3)	27.9 (65.0)	212 (4.4)
	I100	0.164	17.3 (59.9)	127 (2.7)	18.1 (62.6)	164 (3.4)
	I100R	0.185	13.6 (55.3)	145 (2.7)	15.9 (64.6)	193 (3.7)
Batch 3	IIICM2	0.218	35.9 (60.1)	169 (3.8)	38.9 (65.1)	199 (4.5)
	III0	0.215	28.5 (57.9)	143 (3.6)	31.8 (64.6)	211 (5.3)
	III50	0.195	27.6 (59.7)	172 (3.9)	29.8 (64.5)	215 (4.9)
	III100	0.176	22.3 (57.3)	168 (3.6)	25.3 (65.0)	228 (4.9)
	III100R	0.191	18.6 (61.0)	183 (3.5)	19.5 (63.9)	237 (4.6)

Table 6.7 (continued). Characteristic values of stress-strain behavior in the transversal direction. The values between brackets are the percentage ratios (%) in relation to the peak point

Batch	Mix	PLASTIC BEHAVIOR				
		Final point of yield step		Peak point		Strain at fracture ($\mu\epsilon$)
		Stress (MPa)	Strain ($\mu\epsilon$)	Compressive strength (MPa)	Strain ($\mu\epsilon$)	
Batch 1	ICM	39.3 (68.7)	1,211 (23.4)	57.2	5,165	7,427 (143.8)
	I50N	32.7 (68.6)	1,025 (22.2)	47.7	4,612	6,906 (149.7)
	I50R	20.6 (68.4)	1,117 (22.1)	30.1	5,062	7,613 (150.4)
	IIICM1	35.8 (69.6)	1,382 (25.8)	51.4	5,361	7,763 (144.8)
	III50N	26.0 (68.6)	1,179 (23.8)	37.9	4,960	7,124 (143.6)
	III50R	17.7 (68.6)	1,560 (25.9)	25.8	6,027	8,147 (135.2)
Batch 2	ICM	39.3 (68.7)	1,211 (23.4)	57.2	5,165	7,427 (143.8)
	IO	31.2 (68.4)	1,016 (23.7)	45.6	4,288	6,172 (143.9)
	I50	29.4 (68.5)	1,036 (21.7)	42.9	4,768	7,233 (151.7)
	I100	19.8 (68.5)	886 (18.6)	28.9	4,762	7,820 (164.2)
	I100R	16.9 (68.7)	1,078 (20.4)	24.6	5,286	8,302 (157.1)
Batch 3	IIICM2	40.7 (68.2)	1,123 (25.2)	59.7	4,451	6,222 (139.8)
	III0	33.7 (68.5)	973 (24.2)	49.2	4,016	5,697 (141.9)
	III50	31.7 (68.6)	1,124 (25.4)	46.2	4,419	6,052 (137.0)
	III100	26.7 (68.6)	1,149 (24.7)	38.9	4,650	6,505 (139.9)
	III100R	20.9 (68.5)	1,197 (23.0)	30.5	5,206	7,638 (146.7)

That region was followed by a quasi-linear region with a very low (almost horizontal) slope; similar to a yield step in a tensile test of structural steel. This yield region was extended until the “final point of yield step”, shown under the columns of plastic behavior in Table 6.7. A plastic-strain zone with slight micro-structural damage, in which the transversal strain of the concrete increased from

150-185 to around $1,000 \mu\epsilon$ and the stress increased in the order of 1-2 MPa. This increase in transversal tensile strain was associated with generalized micro-cracking of the specimen increasing the micro-structural damage, moving from the situation in Figure 6.7b to the situation in Figure 6.7c. The micro-cracking was produced by vertical splitting, *i.e.*, the cracks were generated on the lateral periphery of the test specimen, a zone under greater strain and stress due to the bulging of the specimen. They then propagated in both vertical directions throughout the specimen and progressively penetrated towards its central vertical axis on vertical planes, as shown in Figure 6.7b and Figure 6.7c. In addition, this micro-cracking was slow and progressive, so it produced no sudden release of mechanical energy. The generalization of micro-cracking caused a notable increase in the transversal strain of the sample specimen and, at the same time, a significant increase in its apparent (contouring) volume associated with the bulge-barreling.

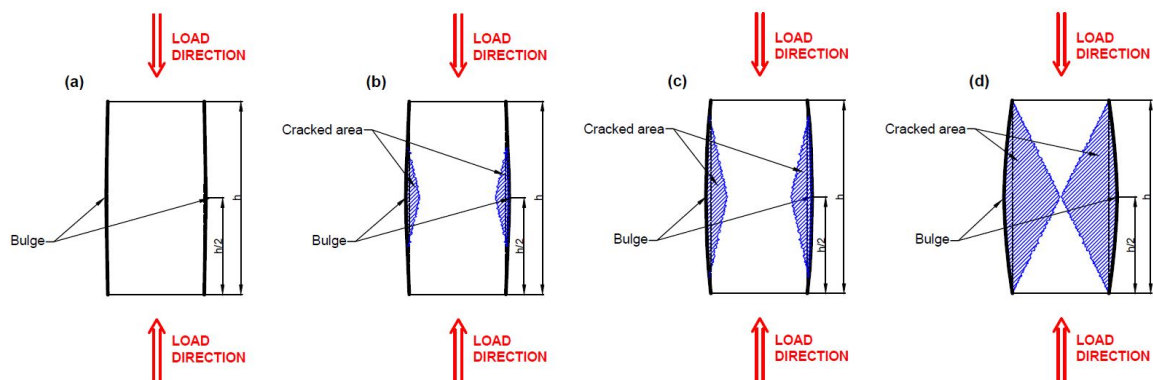


Figure 6.7. Bulging and cracking of a concrete cylindrical sample under compressive loading: (a) elastic region without irreversible damage; (b) halfway intermediate point with partial damage; (c) halfway intermediate point with more extended damage; (d) generalized damage at peak point

From the final point of the yield step to the maximum-stress point (peak point), these curves continued showing a plastic behavior, associated with growth of the damaged region, from the situation of Figure 6.7c to the situation shown in Figure 6.7d. The slope of the curves was firstly higher, but it progressively decreased until the peak point. The zone of the slope reduction (around $3,000 \mu\epsilon$) in this plastic region probably corresponded to the situation shown in Figure 6.7d. The low slopes of this region of the curve, to the left and to the right of the peak point, were associated with a hardly foreseeable behavior in the damaged regions. At the maximum point of this curve (peak point), transversal strain levels of between $4,500$ and $6,000 \mu\epsilon$ were recorded, corresponding to increased stress levels of around 31%. Finally, 14 of the 15 mixtures showed a fracture strain of over $6,000 \mu\epsilon$. Specimen micro-cracking was widespread at the final moment of fracture under compression.

The high transversal strain of the concrete, due to its micro-cracking, produced a high increase in the apparent-contour volume of the specimens. This increase was associated with a value of the “apparent Poisson’s coefficient” of around a theoretical limit of 0.5 units in the plastic zone. A situation that undoubtedly establishes a clear limit for the practical use of this concrete in engineering elements, in terms of mechanical stress: the starting point of the yield step, which corresponded to the Poisson’s coefficients of approximately 0.2 units (62-65% strain at fracture, proportional limit, see Table 6.7), must never be exceeded in service loads.

On the basis of the aspects addressed in both this section and the previous one, it can initially be concluded that the concrete samples showed a linear-elastic behavior under compression and tension. They lost the linearity under compression when cracking appeared along vertical-radial planes (due to tensile tangential-circumferential stresses that appear in horizontal planes), became generalized, and changed both the conditions of the geometric regularity of the tested samples (barreling due to the friction constraint in both bases) and the internal homogeneity of the material,

which became heterogeneous. At this point, instability due to (meso- or micro-) bulging and buckling occurred at many points within the cracked region, and the apparent global behavior of the tested sample was not linear, but plastic or yielding. Hence this vertical cracking, at the beginning superficial and subsequently deeper, involved decisive damage to the material and caused high strains recorded in the transversal direction.

Concerning the influence of the concrete components on mechanical behavior, it can be stated that in the transversal direction, the use of 100% coarse RCA increased the elastic and plastic stiffness of the concrete specimens, as shown by the decrease in both the Poisson's coefficient and the strain at fracture (see Table 6.7). The effect of the fine fraction of this residue was the same for the elastic zone, but different in the plastic zone, because when this RCA fraction was incorporated in the SCC, its plastic deformability increased. The joint use in the mixtures of both RCA fractions, 100% coarse RCA and 50% fine RCA, produced strain levels and a plastic behavior that were similar in the mixtures with 100% NA. Mixtures with CEM III/A in the same amount as CEM I also increased their deformability. In this way, mix III50R had a strain at fracture of 8,147 $\mu\epsilon$. On the other hand, the increase of binder content (batch 3 mixes) increased the plastic stiffness of the mixes, despite the higher deformability of the GGBFS compared to the conventional cement clinker. Thus, mix III0 showed a strain at fracture of only 5,697 $\mu\epsilon$, 43% less than mix III50R (8,147 $\mu\epsilon$). Regardless of the composition of the mixture, the ratio between the stress and strain at the most representative points of the curve and the values at the maximum point of the curve were similar in all the mixtures (see Table 6.7).

3.3.3. RELATIONSHIP BETWEEN TRANSVERSAL AND LONGITUDINAL STRAIN LEVELS

The monotonic-load test results showed a close relationship between the strain of the concrete in both the longitudinal and transversal directions, as may be seen in Figure 6.8, which represents this magnitude versus the percentage of applied stress with respect to the compressive strength of each mixture. This relationship was similar in all the mixtures, regardless of their composition. Initially, it had a constant value, equal to the Poisson's coefficient, up to approximately 60-65% of the compressive strength. Then, the relationship was an almost vertical line, due to the large increase in transversal strain within the yielding zone. The transversal strain equaled the longitudinal strain when 67-70% of the compressive strength was reached. Subsequently, another approximately constant region was obtained with a quotient value of 1.3-1.6 up to 95% of the compressive strength. At this point, the ratio suddenly increased until reaching the maximum point of the stress-strain curve, in which the transversal strain was 1.6-1.8 times the longitudinal strain. Finally, the transversal strain reached twice the longitudinal strain at the fracture point.

3.3.4. VOLUMETRIC VARIATION

The variation of the external volume of the specimens (enveloping volume) throughout the monotonic-load test is depicted in Figure 6.9, in which this magnitude and the applied stress are shown by the rectilinear coordinates of the graph. The plastic regions of the corresponding curves of the different mixes are clearly similar to those of Figure 6.6 that represent transversal strain versus stress (left-hand-side curves). The difference was evident (negative volumetric variation) in the elastic region, due to the contraction of the specimens with no notable bulging.

Several hypotheses and simplifications that also refer to other calculations are needed to obtain these curves of relative volumetric variation regarding the geometric form of the bulging (or barreling) of the specimens depicted in Figure 6.7:

- The form of the vertical profile of the specimens (transversal section, Figure 6.7) was chosen as parabolic (Equation 6.2), in which "2b" is the total height of the specimen, and "a" is the increase of the diameter of the specimens in half of their height. The integrated

area of this parabola above the y-axis is given by $4ab/3$, and the position of the mass center is roughly approximated by $3a/8$.

$$y = a \cdot \left(1 - \frac{x^2}{b^2}\right) \tag{6.2}$$

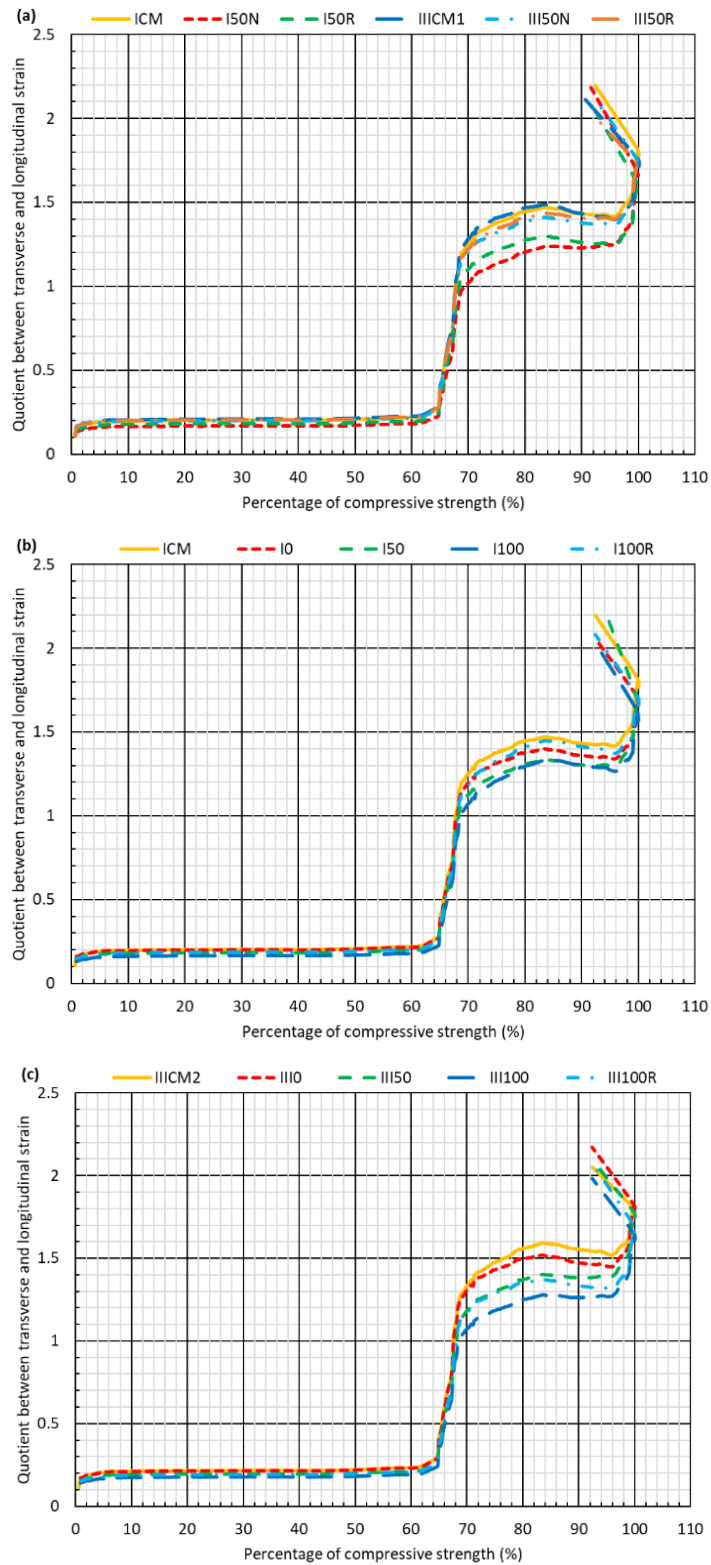


Figure 6.8. Relationship between transversal and longitudinal strain in the monotonic-load test: (a) batch 1; (b) batch 2; (c) batch 3

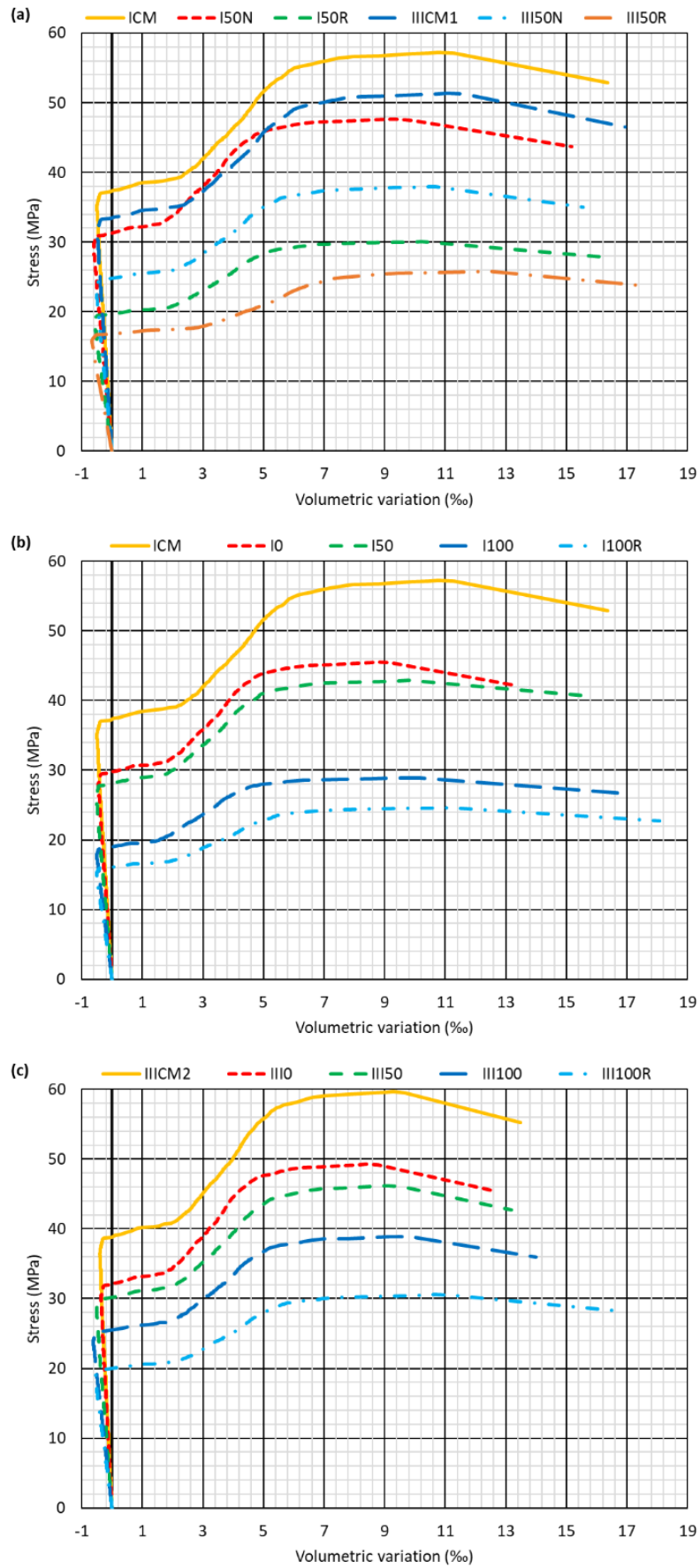


Figure 6.9. Relationship between volumetric variation versus stress in the monotonic-load test: (a) batch 1; (b) batch 2; (c) batch 3

- The application of Pappus-Guldin's second theorem yielded Equation 6.3, which provided the bulging volume of the specimen (ΔV). In this formula, D is the diameter of the specimen. In this way, the total volume V_t of the specimen is approximated by Equation 6.4.

$$\Delta V = \pi \cdot a \cdot b \cdot \left(a + \frac{4 \cdot D}{3} \right) \quad (6.3)$$

$$V_t = \frac{\pi \cdot D^2 \cdot b}{2} + \Delta V \quad (6.4)$$

- If ΔV is divided by V_t , the transversal volumetric variation, due to the dilatation (bulging) in this direction, is calculated with Equation 6.5 (ε_t is the transversal strain). In this calculation, the very small magnitudes, such as a , can be disregarded whenever in summation with very much larger magnitudes, such as D .

$$\frac{\Delta V}{V_t} = \frac{8 \cdot a}{3 \cdot D} = \frac{8}{3} \cdot \varepsilon_t \quad (6.5)$$

- Finally, it is necessary to subtract the volumetric contraction in the longitudinal direction, *i.e.*, the longitudinal strain, ε_l . The volumetric variation ($\Delta V/V_0$) of the specimens is provided by Equation 6.6.

$$\frac{\Delta V}{V_0} = \frac{8}{3} \cdot \varepsilon_t - \varepsilon_l \quad (6.6)$$

In verification of these calculations, we must locate a volumetric contraction in the elastic field given by one of the Hooke-Poisson's formulas (Equation 6.7, where σ_h is the hydrostatic stress and K is the volumetric coefficient according to Equation 6.8, which depends of the modulus of elasticity and the Poisson's coefficient). Considering ordinary values that are suitable for the mixes such as a Poisson's coefficient of 0.2, a modulus of elasticity of 35 GPa and $\sigma_h = \sigma_z/3$, where the vertical stress, σ_z , is around 35 MPa in the elastic region, a negative value (contraction) of the volumetric variation ($\Delta V/V_0$) of 0.6 ‰ is obtained, as depicted in Figure 6.9.

$$\frac{\Delta V}{V_0} = -\frac{\sigma_h}{K} \quad (6.7)$$

$$K = \frac{E}{3 \cdot (1 - 2 \cdot \nu)} \quad (6.8)$$

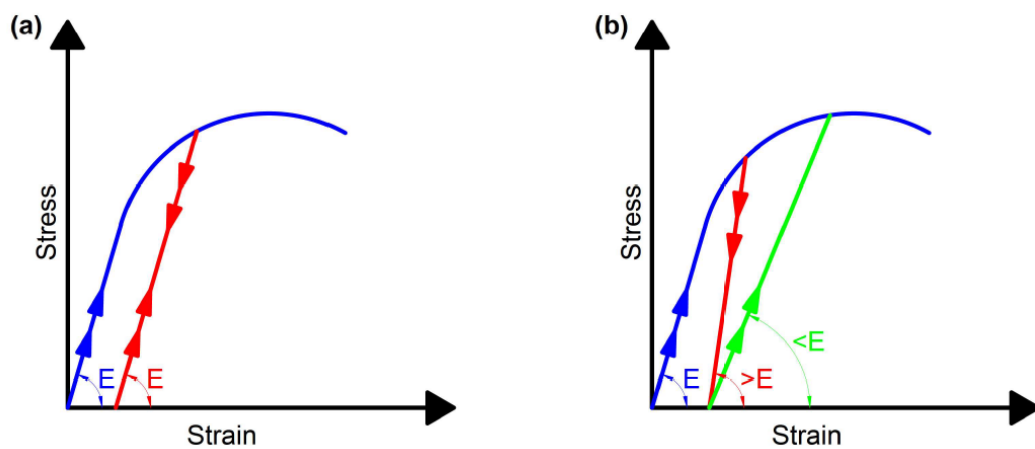


Figure 6.10. Loading/unloading process: (a) theoretical situation; (b) real situation

3.4. LOADING/UNLOADING TEST

If a material is loaded until it moves into a plastic regime and is then unloaded, the unloading will theoretically occur linearly. The slope of this line is the modulus of elasticity (Figure 6.10a) and when the unloading finishes the material will present residual strain, as depicted in the graph. If the material is loaded again, the new loading line will coincide with the previous unloading one [53]. However, the material actually presents hysteresis and, generally, a slight increase of its stiffness during the unloading is observed, as well as a slight decrease in its elastic stiffness in the subsequent loading process (Figure 6.10b) [33].

The mixtures developed in this study were subjected to a loading/unloading test of 5 cycles, to evaluate the above-mentioned behavior. In each cycle, the maximum applied stress was progressively increased, as shown in Table 6.8. In the first two cycles, 25% and then 40% of the compressive strength obtained in the monotonic-load test were applied, in order to evaluate the variations of their theoretical elastic behavior. In the third cycle, the maximum load applied was slightly lower (around 1-2 MPa) than the proportional limit; hence the tests applied around 55% of compressive strength. The aim of this third cycle was to study the performance of the mixtures after applying the maximum usual stress considered in the design of concrete structures (see discussion in section 3.3.2).

Table 6.8. Maximum stress (MPa) applied in each cycle of the loading/unloading test. For the 5th cycle, the percentage decrease of the failure stress in relation to the compressive strength is displayed in brackets

Batch	Mix	1 st cycle	2 nd cycle	3 rd cycle	4 th cycle	5 th cycle	PL ¹	CS ²
Batch 1	ICM	15.6	24.0	32.1	45.8	51.3 (-10.3)	33.2	57.2
	I50N	12.7	19.5	26.2	38.2	41.8 (-12.4)	27.9	47.7
	I50R	8.3	12.8	16.2	24.1	27.4 (-9.0)	16.8	30.1
	IIICM1	13.7	21.1	28.3	41.1	45.3 (-12.1)	30.0	51.4
	III50N	10.0	15.3	20.6	30.2	32.8 (-13.5)	22.6	37.9
	III50R	6.8	10.4	14.0	20.6	22.3 (-13.6)	15.3	25.8
Batch 2	ICM	15.6	24.0	32.1	45.8	51.3 (-10.3)	33.2	57.2
	I0	11.9	18.4	24.6	36.5	39.3 (-13.8)	25.9	45.6
	I50	11.5	17.8	23.8	34.3	38.0 (-11.4)	25.7	42.9
	I100	8.1	12.4	16.7	23.1	26.6 (-8.0)	17.4	28.9
	I100R	7.2	11.1	12.9	19.7	23.8 (-3.3)	13.8	24.6
Batch 3	IIICM2	16.0	24.6	33.0	47.8	52.7 (-11.7)	35.8	59.7
	IIIO	12.4	19.1	27.1	39.3	40.8 (-17.1)	28.3	49.2
	III50	12.0	18.4	26.2	36.9	39.4 (-14.7)	27.5	46.2
	III100	10.8	16.7	21.4	31.2	35.7 (-8.2)	22.5	38.9
	III100R	8.8	13.6	18.2	24.9	29.1 (-4.6)	18.4	30.5

¹ PL: stress (MPa) at the proportional limit according to the monotonic-load test

² CS: compressive strength (MPa) according to the monotonic-load test

The fourth cycle evaluated the behavior of the mixtures when they underwent significant plastic strain. Therefore, the maximum load of this cycle was around 80% of the maximum value reached in the monotonic-load test. Finally, the specimens were broken in the fifth and last cycle, and the variations of the peak stress, the peak strain, and the strain at fracture (Table 6.9 and Table 6.10) were analyzed. In these loading/unloading tests, the load application rate was also 1 kN/s, and a minimum load of 1 kN was maintained throughout the whole test to avoid any slippage of the specimens. Data collection was performed at 20 Hz.

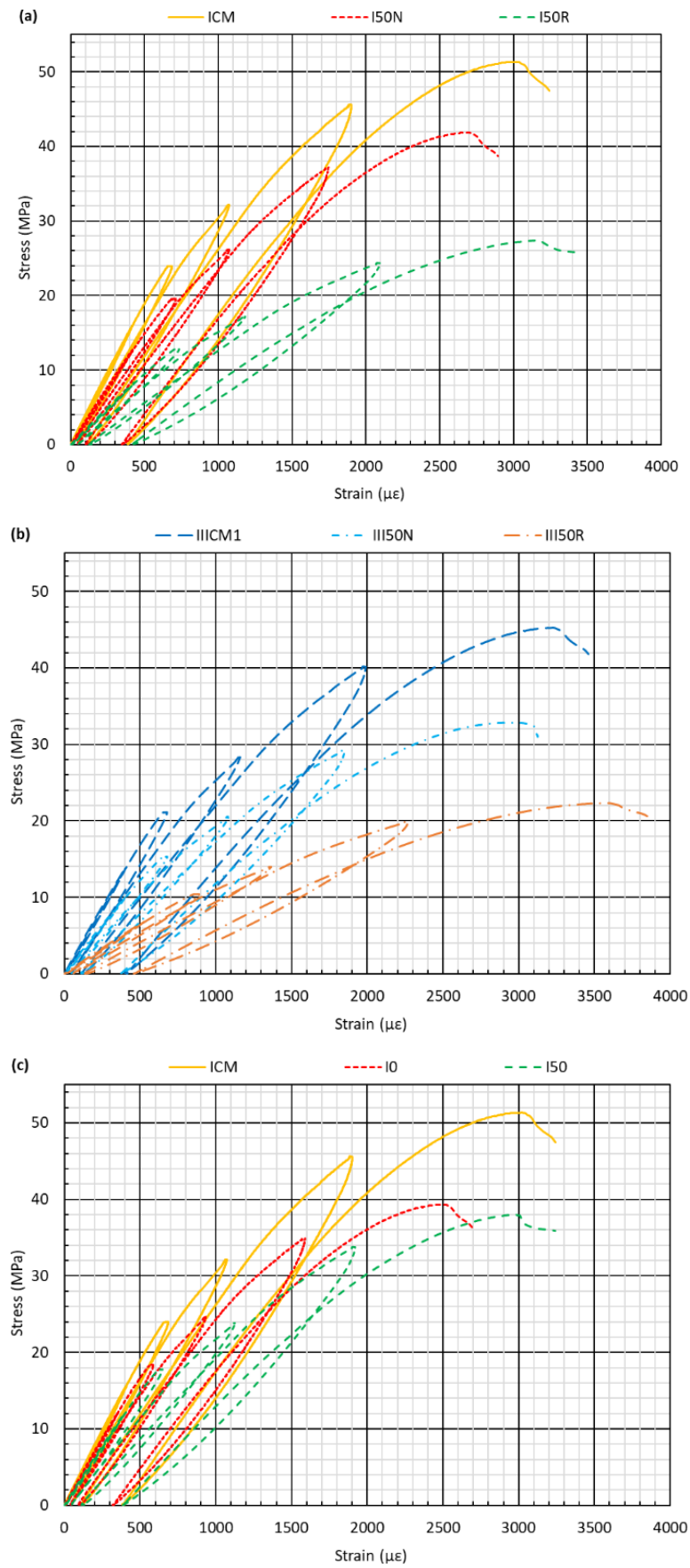


Figure 6.11. Longitudinal stress-strain behavior in the loading/unloading test: (a, b) batch 1; (c, d) batch 2; (e, f) batch 3

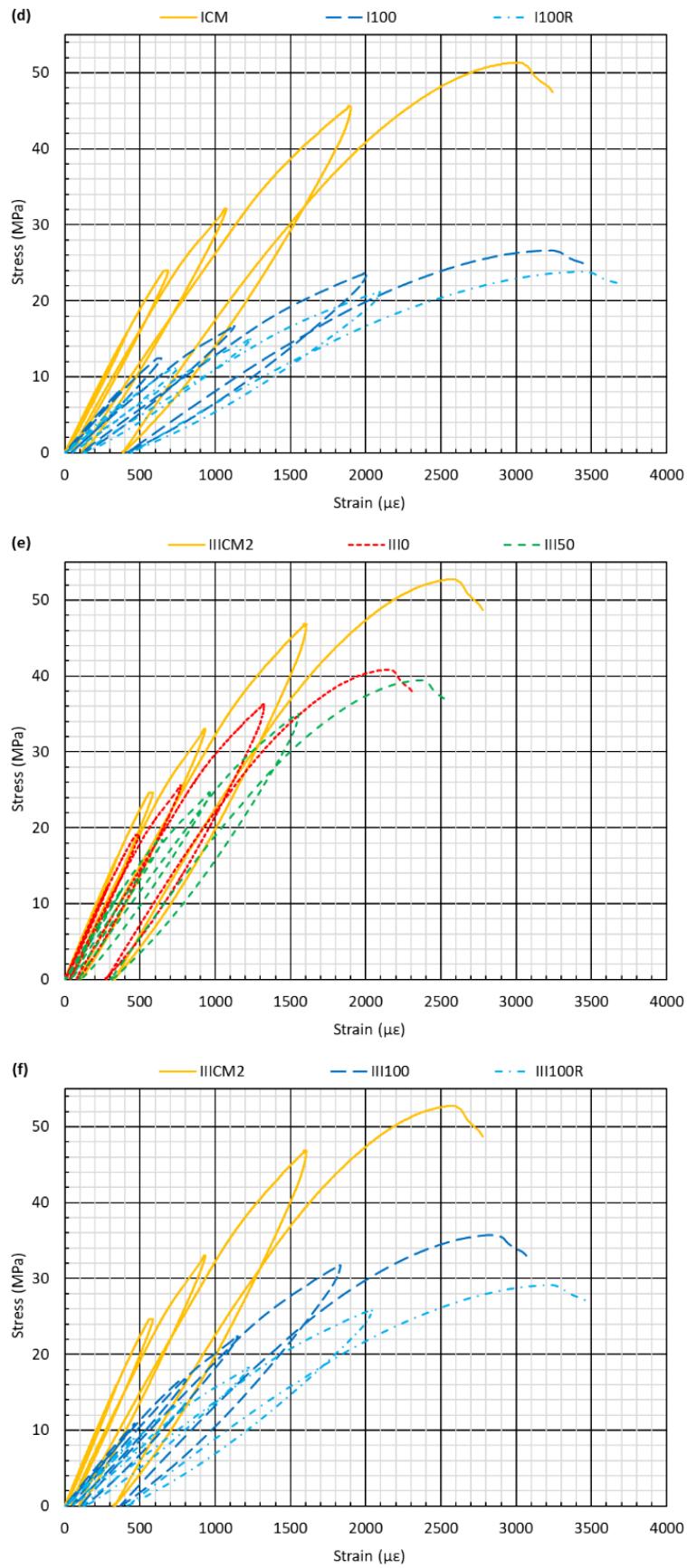


Figure 6.11 (continued). Longitudinal stress-strain behavior in the loading/unloading test: (a, b) batch 1; (c, d) batch 2; (e, f) batch 3

3.4.1. LONGITUDINAL DIRECTION

As shown in Figure 6.11, the stress-strain behavior in the longitudinal direction of the mixtures in this cyclic test progressively deviated from the theoretical behavior indicated in Figure 6.10a. The application of a load equal to 25% of the compressive strength (first cycle), notably below the proportional limit, caused a mismatch with the previously explained theoretical behavior that was practically negligible. In the second cycle (40% of the compressive strength), a little hysteresis and residual strain (from 40 to 60 $\mu\epsilon$, see Table 6.9) appeared, with no significant change of stiffness during the loading test. Furthermore, the unloading section of the curves (see Figure 6.) was slightly curved in this cycle, which meant that it was not coincident with the loading of the third cycle. Although theoretically, the applied load in this second cycle was lower than the stress corresponding to the proportional limit (see Table 6.8), local creep behavior was observed at a crystalline scale in the Calcium-Silicate-Hydrate (C-S-H) gel, reminiscent of the beginning of a plain creep test [8]. In practical terms, due to its lengthy duration, this kind of test is a realistic superposition between an elastic-plastic loading regime and creep-yielding, which is representative of engineering concrete structures in which the in-service load is submitted to variations of high intensity-severity (for instance, flyovers and railway bridges).

The incipient behavior observed in the second cycle increased in subsequent cycles, in which notably enhanced hysteretic regions appeared. The modulus of elasticity decreased throughout these cycles, while the remaining strain increased. In addition, micro-structural damage may be suspected at around the start of the third cycle, due to the change in behavior experienced by the mixtures, although it is difficult to verify its importance in current terms. This issue is explained in detail in section 3.4.2.

The loading regions of the graphics from these last cycles were curved, so the elastic modulus was calculated by considering the points of the loading section corresponding to 5 and 25% of the compressive strength obtained in the monotonic-load test (see Table 6.9). The failure stress (Table 6.8) and the strain at fracture (Table 6.9) were lower than those obtained in the monotonic-load test.

The loss of strength and strain at fracture ranged between 4-14% for all mixtures. Regardless of the amount of cement added to the mix, the loss of strength was greater when using CEM III/A, although the use of this type of cement reduced the decrease in strain at fracture. In terms of deformability, the mixes with GGBFS therefore withstood the application of increasing cyclic load better than conventional cement clinker, although their strength behavior was worse. As with the monotonic-load test, the addition of 100% coarse RCA increased the brittleness of the mixtures and increased the percentage loss of strength and deformability. On the contrary, the higher deformability of fine RCA compensated for this decrease: compressive strength and strain at fracture decreases were 10.3 and 6.1% for mixture ICM, 13.8 and 12.4% for mixture IO, and 3.3 and 9.0% for mixture I100R. The residual strain after each cycle was in percentage terms similar in all the mixtures, regardless of their composition.

The addition of 100% coarse RCA had no appreciable effect on the evolution of the modulus of elasticity throughout the test, as shown by the results of mixtures ICM and IO, and IICM2 and III0. However, the effect of fine RCA 0/4 mm depended on the amount of cement added to the mix. In the CEM I mixtures, the loss of the modulus of elasticity increased with additions of RCA. On the contrary, in the batch 3 mixtures (produced with CEM III/A and 40% more cement than the batch 2 mixtures), the higher the amount of fine RCA, the lower the decrease in the modulus of elasticity. Moreover, mixture I100 showed the maximum decrease in the modulus of elasticity (38.4%). The delayed release of water absorbed by RCA 0/1 mm and 0/0.125 mm during mixing [49] meant that the effect of these fractions was exactly the opposite: reduced loss of stiffness of the CEM I mixtures and increased stiffness of the CEM III/A mixtures. Finally, mixtures with up to 50% RCA 0/4 mm

showed a higher modulus of elasticity in the second cycle than in the first one, which meant that the addition of large amounts of fine RCA reduced the ability of the mixtures to maintain their initial stiffness following compressive stress.

Table 6.9. Most representative values of the longitudinal stress-strain behavior in the loading/unloading test

Batch	Mix	1 st cycle		2 nd cycle		3 rd cycle	
		E (GPa)	S ($\mu\epsilon$)	E (GPa)	S ($\mu\epsilon$)	E (GPa)	S ($\mu\epsilon$)
Batch 1	ICM	38.1	14 (0.4)	38.8 (+1.8)	47 (1.5)	35.0 (-8.1)	118 (3.6)
	I50N	30.3	14 (0.5)	30.5 (+0.7)	49 (1.7)	28.5 (-5.9)	118 (4.1)
	I50R	19.3	14 (0.4)	19.4 (+0.5)	50 (1.4)	17.0 (-11.9)	130 (3.8)
	IIICM1	34.2	13 (0.4)	34.6 (+1.2)	46 (1.3)	28.6 (-16.4)	128 (3.7)
	III50N	24.9	13 (0.4)	25.1 (+0.8)	46 (1.5)	22.2 (-10.8)	119 (3.8)
	III50R	12.9	17 (0.4)	13.0 (+0.8)	61 (1.6)	12.0 (-7.0)	150 (3.9)
Batch 2	ICM	38.1	14 (0.4)	38.8 (+1.8)	47 (1.5)	35.0 (-8.1)	118 (3.6)
	I0	34.3	12 (0.4)	34.7 (+1.2)	40 (1.5)	30.8 (-10.2)	103 (3.8)
	I50	30.3	13 (0.4)	30.5 (+0.7)	44 (1.4)	24.7 (-18.5)	124 (3.8)
	I100	22.4	12 (0.3)	21.6 (-3.6)	44 (1.3)	17.3 (-22.8)	124 (3.6)
	I100R	17.2	14 (0.4)	16.5 (-4.1)	51 (1.4)	14.1 (-18.0)	136 (3.7)
Batch 3	IIICM2	46.3	12 (0.4)	46.8 (+1.1)	40 (1.4)	41.3 (-10.8)	103 (3.6)
	III0	42.8	10 (0.4)	43.1 (+0.7)	34 (1.5)	38.7 (-9.6)	85 (3.7)
	III50	31.4	13 (0.5)	31.6 (+0.6)	44 (1.7)	29.9 (-4.8)	106 (4.2)
	III100	23.4	15 (0.5)	23.0 (-1.7)	55 (1.8)	22.8 (-2.6)	126 (4.1)
	III100R	19.4	15 (0.4)	19.0 (-2.1)	55 (1.6)	17.4 (-10.3)	135 (3.9)

Table 6.9 (continued). Most representative values of the longitudinal stress-strain behavior in the loading/unloading test

Batch	Mix	4 th cycle		5 th cycle	
		E (GPa)	S ($\mu\epsilon$)	E (GPa)	FS ($\mu\epsilon$)
Batch 1	ICM	29.8 (-21.8)	381 (11.8)	28.6 (-24.9)	3,241 (-6.1)
	I50N	26.4 (-12.9)	349 (12.3)	26.1 (-13.9)	2,894 (-10.3)
	I50R	14.4 (-25.4)	419 (12.0)	14.3 (-25.9)	3,458 (-9.2)
	IIICM1	25.1 (-26.6)	398 (11.5)	23.6 (-31.0)	3,461 (-7.8)
	III50N	15.6 (-37.3)	370 (11.9)	18.9 (-24.1)	3,125 (-9.5)
	III50R	10.8 (-16.2)	454 (11.7)	10.5 (-18.6)	3,849 (-6.7)
Batch 2	ICM	29.8 (-21.8)	381 (11.8)	28.6 (-24.9)	3,241 (-6.1)
	I0	27.3 (-20.4)	318 (11.9)	26.4 (-23.0)	2,691 (-12.4)
	I50	21.8 (-28.1)	384 (11.5)	21.2 (-30.0)	3,241 (-4.3)
	I100	14.6 (-34.8)	402 (11.6)	13.8 (-38.4)	3,472 (-11.5)
	I100R	12.5 (-27.3)	419 (11.3)	11.6 (-32.6)	3,704 (-9.0)
Batch 3	IIICM2	36.2 (-21.8)	321 (11.6)	34.2 (-26.1)	2,778 (-10.7)
	III0	33.9 (-20.8)	266 (11.5)	31.8 (-25.7)	2,315 (-13.8)
	III50	28.0 (-10.8)	311 (12.4)	27.9 (-11.1)	2,547 (-13.7)
	III100	21.5 (-8.1)	367 (12.1)	21.0 (-10.3)	3,067 (-8.5)
	III100R	15.7 (-19.1)	409 (11.8)	15.1 (-22.2)	3,473 (-7.7)

E: modulus of elasticity (GPa); S: remaining strain at the end of the cycle ($\mu\epsilon$); FS: strain at fracture point ($\mu\epsilon$)

Values in brackets are:

- For the modulus of elasticity, the percentage variation of its value regarding the value in the first cycle
- For the remaining strain, the percentage that it represents with respect to the strain at fracture after the fifth cycle
- For the strain at fracture, the decrease from the values of this strain obtained in the continuously-increasing-load test

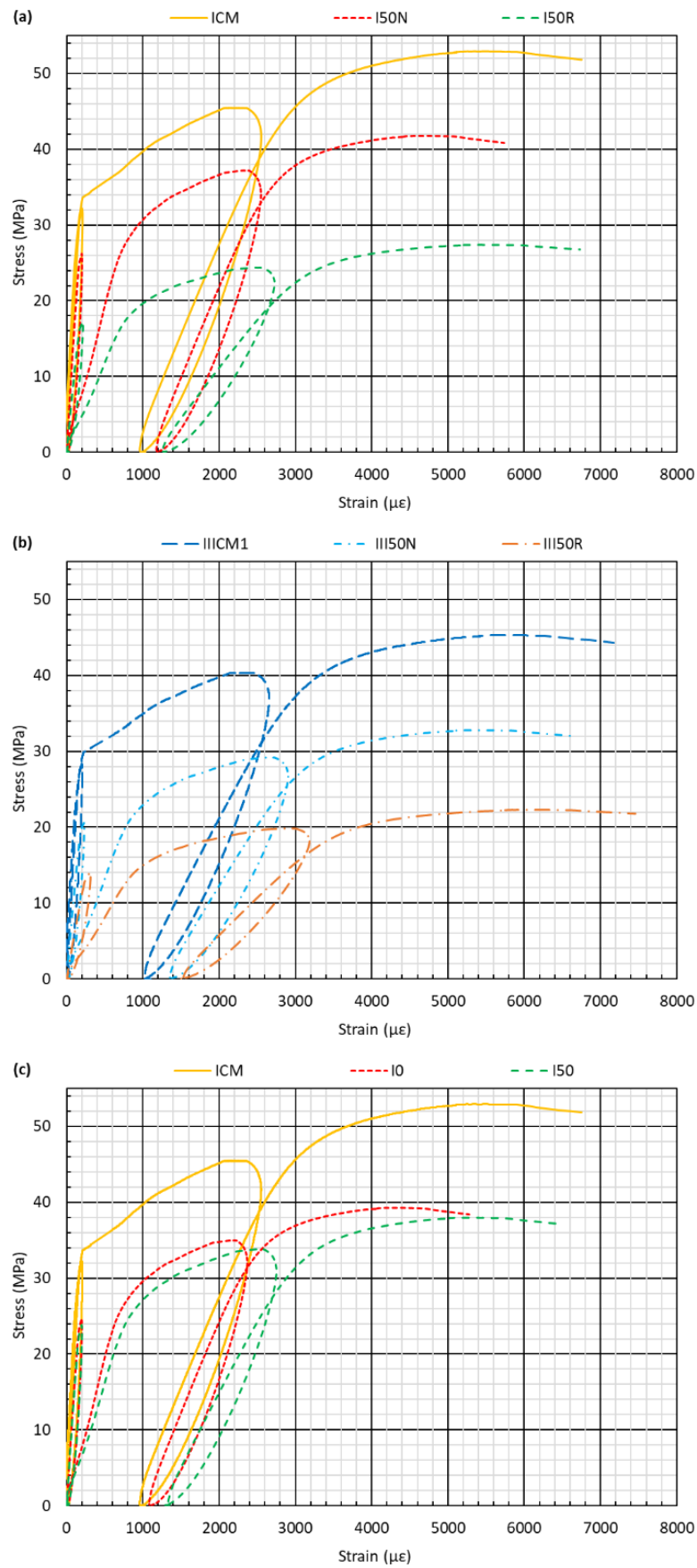


Figure 6.12. Transversal stress-strain behavior in loading/unloading test: (a, b) batch 1; (c, d) batch 2; (e, f) batch 3

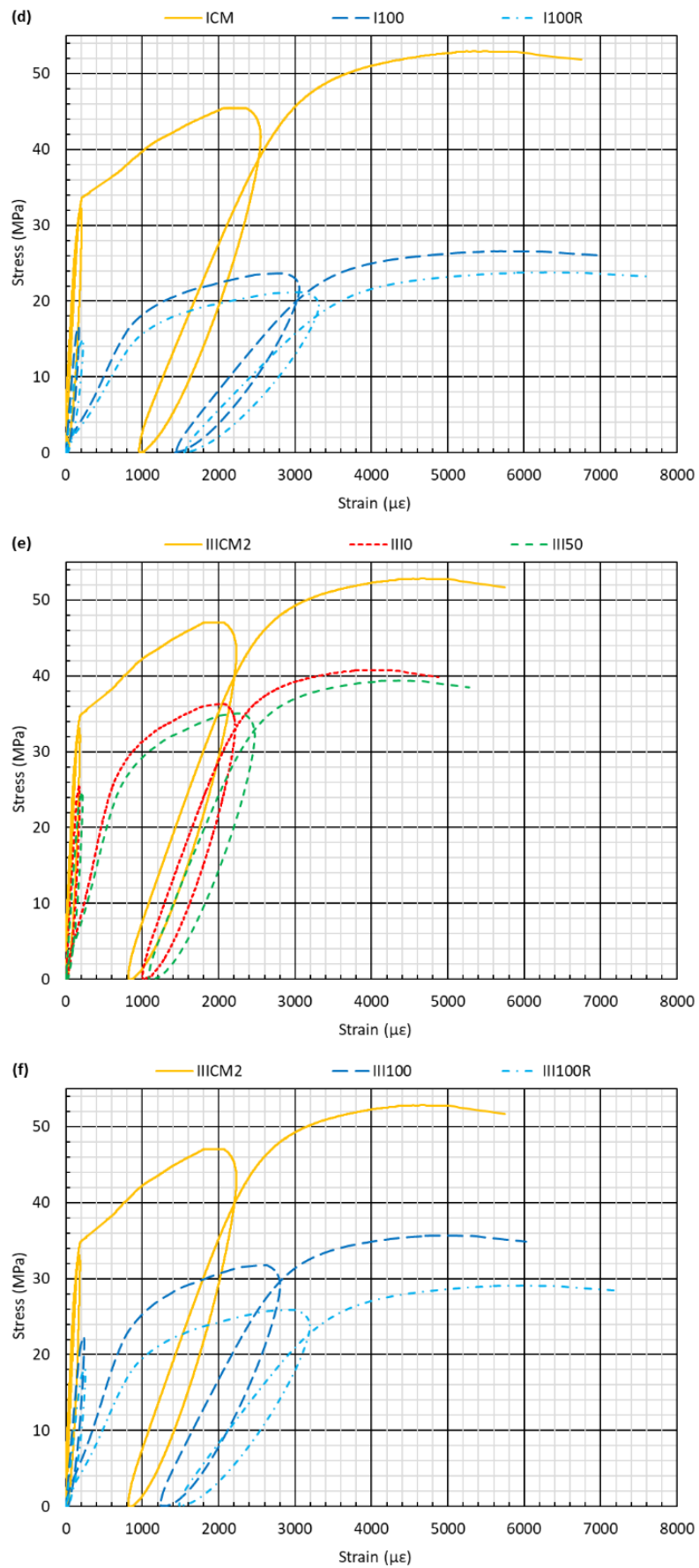


Figure 6.12 (continued). Transversal stress-strain behavior in loading/unloading test: (a, b) batch 1; (c, d) batch 2; (e, f) batch 3

3.4.2. TRANSVERSAL DIRECTION

The longitudinal stress versus transversal strain curves throughout the five test cycles (Figure 6. and Table 6.10) showed similarities with those obtained in the longitudinal direction: non-coincidence of load/unload regions, decreased stress and strain at fracture with respect to the values of the monotonic-load test, and increased deformability with the number of cycles. All the mixtures showed a highly defined linear elastic behavior during the first two cycles, under loading lower than 40% of their compressive strength.

In the third cycle, the theoretically applied stress never exceeded the proportional limit of the mixtures estimated in the monotonic-load test (see Figure 6.), so it could be hypothetically assumed that the transversal strain should not be associated with obvious damage, which could otherwise be confirmed by the lack of residual strain, perhaps for the same reasons as proposed in section 3.3.2. However, that hypothetical assumption is false, because micro-structural damage in this third cycle occurred in most of the mixtures, with the exception of mixes ICM, IIICM1, and IIICM2 (reference mixtures with 100% coarse and fine NA). As much is substantiated in Figure 6. where two types of behavior were obtained during the loading period of the fourth cycle, which are key to any analysis of these test results. In general, the graph of the mixtures was similar to the curve obtained for mix I50N or I50R (Figure 6.a), in which the slope of the fourth cycle load region was notably lower than the loading regions in the previous cycles. However, the aforementioned exceptions, mixes ICM, IIICM1, and IIICM2, presented a curve with two loading regions for the fourth cycle (Figure 6.). The first region clearly coincided with the loading-unloading of the third cycle, and the second region of loading underwent a remarkable loss of slope, flattening out until the point of maximum loading in the cycle. The other mixtures (100% coarse RCA) showed a remarkably smaller load slope at the beginning of the fourth cycle than the load slope of the third cycle, which constitutes evidence of generalized and irreversible damage at the micro-structural level generated throughout the third cycle.

Among all the mixtures, the “plastic behavior” in the fourth cycle showed some similarity with the behavior of the concrete material described in section 3.3.2, as local micro-cracking had damaged it, as shown in Figure 6.7. This zone was associated with a loss of slope in the loading region of the curves shown in Figure 6., starting from a certain level of loading, clearly shown at the point of inflection leading to the flattening out of the curves of mixtures ICM, IIICM1, and IIICM2, though less well defined in the other mixes, that might be roughly situated within the interval of 45-55% of the compressive strength of the mixture. Residual strain between 800 and 2,000 $\mu\epsilon$ after the unloading of this fourth cycle confirmed this performance.

Therefore, the addition of 100% coarse RCA had significant effects on the behavior of the mixtures in this fourth cycle:

- The mixtures manufactured with 100% NA in the coarse and fine fractions withstood the damage caused by the variable loading better than all others, as they retained their stiffness in the elastic zone. In addition, the load under which the plastic behavior began in the fourth cycle was approximately 2 MPa greater than the maximum load in the third cycle.
- The mixes manufactured with 100% coarse RCA, regardless of the fine RCA content or the type of cement used, largely decreased in elastic stiffness from the third cycle. This performance can be attributed to the fact that the damage affected the ITZ between the coarse RCA and the cementitious matrix more significantly than when NA was used.

The behavior in the fifth cycle was the same in all the mixtures, with a large increase in the elastic compliance (loading) compared to that obtained in the initial cycles, and notable hysteresis with respect the unloading of the fourth cycle. As with the monotonic-load test, the post-failure yielding section showed a more ductile fracture than the one produced in the longitudinal direction.

Table 6.10. Most representative values of the transversal stress-strain behavior in the loading/unloading test

Batch	Mix	1 st cycle		2 nd cycle		3 rd cycle	
		ν	S ($\mu\epsilon$)	ν	S ($\mu\epsilon$)	ν	S ($\mu\epsilon$)
Batch 1	ICM	0.205	2 (0)	0.209 (2.0)	9 (0.1)	0.189 (-9.8)	25 (0.4)
	I50N	0.166	1 (0)	0.167 (0.6)	10 (0.2)	0.157 (-5.4)	22 (0.4)
	I50R	0.179	1 (0)	0.181 (1.1)	13 (0.2)	0.150 (-16.2)	23 (0.3)
	IIICM1	0.211	1 (0)	0.214 (1.4)	12 (0.2)	0.176 (-16.6)	24 (0.3)
	III50N	0.198	3 (0)	0.199 (0.5)	11 (0.2)	0.176 (-11.1)	25 (0.4)
	III50R	0.204	2 (0)	0.206 (1.0)	15 (0.2)	0.189 (-7.4)	34 (0.5)
Batch 2	ICM	0.205	2 (0)	0.209 (2.0)	9 (0.1)	0.189 (-9.8)	25 (0.4)
	I0	0.198	1 (0)	0.201 (1.5)	8 (0.2)	0.178 (-10.1)	22 (0.4)
	I50	0.181	3 (0)	0.182 (0.6)	11 (0.2)	0.148 (-18.2)	22 (0.3)
	I100	0.164	2 (0)	0.158 (-3.7)	12 (0.2)	0.127 (-22.6)	19 (0.3)
	I100R	0.185	1 (0)	0.177 (-4.3)	15 (0.2)	0.151 (-18.4)	25 (0.4)
Batch 3	IIICM2	0.217	1 (0)	0.220 (1.4)	7 (0.1)	0.194 (-12.0)	21 (0.4)
	III0	0.215	3 (0)	0.216 (0.5)	6 (0.1)	0.194 (-9.8)	20 (0.4)
	III50	0.195	2 (0)	0.196 (0.5)	8 (0.2)	0.185 (-5.1)	24 (0.5)
	III100	0.176	1 (0)	0.173 (-1.7)	12 (0.2)	0.171 (-2.8)	26 (0.4)
	III100R	0.191	3 (0)	0.186 (-2.6)	13 (0.2)	0.171 (-10.5)	28 (0.4)

Table 6.10 (continued). Most representative values of the transversal stress-strain behavior in the loading/unloading test

Batch	Mix	4 th cycle		5 th cycle	
		ν	S ($\mu\epsilon$)	ν	FS ($\mu\epsilon$)
Batch 1	ICM	0.156 (-25.9)	1,032 (15.3)	2.096 (920.5)	6,750 (9.1)
	I50N	0.698 (320.5)	1,191 (20.8)	2.198 (1,224.1)	5,737 (16.9)
	I50R	0.622 (247.5)	1,274 (18.9)	2.082 (1,063.1)	6,730 (11.6)
	IIICM1	0.160 (-24.2)	1,097 (15.4)	2.148 (918.0)	7,176 (7.6)
	III50N	0.750 (278.8)	1,358 (20.6)	2.340 (1,081.8)	6,597 (7.4)
	III50R	0.671 (228.9)	1,489 (20.0)	2.148 (952.9)	7,458 (8.5)
Batch 2	ICM	0.156 (-25.9)	1,032 (15.3)	2.096 (920.5)	6,750 (9.1)
	I0	0.713 (260.1)	1,107 (21.0)	2.174 (998.0)	5,278 (14.5)
	I50	0.685 (278.5)	1,286 (19.8)	2.218 (1,125.4)	6,482 (10.4)
	I100	0.728 (343.9)	1,429 (20.3)	2.253 (1,273.8)	7,056 (9.8)
	I100R	0.756 (308.6)	1,548 (20.3)	2.284 (1,134.6)	7,630 (8.1)
Batch 3	IIICM2	0.167 (-24.4)	878 (15.3)	2.140 (884.8)	5,741 (7.7)
	III0	0.799 (271.6)	1,036 (21.2)	2.335 (986.0)	4,876 (14.4)
	III50	0.760 (289.7)	1,155 (21.9)	2.298 (1,078.5)	5,278 (12.8)
	III100	0.731 (315.3)	1,309 (21.7)	2.177 (1,136.9)	6,023 (7.4)
	III100R	0.747 (291.1)	1,492 (20.6)	2.308 (1,108.4)	7,228 (5.4)

ν : Poisson coefficient; S: remaining strain at the cycle end ($\mu\epsilon$); FS: strain at fracture ($\mu\epsilon$); CS: compressive strength (MPa)
Values between brackets represent:

- For the Poisson coefficient, the percentage variation in its value relative to the value in the first cycle
- For the remaining strain, the percentage that it represents with respect to the strain at fracture of the fifth cycle
- For strain at fracture, the decreasing values compared to the ones obtained in the continuously-increasing-load test

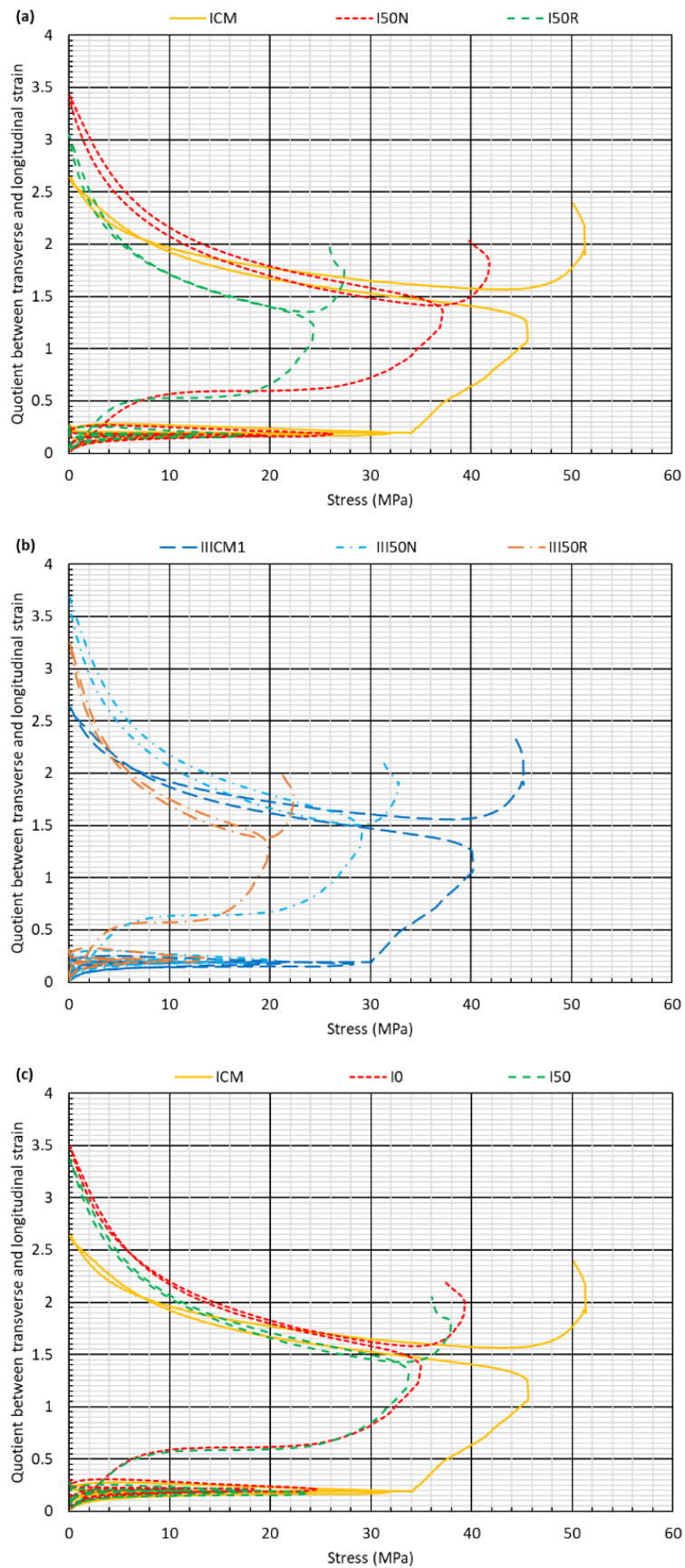


Figure 6.13. Relationship between transversal and longitudinal strain (ν -value) in the loading/unloading test: (a, b) batch 1; (c, d) batch 2; (e, f) batch 3

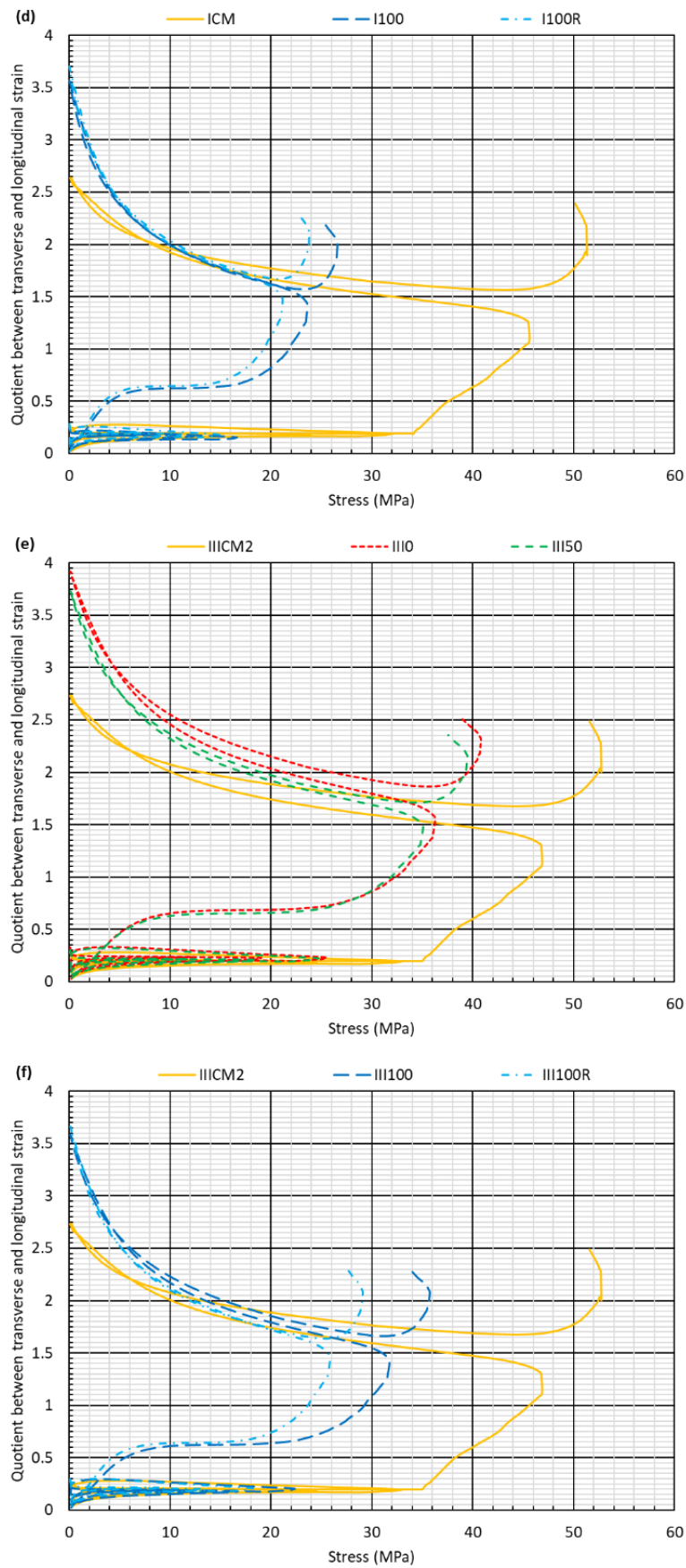


Figure 6.13 (continued). Relationship between transversal and longitudinal strain (ν -value) in the loading/unloading test: (a, b) batch 1; (c, d) batch 2; (e, f) batch 3

3.4.3. RELATIONSHIP BETWEEN TRANSVERSAL AND LONGITUDINAL STRAIN

The relationships between the transversal and the longitudinal strains are depicted in Table 6.10 (Poisson's coefficient from elastic region) and in Figure 6.. It must be recalled that the Poisson's coefficient displayed in Table 6.10 was calculated using the strain gauge data in the interval of loading from 5 to 25% of compressive strength. During the first three cycles, this relationship was approximately constant, and its value approximately coincided with the Poisson's coefficient displayed in Table 6.10. This coefficient showed a slight decrease from the first to the third cycle associated with the slight hysteresis in each cyclic load. The values of this coefficient in the fourth and fifth cycle are improper, due to the absence of pure elastic behavior and could be qualified as "fictitious Poisson's coefficients".

Once again, the most notable difference occurred in the fourth cycle between mixtures that either incorporated 100% coarse RCA or otherwise, as was described in the previous section. In Table 6.10, the values of the Poisson's coefficient for the mixtures ICM, IIICM1, and IIICM2 in the fourth cycle were even slightly lower than in the earlier cycles. However, considering the fourth cycle globally (see Figure 6.), it can be seen that the differences between the mixtures tended to mitigate over this cycle. The values of this "fictitious Poisson's coefficient" were between 1.2 and 1.7 units at maximum load, and between 2.6 and 3.9 units after unloading; this behavior was associated with greater barreling of the specimens.

Finally, the loading of the fifth cycle roughly coincided with the unloading of the fourth cycle in all the mixtures. The relationship between both strains at the peak point (ultimate stress) was 1.7-2.3 units. This value was roughly coincident with the values corresponding to the ultimate stresses of the mixtures observed in Figure 6.8.

4. CONCLUSIONS AND RECOMMENDATIONS

In this paper, the elastic and plastic stress-strain behavior in both the longitudinal and the transversal directions of a Self-Compacting Concrete (SCC) containing Recycled Concrete Aggregate (RCA) and Ground Granulated Blast Furnace Slag (GGBFS) in varying proportions has been compared with a conventional SCC containing natural aggregates (NA) as a reference mixture. The 15 mixtures manufactured with and without GGBFS and coarse RCA, and different contents and fractions of fine RCA were tested up to failure in conventional compressive tests, under monotonic compressive loading and under cyclic loading/unloading processes, in which the maximum applied load increased over the cycles. The following conclusions can be drawn from the aspects discussed throughout this article:

- In all cases, the additions of both coarse and fine RCA decreased the compressive strength, modulus of elasticity, and Poisson's coefficient of the concrete, *i.e.*, the mechanical behavior of the RCA concrete was notably worse than that of NA concrete. The addition of RCA should therefore be carefully studied when using this waste to produce structural concretes with high-load bearing capacity.
- The stress-strain behavior of the mixtures both in the longitudinal and in the transversal directions under monotonic compressive loading showed important differences. First, a yield step was only noted in the transversal direction. Second, the plastic yielding deformability was much higher in the transversal direction, so that the strain at fracture in that direction was approximately twice as high as in the longitudinal direction. These two phenomena were associated with the appearance of vertical cracking in the contour of the test specimen.
- The use of coarse RCA decreased strain at fracture, while the addition of fine RCA increased it. These additions meant that mixtures with 100% NA and mixtures with 100% and 50% coarse and fine RCA, respectively, had almost identical strain levels at fracture. The total

replacement of the traditional cement clinker by CEM III/A in the same amounts also increased the plastic deformability of the mixtures and, consequently, both the longitudinal and the transversal strain at fracture.

- The application of loading/unloading cycles of growing severity increased deformability throughout the cycles and reduced the compressive strength of the mixtures and their strain at fracture. The stress-strain behavior in the longitudinal direction was not dependent on the composition of the mixture. Nevertheless, mixture composition was a key performance factor in the transversal direction, because the mixtures with coarse RCA experienced a higher increase in their elastic deformability when they were subjected to a small plastic strain (55% failure stress), tripling the Poisson's coefficient. In mixtures with 100% NA, this behavior occurred when 75-80% of the failure stress was applied. However, the yield step disappeared, due to micro-cracking during the cycles applied before reaching this zone of the curve. The effects of RCA and the cement type were very similar in the monotonic-load test.

A comparison of the results of both tests shows that the damage accumulated in the first three cycles in the loading/unloading test reduced the "admissible" stress from 62-65% of the failure load in NA mixtures to less than 55% in mixtures containing RCA. From an engineering point of view, the generalized damage mentioned in section 3.4.2 is an undesirable situation that should be avoided in structural concrete elements designed to support variable mechanical stresses. Therefore, RCA should be used with caution, and the amount of RCA added to the SCC mixes should be defined and limited according to serviceability conditions rather than conventional failure design. In this way, no tensile damage will be observed due to transversal strain when the concrete is subjected to axial loading, and SCC with RCA can be successfully used.

Finally, from all the above, it is clear that the addition of RCA and GGBFS significantly modified not only the elasticity of the mixes, but also their plastic, stress-strain behavior in both directions. This area of research, with very few studies, is therefore of great importance for the successful application of recycled concrete in real structures and, it still has many research avenues that remain open, such as studying the effect of other contents of coarse RCA, and evaluating the application of other load levels in the loading/unloading test. This study has therefore contributed to understanding the plastic behavior and, especially, the transversal strain patterns of concrete under axial loading.

REFERENCES

- [1] Y.Y. Lim, K.Z. Kwong, W.Y.H. Liew, R.V. Padilla, C.K. Soh, Parametric study and modeling of PZT based wave propagation technique related to practical issues in monitoring of concrete curing, *Constr. Build. Mater.* 176 (2018) 519-530.
- [2] R.V. Silva, J. De Brito, R.K. Dhir, The influence of the use of recycled aggregates on the compressive strength of concrete: A review, *Eur. J. Environ. Civ. Eng.* 19 (7) (2015) 825-849.
- [3] EC-2, Eurocode 2: Design of concrete structures. Part 1-1: General rules and rules for buildings, CEN (European Committee for Standardization) (2010).
- [4] R.V. Silva, J. de Brito, R.K. Dhir, Fresh-state performance of recycled aggregate concrete: A review, *Constr. Build. Mater.* 178 (2018) 19-31.
- [5] V. Revilla-Cuesta, M. Skaf, F. Faleschini, J.M. Manso, V. Ortega-López, Self-compacting concrete manufactured with recycled concrete aggregate: An overview, *J. Clean. Prod.* 262 (2020) 121362.
- [6] H. Okamura, M. Ouchi, Self-compacting concrete, *J. Adv. Concr. Technol.* 1 (2003) 5-15.
- [7] M.S. Abo Dhaheer, S. Kulasegaram, B.L. Karihaloo, Simulation of self-compacting concrete flow in the J-ring test using smoothed particle hydrodynamics (SPH), *Cem. Concr. Res.* 89 (2016) 27-34.
- [8] A. Santamaría, V. Ortega-López, M. Skaf, J.A. Chica, J.M. Manso, The study of properties and behavior of self compacting concrete containing Electric Arc Furnace Slag (EAFS) as aggregate, *Ain Shams Eng. J.* 11 (1) (2020) 231-243.

- [9] W.S. Alyhya, S. Kulasegaram, B.L. Karihaloo, Simulation of the flow of self-compacting concrete in the V-funnel by SPH, *Cem. Concr. Res.* 100 (2017) 47-59.
- [10] N.H. Roslan, M. Ismail, N.H.A. Khalid, B. Muhammad, Properties of concrete containing electric arc furnace steel slag and steel sludge, *J. Build. Eng.* 28 (2020) 101060.
- [11] L. Jin, M. Liu, R. Zhang, X. Du, Cracking of cover concrete due to non-uniform corrosion of corner rebar: A 3D meso-scale study, *Constr. Build. Mater.* 245 (2020) 118449.
- [12] R.V. Silva, J. De Brito, R.K. Dhir, Establishing a relationship between modulus of elasticity and compressive strength of recycled aggregate concrete, *J. Clean. Prod.* 112 (2016) 2171-2186.
- [13] F. Aslani, S. Nejadi, Mechanical characteristics of self-compacting concrete with and without fibres, *Mag. Concr. Res.* 65 (10) (2013) 608-622.
- [14] J.T. San-José, J.M. Manso, Fiber-reinforced polymer bars embedded in a resin concrete: Study of both materials and their bond behavior, *Polym. Compos.* 27 (3) (2006) 315-322.
- [15] P. Li, L. Sui, F. Xing, Y. Zhou, Static and cyclic response of low-strength recycled aggregate concrete strengthened using fiber-reinforced polymer, *Compos. Part B: Eng.* 160 (2019) 37-49.
- [16] F. Aslani, S. Nejadi, Self-compacting concrete incorporating steel and polypropylene fibers: Compressive and tensile strengths, moduli of elasticity and rupture, compressive stress-strain curve, and energy dissipated under compression, *Compos. Part B: Eng.* 53 (2013) 121-133.
- [17] ACI-318-19, Building Code Requirements for Structural Concrete (2019).
- [18] A.L.B. Marinho, C.M. Mol Santos, J.M.F. de Carvalho, J.C. Mendes, G.J. Brigolini, R.A.F. Peixoto, Ladle furnace slag as binder for cement-based composites, *J. Mater. Civ. Eng.* 29 (11) (2017) 04017207.
- [19] H. Qasrawi, I. Asi, Effect of bitumen grade on hot asphalt mixes properties prepared using recycled coarse concrete aggregate, *Constr. Build. Mater.* 121 (2016) 18-24.
- [20] M. Pasetto, A. Baliello, G. Giacomello, E. Pasquini, Sustainable solutions for road pavements: A multi-scale characterization of warm mix asphalts containing steel slags, *J. Clean. Prod.* 166 (2017) 835-843.
- [21] L. Lei, H.-K. Chan, Investigation into the molecular design and plasticizing effectiveness of HPEG-based polycarboxylate superplasticizers in alkali-activated slag, *Cem. Concr. Res.* 136 (2020) 106150.
- [22] H.L. Wu, F. Jin, Y.L. Bo, Y.J. Du, J.X. Zheng, Leaching and microstructural properties of lead contaminated kaolin stabilized by GGBS-MgO in semi-dynamic leaching tests, *Constr. Build. Mater.* 172 (2018) 626-634.
- [23] M.D.S. Magalhães, F. Faleschini, C. Pellegrino, K. Brunelli, Influence of alkali addition on the setting and mechanical behavior of cement pastes and mortars with electric arc furnace dust, *Constr. Build. Mater.* 214 (2019) 413-419.
- [24] J.A. Fuente-Alonso, V. Ortega-López, M. Skaf, Á. Aragón, J.T. San-José, Performance of fiber-reinforced EAF slag concrete for use in pavements, *Constr. Build. Mater.* 149 (2017) 629-638.
- [25] M. Etxeberria, A. Gonzalez-Corominas, P. Pardo, Influence of seawater and blast furnace cement employment on recycled aggregate concretes' properties, *Constr. Build. Mater.* 115 (2016) 496-505.
- [26] A.L. Beaucour, P. Pliya, F. Faleschini, R. Njinwoua, C. Pellegrino, A. Noumowé, Influence of elevated temperature on properties of radiation shielding concrete with electric arc furnace slag as coarse aggregate, *Constr. Build. Mater.* 256 (2020) 119385.
- [27] V. Revilla-Cuesta, M. Skaf, J.A. Chica, J.A. Fuente-Alonso, V. Ortega-López, Thermal deformability of recycled self-compacting concrete under cyclical temperature variations, *Mater. Lett.* 278 (2020) 128417.
- [28] A.R. Khan, S. Fareed, M.S. Khan, Use of recycled concrete aggregates in structural concrete, *Sustain. Constr. Mater. Technol.* 2 (2019).
- [29] F. Fiol, C. Thomas, C. Muñoz, V. Ortega-López, J.M. Manso, The influence of recycled aggregates from precast elements on the mechanical properties of structural self-compacting concrete, *Constr. Build. Mater.* 182 (2018) 309-323.

- [30] I. González-Taboada, B. González-Fonteboa, J.L. Pérez-Ordóñez, J. Eiras-López, Prediction of self-compacting recycled concrete mechanical properties using vibrated recycled concrete experience, *Constr. Build. Mater.* 131 (2017) 641-654.
- [31] A.S. Brand, A.N. Amirkhani, J.R. Roesler, Flexural capacity of full-depth and two-lift concrete slabs with recycled aggregates, *Transp. Res. Rec.* 2456 (2014) 64-72.
- [32] K.H. Yang, Y.H. Hwang, Y. Lee, J.H. Mun, Feasibility test and evaluation models to develop sustainable insulation concrete using foam and bottom ash aggregates, *Constr. Build. Mater.* 225 (2019) 620-632.
- [33] C. Wang, J. Xiao, Evaluation of the stress-strain behavior of confined recycled aggregate concrete under monotonic dynamic loadings, *Cem. Concr. Compos.* 87 (2018) 149-163.
- [34] Z. Tang, W. Li, V.W.Y. Tam, Z. Luo, Investigation on dynamic mechanical properties of fly ash/slag-based geopolymetric recycled aggregate concrete, *Compos. Part B: Eng.* 185 (2020) 107776.
- [35] H. Zhao, F. Liu, H. Yang, Residual compressive response of concrete produced with both coarse and fine recycled concrete aggregates after thermal exposure, *Constr. Build. Mater.* 244 (2020) 118397.
- [36] S. Luo, S. Ye, J. Xiao, J. Zheng, Y. Zhu, Carbonated recycled coarse aggregate and uniaxial compressive stress-strain relation of recycled aggregate concrete, *Constr. Build. Mater.* 188 (2018) 956-965.
- [37] S.M.S. Kazmi, M.J. Munir, Y.F. Wu, I. Patnaikuni, Y. Zhou, F. Xing, Axial stress-strain behavior of macro-synthetic fiber reinforced recycled aggregate concrete, *Cem. Concr. Compos.* 97 (2019) 341-356.
- [38] F. Faleschini, M.A. Zanini, L. Hofer, K. Toska, D. De Domenico, C. Pellegrino, Confinement of reinforced concrete columns with glass fiber reinforced cementitious matrix jackets, *Eng. Struct.* 218 (2020) 110847.
- [39] Z. Xiong, Q. Cai, F. Liu, L. Li, Y. Long, Dynamic performance of RAC-filled double-skin tubular columns subjected to cyclic axial compression, *Constr. Build. Mater.* 248 (2020) 118665.
- [40] J.M. Lee, Y.J. Lee, Y.J. Jung, J.H. Park, B.S. Lee, K.H. Kim, Ductile capacity of reinforced concrete columns with electric arc furnace oxidizing slag aggregate, *Constr. Build. Mater.* 162 (2018) 781-793.
- [41] S.W. Kim, Y.S. Kim, J.M. Lee, K.H. Kim, Structural performance of spirally confined concrete with EAF oxidising slag aggregate, *Eur. J. Environ. Civ. Eng.* 17 (8) (2013) 654-674.
- [42] A. Gholampour, T. Ozbakkaloglu, O. Gencel, T.D. Ngo, Concretes containing waste-based materials under active confinement, *Constr. Build. Mater.* 270 (2021) 121465.
- [43] Y. Chen, Z. Chen, J. Xu, E.M. Lui, B. Wu, Performance evaluation of recycled aggregate concrete under multiaxial compression, *Constr. Build. Mater.* 229 (2019) 116935.
- [44] X. Hu, Q. Lu, Z. Xu, W. Zhang, S. Cheng, Compressive stress-strain relation of recycled aggregate concrete under cyclic loading, *Constr. Build. Mater.* 193 (2018) 72-83.
- [45] EN-Euronorm, Rue de stassart, 36. Belgium-1050 Brussels, European Committee for Standardization.
- [46] H. Salehi, M. Mazloom, Opposite effects of ground granulated blast-furnace slag and silica fume on the fracture behavior of self-compacting lightweight concrete, *Constr. Build. Mater.* 222 (2019) 622-632.
- [47] V. Revilla-Cuesta, V. Ortega-López, M. Skaf, J.M. Manso, Effect of fine recycled concrete aggregate on the mechanical behavior of self-compacting concrete, *Constr. Build. Mater.* 263 (2020) 120671.
- [48] S.A. Santos, P.R. da Silva, J. de Brito, Self-compacting concrete with recycled aggregates – A literature review, *J. Build. Eng.* 22 (2019) 349-371.
- [49] M.C.S. Nepomuceno, L.A. Pereira-De-Oliveira, S.M.R. Lopes, Methodology for the mix design of self-compacting concrete using different mineral additions in binary blends of powders, *Constr. Build. Mater.* 64 (2014) 82-94.

- [50] A. Santamaría, A. Orbe, M.M. Losañez, M. Skaf, V. Ortega-Lopez, J.J. González, Self-compacting concrete incorporating electric arc-furnace steelmaking slag as aggregate, *Mater. Des.* 115 (2017) 179-193.
- [51] V. Revilla-Cuesta, M. Skaf, R. Serrano-López, V. Ortega-López, Models for compressive strength estimation through non-destructive testing of highly self-compacting concrete containing recycled concrete aggregate and slag-based binder, *Constr. Build. Mater.* 280 (2021) 122454.
- [52] D. Pedro, J. de Brito, L. Evangelista, Mechanical characterization of high performance concrete prepared with recycled aggregates and silica fume from precast industry, *J. Clean. Prod.* 164 (2017) 939-949.
- [53] ANSI/AISC-360-16, Specification for Structural Steel Buildings (2016).
- [54] M. Behera, S.K. Bhattacharyya, A.K. Minocha, R. Deoliya, S. Maiti, Recycled aggregate from C&D waste & its use in concrete - A breakthrough towards sustainability in construction sector: A review, *Constr. Build. Mater.* 68 (2014) 501-516.
- [55] CEB-FIP, Model Code 2010 (Volumes 1 and 2) (2012).

Article 7

Thermal deformability of recycled self-compacting concrete under cyclical temperature variations

Title: Thermal deformability of recycled self-compacting concrete under cyclical temperature variations

Authors: Víctor Revilla-Cuesta, Marta Skaf, José A. Chica, José A. Fuente-Alonso, Vanesa Ortega-López

Journal: Materials Letters

Year: 2020

Volume: 278

Article number: 128417

DOI: <https://doi.org/10.1016/j.matlet.2020.128417>

Journal classification (2019 JCR ranking data): 43/155 (physics, applied). Second quartile (Q2)

ABSTRACT

Recycled Concrete Aggregate (RCA) has greater elasticity than natural aggregate, due to the presence of adhered hydrated mortar in the coarse fraction, and mortar particles in the fine fraction. To evaluate this aspect under temperature variations, four Self-Compacting Concretes (SCC) made with 100% coarse and/or fine RCA were subjected to cyclical temperature variations between 70 °C and 20 °C and between -15 °C and 20 °C. The addition of RCA, especially in the coarse fraction, increased the thermal deformability, although the difference tended to decrease with the number of cycles, especially in positive temperature variations. This study concludes that the traditional upper limit of the linear thermal expansion coefficient for concrete ($1.2 \cdot 10^{-5} \text{ }^\circ\text{C}^{-1}$) is also suitable when RCA is incorporated.

Keywords: cyclical temperature variations; linear thermal expansion coefficient; recycled concrete aggregate; self-compacting concrete; thermal deformability; thermal remaining strain.

1. INTRODUCTION

The dimensional stability and thermal deformability of concrete are conditioned by the curing conditions (temperature and humidity) [1], the environmental temperature during its lifetime [2], some of its properties (porosity, or workability) [3], and the elasticity/expansivity of its components, including by-products [4, 5].

Recycled Concrete Aggregate (RCA), obtained from the crushing of rejected or demolished concrete elements, is one of the most studied wastes, due to its great abundance around the world and its interesting mechanical properties [6]. Its addition to concrete causes varied effects, shrinkage increase, among others, that usually depend on the original concrete's strength [7] or the RCA fraction used [8], although an accurate estimation of these effects is possible [9]. Nevertheless, there is a lack of knowledge regarding the effect of RCA on the concrete deformability due to temperature variations.

This letter aims to evaluate the effect of RCA on the thermal expansion of concrete. The effect of coarse and fine fractions is analyzed in both increase and decrease of temperature. This study was performed on Self-Compacting Concrete (SCC), with high content of fine aggregate to reach self-compactability, so it is very sensitive to the harmful effects of fine RCA [5].

2. MATERIALS AND METHODS

Four SCCs were manufactured with CEM I 52.5 R (EN 197-1 [10]), a plasticizer, a viscosity regulator, limestone fines 0/1 mm, limestone filler, siliceous or RCA gravel (4/12.5 mm) and siliceous or RCA sand (0/4 mm). The RCA used was obtained from concrete with a minimum compressive strength of 45 MPa. The mixes were labelled as *N* (100% natural aggregate), *F* (100% fine RCA), *C* (100% coarse RCA) and *CF* (100% coarse and fine RCA). In mix *N* a water-to-cement ratio of 0.55 was established. The high water absorption and the irregular shape of RCA required an increase in the water content to maintain similar flowability in RCA mixes. Table 7.1 shows the mix design and the aggregates' physical properties.

The mixtures were tested to slump flow (EN 12350-8), capillary porosity in 72 h (UNE 83982), compressive strength (EN 12390-3) and modulus of elasticity (EN 12390-13) at 28 days (two 10x20-cm cylindrical specimens for each test). The freezing and heating tests (two 7.5x7.5x28.5-cm prismatic specimens for each test) were performed at 90 days and consisted in 20 cycles of 12 hours at -15 °C in a freezer (freezing test) or at 70 °C in an oven (heating test), followed by 12 hours at 20 °C in a climatic chamber. During the cycles, the strain was recorded. The temperature variation in the specimens until stabilization was 0.1 °C/minute.

Table 7.1. Mix design. Properties of aggregates and mixes

Material/property	Aggregates' physical properties	Mix design (kg)			
	Density (Mg/m ³); 24 h water absorption (%); fineness modulus	N	F	C	CF
CEM I 52.5 R	-	300			
Water	-	165	230	190	285
Plasticizer	-	4.50			
Viscosity regulator	-	2.20			
Limestone filler	2,77; 0.54	225			
Limestone fines	2.62; 2.53; 2.12	115			
Siliceous gravel	2.62; 0.84; 5.27	575		0	
Siliceous sand	2.58; 0.25; 3.49	940	0	940	0
Coarse RCA	2.42; 6.25; 6.30	0		530	
Fine RCA	2.37; 7.36; 3.12	0	865	0	865
Slump flow (mm)	-	765	810	750	800
Capillary porosity (%)	-	8.1	11.8	9.8	14.7
Compressive strength (MPa)	-	55.7	42.1	44.3	27.8
Modulus of elasticity (GPa)	-	37.5	29.2	32.9	20.9

3. RESULTS AND DISCUSSION

All mixtures had a slump flow between 750 and 850 mm. Furthermore, as expected [7, 8], the mechanical properties and capillary porosity were worse when RCA was added. The adjustment of water content in the mix design produced similar impact in mixes *C* and *F*, and the joint use of both RCA fractions had the most harmful effect.

In thermal tests, all the mixtures had the same general behavior regarding the evolution of strain throughout the cycles (Figure 7.1). On the one hand, during the freezing test, all the mixes increased their absolute strain, due to the remaining negative strain that appeared progressively, mainly from cycle 9-10. However, the strain increase of each individual cycle was approximately the same. The remaining strain is explained by the inability of some cement hydration products (gel Calcium-Silicate-Hydrate, C-S-H) to recover their original dimensions after being cyclically subjected to sub-zero temperatures [11]. On the other hand, in the heating test, the temperature variation (between

70 °C and 20 °C) caused that some gel C-S-H products were less sensitive to positive temperature variations, which led to smaller strain increases in the last cycles, than in the first ones. The phenomena observed in both tests showed a tendency for all mixtures to shrink when they were subjected to cyclical temperature variations.

If the maximum strains of each mix are analyzed, the effect of RCA, mainly characterized for the presence of adhered mortar in the coarse fraction and of mortar particles in the fine fraction [8], can be defined. The maximum strains for the reference mix N were -0.3 and 0.41 mm/m. Mix C reached maximum strains in both tests of -0.38 and 0.48 mm/m respectively. The values for mix F were -0.32 and 0.45 mm/m and, finally, mix CF presented values of -0.40 mm/m and 0.48 mm/m. Therefore, the effect on the thermal deformability of the adhered mortar was greater than the effect of the mortar particles of fine RCA. The average remaining strain in the freezing test for the mixes N, F, C, and CF was 0.030, 0.035, 0.045 and 0.050 mm/m respectively, while the strain decrease in the heating test was 0.110, 0.140, 0.180 and 0.175 mm/m. The use of RCA, especially the coarse fraction, increased the tendency of the mixtures to shrink due to cyclical temperature increases, because of the incorporation of an additional volume of gel C-S-H products, present in the mortar particles of fine fraction and, especially, in the mortar adhered to the coarser particles of RCA [11]. There was no clear influence of porosity on any phenomena discussed.

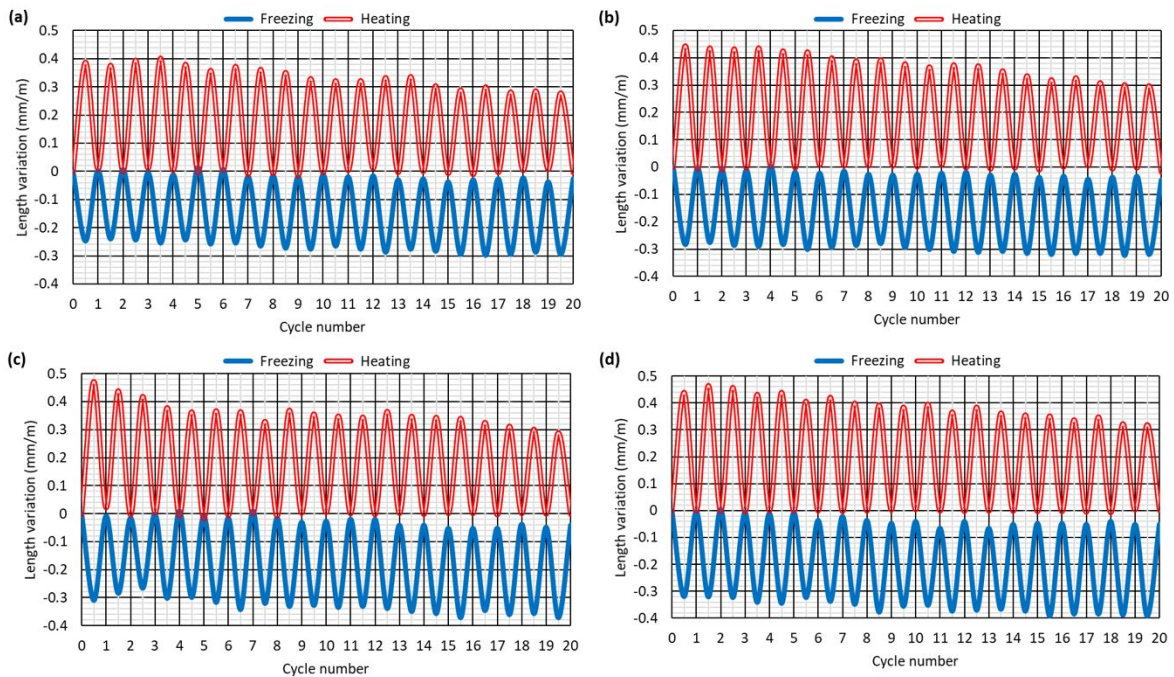


Figure 7.1. Maximum and minimum strains during freezing and heating tests: (a) mix N; (b) mix F; (c) mix C; (d) mix CF

The linear thermal expansion coefficient (α , $^{\circ}\text{C}^{-1}$) is calculated by equation 7.1, in which $\Delta\varepsilon$ is the strain increase (m/m) and ΔT is the temperature increase ($^{\circ}\text{C}$). Its common value for concrete is $1 \cdot 10^{-5} \text{ }^{\circ}\text{C}^{-1}$, although in climates with large temperature variations, a value of $1.2 \cdot 10^{-5} \text{ }^{\circ}\text{C}^{-1}$ is considered to estimate the thermal strains more safely. Figure 7.2 shows this coefficient calculated from the strain of each cycle. Its initial value for all the mixtures was between $7 \cdot 10^{-6}$ and $9 \cdot 10^{-6} \text{ }^{\circ}\text{C}^{-1}$.

- The value obtained from the heating test results was, on average, 6% lower than the one from the freezing test, and showed a clear downward trend, due to the strain decrease over the cycles. The final value was 30% lower than the initial one.
- The coefficient calculated from the freezing test results of each cycle was practically constant. Nevertheless, if the accumulated strain was considered (the strain calculated from the initial length of the specimen before the test), see Figure 7.3, an upward trend appeared, due to the influence of the remaining strain, although with a lower slope than

the heating test. Therefore, it is advisable to estimate thermal strains of concrete with the values from Figure 7.3, as they consider the evolution of the concrete's behavior throughout all the cycles. The maximum value obtained was $1.14 \cdot 10^{-5} \text{ }^\circ\text{C}^{-1}$ (mix CF, freezing test, accumulated strain).

The addition of RCA, especially in the coarse fraction, increased the linear thermal expansion coefficient of concrete. Nevertheless, in all cases, the upper limit of the interval traditionally considered ($1.2 \cdot 10^{-5} \text{ }^\circ\text{C}^{-1}$) would be valid in RCA concrete.

$$\Delta\varepsilon = \alpha \cdot \Delta T \quad (7.1)$$

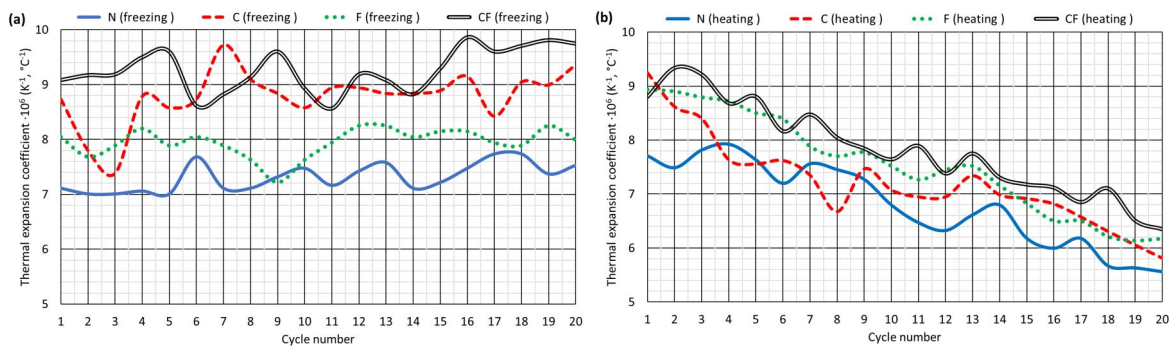


Figure 7.2. Linear thermal expansion coefficient calculated from the strain of each cycle: (a) freezing; (b) heating

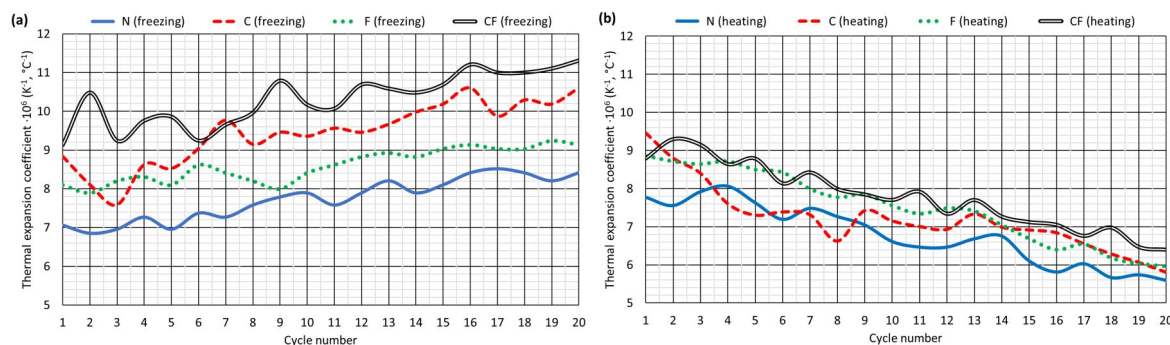


Figure 7.3. Linear thermal expansion coefficient calculated from the accumulated strain: (a) freezing; (b) heating

4. CONCLUSIONS

Regardless of the SCC composition, its linear thermal expansion coefficient decreases when subjected to cyclical positive temperature variations. However, if negative cyclical temperature variations are applied, a remaining strain appears, which causes this coefficient to increase, although the strain in each cycle remains constant. This behavior is mainly attributed to cement hydration products. The common upper limit of this coefficient for concrete, $1.2 \cdot 10^{-5} \text{ }^\circ\text{C}^{-1}$, is also valid when RCA is incorporated. The addition of RCA, especially in the coarse fraction with adhered mortar and, therefore, gel C-S-H products, makes SCC more sensitive to temperature variations, thus experiencing greater strain for an identical temperature increase.

REFERENCES

- [1] H.Y. Aruntaş, S. Cemalgil, O. Şimşek, G. Durmuş, M. Erdal, Effects of super plasticizer and curing conditions on properties of concrete with and without fiber, *Mater. Lett.* 62 (19) (2008) 3441-3443.
- [2] M. Abed, R. Nemes, E. Lublóy, Performance of Self-Compacting High-Performance Concrete Produced with Waste Materials after Exposure to Elevated Temperature, *J. Mater. Civ. Eng.* 32 (1) (2020) 05019004.
- [3] Y. Sun, P. Gao, F. Geng, H. Li, L. Zhang, H. Liu, Thermal conductivity and mechanical properties of porous concrete materials, *Mater. Lett.* 209 (2017) 349-352.

- [4] A. Santamaria, F. Faleschini, G. Giacomello, K. Brunelli, J.T. San José, C. Pellegrino, M. Pasetto, Dimensional stability of electric arc furnace slag in civil engineering applications, *J. Clean. Prod.* 205 (2018) 599-609.
- [5] V. Revilla-Cuesta, M. Skaf, F. Faleschini, J.M. Manso, V. Ortega-López, Self-compacting concrete manufactured with recycled concrete aggregate: An overview, *J. Clean. Prod.* 262 (2020) 121362.
- [6] A.R. Khan, S. Fareed, M.S. Khan, Use of recycled concrete aggregates in structural concrete, *Sustain. Constr. Mater. Technol.* 2 (2019).
- [7] A. Gonzalez-Corominas, M. Etxebarria, Effects of using recycled concrete aggregates on the shrinkage of high performance concrete, *Constr. Build. Mater.* 115 (2016) 32-41.
- [8] M. Bravo, J. de Brito, L. Evangelista, J. Pacheco, Durability and shrinkage of concrete with CDW as recycled aggregates: Benefits from superplasticizer's incorporation and influence of CDW composition, *Constr. Build. Mater.* 168 (2018) 818-830.
- [9] B. Delsaute, S. Staquet, Impact of recycled sand and gravels in concrete on volume change, *Constr. Build. Mater.* 232 (2020) 117279.
- [10] EN-Euronorm, European Committee for Standardization.
- [11] A. Mateos, J. Harvey, J. Bolander, R. Wu, J. Paniagua, F. Paniagua, Field evaluation of the impact of environmental conditions on concrete moisture-related shrinkage and coefficient of thermal expansion, *Constr. Build. Mater.* 225 (2019) 348-357.

Conclusiones y futuras líneas de investigación

Cada uno de los artículos recogidos en la presente Tesis Doctoral tiene sus propias conclusiones debido a su carácter autónomo. Sin embargo, en este apartado final se pretende fusionar todos los aspectos estudiados a lo largo de los mismos, estableciéndose unas conclusiones de carácter general. Además, se indican futuras líneas de investigación por las cuales el trabajo recogido en esta Tesis Doctoral puede continuar.

1. CONCLUSIONES

Se presentan a continuación las conclusiones generales derivadas del análisis conjunto de los diferentes artículos incluidos en la presente Tesis Doctoral. Puede observarse que cada una de ellas se vincula con uno de los objetivos recogidos en la primera sección de esta Tesis, la introducción, lo cual permite dar una respuesta clara a los interrogantes planteados al comienzo de este trabajo de investigación.

1. El efecto del árido reciclado de hormigón en la resistencia a compresión del hormigón autocompactante depende en gran medida de la composición de la mezcla. La modificación de la proporción entre árido grueso y fino, la modificación de la fracción 0/0.5 mm, o la modificación de la relación agua/cemento efectiva pueden compensar el efecto, en principio negativo, que el árido reciclado de hormigón tiene en el hormigón autocompactante. De este modo, es posible encontrar hormigones autocompactantes elaborados con árido reciclado de hormigón que presentan una resistencia a compresión superior a los hormigones autocompactantes convencionales. La sensibilidad de este tipo de hormigón a los cambios en su composición puede explicar este comportamiento.
2. La dispersión del efecto del árido reciclado de hormigón en la resistencia a compresión del hormigón autocompactante no se observa en la resistencia a tracción indirecta. Posiblemente, la mayor influencia de las zonas interfaciales de transición entre el árido y la matriz cementicia justifican esta tendencia. Así, la aparición de zonas interfaciales de transición de menor calidad al añadir árido reciclado de hormigón lleva inevitablemente a una disminución de la resistencia a tracción indirecta.
3. Los estudios que aborden el comportamiento del hormigón autocompactante con árido reciclado de hormigón deben centrarse fundamentalmente en la fracción fina de este residuo. Los estudios también deberían enfocarse en la interacción de esta fracción de árido reciclado de hormigón con conglomerantes alternativos como la ceniza volante o el humo de sílice.
4. De acuerdo con los trabajos realizados en esta Tesis Doctoral, el empleo de un 50% o un 100% de árido grueso de hormigón reciclado no afectó significativamente a las propiedades mecánicas del hormigón autocompactante. Por ello, en caso de introducirse este residuo en una mezcla cementicia de estas características, se recomienda emplear un 100% para conseguir una mayor sostenibilidad del material.
5. El efecto del árido fino de hormigón reciclado cuando se combina con la fracción gruesa de este mismo residuo para producir hormigón autocompactante depende de si su contenido es bajo (0-25%), medio (50%) o alto (75-100%). Puede afirmarse que el empleo de un 100% y un 25% respectivamente, de árido grueso y fino de hormigón reciclado, permite obtener un hormigón autocompactante con un comportamiento mecánico estadísticamente idéntico a aquel que incorpora únicamente un 100% de la fracción gruesa de este material.

6. El empleo simultáneo de un 100% de árido grueso de hormigón reciclado y de un cierto contenido (25-100%) de árido fino de hormigón reciclado ocasiona que la resistencia a compresión del hormigón presente una distribución de probabilidad con una reducida dispersión si las condiciones de la mezcla son controladas y repetidas. Estas condiciones se refieren fundamentalmente a la no modificación de la relación agua/cemento, y a la forma de trabajo habitual en una planta de fabricación de hormigón, cuya modificación favorece la dispersión citada en la primera conclusión. Este planteamiento lleva a que la resistencia característica de los hormigones autocompactantes que contienen este material sea subestimada por la formulación actual, siendo necesario su reajuste para maximizar su aprovechamiento en el diseño de elementos estructurales de hormigón.
7. El desarrollo de hormigones autocompactantes con un elevado contenido de escoria siderúrgica granulada molida (45% del total de conglomerante añadido) y un 100% de árido grueso de hormigón reciclado precisa de un reajuste de la relación entre el contenido de conglomerante y de árido grueso del hormigón. La forma altamente irregular de este árido en la fracción gruesa y la elevada finura de molido de la escoria siderúrgica granulada molida dificulta el arrastre homogéneo de las partículas más gruesas de árido por parte de la pasta de cemento. Este problema puede solucionarse mediante una disminución del contenido de árido grueso y el aumento del contenido total de conglomerante. Este reajuste de la composición permite obtener una alta autocompactabilidad en los hormigones con la composición indicada, a la vez que no afecta en gran medida a la menor huella de carbono conseguida con el empleo de escoria siderúrgica granulada molida y, además, permite compensar el esperable descenso de resistencia del hormigón al sustituir el cemento Portland ordinario por este conglomerante alternativo.
8. El empleo de fracciones finas de árido 0/1 mm o 0/0.5 mm, aunque sean de naturaleza caliza, permiten dotar al hormigón autocompactante de una mayor sostenibilidad (menor huella de carbono) que si se emplea filler calizo < 0.063 mm. Además, el empleo de arena caliza 0/0.5 mm permite mejorar la resistencia y el comportamiento en estado fresco del hormigón autocompactante.
9. Para alcanzar un hormigón de alta autocompactabilidad (clase de escurrimiento SF3, escurrimiento comprendido entre 750 mm y 850 mm) con árido fino y grueso de hormigón reciclado es recomendable emplear un proceso de mezcla por etapas que permita compensar la elevada absorción de agua de este material. En este proceso de mezclado por etapas, en primer lugar, debe añadirse exclusivamente el árido reciclado de hormigón y la fracción de árido fina 0/1 mm o 0/0.5 mm junto con, al menos, la mitad del agua de mezcla. De este modo, se potencia una elevada absorción de agua inicial del árido reciclado de hormigón, evitándose que sea absorbida de forma diferida en el tiempo, lo cual afectaría negativamente a su autocompactabilidad. La eficacia de este procedimiento no se ve afectada por el empleo de escoria siderúrgica granulada molida o de fracciones de árido 0/1 mm o 0/0.5 mm de diferente naturaleza (caliza, o árido reciclado de hormigón).
10. Un proceso de mezcla como el definido en la conclusión anterior permite conservar la autocompactabilidad del hormigón elaborado con escoria siderúrgica granulada molida, un 100% de árido grueso de hormigón reciclado, un 0-100% de árido fino de hormigón reciclado, y arena caliza 0/0.5 mm durante 60 minutos. Al final de este tiempo, el hormigón presentará, como mínimo, una clase de escurrimiento SF1 (escurrimiento comprendido entre 550 mm y 650 mm). Para un hormigonado rápido (15 minutos desde la finalización del proceso de mezcla), el empleo de escoria siderúrgica granulada molida es adecuado. Sin embargo, para hormigonados a gran distancia el cemento Portland ordinario y la arena caliza 0/0.5 mm son la mejor opción.
11. Los modelos estadísticos existentes que permiten estimar de forma indirecta la resistencia a compresión en hormigones vibrados convencionales subestiman la resistencia del hormigón autocompactante. Esto se debe a la menor dureza superficial (índice de rebote)

y a la composición más uniforme (menos zonas de transición entre el árido y la matriz cementicia, aspecto que influye en la velocidad del impulso ultrasónico) de este tipo de hormigón, lo cual está ocasionado por su menor contenido de árido grueso. El empleo de árido reciclado de hormigón, de mayor flexibilidad que el árido natural, y de escoria siderúrgica granulada molida, cuyo uso implica una reducción del contenido de árido grueso, amplifica este fenómeno. No obstante, se detectó una estrecha interrelación entre el índice de rebote, la velocidad del impulso ultrasónico y la resistencia a compresión que permitió desarrollar modelos sencillos y precisos para estimar la resistencia a compresión de las mezclas desarrolladas a partir de estas medidas indirectas. Esto muestra que los métodos habituales de control indirecto de la resistencia del hormigón pueden ser también empleados en hormigones de alta autocompactabilidad elaborados con grandes cantidades de árido reciclado de hormigón, grueso y fino, y escoria siderúrgica granulada molida.

12. El hormigón en su dirección transversal, bajo una carga de compresión, presenta un comportamiento plástico caracterizado por la aparición de una zona de fluencia (incremento de la deformación con un mínimo incremento de la carga) y una mayor deformabilidad que en la dirección longitudinal. La aparición de una fisuración por hendimiento vertical explica la zona de fluencia, mientras que el abarrilamiento (bulging) del elemento de hormigón explica la elevada deformabilidad.
13. Las zonas interfaciales de transición (ITZ) de menor calidad que se originan al añadir árido reciclado de hormigón ocasionan que el empleo de la fracción gruesa de este material facilite el daño del hormigón autocompactante por fenómenos plásticos transversales ante cargas cíclicas crecientes. El empleo de la fracción fina aumenta la deformabilidad en esta dirección transversal, al igual que el empleo de escoria siderúrgica granulada molida siempre que se mantenga constante el contenido total de conglomerante de la mezcla. Por estos motivos, el contenido de estos materiales alternativos debe ser definido en detalle para conseguir un óptimo comportamiento mecánico con una finalidad estructural.
14. El empleo de árido reciclado de hormigón aumenta la deformabilidad térmica del hormigón autocompactante debido a la presencia de mortero adherido y a que este árido favorece la microfisuración ante variaciones cíclicas de temperatura. Se recomienda emplear un coeficiente de dilatación térmica lineal de $1.2 \cdot 10^{-5} \text{ } ^\circ\text{C}^{-1}$ para una estimación segura de estas deformaciones.

2. FUTURAS LÍNEAS DE INVESTIGACIÓN

La presente Tesis Doctoral recoge aspectos muy diferentes en relación con el comportamiento del hormigón autocompactante elaborado con árido reciclado de hormigón. No obstante, existen muchos aspectos en los cuales todavía se puede profundizar para efectuar una caracterización más precisa del comportamiento de este material. Así, algunas líneas de investigación por las cuales el trabajo de esta Tesis Doctoral puede continuar son:

1. Realizar análisis multicriterio para determinar la factibilidad del empleo real de las mezclas desarrolladas respecto del hormigón autocompactante convencional.
2. Establecer árboles de preferencias entre las mezclas desarrolladas que permitan determinar composiciones indiferentes del hormigón autocompactante desde un enfoque multicriterio.
3. Estudiar los efectos sinérgicos en estado fresco entre las modificaciones de la composición del hormigón autocompactante: adición de árido grueso de hormigón reciclado y escoria siderúrgica granulada molida, empleo de diferentes contenidos de árido fino de hormigón reciclado, o fracciones finas 0/1 mm o 0/0.5 mm de diferente naturaleza. Desarrollar cajas de trabajabilidad que consideren estos aspectos.

4. Analizar los cambios espontáneos de longitud (retracción) y forzados (expansión) del hormigón de alta autocompactabilidad elaborado con árido grueso de hormigón reciclado y fino y escoria siderúrgica granulada molida.
5. Evaluar en detalle el efecto del árido grueso y fino de hormigón reciclado y de la escoria siderúrgica granulada molida en la deformabilidad térmica del hormigón autocompactante.
6. Estudiar la durabilidad de los hormigones desarrollados, tanto en relación con los mecanismos de transporte de agua como respecto al ataque de agentes agresivos externos.
7. Ensayar a flecha diferida, flexión y cortante, elementos estructurales como, por ejemplo, vigas, fabricados con hormigón autocompactante con árido grueso y fino de hormigón reciclado y escoria siderúrgica granulada molida.

Conclusions and future research lines

Each article included in this PhD Thesis has its own conclusions due to its autonomous character. However, in this final section it is intended to merge all the aspects studied throughout them, establishing some overall conclusions. In addition, future research lines are also suggested, which enable to continue the work described in this PhD Thesis.

1. CONCLUSIONS

The overall conclusions derived from the joint analysis of the different articles included in this PhD Thesis are presented below. It can be noted that each of them is linked to one of the objectives set out in the first section of this Thesis, the introduction, which allows a clear answer to the questions posed at the beginning of this research work.

1. The effect of recycled concrete aggregate on the compressive strength of self-compacting concrete largely depends on the mix composition. The modification of the coarse to fine aggregate ratio, the adjustment of the content of the aggregate fraction 0/0.5 mm, or the alteration of the effective water/cement ratio can compensate for the expected negative effect that recycled concrete aggregate has on the mechanical performance of self-compacting concrete. Thus, it is possible to obtain self-compacting concrete made with recycled concrete aggregate that have a higher compressive strength than conventional self-compacting concrete. The sensitivity of this type of concrete to changes in its composition may explain this behavior.
2. The dispersion of the effect of recycled concrete aggregate on the compressive strength of self-compacting concrete is not observed in the splitting tensile strength. Probably, the higher influence of the interfacial transition zones (ITZ) between the aggregate and the cementitious matrix justifies this tendency. Therefore, the appearance of lower quality interfacial transition zones when adding recycled concrete aggregate inevitably leads to a decrease of the splitting tensile strength.
3. The studies addressing the behavior of self-compacting concrete with recycled concrete aggregate should focus mainly on the fine fraction of this waste. These studies should also focus on the interaction of this fraction of recycled concrete aggregate with alternative binders such as fly ash or silica fume.
4. According to the work conducted in this PhD Thesis, the use of 50% or 100% coarse recycled concrete aggregate did not significantly affect the mechanical properties of self-compacting concrete. Therefore, when introducing this waste in a concrete mix of these characteristics, it is recommended to use 100% in order to achieve greater sustainability of the material.
5. The effect of fine recycled concrete aggregate when combined with the coarse fraction of this same waste to produce self-compacting concrete depends on whether its content is low (0-25%), medium (50%) or high (75-100%). It can be stated that the use of 100% and 25%, of coarse and fine recycled concrete aggregate, respectively, allows obtaining a self-compacting concrete with a mechanical behavior statistically identical to that which incorporates only 100% of the coarse fraction of this aggregate.
6. The simultaneous use of 100% coarse recycled concrete aggregate and a certain content (25-100%) of fine recycled concrete aggregate causes the compressive strength of self-compacting concrete to exhibit a probability distribution with a reduced dispersion if the conditions of the mixture are controlled and repeated. These conditions refer mainly to the non-modification of the water/cement ratio, and to the usual way of working in a concrete manufacturing plant, whose alteration favors the dispersion mentioned in the first conclusion. This approach leads to the fact that the characteristic strength of self-

compacting concretes containing this aggregate is underestimated by the current formulation, and needs to be readjusted in order to maximize the use of this type of concrete in the design of concrete structural elements.

7. The development of self-compacting concrete with a high content of ground granulated blast furnace slag (45% of the total amount of binder) and 100% coarse recycled concrete aggregate requires a readjustment of the ratio between the binder and coarse aggregate content. The highly irregular shape of this aggregate in the coarse fraction and the high grinding fineness of ground granulated blast furnace slag hinder the uniform dragging of the coarser aggregate particles through the cement paste. This problem can be solved by decreasing the coarse aggregate content and increasing the total amount of binder. This readjustment of the composition enables high self-compactability to be obtained in concretes with this composition, while not greatly affecting the lower carbon footprint achieved with the use of ground granulated blast furnace slag. In addition, it allows compensating for the expected decrease of concrete strength when replacing ordinary Portland cement with this alternative binder.
8. The use of aggregate fines 0/1 mm or 0/0.5 mm, even limestone fines, allows increasing the sustainability of self-compacting concrete (lower carbon footprint) than when using limestone filler < 0.063 mm. Furthermore, the use of limestone fines 0/0.5 mm improves the strength and fresh behavior of self-compacting concrete.
9. To achieve a concrete with high self-compactability (slump-flow class SF3, slump flow between 750 mm and 850 mm) with coarse and fine recycled concrete aggregate, it is advisable to use a staged mixing process to compensate for the high water absorption of this aggregate. In this staged mixing process, the recycled concrete aggregate and the aggregate fines 0/1 mm or 0/0.5 mm should be added at first, along with at least half of the mixing water. In this way, a high initial water absorption of the recycled concrete aggregate is induced, avoiding its delayed absorption over time, which would negatively affect its self-compactability. The effectiveness of this procedure is not affected by the use of ground granulated blast furnace slag or aggregate fines 0/1 mm or 0/0.5 mm of different nature (limestone or recycled concrete aggregate).
10. A mixing process, as defined in the previous conclusion, allows preserving the self-compactability of concrete produced with ground granulated blast furnace slag, 100% coarse recycled concrete aggregate, 0-100% fine recycled concrete aggregate, and limestone fines 0/0.5 mm for 60 minutes. At the end of this time, the concrete will exhibit, at least, a slump-flow class SF1 (slump flow between 550 mm and 650 mm). For fast concreting (15 minutes after the end of the mixing process), the use of ground granulated blast furnace slag is adequate. However, for long-distance concreting, ordinary Portland cement and limestone fines 0/0.5 mm are the best choice.
11. Existing statistical models for indirect estimation of compressive strength in conventional vibrated concrete underestimate the compressive strength of self-compacting concrete. This is due to the lower surface hardness (hammer rebound index) and the more uniform composition (fewer interfacial transition zones between the aggregate and the cementitious matrix, an aspect that influences ultrasonic pulse velocity) of this type of concrete, which is caused by its lower coarse aggregate content. The use of recycled concrete aggregate, which is more flexible than natural aggregate, and ground granulated blast furnace slag, whose use implies a reduction in coarse aggregate content, amplifies this phenomenon. However, a close relationship between the hammer rebound index, the ultrasonic pulse velocity and the compressive strength was detected, which allowed the development of simple and accurate models to estimate the compressive strength of the mixtures developed from these indirect measurements. This shows that the usual methods of indirect control of concrete strength can also be employed in highly self-compacting

concretes made with large quantities of coarse and fine recycled concrete aggregate and ground granulated blast furnace slag.

12. Concrete in its transversal direction, under a compressive load, exhibits a plastic behavior characterized by the appearance of a creep zone (increase in strain with a minimum increase in load) and a higher deformability than in the longitudinal direction. The appearance of vertical-splitting cracking explains the creep zone, while the bulging of the concrete specimens explains the high deformability.
13. The lower quality interfacial transition zones (ITZ) caused by the addition of recycled concrete aggregate results that the use of the coarse fraction of this material facilitates damage of self-compacting concrete by transversal plastic phenomena under increasing cyclic compressive loads. The use of the fine fraction of this aggregate increases the deformability in this transversal direction. The addition of ground granulated blast furnace slag also has the same effect, as long as the total binder content of the mix is kept constant. For these reasons, the content of these alternative materials must be defined in detail in order to achieve an optimum mechanical behavior in structural applications.
14. The use of recycled concrete aggregate increases the thermal deformability of self-compacting concrete due to the presence of adhered mortar and to the fact that this aggregate favors micro-cracking under cyclical temperature variations. It is recommended to use a linear thermal expansion coefficient of $1.2 \cdot 10^{-5} \text{ } ^\circ\text{C}^{-1}$ for a safe estimation of these strains.

2. FUTURE RESEARCH LINES

This PhD Thesis addresses very different aspects related to the in-fresh and hardened behavior of self-compacting concrete made with recycled concrete aggregate. Nevertheless, there are still many aspects that can be explored for a better understanding of the behavior of recycled aggregate self-compacting concrete. Thus, some research lines to continue the work of this PhD Thesis are:

1. Performing a multi-criteria analysis to determine the feasibility of the real use of the mixes developed regarding conventional self-compacting concrete.
2. Establishing preference trees among the developed mixes to determine indifferent compositions of self-compacting concrete from a multi-criteria approach.
3. Studying the synergistic effects in the fresh state between the different modifications in the composition of self-compacting concrete: addition of coarse recycled concrete aggregate and ground granulated blast furnace slag, use of different contents of fine recycled concrete aggregate, and addition of aggregate fines 0/1 mm or 0/0.5 mm of different nature. Developing workability boxes that address these aspects.
4. Analyzing the spontaneous (shrinkage) and forced (expansion) length changes of highly self-compacting concrete made with coarse and fine recycled concrete aggregate and ground granulated blast furnace slag.
5. Evaluating in detail the effect of coarse and fine recycled concrete aggregate and ground granulated blast furnace slag on the thermal deformability of self-compacting concrete.
6. Studying the durability of the developed concretes, both in relation to the water transport mechanisms and to the attack of external aggressive agents.
7. Testing in both long-term deflection and, bending and shear strength, structural elements, such as beams, manufactured with self-compacting concrete with coarse and fine recycled concrete aggregate and ground granulated blast furnace slag.

Scientific productivity during the PhD Thesis

1. SCIENTIFIC RESEARCH ARTICLES

1. **Title:** Performance and durability of porous asphalt mixtures manufactured exclusively with electric steel slags
Authors: Marta Skaf, Emiliano Pasquini, **Víctor Revilla-Cuesta**, Vanesa Ortega-López
Journal: Materials
Year: 2019
Volume: 12
Issue: 20
Article number: 3306
DOI: <https://doi.org/10.3390/ma12203306>
Journal classification (2019 JCR ranking data): 132/314 (materials science, multidisciplinary; SCIE). Second quartile (Q2)
2. **Title:** Self-compacting concrete with recycled concrete aggregate: an overview
Authors: **Víctor Revilla-Cuesta**, Marta Skaf, Flora Faleschini, Juan M. Manso, Vanesa Ortega-López
Journal: Journal of Cleaner Production
Year: 2020
Volume: 262
Article number: 121362
DOI: <https://doi.org/10.1016/j.jclepro.2020.121362>
Journal classification (2019 JCR ranking data): 19/265 (environmental sciences; SCIE). First quartile (Q1), first decile (D1)
3. **Title:** Thermal deformability of recycled self-compacting concrete under cyclical temperature variations
Authors: **Víctor Revilla-Cuesta**, Marta Skaf, José A. Chica, José A. Fuente-Alonso, Vanesa Ortega-López
Journal: Materials Letters
Year: 2020
Volume: 278
Article number: 128417
DOI: <https://doi.org/10.1016/j.matlet.2020.128417>
Journal classification (2019 JCR ranking data): 43/155 (physics, applied; SCIE). Second quartile (Q2)
4. **Title:** Effect of fine recycled concrete aggregate on the mechanical behavior of self-compacting concrete
Authors: **Víctor Revilla-Cuesta**, Vanesa Ortega-López, Marta Skaf, Juan M. Manso
Journal: Construction and Building Materials
Year: 2020
Volume: 263
Article number: 120671
DOI: <https://doi.org/10.1016/j.conbuildmat.2020.120671>

- Journal classification (2019 JCR ranking data):** 11/134 (engineering, civil; SCIE). First quartile (Q1), first decile (D1)
5. **Title:** Statistical approach for the design of structural self-compacting concrete with fine recycled concrete aggregate
Authors: **Víctor Revilla-Cuesta**, Marta Skaf, Ana B. Espinosa, Amaia Santamaría, Vanesa Ortega-López
Journal: Mathematics
Year: 2020
Volume: 8
Issue: 12
Article number: 2190
DOI: <https://doi.org/10.3390/math8122190>
Journal classification (2019 JCR ranking data): 28/325 (mathematics; SCIE). First quartile (Q1), first decile (D1)
6. **Title:** Models for compressive strength estimation through non-destructive testing of highly self-compacting concrete containing recycled concrete aggregate and slag-based binder
Authors: **Víctor Revilla-Cuesta**, Marta Skaf, Roberto Serrano-López, Vanesa Ortega-López
Journal: Construction and Building Materials
Year: 2021
Volume: 280
Article number: 122454
DOI: <https://doi.org/10.1016/j.conbuildmat.2021.122454>
Journal classification (2019 JCR ranking data): 11/134 (engineering, civil; SCIE). First quartile (Q1), first decile (D1)
7. **Title:** Temporal flowability evolution of slag-based self-compacting concrete with recycled concrete aggregate
Authors: **Víctor Revilla-Cuesta**, Marta Skaf, Amaia Santamaría, Jorge J. Hernández-Bagaces, Vanesa Ortega-López
Journal: Journal of Cleaner Production
Year: 2021
Volume: 299
Article number: 126890
DOI: <https://doi.org/10.1016/j.jclepro.2021.126890>
Journal classification (2019 JCR ranking data): 19/265 (environmental sciences; SCIE). First quartile (Q1), first decile (D1)
8. **Title:** Bending tests on building beams containing electric arc furnace slag and alternative binders and manufactured with energy-saving placement techniques
Authors: Amaia Santamaría, Aratz García-Llona, **Víctor Revilla-Cuesta**, Ignacio Piñero, Vanesa Ortega-López
Journal: Structures
Year: 2021
Volume: 32
Pages: 1921-1933
DOI: <https://doi.org/10.1016/j.istruc.2021.04.003>
Journal classification (2019 JCR ranking data): 65/134 (engineering, civil; SCIE). Second quartile (Q2)

9. **Title:** Fiber-reinforcement and its effect on the mechanical properties of high-workability concretes manufactured with slag as aggregate and binder
Authors: Vanesa Ortega-López, Aratz García-Llona, **Víctor Revilla-Cuesta**, Amaia Santamaría, José T. San-José
Journal: Journal of Building Engineering
Year: 2021
Volume: 43
Article number: 102548
DOI: <https://doi.org/10.1016/j.jobe.2021.102548>
Journal classification (2019 JCR ranking data): 22/134 (engineering, civil; SCIE). First quartile (Q1)
10. **Title:** Assessment of longitudinal and transversal plastic behavior of recycled aggregate self-compacting concrete: a two-way study
Authors: **Víctor Revilla-Cuesta**, Marta Skaf, Amaia Santamaría, Vanesa Ortega-López, Juan M. Manso
Journal: Construction and Building Materials
Year: 2021
Volume: 292
Article number: 123426
DOI: <https://doi.org/10.1016/j.conbuildmat.2021.123426>
Journal classification (2019 JCR ranking data): 11/134 (engineering, civil; SCIE). First quartile (Q1), first decile (D1)
11. **Title:** Preliminary validation of steel slag-aggregate concrete for rigid pavements: A Full-Scale Study
Authors: **Víctor Revilla-Cuesta**, Vanesa Ortega-López, Marta Skaf, Emiliano Pasquini, Marco Pasetto
Journal: Infrastructures
Year: 2021
Volume: 6
Issue: 5
Article number: 64
DOI: <https://doi.org/10.3390/infrastructures6050064>
Journal classification (2019 SJR ranking data): Third quartile (Q3) in the category of “construction and building”. Indexed in Web of Science (WoS)
12. **Title:** Performance assessment of a self-compacting concrete with coarse and fine recycled aggregate
Authors: **Víctor Revilla-Cuesta**, José A. Fuente-Alonso, Jorge J. Hernández-Bagaces, José A. Chica-Páez, Estibaliz Briz, Vanesa Ortega-López
Journal: Hormigón y acero
DOI: <https://doi.org/10.33586/hya.2020.2742>
 Indexed in Web of Science (WoS)

2. BOOK CHAPTERS

1. **Title:** Optimization of self-compacting recycled concrete manufactured with waste and byproducts
Authors: Juan M. Manso, Francisco Fiol, Carlos Thomas, Vanesa Ortega-López, **Víctor Revilla-Cuesta**, Marta Skaf
Book: Waste and Byproducts in Cement-Based Materials
Year of publication: 2021

Paperback ISBN: 9780128205495

Editorial: Woodhead Publishing, Elsevier

3. TEACHING INNOVATION ARTICLES

1. **Title:** Student perceptions of formative assessment and cooperative work on a technical engineering course
Authors: **Víctor Revilla-Cuesta**, Marta Skaf, Juan M. Manso, Vanesa Ortega-López
Journal: Sustainability
Year: 2020
Volume: 12
Issue: 11
Article number: 4569
DOI: <https://doi.org/10.3390/su12114569>
Journal classification (2019 JCR ranking data): 53/123 (environmental studies; SSCI). Second quartile (Q1)
2. **Title:** The outbreak of the COVID-19 pandemic and its social impact on education: were engineering teachers ready to teach online?
Authors: **Víctor Revilla-Cuesta**, Marta Skaf, Juan M. Varona, Vanesa Ortega-López
Journal: International Journal of Environmental Research and Public Health
Year: 2021
Volume: 18
Issue: 4
Article number: 2127
DOI: <https://doi.org/10.3390/ijerph18042127>
Journal classification (2019 JCR ranking data): 32/171 (public, environmental & occupational health; SSCI). First quartile (Q1)

4. SCIENTIFIC PRESENTATIONS AT NATIONAL AND INTERNATIONAL CONGRESSES AND CONFERENCES

1. **Title:** Fracture toughness evaluation of fiber-reinforced concrete manufactured with siderurgic aggregates
Authors: Vanesa Ortega-López, **Víctor Revilla-Cuesta**, Marta Skaf, Francisco Fiol, Amaia Santamaría, Aratz García-Llona, Ignacio Piñero
Congress/conference: 5th International Conference on Sustainable Construction Materials and Technologies (SCMT5)
Place/date: London (United Kingdom), July 14-17, 2019
ISSN proceedings: 2515-3048 (print), 2515-3056 (online)
2. **Title:** Puente arco sobre el río Arlanzón en le bulevar de Burgos. Análisis del impacto ambiental de un puente urbano
Authors: **Víctor Revilla-Cuesta**, Vanesa Ortega-López, Juan M. Manso, José A. Martínez
Congress/conference: I Congreso Nacional de TFG y TFM Ambientales
Place/date: Burgos (Spain), November 7-9, 2019
ISBN proceedings: 978-84-14865-00-0
3. **Title:** Economía circular en el sector de la construcción: fabricación de hormigones con residuos
Authors: **Víctor Revilla-Cuesta**, Juan M. Manso, Marta Skaf, Vanesa Ortega-López
Congress/conference: VI Jornadas de Doctorandos de la Universidad de Burgos
Place/date: Burgos (Spain), December 2-3, 2019

- ISBN proceedings:** 978-84-16283-86-6
4. **Title:** Self-compacting concrete manufactured with recycled concrete aggregate
Authors: **Víctor Revilla-Cuesta**, Francisco Fiol, Marta Skaf, Roberto Serrano-López, Juan M. Manso, Vanesa Ortega-López
Congress/conference: Euro-American Congress in Construction Pathology, Rehabilitation, Technology and Heritage Management (REHABEND2020)
Place/date: Granada (Spain), March 24-27, 2020
ISSN proceedings: 2386-8198 (print)
ISBN proceedings: 978-84-09-17871-1 (book of abstracts), 978-84-09-17873 (book of articles)
 5. **Title:** Self-compacting concrete with recycled concrete aggregate: resistance against aggressive external agents
Authors: **Víctor Revilla-Cuesta**, Marta Skaf, Aratz García-Llona, Ignacio Piñero, Juan M. Manso, Vanesa Ortega-López
Congress/conference: XV International Conference on Durability of Building Materials and Components (DBMC2020)
Place/date: Barcelona (Spain), October 20-23, 2020
ISBN proceedings: 978-84-121101-8-0
 6. **Title:** Durability studies on fiber-reinforced siderurgic concrete
Authors: Vanesa Ortega-López, **Víctor Revilla-Cuesta**, Amaia Santamaría, Ana B. Espinosa, José A. Fuente-Alonso, José A. Chica
Congress/conference: XV International Conference on Durability of Building Materials and Components (DBMC2020)
Place/date: Barcelona (Spain), October 20-23, 2020
ISBN proceedings: 978-84-121101-8-0
 7. **Title:** Evolución temporal de las propiedades mecánicas del hormigón autocompactante con el empleo de árido reciclado fino
Authors: **Víctor Revilla-Cuesta**, Marta Skaf, Vanesa Ortega-López, Juan M. Manso
Congress/conference: VII Jornadas de Doctorandos de la Universidad de Burgos
Place/date: Burgos (Spain), March 9-10, 2021
ISBN proceedings: 978-84-18465-03-1

5. TEACHING INNOVATION PRESENTATIONS AT INTERNATIONAL CONGRESSES

1. **Title:** Posibilidades del aprendizaje cooperativo para la simulación del entorno laboral en ingeniería
Authors: **Víctor Revilla-Cuesta**
Congress/conference: 4th International Virtual Conference on Educational Research and Innovation (CIVINEDU2020)
Place/date: Online, September 23-24, 2020
ISSN proceedings: 978-84-22966-6
2. **Title:** ¿Qué opina un profesor de ingeniería tras alicar por primera vez el trabajo grupal autónomo en sus clases?
Authors: **Víctor Revilla-Cuesta**
Congress/conference: 5th Virtual International Conference on Education, Innovation and ICT (EDUNAVATIC2020)
Place/date: Online, December 10-11, 2020
ISSN proceedings: 978-84-22967-3

3. **Title:** Análisis mixto de la percepción de los estudiantes de ingeniería ante el aprendizaje colaborativo
Authors: **Víctor Revilla-Cuesta**
Congress/conference: 5th Virtual International Conference on Education, Innovation and ICT (EDUNAVATIC2020)
Place/date: Online, December 10-11, 2020
ISSN proceedings: 978-84-22967-3

6. PATENTS

1. **Patent number:** P202030746
Title: Hormigón autocompactante con árido reciclado de hormigón y su procedimiento de elaboración
Authors: Vanesa Ortega-López, José A. Fuente-Alonso, Marta Skaf, Juan M. Manso, **Víctor Revilla-Cuesta**
Country: Spain
Application date: 17/07/2020
Holder: University of Burgos
2. **Patent number:** P202030748
Title: Hormigón autocompactante con árido reciclado de hormigón y de baja retracción y su procedimiento de elaboración
Authors: Vanesa Ortega-López, Francisco Fiol, Marta Skaf, Juan M. Manso, **Víctor Revilla-Cuesta**
Country: Spain
Application date: 17/07/2020
Holder: University of Burgos
3. **Patent number:** P202030750
Title: Hormigón autocompactante siderúrgico de alta resistencia y su procedimiento de elaboración
Authors: Vanesa Ortega-López, Roberto Serrano-López, Marta Skaf, Juan M. Manso, **Víctor Revilla-Cuesta**
Country: Spain
Application date: 17/07/2020
Holder: University of Burgos
4. **Patent number:** P202030878
Title: Hormigón siderúrgico de consistencia seca y su procedimiento de elaboración
Authors: Vanesa Ortega-López, Marta Skaf, Juan M. Manso, **Víctor Revilla-Cuesta**, Amaia Santamaría
Country: Spain
Application date: 20/08/2020
Holder: University of Burgos, University of the Basque Country
5. **Patent number:** P202030881
Title: Hormigón sostenible de consistencia seca y su procedimiento de elaboración
Authors: Vanesa Ortega-López, Marta Skaf, Juan M. Manso, **Víctor Revilla-Cuesta**, Aimar Orbe
Country: Spain
Application date: 20/08/2020
Holder: University of Burgos, University of the Basque Country

7. STAYS

1. **Place:** Lisbon, Portugal
Institution: Instituto Superior Técnico (IST), University of Lisbon
Type: Pre-doctoral stay
Dates: September-December 2020 (4 months)
Researcher in charge: Prof. Dr. Jorge de Brito, Prof. Dr. Luís Evangelista

8. CONTRACTS, KNOWLEDGE TRANSFER

1. **Reference:** W29W06
Contract title: Asistencia técnica en el diseño y ensayo de fluencia en flexión para 4 vigas con EAFS. Proyecto Retos 2018 "DESCLIMA" (RTI2018-097079-B-C37; MCIU/AEI/FEDER, EU)
Funding entity: University of the Basque Country
Duration: from 22/07/2019 to 31/12/2019
Principal researcher: Vanesa Ortega-López
2. **Reference:** W18X06
Contract title: Asistencia técnica en el diseño y ensayo de hormigones siderúrgicos para el grupo CLIM-ADAPT
Funding entity: University of the Basque Country
Duration: from 29/07/2020 to 22/09/2020
Principal researcher: Vanesa Ortega-López
3. **Reference:** W19X06
Contract title: Asistencia técnica sobre ensayos en morteros/hormigones
Funding entity: Fundación Tecnalia Research & Innovacion
Duration: from 01/09/2020 to 09/10/2020
Principal researcher: Vanesa Ortega-López, Marta Skaf
4. **Reference:** W21X06
Contract title: Estudio de patologías constructivas en obra de adecuación de parcela dotacional para espacio libre fase I de Aranda de Duero (Burgos)
Funding entity: EYPO Ingeniería S.L.
Duration: from 15/07/2020 to 23/10/2020
Principal researcher: Juan M. Manso

9. PhD THESIS FUNDING

1. **Reference:** FPU17/03374
Call: Convocatoria 2017 de las Ayudas para la Formación de Profesorado Universitario (FPU)
Funding entities: Ministerio de Ciencia e Innovación (MICINN), Agencia Estatal de Investigación (AEI), Fondos Europeos de Desarrollo Regional (FEDER)
Duration: from 26/09/2018 to 25/09/2022
2. **Reference:** EST19/00263
Call: Convocatoria 2020 de las Ayudas a la movilidad para estancias breves y traslados temporales para beneficiarios del programa de Formación del Profesorado Universitario (FPU)
Funding entities: Ministerio de Ciencia e Innovación (MICINN), Agencia Estatal de Investigación (AEI), Fondos Europeos de Desarrollo Regional (FEDER)
Duration: from 20/09/2020 to 19/12/2020



UNIVERSITY OF BURGOS
HIGHER POLYTECHNIC SCHOOL

